



National Library  
of Canada

Bibliothèque nationale  
du Canada

Canadian Theses Service

Services des thèses canadiennes

Ottawa, Canada  
K1A 0N4

## CANADIAN THESES

## THÈSES CANADIENNES

### NOTICE

The quality of this microfiche is heavily dependent upon the quality of the original thesis submitted for microfilming. Every effort has been made to ensure the highest quality of reproduction possible.

If pages are missing, contact the university which granted the degree.

Some pages may have indistinct print especially if the original pages were typed with a poor typewriter ribbon or if the university sent us an inferior photocopy.

Previously copyrighted materials (journal articles, published tests, etc.) are not filmed.

Reproduction in full or in part of this film is governed by the Canadian Copyright Act, R.S.C. 1970, c. C-30.

### AVIS

La qualité de cette microfiche dépend grandement de la qualité de la thèse soumise au microfilmage. Nous avons tout fait pour assurer une qualité supérieure de reproduction.

S'il manque des pages, veuillez communiquer avec l'université qui a conféré le grade.

La qualité d'impression de certaines pages peut laisser à désirer, surtout si les pages originales ont été dactylographiées à l'aide d'un ruban usé ou si l'université nous a fait parvenir une photocopie de qualité inférieure.

Les documents qui font déjà l'objet d'un droit d'auteur (articles de revue, examens publiés, etc.) ne sont pas microfilmés.

La reproduction, même partielle, de ce microfilm est soumise à la Loi canadienne sur le droit d'auteur, SRC 1970, c. C-30.

**THIS DISSERTATION  
HAS BEEN MICROFILMED  
EXACTLY AS RECEIVED**

**LA THÈSE A ÉTÉ  
MICROFILMÉE TELLE QUE  
NOUS L'AVONS REÇUE**

THE UNIVERSITY OF ALBERTA  
PHOTOCHEMISTRY OF  $\text{Os}_3(\text{CO})_{12}$  WITH UNSATURATED  
ORGANIC SUBSTRATES.

---

by

MICHAEL RICHARD BURKE

A THESIS

SUBMITTED TO THE FACULTY OF GRADUATE STUDIES AND  
RESEARCH IN PARTIAL FULFILMENT OF THE REQUIREMENTS  
FOR THE DEGREE OF DOCTOR OF PHILOSOPHY

DEPARTMENT OF CHEMISTRY

EDMONTON, ALBERTA

SPRING, 1987

Permission has been granted to the National Library of Canada to microfilm this thesis and to lend or sell copies of the film.

The author (copyright owner) has reserved other publication rights, and neither the thesis nor extensive extracts from it may be printed or otherwise reproduced without his/her written permission.

L'autorisation a été accordée à la Bibliothèque nationale du Canada de microfilmer cette thèse et de prêter ou de vendre des exemplaires du film.

L'auteur (titulaire du droit d'auteur) se réserve les autres droits de publication; ni la thèse ni de longs extraits de celle-ci ne doivent être imprimés ou autrement reproduits sans son autorisation écrite.

SBN 0-315-37595-7



University of Alberta  
Edmonton

Department of Chemistry  
Faculty of Science

Canada T6G 2G2

E3-43 Chemistry Building East, Telephone (403) 432-3254

February 17, 1987.

To Whom It May Concern:

Permission is hereby granted to Dr. Michael R. Burke to use the following X-ray figures in his Ph.D. Thesis and to have them reproduced as necessary.

(1) Figure VI. Structure of  $\text{Fe}(\text{CO})_3(\text{PPh}_3)(\eta^2\text{-DEM})$

J. Takats for

(J. Takats & M.V.R. Stainer)

(2) Figures II, VII, VIII, IX, X, XI, XVIII and XIX.

R.G. Ball

Structure Determination Laboratory  
University of Alberta

In addition, parts of Chapters II and IV have been published and Chapter VI has been submitted for publication and we (Burke and Takats) hereby grant permission to reproduce the relevant material.

J. Takats

M.R. Burke



THE UNIVERSITY OF ALBERTA

RELEASE FORM

NAME OF AUTHOR Michael Richard Burke  
TITLE OF THESIS Photochemistry of  $\text{Os}_3(\text{CO})_{12}$  with Unsaturated  
Organic Substrates.

DEGREE FOR WHICH THESIS WAS PRESENTED Ph. D.

YEAR THIS DEGREE GRANTED 1987

Permission is hereby granted to THE UNIVERSITY OF ALBERTA  
LIBRARY to reproduce single copies of this thesis and to lend or sell  
such copies for private, scholarly or scientific research purposes only.

The author reserves other publication rights, and neither the  
thesis nor extensive extracts from it may be printed or otherwise re-  
produced without the author's written permission.

(Signed) Michael R. Burke

PERMANENT ADDRESS:

10, 6233-124 St.  
Edmonton, Alberta

DATED Feb 18, 1987.

THE UNIVERSITY OF ALBERTA  
FACULTY OF GRADUATE STUDIES AND RESEARCH

The undersigned certify that they have read, and recommend to the Faculty of Graduate Studies and Research, for acceptance, a thesis entitled PHOTOCHEMISTRY OF  $\text{Os}_3(\text{CO})_{12}$  WITH UNSATURATED ORGANIC SUBSTRATES submitted by Michael R. Burke in partial fulfilment of the requirements for the degree of Doctor of Philosophy in Chemistry.

Josef Takats  
Josef Takats, Supervisor

[Signature]

[Signature]

9/77 & 9/11/77

Harrison

[Signature]

Date Feb. 12, 1987

To the funniest and most lovable child that can be

RYAN KENT BURKE

To the woman I adore with my wholeness

ELAINE VICTORIA KENT BURKE

To my wonderful mother

JEANNETTE MARIE BURKE

# ABSTRACT

The photochemical behaviour of  $\text{Os}_3(\text{CO})_{12}$  (**3c**) toward a variety of alkenes (ethylene, propylene, cis-cyclooctene, methyl vinyl ketone, acrylic acid, methyl acrylate, ethyl acrylate, 3-penten-2-one, tetrafluoroethylene, perfluoro-2-butene, maleic anhydride) was investigated. Long wavelength photolysis ( $\lambda > 370$  nm,  $15^\circ\text{C}$ ) in benzene resulted, in most cases, in fragmentation of the cluster to give mononuclear,  $\text{Os}(\text{CO})_4[\eta^2\text{-alkene}]$ , and dinuclear,  $\text{Os}_2(\text{CO})_8[\mu\text{-alkene}]$  derivatives. Methyl acrylate [MA] afforded the best yields of products and the subsequent solid state structure determination of  $\text{Os}_2(\text{CO})_8[\mu\text{-MA}]$  (**14**) revealed that the dinuclear complexes are rare examples of stable 1,2-diosmacyclobutanes. The photolysis with some 1,2-disubstituted alkenes (dimethyl maleate, diethyl maleate, cis-stilbene) led to facile cis-to-trans isomerization of the bulk free alkene. In one instance, with dimethyl maleate, isolation of the isomeric compounds- $\text{Os}_2(\text{CO})_8[\mu\text{-C}_2\text{H}_2(\text{CO}_2\text{CH}_3)_2]$ , **28** and **30**, was achieved and the stereochemistry of the bridging groups was corroborated by X-ray crystallography. The relevance of these observations concerning the photofragmentation of **3c** is discussed.

The photochemical synthesis was extended to alkynes with a view of preparing unsaturated 1,2-diosmacyclobutenes. However, mixtures of products were obtained and only three  $\text{Os}_2(\text{CO})_8[\mu\text{-RCCR}]$  ( $\text{R}=\text{CO}_2\text{Me}$  (**33**),  $\text{Ph}$  (**40**),  $\text{CF}_3$  (**43**)) complexes could be isolated and only in low yields. The structure of **33** confirmed the unsaturated diosmacycle, whereas that of  $\text{Os}_2(\text{CO})_6(\text{MeO}_2\text{CC}_2\text{CO}_2\text{Me})_4$  (**34**) from the same reaction showed an unusual coupling of the alkyne moieties.

The thermal exchange reactions between the saturated diosmacycle 14 and alkynes provided an alternate synthesis for the diosmacyclobutenes 33, 40 and 43. Even though this resulted in an improved yield over the photochemical route, these reactions were complicated and also gave mixtures of products.

Modifications in the photochemical reaction conditions allowed the synthesis of the first simple carbonyl-alkyne derivatives of ruthenium and osmium,  $M(CO)_4[\eta^2-Me_3SiC_2SiMe_3]$  ( $M=Ru$  55,  $Os$  54). The structure of 54, determined by X-ray analysis, showed an interesting canting of the axial carbonyl groups toward the equatorial alkyne moiety. With the availability of the analogous iron complex, a detailed triad comparison of properties was carried out.

## ACKNOWLEDGEMENTS

In crossing the paths of many throughout the tenure of this project, the author would like to express his sincere appreciation to the following in particular:

First, and foremost, Professor Josef Takats, for his unyielding inspiration, confidence, dedication and friendship, the last of which I hope I will never forget.

Dr. Gong-Yu Kiel, for her wonderful wit, warmhearted companionship, and willingness to share her expertise (and hockey tickets!). Everyone should have such a dedicated person in their lab.

To other members of the research group through the years, who gave me someone to talk to when things went awry and to bounce ideas off during the better times (Drs. Janis Matisons, Frank Edelmann, Frank Seils, and Achutha Vasudevamurthy, Steve Astley, Mike (Junior) Gagné).

To the best service staff available, specifically John Olekszyk (mass spec) who did lots of counting and cleaning after numerous runs with osmium; Dr. Tom Nakashima and the NMR staff, especially Glen Bigam, for showing interest and spending hours collecting data on often small quantities of sometimes insoluble compounds; Dr. Rick Ball (SDL) for providing expedient crystallographic service of the highest quality.

To other friends through the years who have made my time in Edmonton much more enjoyable (Dr. Bruce Sutherland, Richard Krentz, Drs. John Arenivar, Evert Ditzel, Neil Meanwell, Bill Kiel).

To Dr. Friedrich-Wilhelm Grevels, Max Planck Institut, Mülheim  
a. d. Ruhr, West Germany for the opportunity to study abroad early  
in my graduate career; an experience I will never forget.

To Dr. Mary Frances Richardson (Brock University) whose belief  
in me inspired me to continue in Chemistry.

To my cats, Simba and Frisco, who allowed me to vent some  
frustration (harmlessly) and to witness some incredible acts of acrobatics.

And lastly (because it usually gets put here), to my wife Elaine,  
whose expert preparation of this thesis and her patience and understanding  
only confirm my strongest beliefs that she is truly a remarkable person.

I would be remiss if I didn't mention the one who made me realize that  
there is more to life, my wonderful son, Ryan.

# TABLE OF CONTENTS

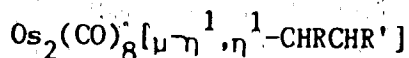
	<u>PAGE</u>
ABSTRACT	v
ACKNOWLEDGEMENTS	vii
LIST OF TABLES	xii
LIST OF FIGURES	xv
LIST OF SCHEMES	xvii
LIST OF ABBREVIATIONS	xviii

## CHAPTER ONE- INTRODUCTION

I. Brief History of Iron-group Carbonyls	1
II. Physical and Spectral Characteristics of $\text{Os}_3(\text{CO})_{12}$ (3c)	2
III. Reactivity of $\text{Os}_3(\text{CO})_{12}$ (3c).	4
A. Thermal Reactions of 3c with Alkenes and Alkynes.	4
B. Photochemical Behaviour of 3c.	7
IV. Scope of the Present Research.	17

## CHAPTER TWO- PHOTOREACTIVITY OF $\text{Os}_3(\text{CO})_{12}$ TOWARDS ALKENES:

### UNEXPECTED FORMATION OF DIOSMACYCLOBUTANES



I. Introduction.	20
II. Reaction of 3c with Methyl Acrylate.	20
III. Photoreactivity of 3c with Other Alkenes.	36
IV. The $\text{Os}(\text{CO})_4[\eta^2\text{-alkene}]$ Complexes.	42
V. Conclusions.	48

## CHAPTER THREE- PHOTOREACTIONS OF $\text{Os}_3(\text{CO})_{12}$ WITH 1,2-DISUBSTITUTED ALKENES

I. Introduction.	51
------------------	----



	<u>PAGE</u>
II. Reactions of 3c with Dimethyl Maleate and Dimethyl Fumarate.	51
A. Initial Investigations.	51
B. Solid State Structure of Isomeric $Os_2(CO)_8[\mu-DMM]$ and $Os_2(CO)_8[\mu-DMF]$ .	58
C. Experimental Attempts to Identify the Origin of the Isomerization Process.	66
III. Photoreactions of 3c with Other Disubstituted Alkenes.	71
IV. Conclusions.	72
 <u>CHAPTER FOUR- PHOTOREACTIONS OF <math>Os_3(CO)_{12}</math> WITH ALKYNES</u>	
I. Introduction.	74
II. Reaction with Dimethylacetylenedicarboxylate [DMAD]. Preparation and Characterization of $Os_2[\mu_1\text{-alkyne}]$ and an Unusual Alkyne-Linked Species.	74
III. Reactions with Other Alkynes.	95
IV. Conclusions.	101
 <u>CHAPTER FIVE- THERMAL ACTIVATION OF DIOSMACYCLES</u>	
I. Introduction.	102
II. Alkyne Exchange Reactions.	103
A. Reactions with DMAD, $C_2H_2$ , DPA.	103
B. Reaction with HFB.	106
III. Alkene Exchange Reactions.	120
IV. Phosphine Substitution Reactions.	121
V. Conclusions.	124

## CHAPTER SIX- SYNTHESIS AND COMPARATIVE STUDY OF AN IRON

### TRIAD $M(CO)_4[\eta^2\text{-ALKYNE}]$ COMPLEXES

I. Introduction.	125
II. The $M[\eta^2\text{-BTMSA}]$ Complexes.	125
A. Synthesis and Characterization of $M(CO)_4[\eta^2\text{-Me}_3\text{SiC}_2\text{SiMe}_3]$ .	125
B. Molecular Structure of 54.	127
C. Variable Temperature $^{13}\text{C}$ NMR Behaviour.	139
III. Triad Comparison of $M(CO)_4[\eta^2\text{-Me}_3\text{SiC}_2\text{SiMe}_3]$ Compounds and Nature of the $M\text{-}[\eta^2\text{-alkyne}]$ Interaction.	141
IV. Conclusions.	148

## CHAPTER SEVEN- EXPERIMENTAL PROCEDURES

I. General Techniques.	150
II. Photochemical Techniques.	150
III. Physical Measurements.	153
IV. Reagents and Reactions, Chapter Two.	154
V. Reagents and Reactions, Chapter Three.	161
VI. Reagents and Reactions, Chapter Four.	167
VII. Reagents and Reactions, Chapter Five.	176
VIII. Reagents and Reactions, Chapter Six.	187

## REFERENCES

192

## TABLE

## PAGE

I	Physical and Spectral Characteristics for $N_3(CO)_{12}$	3
II	Electronic Spectral Characterizations for $N_3(CO)_{12}$	11
III	Summary of Photoreactions of $Os_3(CO)_{12}(3c)$ with Alkenes	21
IV	Carbonyl Stretching Frequencies for $Os(CO)_4[\eta^2\text{-alkene}]$ and $Os_2(CO)_8[\mu\text{-alkene}]$	24
V	Analytical and Mass Spectral Data for $Os(CO)_4[\eta^2\text{-alkene}]$ and $Os_2(CO)_8[\mu\text{-alkene}]$	27
VI	Summary of Crystallographic Data for $Os_2(CO)_8[\mu-\eta^1, \eta^1\text{-CH}_2\text{CH(CO}_2\text{CH}_3)](14)$	28
VII	Relevant Bond Distances (Å) for $Os_2(CO)_8[\mu-\eta^1, \eta^1\text{-CH}_2\text{CH(CO}_2\text{CH}_3)](14)$	29
VIII	Selected Bond Angles (deg) for $Os_2(CO)_8[\mu-\eta^1, \eta^1\text{-CH}_2\text{CH(CO}_2\text{CH}_3)](14)$	30
IX	Relevant Torsional Angles (deg) for $Os_2(CO)_8[\mu-\eta^1, \eta^1\text{-CH}_2\text{CH(CO}_2\text{CH}_3)](14)$	31
X	$^1H$ Chemical Shifts for Complexes $Os_2(CO)_8[\mu\text{-alkene}]$	34
XI	$^{13}C$ Chemical Shifts for Complexes $Os_2(CO)_8[\mu\text{-alkene}]$	37
XII	$^1H$ Chemical Shifts for Complexes $Os(CO)_4[\eta^2\text{-alkene}]$	43
XIII	$^{13}C$ Chemical Shifts for Complexes $Os(CO)_4[\eta^2\text{-alkene}]$	44
XIV	Summary of Photoreactions of $Os_3(CO)_{12}(3c)$ with 1,2-disubstituted Alkenes	52

XV	Summary of Crystallographic Data for the Isomeric Compounds $\text{Os}_2(\text{CO})_8[\mu\text{-}\eta^1, \eta^1\text{-C}_2\text{H}_2(\text{CO}_2\text{CH}_3)_2]$	59.
XVI	Comparison of Relevant Bond Distances (Å) for the Isomeric Compounds $\text{Os}_2(\text{CO})_8[\mu\text{-}\eta^1, \eta^1\text{-C}_2\text{H}_2(\text{CO}_2\text{CH}_3)_2]$	64
XVII	Comparison of Relevant Torsional Angles (deg) for the Isomeric Compounds $\text{Os}_2(\text{CO})_8[\mu\text{-}\eta^1, \eta^1\text{-C}_2\text{H}_2(\text{CO}_2\text{CH}_3)_2]$	65
XVIII	Comparison of Relevant Bond Angles (deg) for the Isomeric Compounds $\text{Os}_2(\text{CO})_8[\mu\text{-}\eta^1, \eta^1\text{-C}_2\text{H}_2(\text{CO}_2\text{CH}_3)_2]$	67
XIX	Summary of Photoreactions of $\text{Os}_3(\text{CO})_{12}(3\text{c})$ with Alkynes	75
XX	Summary of Crystallographic Data for $\text{Os}_2(\text{CO})_8[\mu\text{-C}_2(\text{CO}_2\text{CH}_3)_2](33)$ and $\text{Os}_2(\text{CO})_6(\text{DMAD})_4(34)$	78
XXI	Relevant Bond Distances (Å) for $\text{Os}_2(\text{CO})_8[\mu\text{-C}_2(\text{CO}_2\text{CH}_3)_2](33)$	80
XXII	Relevant Bond Angles and Torsional Angles (deg) for $\text{Os}_2(\text{CO})_8[\mu\text{-C}_2(\text{CO}_2\text{CH}_3)_2](33)$	82
XXIII	Comparison of Relevant Bond Distances (Å) for the Independent Molecules of $\text{Os}_2(\text{CO})_6[\text{C}_2(\text{CO}_2\text{CH}_3)_2]_4(34)$	86
XXIV	Comparison of Relevant Bond Angles (deg) for the Independent Molecules of $\text{Os}_2(\text{CO})_6[\text{C}_2(\text{CO}_2\text{CH}_3)_2]_4(34)$	87
XXV	Some Reported Os-O Donor Bond Distances	90
XXVI	Spectral Parameters for $\text{Os}(\text{CO})_3(\text{butadiene})$ Complexes	98
XXVII	Characterization of the Isomeric Compounds $\text{Os}(\text{CO})_3[(\text{HFB})_2(\text{MA})]$	109

XXVIII	Spectral Data for Complexes $M(CO)_4[\eta^2-C_2(SiMe_3)_2]$	129
XXIX	Summary of Crystallographic Data for $Os(CO)_4[\eta^2-C_2(SiMe_3)_2](54)$	130
XXX	Relevant Bond Distances (Å) for $Os(CO)_4[\eta^2-C_2(SiMe_3)_2](54)$	131
XXXI	Selected Bond Angles (deg) for $Os(CO)_4[\eta^2-C_2(SiMe_3)_2](54)$	132
XXXII	Some Reported Structural Data for $\eta^2$ -Alkyne Complexes	134
XXXIII	Comparison of Spectroscopic and Energetic Data on Complexes $M(CO)_4[\eta^2-C_2(SiMe_3)_2]$	143
XXXIV	Drying Agents	151
XXXV	Positional and Thermal Parameters for $Os_2(CO)_8[\mu-\eta^1, \eta^1-CH_2CH(CO_2CH_3)](14)$	159
XXXVI	Positional and Thermal Parameters for $Os_2(CO)_8[\mu-\eta^1, \eta^1-Z-C_2H_2(CO_2CH_3)_2](28)$	168
XXXVII	Positional and Thermal Parameters for $Os_2(CO)_8[\mu-\eta^1, \eta^1-E-C_2H_2(CO_2CH_3)_2](30)$	170
XXXVIII	Positional and Thermal Parameters for $Os_2(CO)_8[\mu-\eta^1, \eta^1-C_2(CO_2CH_3)_2](33)$	177
XXXIX	Positional and Thermal Parameters for $Os_2(CO)_6-[C_2(CO_2CH_3)_2]_4(34)$	178
XL	Positional and Thermal Parameters for $Os(CO)_4[\eta^2-C_2(SiMe_3)_2](54)$	191

# LIST OF FIGURES

FIGURE		PAGE
I	Infrared spectra of the different stages of product isolation from the reaction of 3c with MA	23
II	Perspective view of $\text{Os}_2(\text{CO})_8[\mu-\eta^1, \eta^1-\text{CH}_2\text{CH}(\text{CO}_2\text{CH}_3)](14)$	32
III	100.6 MHz $^{13}\text{C}$ variable temperature NMR spectra for $\text{Os}(\text{CO})_4[\eta^2-\text{CH}_2\text{CH}(\text{CO}_2\text{CH}_3)](13)$	46
IV	The turnstile rotation	47
V	IR spectra for $[\eta^2\text{-DMM}]^-$ and $[\eta^2\text{-DMF}]\text{Os}(\text{CO})_4$	54
VI	Structure of $\text{Fe}(\text{CO})_3(\text{PPh}_3)[\eta^2\text{-DEM}]$	56
VII	Molecular structures of $\text{Os}_2(\text{CO})_8[\mu\text{-DMM}](28)$ and $\text{Os}_2(\text{CO})_8[\mu\text{-DMF}](30)$	61
VIII	Views of 28 and 30 looking down the C(9)-C(12) vector	63
IX	Molecular structure of $\text{Os}_2(\text{CO})_8[\mu-\eta^1, \eta^1-\text{C}_2(\text{CO}_2\text{CH}_3)_2](33)$	77
X	Molecular structure of $\text{Os}_2(\text{CO})_6(\text{DMAD})_4(34)$	84
XI	View of cyclobutane ring in 34	88
XII	The $\text{Os}(\text{CO})_3[\eta^4\text{-butadiene}]$ complexes	97
XIII	IR spectra for the thermal exchange reaction between $\text{Os}_2(\text{CO})_8[\mu\text{-MA}](14)$ and DMAD	104
XIV	376 MHz $^{19}\text{F}$ NMR spectrum of 44	108
XV	Proposed structure for 44	114
XVI	376 MHz $^{19}\text{F}$ variable temperature NMR spectra for 45	115

<u>FIGURE</u>		<u>PAGE</u>
XVII	Proposed possible structures for 45	119
XVIII	Perspective view of $\text{Os}(\text{CO})_4[\eta^2\text{-C}_2(\text{SiMe}_3)_2](54)$	128
XIX	View of 54 emphasizing the axial carbonyls bending toward the equatorial alkyne	136
XX	100.6 MHz $^{13}\text{C}$ variable temperature NMR spectra for complexes $\text{M}(\text{CO})_4[\eta^2\text{-C}_2(\text{SiMe}_3)_2]$	140
XXI	Graphical comparison of the variation in coordination shifts (IR and NMR) versus $\Delta G^\ddagger$ for carbonyl scrambling in complexes $\text{M}(\text{CO})_4[\eta^2\text{-C}_2(\text{SiMe}_3)_2]$	147
XXII	Immersion well apparatus	152

# LIST OF SCHEMES

<u>SCHEMES</u>	<u>PAGE</u>
I Thermal reactivity of $\text{Ru}_3(\text{CO})_{12}$ toward alkenes	6
II Thermal reactivity of $\text{Os}_3(\text{CO})_{12}$ with diphenylacetylene (DPA)	8
III Long wavelength photofragmentation of $\text{Ru}_3(\text{CO})_{12}$	15
IV Short wavelength photosubstitution of $\text{Ru}_3(\text{CO})_{12}$	16
V Long wavelength photobehaviour of $\text{Os}_3(\text{CO})_{12}$	18
VI Alkyne linkage at a dimetal center (Knox)	92
VII Alkyne linkage at a dimetal center (Green)	93
VIII Proposed formation of 34	94
IX Homo- and heteronuclear $^1\text{H}$ and $^{19}\text{F}$ couplings for 44	112
X Assignment of olefinic and trifluoromethyl carbons from $^{13}\text{C}$ ( $^{19}\text{F}$ ) experiments for 45	117
XI Proposed fragmentation of $\text{Os}_2[\mu\text{-alkene}]$ induced by $\text{PPh}_3$	122
XII Proposed orbital interaction to account for axial carbonyl bending	138
XIII The coupled alkyne rotation - Berry pseudorotation	142



# LIST OF ABBREVIATIONS

AA	acrylic acid, $\text{CH}_2=\text{CHCO}_2\text{H}$
br	broad
<sup>t</sup> Bu	tert-butyl, $\text{C}(\text{CH}_3)_3$
BTMSA	bis(trimethylsilyl)acetylene, $\text{C}_2(\text{Si}(\text{CH}_3)_3)_2$
cis-COE	cis-cyclooctene, $\text{C}_8\text{H}_{14}$
DEF	diethyl fumarate, $\text{E}-\text{C}_2\text{H}_2(\text{CO}_2\text{CH}_2\text{CH}_3)_2$
DEM	dimethyl maleate, $\text{Z}-\text{C}_2\text{H}_2(\text{CO}_2\text{CH}_3)_2$
DMAD	dimethylacetylenedicarboxylate, $\text{C}_2(\text{CO}_2\text{CH}_3)_2$
DMF	dimethyl fumarate, $\text{E}-\text{C}_2\text{H}_2(\text{CO}_2\text{CH}_3)_2$
DMM	dimethyl maleate, $\text{Z}-\text{C}_2\text{H}_2(\text{CO}_2\text{CH}_3)_2$
DPA	diphenylacetylene, $\text{C}_2(\text{C}_6\text{H}_5)_2$
EA	ethyl acrylate, $\text{CH}_2=\text{CHCO}_2\text{CH}_2\text{CH}_3$
Et	ethyl
HFB	hexafluoro-2-butyne, $\text{C}_2(\text{CF}_3)_2$
m	medium
MA	methyl acrylate, $\text{CH}_2=\text{CHCO}_2\text{CH}_3$
MAH	maleic anhydride, $\text{CH}=\text{CHC}(\text{O})\text{OC}(\text{O})$
MCD	magnetic circular dichroism
Me	methyl
MLCT	metal-to-ligand charge transfer
MVK	methyl vinyl ketone, $\text{CH}_2=\text{CHC}(\text{O})\text{CH}_3$
OFB	octafluoro-2-butene, $\text{CF}(\text{CF}_3)=\text{CF}(\text{CF}_3)$
	parallel
Ph	phenyl

LIST OF ABBREVIATIONS (continued)

s	sharp
TFE	tetrafluoroethylene, $C_2F_4$
THF	tetrahydrofuran, $C_4H_8O$
TLC	thin layer chromatography
3P2O	3-penten-2-one, $CH(CH_3)=CHC(O)CH_3$
TMS	tetramethylsilane, $Si(CH_3)_4$
Ts	para-tosylate, $p-OSO_2C_6H_4CH_3$
w	weak

## CHAPTER ONE

### INTRODUCTION

#### I. Brief History of Iron-group Carbonyls.

The binary carbonyl derivatives of iron, ruthenium and osmium constitute an excellent example of the regular trends observed within transition-metal sub-groups.

In keeping with the tendency of first-row transition-metal elements to form mononuclear compounds,  $\text{Fe}(\text{CO})_5$  (1a) is the most common binary carbonyl of iron. The compound is easily obtained<sup>1a</sup> and it is the starting material of choice for further chemistry.<sup>1b</sup> 1a can be converted to the other iron carbonyls,  $\text{Fe}_2(\text{CO})_9$  (2a)<sup>2</sup> and  $\text{Fe}_3(\text{CO})_{12}$  (3a).<sup>1c</sup>

However, the most stable (and consequently most studied) carbonyls of ruthenium and osmium are the trinuclear cluster compounds  $\text{M}_3(\text{CO})_{12}$  (M=Ru, 3b; Os, 3c). It is now known that the increase in metal-metal bond strength accounts for this feature. This was not recognized in earlier times. The high temperature and high pressure reaction of  $\text{OsO}_4$  with CO, said to produce  $\text{Os}(\text{CO})_5$  (1c) which, under these conditions, decarbonylated to form  $\text{Os}_2(\text{CO})_9$  (2c).<sup>3</sup> The formulation was based on elemental analysis of the yellow crystals obtained from the reaction and the previously known preparation of  $\text{Fe}_2(\text{CO})_9$  (2a) from 1a.<sup>4</sup> The issue was resolved in 1962<sup>5</sup> when the crystal structure of  $\text{Os}_3(\text{CO})_{12}$  (3c), the yellow solid obtained from the carbonylation of  $\text{OsO}_4$ , was determined and showed the triangular arrangement of the osmium atoms each surrounded by four carbonyl ligands. Since then, 2c has been obtained as a thermally unstable yellow solid.<sup>6</sup> Interestingly, 3b also was mistaken as the enneacarbonyl derivative  $\text{Ru}_2(\text{CO})_9$ , which has proven to be even more unstable than 2c.<sup>6</sup>

## II. Physical and Spectral Characteristics of $\text{Os}_3(\text{CO})_{12}(\underline{3c})$ .

$\text{Os}_3(\text{CO})_{12}(\underline{3c})$  can be prepared in high yields by the high temperature, high pressure carbonylation of  $\text{OsO}_4$  in methanol.<sup>7</sup> The compound is a yellow crystalline solid which is sparingly soluble in hydrocarbon solvents and slightly more soluble in  $\text{CH}_2\text{Cl}_2$ , THF and benzene.  $\underline{3c}$  can be purified by sublimation in vacuo at  $130^\circ\text{C}$  or by recrystallization from hot benzene.

Some of the spectral characteristics for  $\underline{3c}$  are collected in Table I, along with those for  $\underline{3a}$  and  $\underline{3b}$  for comparison. The four carbonyl stretching frequencies obtained for  $\underline{3c}$  can be assigned<sup>8</sup> based on the observed  $D_{3h}$  symmetry<sup>5</sup> of the molecule. The same analysis has been made for  $\underline{3b}$ , whereas the Fe trimer  $\underline{3a}$  exhibits two bands in the bridging carbonyl region, consistent with the observed  $C_{2v}$  symmetry of the molecule.<sup>1d</sup> The  $^{13}\text{C}$  NMR spectrum of  $\underline{3c}$  shows two carbonyl signals of equal intensity, one each for the axial and equatorial carbonyl ligands<sup>9a</sup>, as suggested by the solid state structure.

Coalescence of these resonances occurs at  $156^\circ\text{C}$  whereas a single resonance is observed for  $\underline{3a}$ <sup>9a,b</sup> and  $\underline{3b}$ <sup>9a</sup> down to the lowest recorded temperatures. Carbonyl scrambling, which proceeds either by an axial-equatorial exchange or exchange through a bridged intermediate<sup>9c</sup>, is clearly a much higher energy process in  $\underline{3c}$  than in  $\underline{3a}$  or  $\underline{3b}$ .

Mass spectrometry has given great insight into the relative strengths of the cluster compounds. Under positive electron impact,<sup>10</sup> the parent isotope pattern for  $\underline{3c}$  centered at 908 m/e was observed and this was followed by the subsequent loss of twelve carbonyl ligands to give the  $\text{Os}_3^+$  ion (100% relative abundance) and no lower nuclearity

Table I. Physical and Spectral Characteristics for  $M_3(CO)_3$

		M	
		Fe, 3a	Os, 3c
		green-black	yellow
mp		sublimes 70°C/0.4 mm Hg	sublimes 130°C/0.01 mm Hg
IR <sup>a</sup>		2046(s), 2023(m), 2013(sh) 1867(vw), 1835(w) <sup>b,d</sup>	2070(vs), 2037(vs), 2017(m) 2007(m) <sup>c,d</sup>
<sup>13</sup> C NMR <sup>e</sup>		212.9 o (-150°C) <sup>f,8</sup>	182.3, 170.4 (22°C) <sup>f</sup>
Mass spec		$Fe_3(CO)_n^+$ n=2-7,10 $Fe(CO)^+$ 100% <sup>h,i</sup>	$Os_3(CO)_n^+$ n=0-12 $Os_3^+$ 100% <sup>j</sup>

a)  $cm^{-1}$ ; b) n-hexane; c) isooctane; d) ref. 21; e) ppm downfield from TMS; f) ref. 9a;

g) ref. 9b; h) ref. 11; i) mononuclear and dinuclear fragments also; j) ref 10.

fragments. For  $3b$ , the  $Ru_3^+$  ion was again the most abundant fragment, but both mononuclear and dinuclear fragments were seen also.<sup>11</sup>  $Fe(CO)^+$  was the highest abundance species from  $3a$ .<sup>11</sup> The inherently greater metal-metal bond strength of  $3c$  over  $3a$  and  $3b$  is manifested in reactivity studies which will be highlighted below.

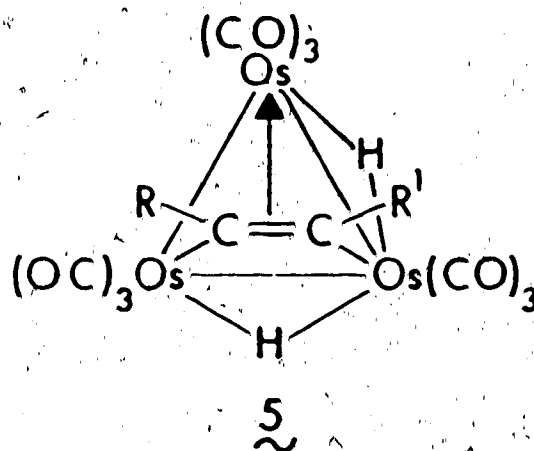
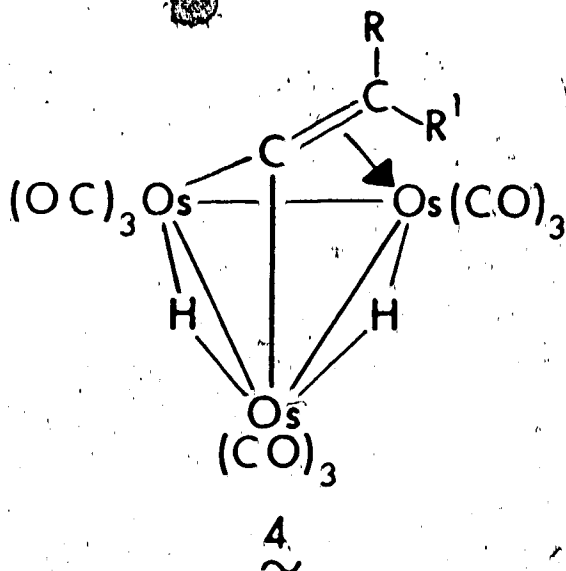
### III. Reactivity of $Os_3(CO)_{12}(3c)$ .

The stability of  $3c$  and that of its derivatives quickly established the molecule as an appealing source for reactivity studies. The initial investigations by Bradford and Nyholm<sup>12</sup> lead to a virtual explosion of studies, from which thousands of compounds are known.<sup>13</sup>

It is not the purpose here to give a comprehensive review of the existing literature concerning the reactivity of  $3c$ . More pertinent to the present study is an overview of the thermal reactivity and photobehaviour of  $3c$  towards alkenes and alkynes.

#### A. Thermal Reactions of $3c$ with Alkenes and Alkynes.

It was clear from the onset that the robustness of the trinuclear osmium cluster would dictate its thermal chemistry. The integrity of the cluster has been consistently maintained in its reactions with alkenes. Under moderate conditions, products from these reactions are of the type  $4$  arising from 1,1-dehydrogenation of terminal olefins and/or the type  $5$  due to 1,2-dehydrogenation of terminal<sup>15</sup> and cyclic<sup>14,16</sup> olefins. 1-octene is the only alkene to give examples of both structures ( $4c$  and  $5a$ ). More extreme conditions give way to cluster aggregation.<sup>17</sup> Contrary to this,  $3a$  has been shown to be an effective isomerization catalyst for terminal olefins<sup>18-22</sup>, from which mononuclear products have been isolated<sup>22</sup> or inferred<sup>19</sup> to arise from



$R = R' = H$  (a)<sup>14</sup>

$R = H, R' = C_6H_{13}$  (a)<sup>15</sup>

$R = H, R' = CH_3$  (b)<sup>14</sup>,  $C_6H_{13}$  (c)<sup>15</sup>

$R = R' = C_3H_6$  (b)<sup>14</sup>,  $C_4H_4$  (c)<sup>14</sup>

$R = Me, R' = Ph$  (d),  $CH_2CHMe_2$  (e),

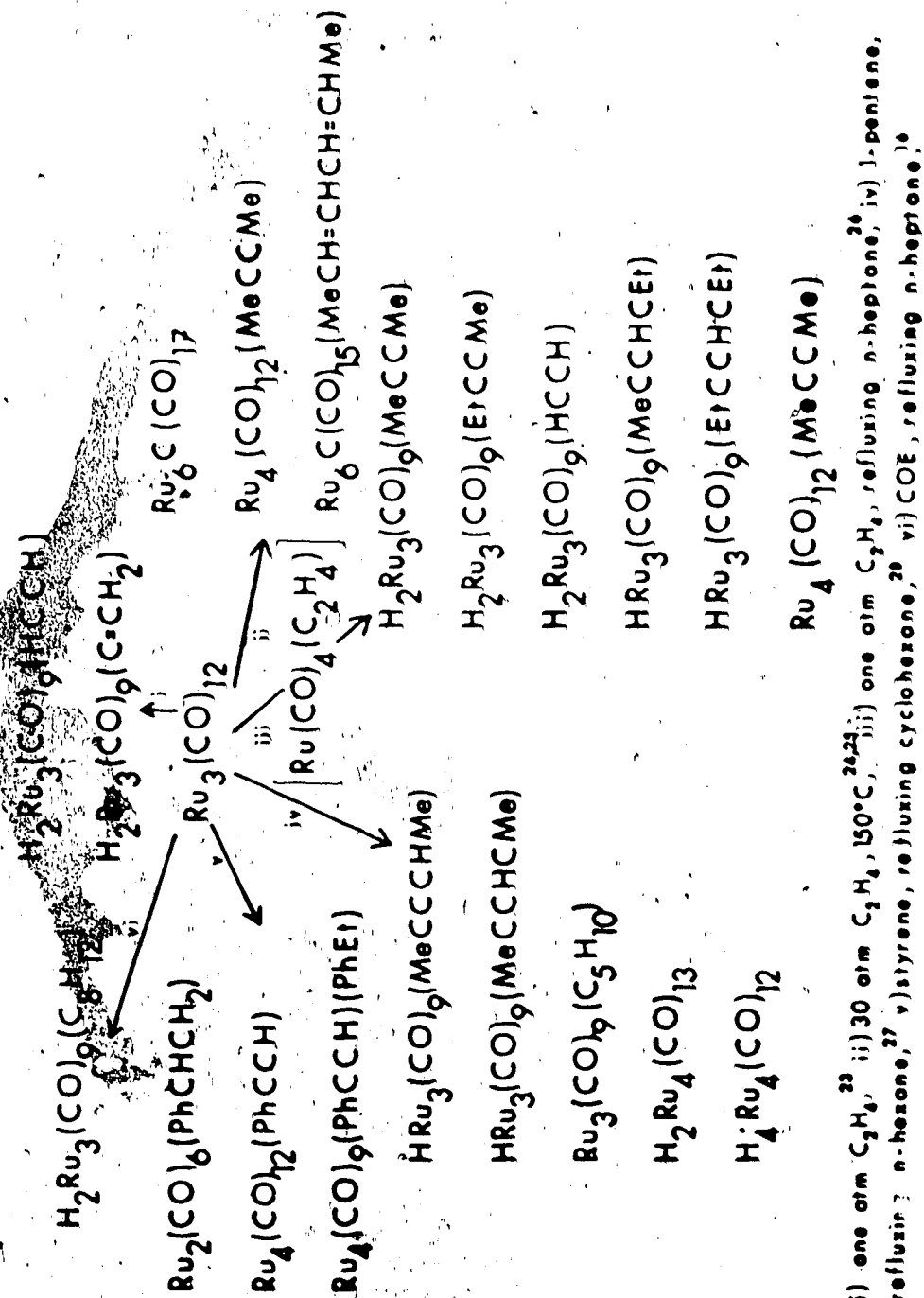
$C_6H_{12}$  (d)<sup>16</sup>

$CHMe_2$  (f)<sup>15</sup>

cluster decomposition. Scheme I outlines the great variety of products from the thermal reactions of 3b with alkenes.<sup>16,23-28</sup> With the observation of  $Ru(CO)_4(C_2H_4)$  generated under mild conditions<sup>26</sup>, it is clear that the obtained products are formed via cluster fragmentation, a feature not observed for 3c.

The thermal reactivity of 3c with alkynes results in a rich derivative chemistry. A recent review<sup>29</sup> and a much earlier one<sup>30</sup> have extensively covered this topic. Only one of the more interesting series of studies will be highlighted here.

The most extensively studied reaction has been with diphenylacetylene [DPA]. The thermal chemistry of 3c and its DPA derivatives



Scheme 1. Thermal reactivity of  $\text{Ru}_3(\text{CO})_{12}$  toward alkenes.



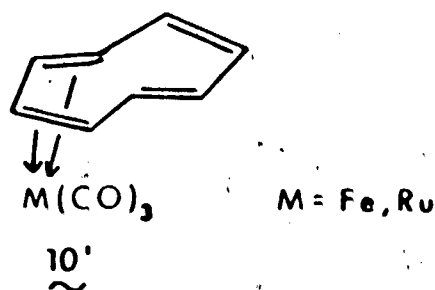
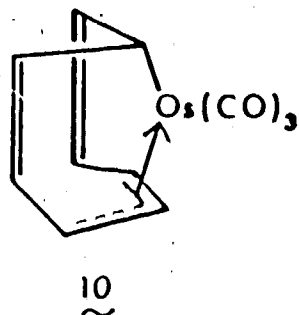
investigations. These studies have also vindicated the stability of the triosmium framework (Scheme II). Compound  $8^{33,35}$  is the final trinuclear substitution product in the series. Further treatment with DPA fragments the cluster and gives mono- and dinuclear compounds and cyclotrimerized DPA, hexaphenylbenzene.<sup>33</sup> Cluster breakdown occurs more readily with  $3a$  and  $3b$  under similar conditions. Six iron-alkyne derivatives are obtained from  $3a$  and DPA, of which only the violet isomer of  $Fe_3(CO)_8[DPA]_2$  is a cluster compound.<sup>37</sup> The same reaction with  $3b$  afforded the isolation of nine alkyne derivatives, including mono-, di-, and trinuclear species.<sup>38</sup>

A number of other studies involving internal<sup>39-41</sup> and terminal<sup>41-43</sup> alkynes have been carried out. In most cases, the major products derive from substitution on the intact trinuclear framework. In references 29 and 30, the variety of compounds available from  $3a$  and  $3b$  and other alkynes lends further credence to the greater metal-metal bond strength in  $3c$  over its Fe and Ru analogues.<sup>44</sup>

#### B. Photochemical Behaviour of $3c$ .

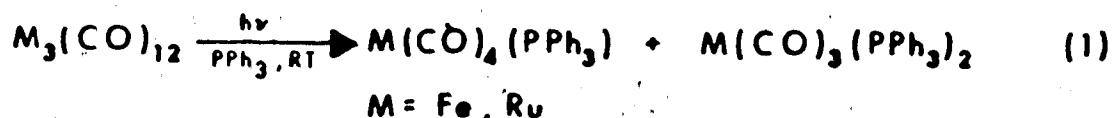
The photoreactivity of  $3c$  towards unsaturated organic substrates is a largely neglected field. Prior to the present study only a limited number of reports appear to have dealt with this area.<sup>21,39,45-47</sup> In every case, the sole product of the photoreaction was a mononuclear species containing an  $Os(CO)_3$  unit. The photoreaction of  $3c$  with cyclo-octatetraene yielded a species with the unusual 1-3,6- $\eta$  bonding mode of the organic moiety  $(10)^{39}$  in contrast to the common 1-4- $\pi$  mode previously observed for the iron<sup>48</sup> and ruthenium<sup>49</sup> analogues  $(10')$ .



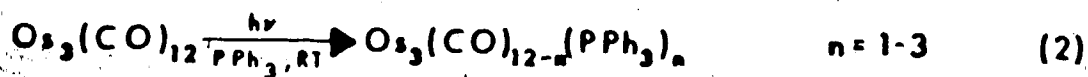


In an interesting reaction, the photolysis of 3c with 1,5-cyclooctadiene afforded some  $\text{Os}(\text{CO})_3[\eta^4\text{-}1,3\text{-cyclooctadiene}]$ .<sup>45</sup> However, the reaction of simple alkenes had only been attempted in an effort to clarify the photocatalytic role of 3c in alkene isomerization.<sup>21</sup>

In a comparative study of the three iron-group carbonyl clusters<sup>21</sup>, 3c showed the least activity towards isomerization of 1-pentene. This result parallels the ease of photofragmentation of the trinuclear compounds, a conclusion which has the support of subsequent studies from the photoreactions of  $\text{M}_3(\text{CO})_{12}$  with  $\text{CO}$ <sup>21,50,51,53,54</sup>,  $\text{PPh}_3$ <sup>21,50-52</sup> and alkenes.<sup>21,51,53,55,56</sup> 1a and 1b were obtained upon irradiation of 3a and 3b under  $\text{CO}$ <sup>21,51,53,54</sup> whereas they react with  $\text{PPh}_3$ <sup>21,51,52</sup> according to equation (1).



Alkenes also have given monosubstituted<sup>21,51,53,55</sup> and disubstituted<sup>56</sup> mononuclear products. Under similar reaction conditions, 1c was not formed<sup>21,50</sup> and substitution on 3c by  $\text{PPh}_3$  is the preferred mode of reaction [equation (2)]<sup>21,50</sup> (Exhaustive photolysis of 3c with



$\text{PPh}_3$  generated  $\text{Os}(\text{CO})_3(\text{PPh}_3)_2$ <sup>50</sup>.

This difference in photochemistry, especially between 3b and 3c, has led to investigations by several groups<sup>57-62</sup> into the electronic structure of the trinuclear clusters. Although there is general agreement that the electronic structure of 3b and 3c is similar and that the first electronic absorptions involve depopulation of the metal-metal bonding levels, some ambiguities remain.

In an early report,<sup>57</sup> the two lowest-lying transitions were identified as  $\sigma \rightarrow \sigma^*$  and  $\sigma^* \rightarrow \sigma^*$  in nature. It was concluded on inspection of electronic and MCD data (Table II) that the ordering of the corresponding MO's for 3b and 3c is different, leading to the energy level diagrams depicted below. The frontier orbitals  $xz$  and  $z^2$

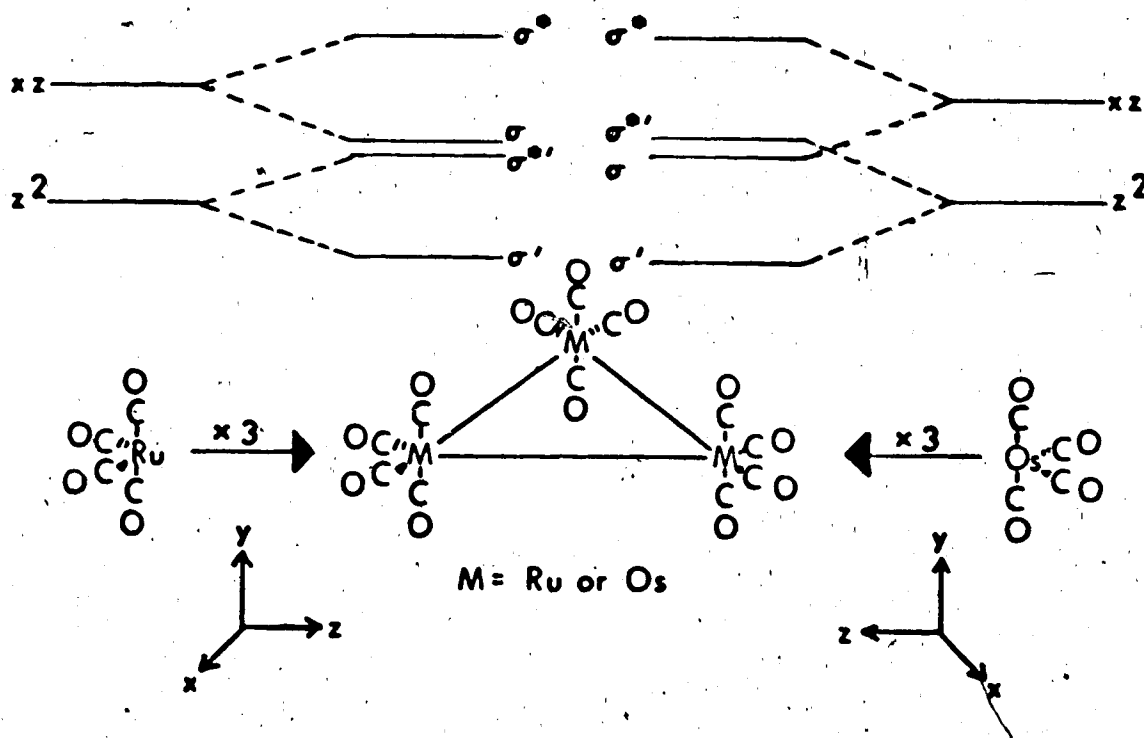


Table II. Electronic Spectral Characterizations for  $M_3(CO)_{12}$

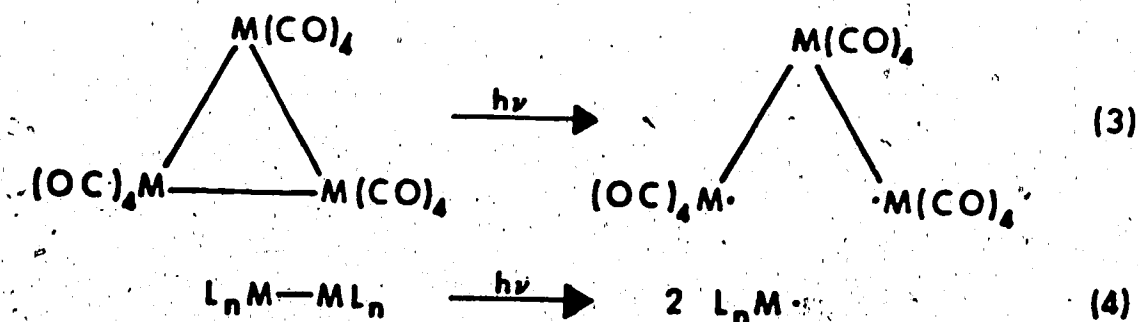
M	298K (isooctane) <sup>a</sup>		300K (2-methylpentane) <sup>b</sup>		MCD	assignment
	$\lambda_{max}, nm$	$\epsilon_M \times 10^{-4} c$	$\lambda_{max}, nm$	$\epsilon_M \times 10^{-4} c$	A term	
Fe	603	0.29	602	0.32	d	$d \rightarrow \sigma^*$ $\sigma \rightarrow \sigma$
	440 sh	0.24	437 sh 360 sh 310 sh 263			MLCT
3a	315 sh 275 sh 192	1.24 1.77 >7.00				
Ru	395	0.77	390	0.64	379 305	$d \rightarrow \sigma^*$ $\sigma \rightarrow \sigma$ MLCT
	268 sh 239 203 sh	2.70 3.55 4.80	320 sh 270 sh 238	3.50		
Os	385	0.37	385 sh	0.36	385	$d \rightarrow \sigma^*$ $\sigma \rightarrow \sigma$
3c	329 288 sh 244	0.93 0.85 2.60	330 280 sh 240	0.86 2.48	327	MLCT

a) ref. 21; b) ref. 57; c)  $L \text{ mol}^{-1} \text{ cm}^{-1}$ ; d) not given.

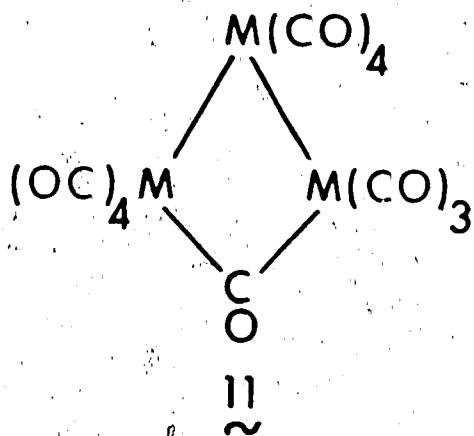
interact to form the cluster orbitals  $\sigma$ ,  $\sigma^*$ ,  $\sigma$  and  $\sigma^*$ . The greater strength of the metal-metal bonding in  $3c$ <sup>44</sup> was suggested to cause greater bonding-antibonding energy splitting, moving the  $\sigma^*$  level above the  $\sigma$  level. The dipole forbidden  $\sigma^* \rightarrow \sigma^*$  transition should be the weaker of the two transitions.<sup>62</sup> The observation of weak bands at relatively different energies for the two trimers bolsters the argument.<sup>21,57</sup>

However, Ellis, Trogler, et al.<sup>62</sup>, through  $X_\alpha$  calculations and He I Photoelectron Spectroscopy, have determined that the same forbidden transition should occur at a lower energy than previously reported.<sup>21,57</sup> As a result, this transition is unobserved in their experiments. They have also suggested that the  $\sigma^*$  level decreases rather than increases in energy with respect to the  $\sigma$  level in going from  $3b$  to  $3c$ . Also as a result of their calculations and experiments, the absolute assignment of the two lowest energy transitions remained ambiguous due to the close degeneracy of the two highest occupied molecular orbitals.

Kinetic studies of the photofragmentation process of  $M_3(CO)_{12}$  have begun to address this disparity. It had been assumed that the primary photoproduct was a diradical species [equation (3)]<sup>21</sup>, based on the photoreactions of dinuclear metal carbonyls [equation (4)]<sup>63</sup>.



Radical-trapping studies for  $3b$ <sup>53,54</sup> and  $3c$ <sup>50</sup> have cast doubt on the photoinduced homolytic fission of one metal-metal bond. Low disappearance quantum yields (0.002<sup>53,54</sup> and 0.001<sup>50</sup> respectively) and the inability to detect  $M_3(CO)_{12}Cl_2$  from reactions with  $CCl_4$  suggested that a non-radical, reactive isomer of  $M_3(CO)_{12}$  should be considered as a plausible intermediate in the photoreaction. The proposed isomer (11) features a site of coordinative unsaturation created by the



migration of a terminal carbonyl ligand across a concomitantly severed metal-metal bond. Fragmentation to products is possible by trapping this isomer with two-electron donors, or, it can quickly revert to starting material.<sup>53,54</sup> Very recently, more extensive investigations have appeared<sup>58-66</sup> which deal with the photochemical behaviour in greater detail.

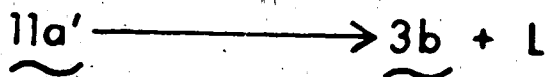
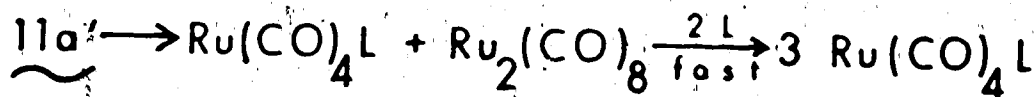
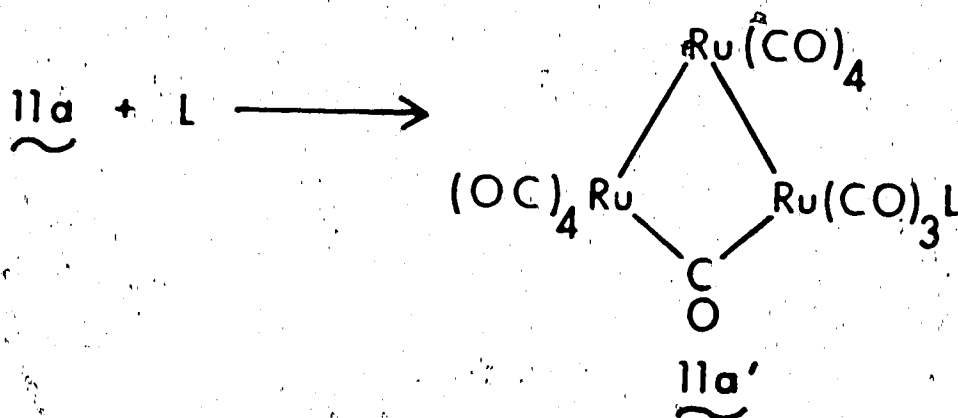
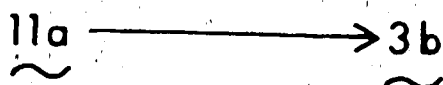
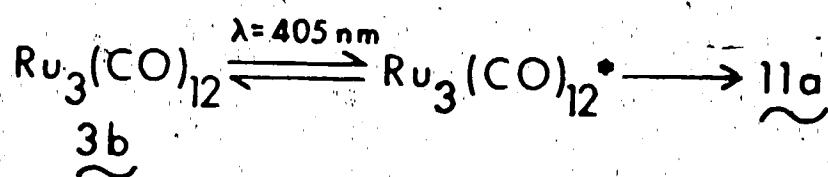
Ford, et al.<sup>64,65</sup> reported that the photoreactivity of  $3b$  is both solvent and wavelength dependent. Photofragmentation is dominant for long wavelength ( $\lambda \sim 405$  nm) irradiation under a CO atmosphere or with  $P(OMe)_3$  or  $PPh_3$ , but it can be quenched by hard donor ligands (solvents) like THF, diglyme and cyclohexene. As well,  $Ru(CO)_5(2b)$  is the initial photoproduct of  $3b$  with CO even in the presence of

$\text{CCl}_4$ . This gives further support to earlier suggestions<sup>53,54</sup> that a diradical intermediate does not form. Based on these results and further evidence from flash photolysis experiments, Scheme III was devised.<sup>65</sup> The coordinatively unsaturated metal center of  $11a$  can accept a two-electron donor to give  $11a'$ . This second intermediate can lose  $L$  to reform  $3b$  or fragment to products with subsequent ligand addition.

Upon shorter wavelength ( $\lambda \sim 313 \text{ nm}$ ) excitation of  $3b$  and  $\text{P(OMe)}_3$  or  $\text{PPh}_3$  in the presence of THF (a photofragmentation quencher), tetra- or trisubstitution of the intact cluster ultimately resulted.<sup>65</sup> It was also discovered that fragmentation and substitution can compete in octane solution to give mixtures of mononuclear and cluster products. The importance of THF in this reaction supports the proposal that CO dissociation is the primary step. That THF is instrumental in stabilizing a reactive form of  $12a$  ( $11a'$  with  $L=\text{THF}$ ) allows for substitution to occur via Scheme IV.<sup>65</sup>

In a separate study<sup>66</sup> on  $3c$ , photofragmentation and photosubstitution were shown to be uniquely dependent on the ligand, and are assumed to occur via the same intermediate. The initial photoreaction generates an excited  $\text{Os}_3(\text{CO})_{12}^*$  which converts to the chemically reactive species  $11b$ , the Os analog of  $11a$ . This species then can accept a ligand  $L$  to give the corresponding  $11b'$ . Depending on the nature of  $L$ , a number of deactivation steps are possible. When  $L = \text{phosphorus}$ , cluster substitution occurs as in the short wavelength photolysis of  $3b$ . It is interesting to note that contrary to an earlier report<sup>50</sup>, no mononuclear products were observed. Fragmentation occurs when  $L = 1\text{-octene}$ ,

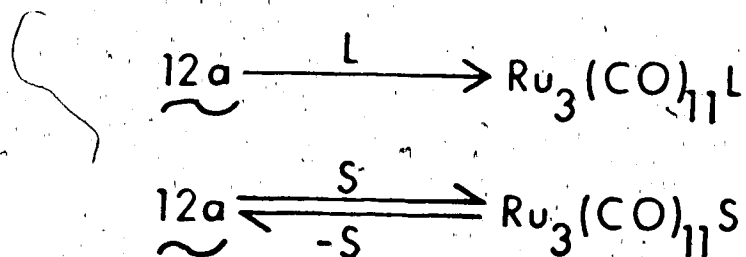
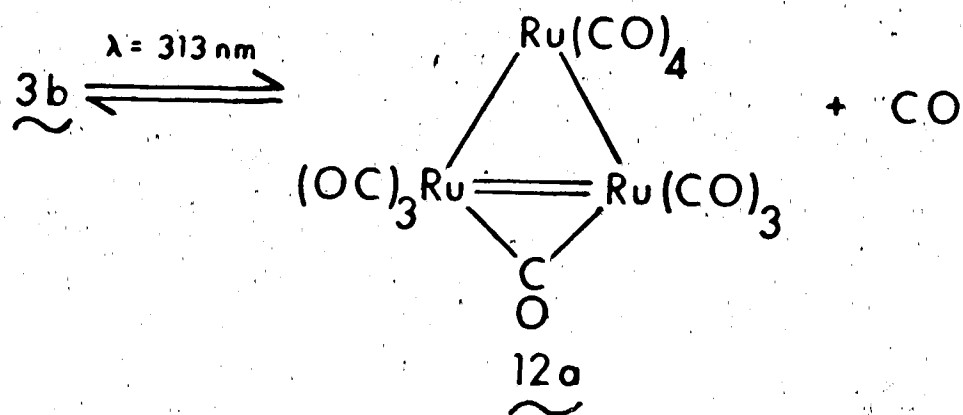




$\text{L} = \text{CO}, \text{C}_2\text{H}_4, \text{activated alkenes}, \text{P donors}$

Scheme III. Long wavelength photofragmentation of  $\text{Ru}_3(\text{CO})_{12}$

(adapted from Ford, et al.<sup>65</sup>).



$\text{L} = \text{P(OMe)}_3, \text{PPh}_3 \quad \text{S} = \text{THF}$

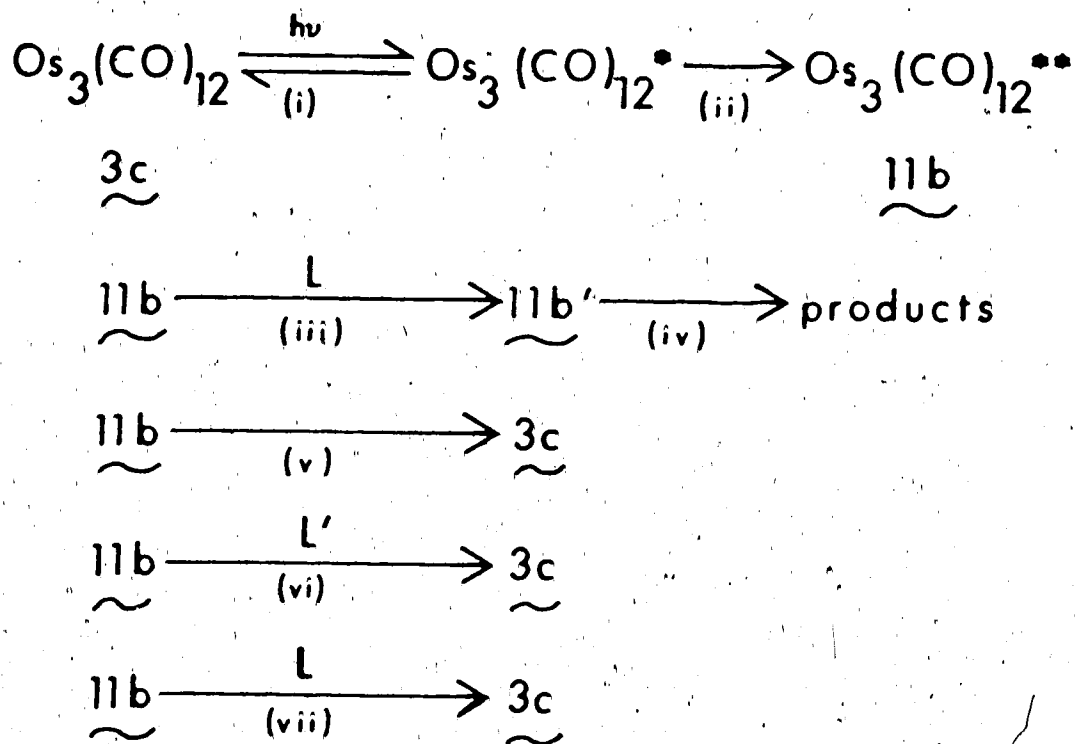
Scheme IV. Short wavelength photosubstitution of  $\text{Ru}_3(\text{CO})_{12}$   
 (adapted from Förd, et al.<sup>65</sup>).

which agrees with previous studies with polyalkenes<sup>39,45-47</sup> and the results to be presented in this Thesis. However, the products are uniquely different from those obtained in experiments with polyolefins, and discussion of this aspect is deferred until Chapter Two. As well, **L** can cause reversion of **11b** back to **3c**. Reversion of **11b** to starting material also can be brought about by spontaneous deactivation or by intervention of a Lewis base (like diglyme). An overall depiction of the photobehaviour of **3c** is summarized by Scheme V.

The difference in photoreactivity between **3b** and **3c** appears to be the ease with which photofragmentation occurs with **3b**. This is most plausibly due to differences in metal-metal bond strengths, an argument previously entertained to account for features of the thermal chemistry of the clusters. As will be seen in Chapter Two, the greater metal-metal bond strength in **3c** will profoundly influence the products obtained from the photofragmentation of **3c** in the presence of alkenes.

#### IV. Scope of the Present Research.

The initial impetus for the present study derived from the observation of facile and virtually quantitative formation of tetracarbonyl-alkene ruthenium complexes via the photolysis of **3b** with alkenes.<sup>55</sup> Similar compounds of osmium with a variety of alkenes would complete the series of  $M(CO)_4[\eta^2\text{-alkene}]$  derivatives for the iron triad and afford informative comparative studies. As well, no photochemical studies of **3c** with monoalkenes had reported the isolation of osmium-containing products at the onset of this research.<sup>21</sup> During the course of this present study, two other groups<sup>66,67</sup> communicated their results of photoreactions between **3c** and alkenes.



- (i) photoexcitation (436 nm)
- (ii) conversion to chemically reactive intermediate
- (iii) reaction with L = P donors, 1-octene
- (iv) substitution (P donors) or fragmentation (1-octene)
- (v) spontaneous reversion
- (vi) relaxation by added Lewis base (i.e. diglyme)
- (vii) relaxation by L

Scheme V. Long wavelength photobehaviour of  $\text{Os}_3(\text{CO})_{12}$   
 (adapted from Poë, et al.<sup>66</sup>).

As a result of the success with alkenes, the photolysis of 3c with a variety of alkynes was attempted in an effort to obtain compounds analogous to those derived from alkenes. As will be discussed in later Chapters, this goal was achieved in a limited sense. The photochemical reactions were complicated with products often emulating those obtained from the thermal activation of 3c.

3100/12 TOWARDS ALKENES. UNEXPECTED FORMATION  
OF DIOSMACYCLOBUTANES  $\text{Os}_2(\text{CO})_8[\mu-\eta^1, \eta^1\text{-CHRCHR}']$

I. Introduction.

In Chapter One, it was shown that efforts to exploit the photochemistry of  $\text{Os}_3(\text{CO})_{12}(\text{3c})$  with unsaturated substrates met with marginal success. In addition, photophysical studies indicated that photofragmentation of  $\text{3c}$  was an unfavourable process. It was not surprising that further synthetic studies via the photoactivation of  $\text{3c}$  were held back.

The results of photochemical reactions of  $\text{3c}$  with a variety of alkenes (Table III) are presented here. Based on the obtained products, the question of the photofragmentation of  $\text{3c}$  will be addressed. During the course of this work, two reports appeared describing the photo-reaction of  $\text{3c}$  with 1-octene<sup>66</sup> and 5,6-dimethylidene-7-oxabicyclo-[2.2.2]hept-2-ene.<sup>67</sup>

II. Reaction of  $\text{3c}$  with Methyl Acrylate.

For the initial investigations, the choice of methyl acrylate [MA] was dictated by two considerations. First, it is well-recognized that electron-withdrawing substituents activate alkenes toward transition metal complex formation, examples of which are presently available in the moderately stable iron<sup>68</sup> and ruthenium<sup>55</sup> tetracarbonyl-methyl acrylate derivatives. Second, the reasonable volatility of MA should facilitate isolation of prospective osmium complexes, especially since large excesses of alkene are usually used.

Table III. Summary of Photoreactions of  $\text{Os}_3(\text{CO})_{12}(\underline{3c})$  with Alkenes.

	Mass of		reaction time(h)	Yields of	
	$\underline{3c}$ (mg)	alkene(g)		$\text{Os}(\text{CO})_4[\eta^2\text{-alkene}]$ mg(%)	$\text{Os}_2(\text{CO})_8[\mu\text{-alkene}]$ mg(%)
MA	500.0	4.11	5.5	$\underline{13}$ , 150.0 (65)	$\underline{14}$ , 200.0 (48)
MA <sup>*</sup>	500.0	4.11	5	$\underline{13}$ , not isolated	$\underline{14}$ , 285.6 (69)
$\text{C}_2\text{H}_4$	307.0	purge	3	$\underline{15}$ , benzene solution	$\underline{16}$ , 107.0 (50)
$\text{C}_2\text{H}_4$ <sup>*</sup>	513.6	purge	2	$\underline{15}$ , benzene solution	$\underline{16}$ , 197.0 (55)
$\text{C}_3\text{H}_6$	502.0	purge	2	$\underline{17}$ , benzene solution	$\underline{18}$ , unstable
cis-COE	508.0	6.09	5.5	$\underline{19}$ , unstable	N/O
EA	441.0	8.32	4	$\underline{20}$ , unstable	$\underline{21}$ , 212.0 (62)
AA	513.0	3.99	7	$\underline{22}$ , 116(mixture)	$\underline{23}$ , 116(mixture)
MVK	521.0	8.42	6	$\underline{24}$ , not isolated	$\underline{25}$ , 11.0 (3)
3P2O	427.0	3.97	13	$\underline{26}$ , < 20.0 impure	N/O
TFE <sup>†</sup>	103.2	1.00	24	N/O	N/O
OFB <sup>†</sup>	105.0	1.20	20	N/O	N/O
MAH	511.0	6.06	24	N/O	N/O

All reactions carried out with photoapparatus (1), except (\*) photoapparatus (3) and (†) photoapparatus (2a). MA-methyl acrylate, cis-COE-cis-cyclooctene, EA-ethyl acrylate, AA-acrylic acid, MVK-methyl vinyl ketone, 3P2O-3-penten-2-one, TFE-tetrafluoroethylene, OFB-octa (or per-)fluoro-2-butene, MAH-maleic anhydride. N/O=not observed.

of excess MA resulted in relatively rapid (ca. 6 hr) consumption of 3c and in IR changes somewhat reminiscent of the formation of carbonyl-alkene type complexes. Following the removal of volatiles, an IR spectrum of the pentane extract of the resulting solid residue showed a complicated set of  $\nu_{\text{CO}}$  bands (Figure Ia). Splitting of the high frequency peak in conjunction with the appearance of two closely spaced carboxylate  $\nu_{\text{CO}_2}$  bands indicated the presence of at least two compounds. The anticipated  $\text{Os}(\text{CO})_4[\eta^2\text{-MA}]$  molecule was expected to show four terminal carbonyl bands, one above  $2100\text{ cm}^{-1}$ , on the basis of the known iron<sup>68</sup> and ruthenium<sup>55</sup> complexes. Initially, it was postulated that the mixture consisted of the osmium derivate with the remaining three  $\nu_{\text{CO}}$  bands due to another species, perhaps tricarbonyl in nature. Separation of the mixture was effected by cooling the pentane solution which caused precipitation of clear, pale yellow crystals whose IR spectrum proved both puzzling and misleading (Figure Ib). The great similarities between the spectra of the original pentane solution and the solid suggested a mixture of compounds still. Slight variations in the spectra were ascribed to changing concentrations of the two species until repeated fractional crystallizations of the solid left a mother liquor which displayed four major terminal carbonyl bands (Figure Ic.). The pattern and intensity distribution (Table IV) was consistent with the anticipated  $\text{Os}(\text{CO})_4[\eta^2\text{-MA}]$  (13), but the band positions were marginally different from any seen in the spectrum of the precipitate. Inescapably the last observation implied that either the solid "mixture" contained



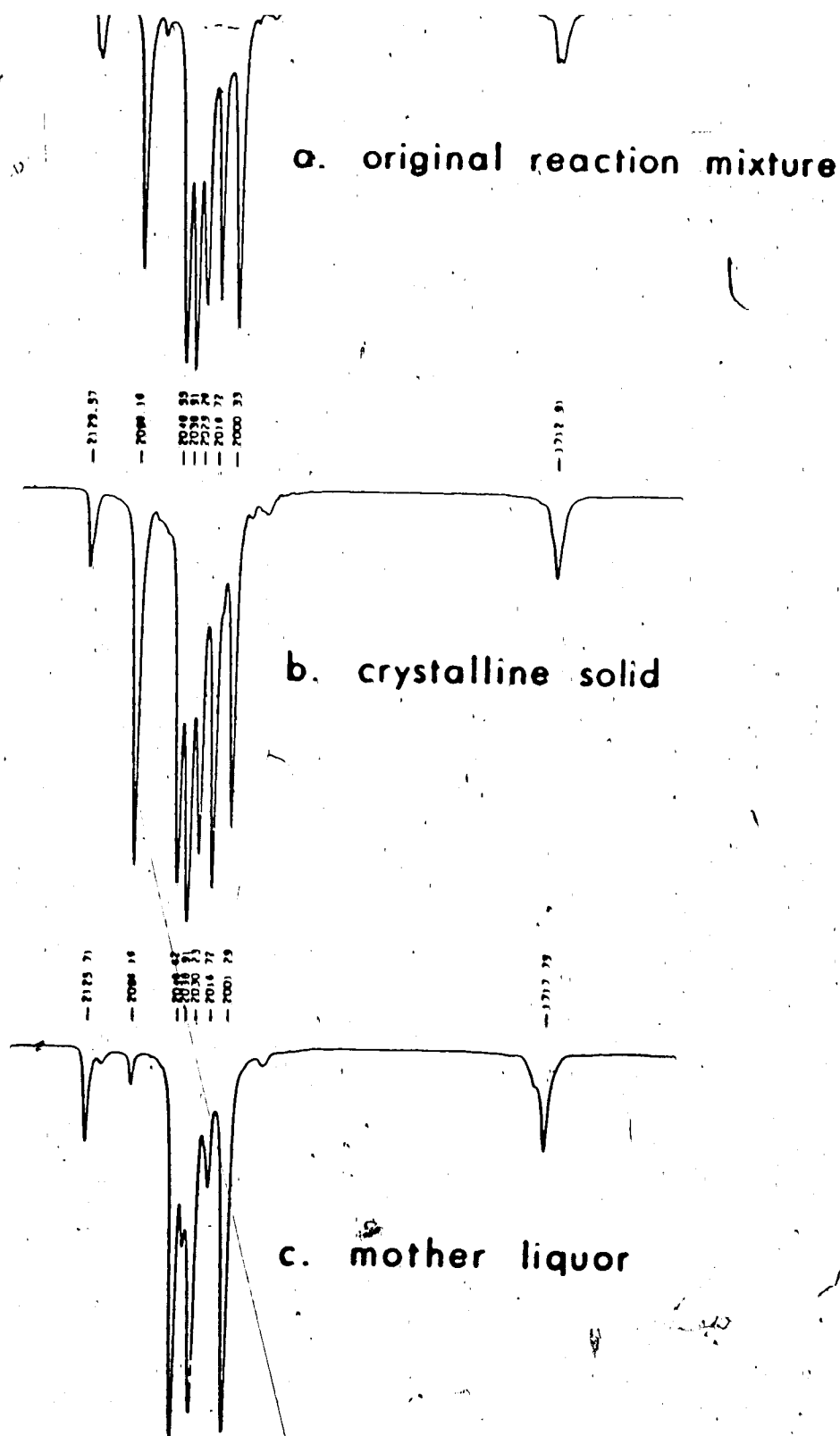


**Figure 1.** Infrared spectra of the different stages of product isolation from the reaction of 3c with MA.

Table IV. Carbonyl Stretching Frequencies for  $\text{Os}(\text{CO})_4[\eta^2\text{-alkene}]$  and  $\text{Os}_2(\text{CO})_8[\mu\text{-alkene}]^a$ .

Alkene	$\text{Os}(\text{CO})_4[\eta^2\text{-alkene}]$		$\text{Os}_2(\text{CO})_8[\mu\text{-alkene}]$	
	$\nu_{\text{CO}}, \text{cm}^{-1}$	$\nu_{\text{CO}_2}$	$\nu_{\text{CO}}, \text{cm}^{-1}$	
MA	13 $\tilde{\sim}$ 2126(m), 2047(s) 2031(s), 2001(s)	1718(m)	14 2130(m), 2086(s), 2049(s), 2039(vs), 2028(s), 2017(s), 2000(s)	17
$\text{C}_2\text{H}_4$	15 $\tilde{\sim}$ 2108(m), 2018(s br), 1982(m) <sup>b,†</sup>		16 2122(m), 2077(s), 2038(s), 2031(vs),	
$\text{C}_3\text{H}_6$	17 $\tilde{\sim}$ 2105(m), 2016(s br), 1977(m) <sup>b,†</sup>		18 2116(m), 2077(s), 2037(s), 2030(vs), 2022(s), 2009(s), 1995(s) <sup>†</sup>	
cis-COE	19 2100(m), 2013(s) 1982(m), 1975(s) <sup>†</sup>		N/O	
EA	20 $\tilde{\sim}$ 2126(m), 2046(s) 2030(s), 2000(s)	1712(m) <sup>†</sup>	21 2129(m), 2086(s), 2048(s), 2039(vs), 2028(s), 2017(s), 2000(s)	17
AA	22 $\tilde{\sim}$ 2127(m), 2049(s), 2035(s), 2004(s)	1675(m) <sup>†</sup>	23 2128(m), 2088(s), 2049(sh), 2040(vs), 2032(s), 2020(s), 2000(s)	16
MVK	24 $\tilde{\sim}$ 2125(m), 2048(s), 2029(s), 2000(s)	1685(m) <sup>†</sup>	25 2130(m), 2087(s), 2049(s), 2038(vs), 2028(s), 2014(s), 1999(s)	16

Table IV. (continued).

3P20	26 2121(m), 2043(s), 2023(s), 1995(s) <sup>c,†</sup>	N/I	N/O	
DNM	27 2138(m), 2062(s), 2036(s), 2009(s)	1733(m) 1717(m)	28 2135(m), 2093(s), 2059(s), 2040(vs), 2034(s), 2023(s), 2010(s), 2005(m)	17 17
DMF	29 2137(m), 2063(s), 2044(m), 2008(s)	1733(vw) 1713(m)	30 2136(m), 2095(s), 2048(s), 2035(s), 2024(s), 2008(m)	16
DEF	31 2136(m), 2062(s), 2044(m), 2008(s)	1726(vw) 1707(m)	32 2135(m), 2095(s), 2048(s), 2037(sh), 2023(s), 2008(m)	16
MAH	48 2146(m), 2065(s), 2050(m), 2032(s)	1824(w) 1763(w) <sup>d</sup>	47 2139(m), 2097(s), 2052(s), 2048(s), 2028(s), 2014(m)	18 17

a) pentane solution unless otherwise noted; b) benzene; c) hexanes; d)  $\text{CH}_2\text{Cl}_2$ ; e) THF.

† not isolated in pure form; N/O=not observed, N/I=not identified.

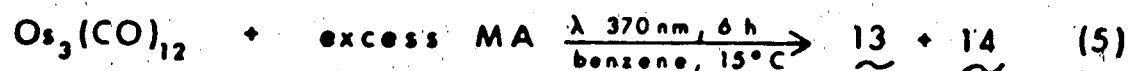
MA-methyl acrylate, cis-COE-cis-cyclooctene, EA-ethyl acrylate, AA-

acrylic acid, MVK-methyl vinyl ketone, 3P20-3-penten-2-one, MAH-maleic

anhydride, DNM-dimethyl maleate, DMF-dimethyl fumarate, DEM-diethyl

maleate, DEF-diethyl fumarate.

osmium complex, 14, incorporating an MA ligand. The latter possibility was verified when recrystallization of 14 gave materials whose IR spectrum was indistinguishable from Figure Ib. As a result, the photoreaction between 3c and MA gave two osmium-containing compounds, equation (5), in contrast to the single mononuclear  $\text{Ru}(\text{CO})_4[\eta^2\text{-MA}]$  derived from



the analogous ruthenium reaction.<sup>55</sup>

The exact nature of 14 was slow to emerge. A parent molecular ion in the mass spectrum at 692 m/e followed by consecutive loss of eight carbonyl units together with an elemental analysis (Table V) pointed to the dinuclear formulation  $\text{Os}_2(\text{CO})_8(\text{MA})$ . Although this information, along with NMR (*vide infra*) and IR data which indicated an intact bound MA moiety, all supported a unique 1,2-diosmacyclobutane formulation, X-ray structural verification was necessary to assign this structure. Hesitation to claim this structure without an X-ray analysis stemmed from the rarity of iron group saturated dimetallacycles, except dimetallacyclopropanes<sup>69</sup>, and the absence of an osmium derivative at the time of deliberation.

Features of the data collection and structure refinement are collected in Table VI, while relevant bond distances and angles and torsional angles appear in Tables VII, VIII and IX, respectively. The molecular structure, with numbering scheme, is shown by the perspective view in Figure II, and corroborates the 1,2-diosmacyclobutane structure of the molecule. The Os(1)-Os(2) bond distance (2.8850(5)Å) closely approximates the redetermined benchmark value for 3c (2.8771(27)Å)<sup>70</sup> and is

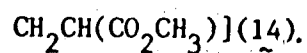
Table V. Analytical and Mass Spectral Data for  $\text{Os}(\text{CO})_4[\eta^2\text{-alkene}]$  and  $\text{Os}_2(\text{CO})_8[\mu\text{-}\eta^1, \eta^1\text{-alkene}]$ .

alkene	$\text{Os}(\text{CO})_4[\eta^2\text{-alkene}]$					$\text{Os}_2(\text{CO})_8[\mu\text{-alkene}]$				
	calc %C	calc %H	found %C	found %H	$M^+$	calc %C	calc %H	found %C	found %H	$M^+$
MA (13/14)	24.74	1.56	23.14	1.43	390	20.87	0.88	21.26	0.93	692
EA (20/21)	26.87	2.00	N/A		N/A	22.16	1.14	22.23	1.14	706
AA (22/23)	22.46	1.08	N/A		376 <sup>†</sup>	19.53	0.60		N/A	678 <sup>†</sup>
MVK (24/25)	25.81	1.62	N/A		N/A	21.37	0.90	21.63	0.96	676
DMM (27/28)	26.91	1.81	N/A		448	22.46	1.08	22.31	1.75	750
DMF (29/30)	26.91	1.81	27.04	1.77	448	22.46	1.08	22.59	1.09	750
DEF (31/32)	30.38	2.55	N/A		476	24.74	1.56	24.52	1.42	778
MAH (48/47)	24.00	0.50	N/A		402	20.52	0.29	21.15	0.57	704

N/A: Not available

<sup>†</sup> MS obtained on mixture of 19 and 20.

MA-methyl acrylate, EA-ethyl acrylate, AA-acrylic acid, MVK-methyl vinyl ketone, DMM-dimethyl maleate, DMF-dimethyl fumarate, DEF-diethyl fumarate, MAH-maleic anhydride.



temperature	-130°C
formula	$\text{C}_{12}\text{H}_{16}\text{O}_{10}\text{S}_2$
formula weight	690.58
crystal dimensions, mm	0.15 x 0.39 x 0.14 mm
crystal system, space group	Monoclinic, $P 2_1/n$
a, Å	16.707 (2)
b, Å	13.604 (2)
c, Å	6.997 (2)
$\beta$ , deg	95.08 (2)
volume, Å <sup>3</sup>	1583.95
Z	4
d, g cm <sup>-3</sup>	2.896
$\mu$ , cm <sup>-1</sup>	161.01
take-off angle, deg	1.7
detector aperture, mm	2.00 + 0.5 tan $\theta$ mm horizontal 4.00 mm vertical
crystal-to-detector distance, mm	205
scan type	$\omega$ -2 $\theta$
scan rate, deg min <sup>-1</sup>	10.1 ~ 1.7
scan width, deg	0.70 + 0.35 tan $\theta$
2 $\theta$ limit, deg	50.00
reflections measured	2789 unique, 2352 with $I > 3.0\sigma(I)$
absorption correction	yes
parameters refined	227
agreement factors	R, 0.044; $R_w$ , 0.058

Table VII. Relevant Bond Distances (Å) for  $\text{Os}_2(\text{CO})_8[\mu\text{-}\eta^1, \eta^1\text{-CH}_2\text{CH}(\text{CO}_2\text{CH}_3)](14)$ .

Metal-Metal		C-C (bridging)	
Os(1)-Os(2)	2.8850(5)	C(9)-C(10)	1.52(1)
Metal-C (bridging)			
Os(1)-C(10)	2.223(9)	Os(2)-C(9)	2.203(9)
Metal-C (carbonyl)			
Os(1)-C(1)	1.92(1)	Os(2)-C(5)	1.90(1)
Os(1)-C(2)	1.97(1)	Os(2)-C(6)	1.95(1)
Os(1)-C(3)	1.94(1)	Os(2)-C(7)	1.94(1)
Os(1)-C(4)	1.962(9)	Os(2)-C(8)	1.945(9)
C-O (carbonyl)			
C(1)-O(1)	1.13(1)	C(5)-O(5)	1.16(1)
C(2)-O(2)	1.13(1)	C(6)-O(6)	1.12(1)
C(3)-O(3)	1.14(1)	C(7)-O(7)	1.14(1)
C(4)-O(4)	1.13(1)	C(8)-O(8)	1.15(1)

Numbers in parentheses are estimated standard deviations in the least significant digits.

Table VIII. Selected Bond Angles (deg) for  $\text{Os}_2(\text{CO})_8[\mu\text{-}\eta^1, \eta^1\text{-CH}_2\text{CH}(\text{CO}_2\text{CH}_3)](14)$ .

Angles at Os(1)		Angles at Os(2)	
Os(2)-Os(1)-C(1)	168.3(3)	Os(1)-Os(2)-C(5)	167.7(3)
Os(2)-Os(1)-C(2)	87.4(3)	Os(1)-Os(2)-C(6)	86.7(3)
Os(2)-Os(1)-C(3)	95.6(3)	Os(1)-Os(2)-C(7)	93.9(3)
Os(2)-Os(1)-C(4)	90.2(3)	Os(1)-Os(2)-C(8)	88.1(3)
Os(2)-Os(1)-C(10)	71.0(2)	Os(1)-Os(2)-C(9)	70.0(2)
C(1)-Os(1)-C(2)	90.2(4)	C(5)-Os(2)-C(6)	90.6(2)
C(1)-Os(1)-C(3)	95.9(4)	C(5)-Os(2)-C(7)	98.4(2)
C(1)-Os(1)-C(4)	91.6(4)	C(5)-Os(2)-C(8)	92.2(4)
C(1)-Os(1)-C(10)	97.6(4)	C(5)-Os(2)-C(9)	97.7(4)
C(2)-Os(1)-C(3)	92.5(4)	C(6)-Os(2)-C(7)	96.8(4)
C(2)-Os(1)-C(4)	176.5(4)	C(6)-Os(2)-C(8)	167.7(4)
C(2)-Os(1)-C(10)	89.6(4)	C(6)-Os(2)-C(9)	80.9(4)
C(3)-Os(1)-C(4)	90.3(4)	C(7)-Os(2)-C(8)	94.6(4)
C(3)-Os(1)-C(10)	166.3(4)	C(7)-Os(2)-C(9)	163.8(4)
C(4)-Os(1)-C(10)	87.1(4)	C(8)-Os(2)-C(9)	86.9(4)
Angles at C (carbonyl)			
Os(1)-C(1)-O(1)	178.1(1)	Os(2)-C(5)-O(5)	177.7(8)
Os(1)-C(2)-O(2)	178.2(8)	Os(2)-C(6)-O(6)	174.3(8)
Os(1)-C(3)-O(3)	177.0(8)	Os(2)-C(7)-O(7)	177.3(9)
Os(1)-C(4)-O(4)	175.1(8)	Os(2)-C(8)-O(8)	172.1(9)
Angles at C (bridging)			
Os(1)-C(10)-C(9)	103.5(6)	Os(2)-C(9)-C(10)	106.5(6)

Numbers in parentheses are estimated standard deviations in the least significant digits.



Table IX. Relevant Torsional Angles (deg) for  $\text{Os}_2(\text{CO})_8[\mu\text{-}\eta^1, \eta^1\text{-CH}_2\text{CH}(\text{CO}_2\text{CH}_3)](14)$ .

---

Carbonyl ligands

C(1)-Os(1)-Os(2)-C(5)	24.0
C(2)-Os(1)-Os(2)-C(6)	24.9
C(3)-Os(1)-Os(2)-C(7)	20.6
C(4)-Os(1)-Os(2)-C(8)	16.5

Bridging ligand

C(10)-Os(1)-Os(2)-C(9)	15.9
Os(1)-Os(2)-C(9)-C(10)	-23.3
Os(2)-Os(1)-C(10)-C(9)	-22.6
Os(2)-C(9)-C(10)-Os(1)	29.7

---

Numbers in parentheses are estimated standard deviations in the least significant digits.

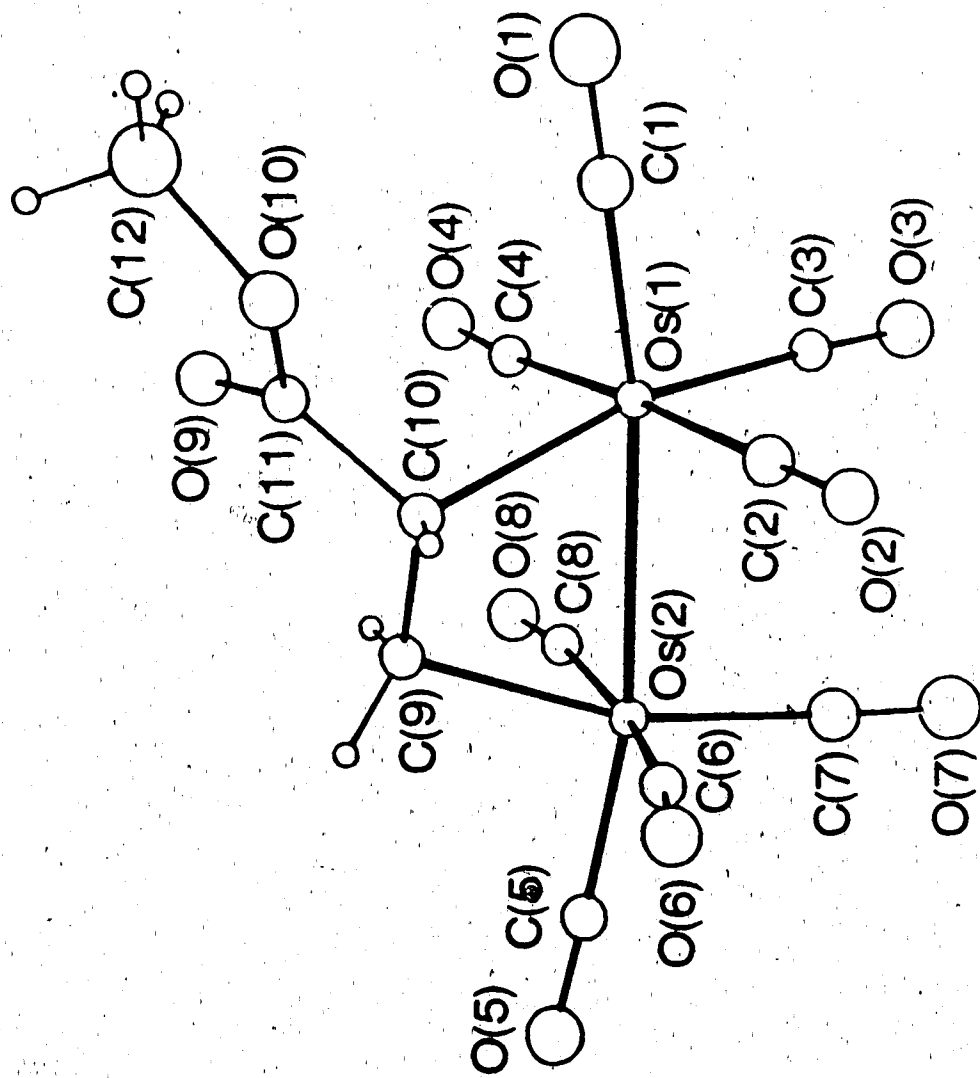


**Figure II.** Perspective view of  $\text{Os}_2(\text{CO})_8[\eta^5\text{-}\eta^1, \eta^1\text{-CH}_2\text{CH}(\text{CO}_2\text{CH}_3)](14)$  (Dr. R.G. Ball, SDL/U of A, 1982).

virtually identical to that found for the parent unsubstituted molecule  $\text{Os}_2(\text{CO})_8[\mu\text{-}\eta^1, \eta^1\text{-C}_2\text{H}_4]$  (2.883(1) Å)<sup>71</sup> which appeared as preliminary results from this study were being submitted for publication. The Os-C (bridge) bond distances of 2.203(9) and 2.223(9) Å are typical single bond values, comparable to the Os-C(sp<sup>3</sup>) distance in  $(\mu\text{-H})\text{Os}_3(\text{CO})_8^-$   $[\text{C}(\text{O}-)\text{C}(\text{C-CH})(\text{Me})\text{CHCHCEt}]$  (2.194(14) Å)<sup>72</sup> and equivalent to the analogous bonds in the parent compound (2.22(2) Å).<sup>71</sup> The length of the 1,2-ethanediyl bridge (1.52(1) Å) is that of a normal C-C single bond<sup>73</sup> (parent compound, 1.53(3) Å). The average Os-CO (axial) bond length of 1.96(1) Å is 0.04 Å longer than the average Os-CO(equatorial) distance. Similar differences have been observed previously in  $\text{Os}_3$ <sup>70</sup> and were interpreted as a consequence of the severe competition for back-bonding electron density from mutually trans carbonyl ligands. Not unexpectedly both in this structure and the parent molecule the four membered ring is distinctly non-planar, but show less deviation than in the hydrocarbon analog  $\text{C}_4\text{H}_8$ .<sup>74</sup> The upshot is a skewed conformation of the ring and twisting of the  $\text{Os}(\text{CO})_4$  moieties about the Os-Os bond by an average angle of 21° (Table IX) comparable to the parent structure (27°). Consequently, the bond angles at C(9) and C(10) (Table VIII) are slightly compressed from the expected 108° for an sp<sup>3</sup> hybridized carbon.

With the solid state structure in hand, the assignment of <sup>1</sup>H and <sup>13</sup>C NMR spectra becomes straightforward. The pattern and multiplicities of proton resonances for **14** are similar to those observed for free<sup>68</sup> and  $\text{M}(\text{CO})_4$ -bound<sup>55,68</sup> MA. The chemical shifts are at higher field from the above species (for M=Os, see section IV) in the region normally associated with alkane protons and consistent with a saturated diosmacycle (Table X). The observed coupling constants reflect the change in hybridization

Table X.  $^1\text{H}$  Chemical Shifts for Complexes  $\text{Os}_2(\text{CO})_8[\text{v-alkene}]^a$

$\begin{array}{c} \text{R}_1 \quad \text{R}_4 \\ \diagdown \quad \diagup \\ \text{C}-\text{C} \\ \diagup \quad \diagdown \\ \text{R}_2 \quad \text{R}_3 \end{array}$	$\delta(\text{R}_1)$	$\delta(\text{R}_2)$	$\delta(\text{R}_3)$	$\delta(\text{R}_4)$	$\delta(\text{OCH}_2)$	$\delta(\text{OCH}_3)$	$\delta(\text{C})$
$\text{MA}^b \text{ R}_1=\text{R}_2=\text{R}_3=\text{H}$ (14) $\text{R}_4=\text{CO}_2\text{CH}_3$	1.98 (t)	1.53 (dd)	2.57 (dd)	-	-	3.45 (s)	-
$\text{C}_2\text{H}_4^c \text{ R}_1=\text{R}_2=\text{R}_3=\text{R}_4=\text{H}$ (16)	1.51	1.51	1.51	1.51	-	-	-
$\text{EA}^d \text{ R}_1=\text{R}_2=\text{R}_3=\text{H}$ (21) $\text{R}_4=\text{CO}_2\text{CH}_2\text{CH}_3$	1.82 (t)	1.69 (dd)	2.57 (dd)	-	4.03 (dq) 4.08 (dq)	-	1.1
$\text{AA}^e \text{ R}_1=\text{R}_2=\text{R}_3=\text{H}$ (23) $\text{R}_4=\text{CO}_2\text{H}$	1.76 (t)	1.69 (dd)	2.63 (dd)	-	-	-	-
$\text{MVX}^g \text{ R}_1=\text{R}_2=\text{R}_3=\text{H}$ (25) $\text{R}_4=\text{C}(=\text{O})\text{CH}_3$	1.85 (t)	1.51 (dd)	2.72 (dd)	-	-	-	1.1
$\text{DM}^h \text{ R}_1=\text{R}_4=\text{H}$ (28) $\text{R}_2=\text{R}_3=\text{CO}_2\text{CH}_3$	3.06 (s)	-	-	3.06 (s)	-	3.57 (s)	-
$\text{DMF}^h \text{ R}_1=\text{R}_3=\text{H}$ (30) $\text{R}_2=\text{R}_4=\text{CO}_2\text{CH}_3$	3.03 (s)	-	3.03 (s)	-	-	3.60 (s)	-

Table X. (continued).

DEF <sup>i</sup> R <sub>1</sub> =R <sub>3</sub> =H	3.10 (s)	-	3.10 (s)	-	4.05 (dq)	-	1
(32) R <sub>2</sub> =R <sub>4</sub> =CO <sub>2</sub> CH <sub>2</sub> CH <sub>3</sub>					4.10 (dq)		
MAH <sup>j</sup> R <sub>1</sub> =R <sub>4</sub> =H	3.33 (s)	-	-	3.33 (s)	-	-	
(47) R <sub>2</sub> -R <sub>3</sub> =C(O)OC(O)							

a) ambient temperature, ppm vs. TMS; b) C<sub>6</sub>D<sub>6</sub>, 200 MHz, J<sub>gem</sub>=J<sub>trans</sub>=11Hz, J<sub>cis</sub>=7.5Hz; c) C<sub>6</sub>D<sub>6</sub>, see reference; d) CDCl<sub>3</sub>, 400 MHz, J<sub>gem</sub>=J<sub>trans</sub>=10.5Hz, J<sub>cis</sub>=7.5Hz; e) mixture with 19: CD<sub>2</sub>Cl<sub>2</sub>, 300 MHz, J<sub>gem</sub>=J<sub>trans</sub>=10.5Hz, J<sub>cis</sub>=8Hz; f) acidic proton not observed; g) CD<sub>2</sub>Cl<sub>2</sub>, 300 MHz, J<sub>gem</sub>=J<sub>trans</sub>=10.5Hz, J<sub>cis</sub>=7Hz; h) CD<sub>2</sub>Cl<sub>2</sub>, 400 MHz; i) CDCl<sub>3</sub>, 300 MHz, J<sub>gem</sub>=11Hz, J<sub>H-H<sub>Me</sub></sub>=7Hz; j) CD<sub>2</sub>Cl<sub>2</sub>, 300 MHz.

MA-methyl acrylate, EA-ethyl acrylate, AA-acrylic acid, MVK-methyl vinyl ketone, DM-dimethyl maleate, DMF-dimethyl fumarate, DEF-diethyl fumarate, MAH-maleic anhydride.

12. However, in 14 there is an equalization of  $J_{gem}$  and  $J_{trans}$  at a value larger than  $J_{cis}$ , presumably reflecting the reduction of the dihedral angle between the trans protons and the increased  $sp^3$  character of C(9). A more dramatic result of this bonding mode is the extreme "coordination shift" experienced by the bridging carbons. In the  $^{13}C$  spectrum of 14 (Table XI), both C(9) and C(10) resonate above TMS at -24.9 and -4.3 ppm respectively ("coordination shifts",  $\Delta\delta$ : C(9)=155.2 and C(10)=133.2 ppm).

### III. Photoreactivity of 3c with Other Alkenes.

Favourable reactivity between 3c and MA with the formation of a remarkable product raised interest to test the generality of the photoreactivity with a variety of alkenes. As a consequence of Section II, other activated alkenes should be particularly suited to stabilize carbonyl-alkene derivatives. It was thus surprising to learn that during the early stages of this study, Norton and coworkers had obtained the corresponding mononuclear<sup>75</sup> and dinuclear<sup>71</sup> ethylene derivatives via totally different thermal routes (equations (6) and (7)):

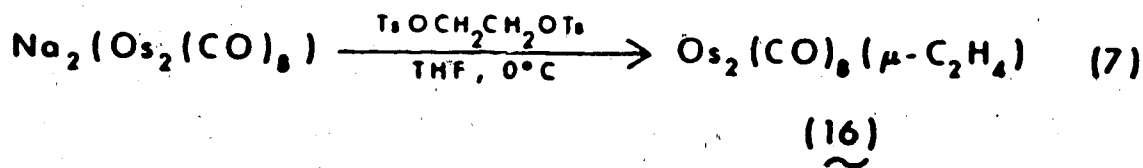
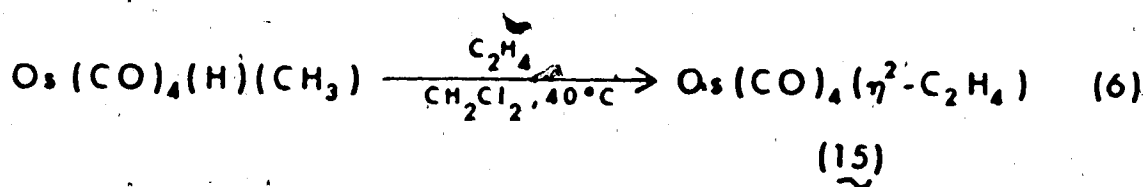


Table XI.  $^{13}\text{C}$  Chemical Shifts for Complexes  $\text{Os}_2(\text{CO})_8[\nu\text{-alkene}]^a$ .

$\begin{array}{c} \text{R}_1 \\ \diagdown \\ \text{C}(1')=\text{C}(1) \\ \diagup \\ \text{R}_2 \end{array} \quad \begin{array}{c} \text{R}_4 \\ \diagup \\ \text{C}(1') \\ \diagdown \\ \text{R}_3 \end{array}$	$\delta(\text{CO} + \text{CO}_2\text{R})$	$\delta(\text{C}(1))$	$\delta(\text{C}(1'))$	$\delta(\text{OCH}_2)$	$\delta(\text{OCH}_3)$
$\text{MA}^b \text{ R}_1=\text{R}_2=\text{R}_3=\text{H}$	182.4, 180.0, 179.1, 178.7,	-4.3	-24.9	-	50.4
(14) $\text{R}_4=\text{CO}_2\text{CH}_3$	178.2, 172.1, 171.9, 168.5, 166.9				
$\text{C}_2\text{H}_4^c \text{ R}=\text{H}$	180.7(2), 172.7(1), 169.7(1)	-25.2	-25.2	-	-
(16)					
$\text{EA}^d \text{ R}_1=\text{R}_2=\text{R}_3=\text{R}_4=\text{H}$	182.8, 179.9, 179.0, 178.7,	-4.6	-25.3	59.6	-
(21) $\text{R}_4=\text{CO}_2\text{CH}_2\text{CH}_3$	178.3, 171.8, 171.6, 168.4, 166.6				
$\text{NVK}^e \text{ R}_1=\text{R}_2=\text{R}_3=\text{H}$	211.8 <sup>f</sup> , 180.2, 179.1, 178.6, -1.0	-25.9	-	-	-
(25) $\text{R}_4=\text{C}(\text{O})\text{CH}_3$	178.2, 172.3, 171.8, 169.0, 168.7				
$\text{DNM}^g \text{ R}_1=\text{R}_4=\text{H}$	179.8(2), 177.9(1), 172.7(1), -1.8 167.1(1)	-1.8	-	-	51.5
(28) $\text{R}_2=\text{R}_3=\text{CO}_2\text{CH}_3$					
$\text{DNF}^g \text{ R}_1=\text{R}_3=\text{H}$	182.7, 178.6, 178.2, 171.7, -2.7 166.3	-2.7	-	-	51.1
(30) $\text{R}_2=\text{R}_4=\text{CO}_2\text{CH}_3$					

Table XI. (continued).

DEF <sup>h</sup> R <sub>1</sub> =R <sub>3</sub> =H	181.7, 179.21, 179.16, 172.7, 167.5	-1.0	59.8	-
(32) R <sub>2</sub> =R <sub>4</sub> =CO <sub>2</sub> CH <sub>2</sub> CH <sub>3</sub>				
MAH <sup>i</sup> R <sub>1</sub> =R <sub>4</sub> =H	181.4, 177.6, 176.5, 170.7	-6.7	-	-
(47) R <sub>2</sub> -R <sub>3</sub> =C(O)C(O)				-

a) ambient temperature, ppm vs. TMS; b) C<sub>6</sub>D<sub>6</sub>, 100.62 MHz; c) toluene-d<sub>8</sub>, 100.62 MHz; d) CDCl<sub>3</sub>, 100.62 MHz; e) CD<sub>2</sub>Cl<sub>2</sub>, 75.469 MHz; f) ketonic carbonyl; g) CD<sub>2</sub>Cl<sub>2</sub>, 100.62 MHz; h) THF-d<sub>8</sub>, 100.62 MHz; i) CDCl<sub>3</sub>, 75.469 MHz.

Numbers in parentheses indicate intensities of peaks when not equal.

MA-methyl acrylate, EA-ethyl acrylate, MVK-methyl vinyl ketone, DMF-dimethyl maleate, DMF-dimethyl fumarate, DEF-diethyl fumarate, MAH-maleic anhydride.



the appropriate work-up afforded 16 in moderate yield (Table III). With recently improved isolation procedures<sup>76</sup>, 16 is routinely obtained in 55-80% yield, rendering the photochemical synthesis the method of choice for this potentially useful molecule.

Encouraged by these results, other similar types of alkenes were attempted. Under the immersion well conditions employed for both  $\text{MA}$  and  $\text{C}_2\text{H}_4$ , the propylene derivatives  $\text{Os}(\text{CO})_4[\eta^2\text{-CH}_2\text{CH}(\text{CH}_3)]$  (17) and  $\text{Os}_2(\text{CO})_8[\mu\text{-}\eta^1, \eta^1\text{-CH}_2\text{CH}(\text{CH}_3)]$  (18) were observed in the IR spectrum of the reaction solution (Table IV). As with its ethylene analog, 17 is volatile and was collected along with the evaporated benzene solvent. However, 17 slowly decomposes while 15 remains stable in benzene solution. Perhaps more surprising was the extreme instability of dinuclear 18. Storing either the impure solid or a pentane solution of 18 in the dark at  $-15^\circ\text{C}$  even under a propylene atmosphere gave back 3c and an unidentified insoluble orange material. In another experiment, cis-cyclooctene [ $\text{cis-COE}$ ] was irradiated with 3c to give as the only identifiable species  $\text{Os}(\text{CO})_4[\eta^2\text{-cis-COE}]$  (19). No bands in the terminal carbonyl region could be assigned to a dinuclear compound. Failed attempts to recrystallize 19 also brought into suspicion its stability. At this time it is unclear whether 19 is either inherently unstable or that some unidentified product(s) obtained during the photochemical preparation adversely affected compound stability. Interestingly, the disubstituted  $\text{cis-Os}(\text{CO})_3[\eta^2\text{-cis-COE}]_2$  has been prepared from  $\text{Os}(\text{CO})_5$  photolysis and has been structurally characterized<sup>77</sup>. Independent observations in our laboratories<sup>78</sup> confirmed the latter route to be far superior than using

and cis-COE shifted the emphasis back to activated alkenes. However, it was quickly discovered that many of the reactions with activated alkenes also proceeded with problems. In most cases, the path towards the formation of mononuclear and dinuclear species was confirmed by IR spectroscopy. However, it was in the attempted isolation of observed products that difficulties arose.

The photoreaction between 3c and ethyl acrylate [EA] appeared identical (by IR) to the homologous MA photolysis. Whereas the dinuclear  $\text{Os}_2(\text{CO})_8[\mu\text{-EA}](\underline{21})$  was obtained as per 14, the mononuclear  $\text{Os}(\text{CO})_4[\eta^2\text{-EA}](\underline{20})$  has eluded separation and complete characterization. In a similar fashion the ruthenium analog of 20 has not been obtained in pure form, although spectroscopic identification was possible.<sup>79</sup> The photoreaction with acrylic acid [AA] was carried out next to determine if changes in solubility characteristics of the products will result in improved isolation. However, the AA species (22, 23; Table IV) appeared only in low concentrations in reaction solution IR spectra. Attempted isolation showed lesser solubilities than the corresponding vinyl ester compounds but similar solubility and chromatographic behaviour to each other. Nevertheless, a sufficient quantity of the mixture could be analysed by comparison of IR (Table IV) and  $^1\text{H}$  NMR data (Tables X and XII) with their MA analogues to satisfactorily establish their existence.

To gauge the intrinsic effects of moderate changes in the activating group, methyl vinyl ketone [MVK] was chosen. Once again, only in a small way did the photoreaction mimic that of MA. The darkly coloured residue, obtained after the reaction was judged complete, defied purification attempts.

...the residue, a variety of separation techniques (extraction, fractional crystallization and chromatography) did not yield further materials. The effect of replacing a methylene hydrogen by a methyl group was investigated by the reaction of 3-penten-2-one [3P20]. Extended photolysis resulted in limited conversion to  $\text{Os}(\text{CO})_4[\eta^2\text{-CH}(\text{CH}_3)\text{-CH}(\text{C}(\text{O})\text{CH}_3)]$  (26) as the only identifiable species (Table IV). In some way this behaviour parallels the differing reactivity between propylene ( $\text{CH}_2\text{CHCH}_3$ ) and ethylene ( $\text{CH}_2\text{CH}_2$ ).

By no means does the above group of activated alkenes represent an exhaustive search for potentially suitable olefins for the photochemical formation of diosmacyclobutanes. Since much of the results were disappointing some final hope rested on a few well-known strong  $\Pi$ -acidic alkenes. Anticipation of complex formation from the photolysis with tetrafluoroethylene [TFE] was based on the ability to prepare  $(\text{TFE})\text{Fe}(\text{CO})_4$ , which along with the  $\text{C}_2\text{H}_4$  analog have had gas-phase electron diffraction studies performed.<sup>80</sup> Equally the iron -  $\text{C}_2\text{H}_4$  and iron-TFE derivatives could be obtained, albeit in low yield, from a photochemical preparation.<sup>81</sup> No products could be isolated and/or identified from the irradiation of 3c with TFE. Some limited polymerization of TFE may have occurred in accord with a previous report.<sup>82</sup> The outcome of the reaction with a second fluoroalkene, perfluoro-2-butene [OFB] was no different. Lastly, the reaction with one of the most  $\Pi$ -acidic alkenes, maleic anhydride [MAH], as well proved unsuccessful. After extended photolysis, there was no indication of product formation from either solution IR spectra or that of the reaction residue. Interestingly,  $\text{Ru}(\text{CO})_4[\eta^2\text{-MAH}]$  could not be prepared photochemically from 3b

derivatives of osmium with MAH subsequently have been obtained. Clearly there are some aspects of the photoreaction of  $\text{Os}_3(\text{CO})_{12}$  which did not manifest in the initial successful reactions. The simplistic approach which required activating substituents appears outweighed by steric and/or other electronic effects which complicate the anticipated straightforward alkene derivative chemistry.

#### IV. The $\text{Os}(\text{CO})_4[\eta^2\text{-alkene}]$ Complexes.

Although the attention was quickly focussed on the heretofore rare diosmacyclic compounds, as is obvious from the preceeding sections, the mononuclear carbonyl-alkene complexes were interesting in their own right. Indeed, the molecules were the anticipated products of the photoreaction and, with the exception of  $\text{Os}(\text{CO})_4[\eta^2\text{-C}_2\text{H}_4]$ <sup>75</sup>, were unavailable at the outset of this study.

With the highly successful reactivity obtained with MA,  $\text{Os}(\text{CO})_4[\eta^2\text{-MA}](13)$  prevails as the most easily accessible mononuclear derivative and as such was subjected to the gamut of spectroscopic characterization. The terminal carbonyl band pattern in the IR spectrum for 13 (Figure 1c) is consistent with a trigonal bipyramidal (tbp) geometry where the asymmetric alkene occupies an equatorial position on an  $\text{Os}(\text{CO})_4$  unit of local  $\text{C}_{2v}$  symmetry.<sup>83</sup> The observed IR frequencies for 13 are higher than in the analagous iron and ruthenium compounds<sup>55</sup> and suggest that  $d \rightarrow \pi^*$  back donation to the carbonyl groups is of lesser importance in the osmium complex. Conversely, the  $\eta^2$ -alkene moiety experiences larger upfield shifts in both  $^1\text{H}$  (Table XII) and  $^{13}\text{C}$  (Table XIII) NMR spectra

Table XII.  $^1\text{H}$  Chemical Shift for Complexes  $\text{Os}(\text{CO})_4[\eta^2\text{-alkene}]^a$ .

$\begin{array}{c} \text{R}_1 \quad \text{R}_4 \\ \diagdown \quad \diagup \\ \text{C}=\text{C} \\ \diagup \quad \diagdown \\ \text{R}_2 \quad \text{R}_3 \end{array}$	$\delta(\text{R}_1)$	$\delta(\text{R}_2)$	$\delta(\text{R}_3)$	$\delta(\text{R}_4)$	$\delta(\text{OCH}_2)$	$\delta(\text{OCH}_3)$	$\delta(\text{oth})$
$\text{MA}^b \text{ R}_1=\text{R}_2=\text{R}_3=\text{H}$	2.12 (dd)	1.58 (dd)	2.59 (dd)	-	-	3.38 (s)	
(13) $\text{R}_4=\text{CO}_2\text{CH}_3$							
$\text{AA}^c \text{ R}_1=\text{R}_2=\text{R}_3=\text{H}$	2.11 (dd)	1.94 (dd)	2.78 (dd)	-	-	-	d
(22) $\text{R}_4=\text{CO}_2\text{H}$							
$\text{DM}^e \text{ R}_1=\text{R}_4=\text{H}$	3.21 (s)	-	-	3.21 (s)	-	3.66 (s)	
(27) $\text{R}_2=\text{R}_3=\text{CO}_2\text{CH}_3$							
$\text{DMF}^f \text{ R}_1=\text{R}_3=\text{H}$	3.39 (s)	-	3.39 (s)	-	-	3.33 (s)	
(29) $\text{R}_2=\text{R}_4=\text{CO}_2\text{CH}_3$							
$\text{DEF}^g \text{ R}_1=\text{R}_3=\text{H}$	3.24 (s)	-	3.24 (s)	-	4.10 (dq)	-	1.24 (t)
(31) $\text{R}_2=\text{R}_4=\text{CO}_2\text{CH}_2\text{CH}_3$					4.15 (dq)		
$\text{MAH}^h \text{ R}_1=\text{R}_4=\text{H}$	3.57 (s)	-	-	3.57 (s)	-	-	
(48) $\text{R}_2-\text{R}_1=\text{C}(\text{O})\text{OC}(\text{O})$							

a) ambient temperature, ppm vs. TMS; b) toluene- $d_8$ , 200 MHz,  $J_{\text{gem}}=4\text{Hz}$ ,  $J_{\text{cis}}=8\text{Hz}$ ,  $J_{\text{trans}}=10\text{Hz}$ ; c) mixture with 20:  $\text{CD}_2\text{Cl}_2$ , 300 MHz,  $J_{\text{gem}}=4\text{Hz}$ ,  $J_{\text{cis}}=8\text{Hz}$ ,  $J_{\text{trans}}=10\text{Hz}$ ; d) acidic proton not observed; e)  $\text{CD}_2\text{Cl}_2$ , 400 MHz; f) toluene- $d_8$ , 400 MHz; g)  $\text{CDCl}_3$ , 300 MHz,  $J_{\text{gem}}=11\text{Hz}$ ,  $J_{\text{H-Me}}=7\text{Hz}$ ; h)  $\text{CD}_2\text{Cl}_2$ , 300 MHz.

Table XIII.  $^{13}\text{C}$  Chemical Shifts for Complexes  $\text{Os}(\text{CO})_4[\eta^2\text{-alkene}]^a$ .

$\begin{array}{c} \text{R}_1 \\ \diagdown \\ \text{C}(1')=\text{C}(1) \\ \diagup \\ \text{R}_2 \end{array} \quad \begin{array}{c} \text{R}_4 \\ \diagup \\ \text{C}(1') \\ \diagdown \\ \text{R}_3 \end{array}$	$\delta(\text{CO} + \text{CO}_2\text{R})$	$\delta(\text{C}(1))$	$\delta(\text{C}(1'))$	$\delta(\text{OCH}_2)$	$\delta(\text{OCH}_3)$	$\delta(\text{CF})$
$\text{MA}^b \text{ R}_1=\text{R}_2=\text{R}_3=\text{H}$	177.2, 176.7 <sup>†</sup> , 175.9	23.6	10.5	-	51.2	-
(13) $\text{R}_4=\text{CO}_2\text{CH}_3$	175.6, 174.4					
$\text{DMN}^b \text{ R}_1=\text{R}_4=\text{H}$	175.0 <sup>†</sup> , 174.3, 173.7, 171.3	27.5	27.5	-	52.0	-
(27) $\text{R}_2=\text{R}_3=\text{CO}_2\text{CH}_3$						
$\text{DMF}^b \text{ R}_1=\text{R}_3=\text{H}$	176.3 <sup>†</sup> , 173.7, 172.3	26.2	26.2	-	51.4	-
(29) $\text{R}_2=\text{R}_4=\text{CO}_2\text{CH}_3$						
$\text{DEF}^c \text{ R}_1=\text{R}_3=\text{H}$	176.2 <sup>†</sup> , 173.4, 172.5	25.9	25.9	60.7	-	14.2
(31) $\text{R}_2=\text{R}_4=\text{CO}_2\text{CH}_2\text{CH}_3$						
$\text{MAH}^d \text{ R}_1=\text{R}_4=\text{H}$	173.7, 172.9, 170.5, 169.8	21.6	21.6	-	-	-
(48) $\text{R}_2-\text{R}_3=\text{C}(\text{O})\text{OC}(\text{O})$						

a) ambient temperature, ppm vs. TMS; b)  $-30^\circ\text{C}$  toluene- $d_8$ , 100.62 MHz; c)  $\text{CDCl}_3$ , 75.469 MHz;

d)  $\text{CD}_2\text{Cl}_2$ , 75.469 MHz. <sup>†</sup> carboxylate carbonyl

olefin interaction in 13. The tbp geometry of 13 also is illustrated in the low temperature limiting  $^{13}\text{C}$  spectrum (Figure III) exhibiting one carboxylate carbonyl and four metal-carbonyl resonances, ca. 175 ppm. The attending variable temperature study showed an interesting coalescence pattern. Upon warming from  $-30^{\circ}\text{C}$ , the three lowest-field signals began to broaden until at  $5^{\circ}\text{C}$ , these peaks had almost disappeared, leaving the fourth high field resonance somewhat broadened. Increasing the temperature to  $90^{\circ}\text{C}$  averaged all metal carbonyl sites to give one broad signal. To account for the unusual coalescence, synchronous Berry-pseudorotation-olefin rotation which exchanges the environment of all carbonyl groups at the same rate cannot be invoked here. However, the "turnstile rotation"<sup>84</sup> consisting of an internal rotation of three sites (one axial, two equatorial) about a pseudo-three-fold axis against pairwise exchange of the remaining sites around a (pseudo-two-fold axis may be operating in this case. This motion, experimentally observed for a series of  $\text{Fe}(\text{CO})_4[\eta^2\text{-(cyclic alkene)}]$  complexes<sup>85</sup>, is depicted in Figure IV. The alkene and  $\text{CO}(4)$  groups are left static at lower temperatures due to what would be an energetically unfavourable conformation with the alkene in an axial site.<sup>86</sup> As the temperature is raised,  $\text{CO}(4)$  also begins to participate in the exchange process, probably via rotation about the other pseudo-three-fold axis of the molecule. The results of a complete study of the iron triad of complexes will appear in a later report.<sup>87</sup>

Unfortunately, the difficulties encountered during the attempted isolation of other mononuclear alkene derivatives (see previous section)

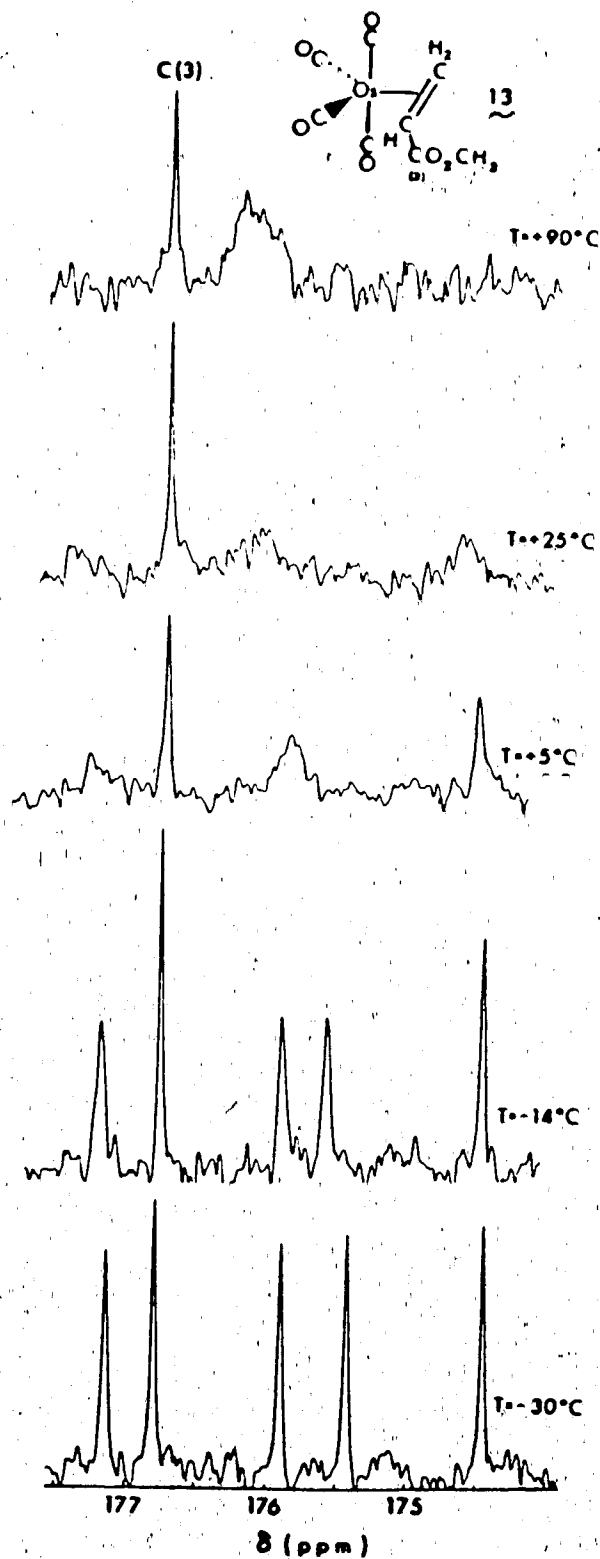
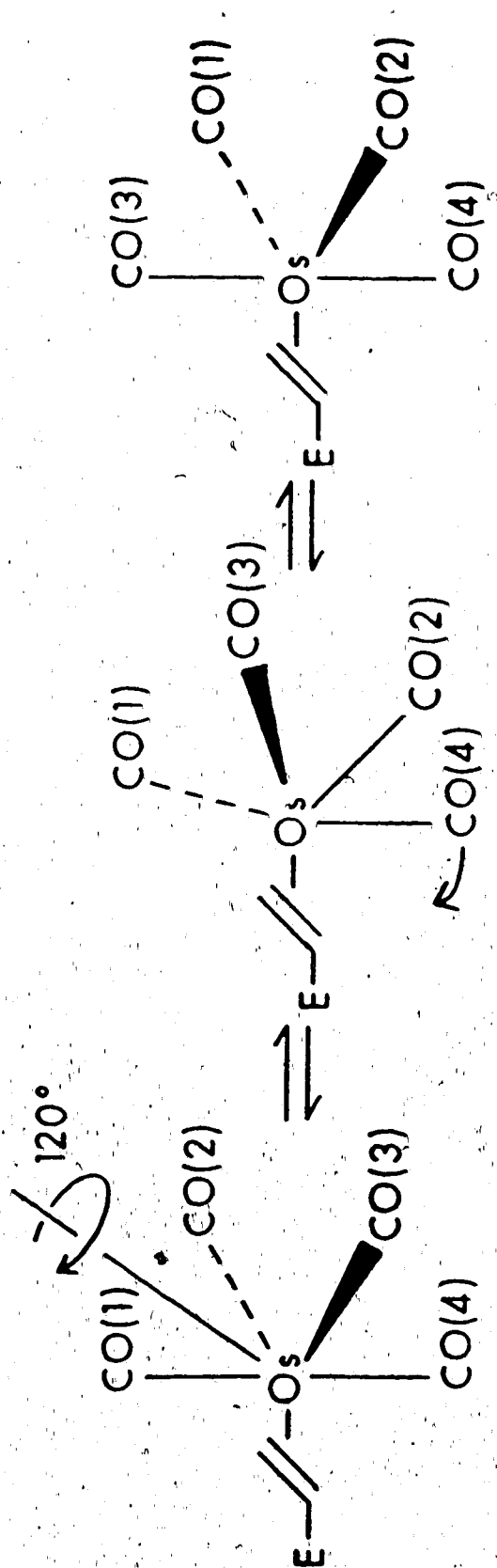


Figure III. 100.6 MHz  $^{13}\text{C}$  variable temperature NMR spectra for  $\text{Os}(\text{CO})_4[\eta^2\text{-CH}_2\text{CH}(\text{CO}_2\text{CH}_3)](13)$ .





**Figure IV.** The turnstile rotation.

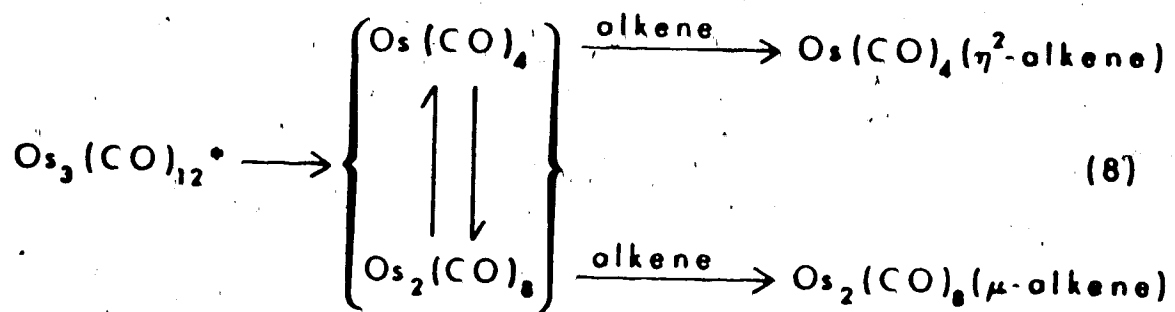
the utility of the photochemical entry via  $3c$  towards  $Os(CO)_4[\eta^2\text{-olefin}]$  species is largely negated. This has led to a search for a more reliable, direct synthetic route to the osmium carbonyl-alkene compounds. Work in our laboratories<sup>78</sup> and elsewhere<sup>88</sup> have established that the photoreaction between  $Os(CO)_5$  and alkenes offers an attractive possibility. An example will be tendered in Chapter Three.

#### V. Conclusions.

In retrospect, although the photochemical reaction between  $3c$  and alkenes proved disappointing especially with a view to a variety of 1,2-diosmacyclobutanes, the limited success must be put into the proper perspective. At the outset of this project only one 1,2-dimetallacyclobutane,  $Pd_2(1,5\text{-COD})_2[\mu\text{-}\eta^1, \eta^1\text{-C}_2\text{F}_4]$ <sup>88</sup>, was known. Bergman and coworkers attempted to prepare related dicobalt complexes<sup>90</sup> and failed, and even the "stabilized"  $Co_2(CO)_2(\eta\text{-C}_5\text{H}_5)_2[\mu\text{-}\eta^1, \eta^1\text{-benzocyclobutene}]$  decomposed at room temperature.<sup>90</sup> An apparent prerequisite for stable dimetallacyclobutane formation is strong metal-carbon  $\sigma$  bonds, which was vividly demonstrated by Norton, et al.<sup>71</sup> in the synthesis of  $Os_2(CO)_8[\mu\text{-}\eta^1, \eta^1\text{-C}_2\text{H}_4]$  (16). This finding lead to the photochemical preparation of 16 in substantially better yields. Professor Norton also has communicated his results<sup>91</sup> concerning the reduced stability of the analogous propylene derivative compared to 16, and confirms the problems encountered in the present study toward the same alkene. In fact, the limited success observed with simple olefins is not unknown for the osmium system. No products were detected in the photolysis of  $3c$  with 1-pentene<sup>21</sup>, whereas the reaction with 1-octene afforded only IR characterization

of the dimetallacyclic species. Since only slight changes in electronic properties are expected upon alkyl-group substitution of alkenes, steric destabilization of the dimetallacycle argues for the failure to isolate saturated diosmacycles from simple alkenes (other than ethylene).

A plausible explanation for the nonreactivity of strongly  $\Pi$ -acidic olefins like tetrafluoroethylene and maleic anhydride is more difficult to arrive at. This is especially so in view of the fact that the stable dipalladium complex contained a  $C_2F_4$  bridge<sup>88</sup> and that the MAH bridged material is available via an alternate route. Based on these events, the question of the photofragmentation of 3c in the presence of alkenes briefly should be considered. An initially postulated mechanism<sup>21,55</sup> for cluster breakdown was eagerly embraced to account for the formation of mononuclear and dinuclear products from 3c and alkenes (equation (8)):



The lack of dinuclear ruthenium derivatives<sup>55</sup> was attributed to the inherently weaker Ru-Ru bond compared to osmium.<sup>44</sup>

Alternatively, the currently popular mechanism<sup>65,66</sup> described in Chapter One proposes the coordinatively unsaturated carbonyl bridged intermediate 17b which is available for attack by an alkene in an  $\eta^2$ -fashion to give 11b' (L=alkene). Further fragmentation produces either  $Os_2(CO)_8(\text{alkene})$  and  $[Os(CO)_4]$  or  $Os(CO)_4(\text{alkene})$  and  $[Os_2(CO)_8]$ .

The coordinatively unsaturated fragments, much like in equation (8), can be rapidly scavenged to yield the observed final products.

Although no direct means of deciding between the two possibilities is availed from the limited experimental results, the disparity of reactivities with different olefins is more easily accommodated by the second pathway. The absence of photoreactivity between  $3c$  and MAH might be equated to the ability of THF and other hard donors to quench the photofragmentation of  $3b$ <sup>65</sup> and  $3c$ <sup>66</sup>. Extension of the argument to include the fluorine lone pairs of TFE may be valid but does not explain the "lack of difficulties" experienced with methyl acrylate which also has potential oxygen donor sites. Understandably a delicate balance must exist between electronic and steric substitutional effects on the alkene which dictates the successful outcome of this reaction.

As a final note of interest, Wrighton, et. al.<sup>92</sup>, have observed important solvent and temperature dependent photobehaviour of  $3b$  and  $3c$  with a variety of ligands. Long wavelength photolysis of  $3c$  and ethylene in hydrocarbon solvents at room temperature gives  $Os_3(CO)_{11}(C_2H_4)$  as the initial photoproduct. Extrapolation to the present benzene solvent system would be hasty at this time. However, even a minor contribution from this, followed by transformation of the cluster-bound alkene as seen in thermal reactions<sup>14-16</sup>, may be responsible for unidentified byproducts and for unexpected and unpredictable difficulties in some isolation attempts.

7

### CHAPTER THREE

#### PHOTOREACTIONS OF $\text{Os}_3(\text{CO})_{12}$ WITH 1,2-DISUBSTITUTED ALKENES

##### I. Introduction.

During the photochemical investigations with alkenes, a sampling of 1,2-disubstituted olefins also were included. Initial expectations that the second substituent would further activate the alkenes toward even more stable products in fact has been realized in the ruthenium system. Both dimethyl maleate [DMN,  $\text{Z-C}_2\text{H}_2(\text{CO}_2\text{CH}_3)_2$ ] and dimethyl fumarate [DMF,  $\text{E-C}_2\text{H}_2(\text{CO}_2\text{CH}_3)_2$ ] have afforded  $\text{Ru}(\text{CO})_4[\eta^2\text{-alkene}]$  species with enhanced stability over analogs of the singly substituted olefins (MA and MVK, for instance) from their photoreactions with  $\text{Ru}_3(\text{CO})_{12}$  (3b).<sup>55</sup> An obvious concern with disubstituted alkenes is the possibility of geometric isomerization.<sup>93</sup> No such problems were encountered in the above reactions, and since isomerization of these olefins by direct photolysis occurs only at short wavelengths (170-190 nm)<sup>93</sup>, it was not anticipated under the present conditions ( $\lambda \geq 370$  nm).

##### II. Reactions of 3c With Dimethyl Maleate and Dimethyl Fumarate.

###### A. Initial Investigations.

Selection of DMN for the first reaction attempt can be traced to physical and reactivity aspects of the ligand. It is a liquid at room temperature (DMF is solid) and the more soluble of the two in common organic solvents. This hopefully should lead to easier isolation of products. Furthermore, the photoreaction of 3b with DMN was shown to proceed directly to  $\text{Ru}(\text{CO})_4[\eta^2\text{-DMN}]$  in good yield.<sup>55</sup>

Photolysis of 3c with an excess of DMN (Table XIV, entry i) appeared to lead to the consumption of 3c in the expected fashion and

Table XIV. Summary of Photoreactions of  $\text{Os}_3(\text{CO})_{12}(\text{3c})$  with 1,2-disubstituted Alkenes.\*

entry	alkene	Mass of		molar ratio alkene(g)/ $\text{3c}$	time isolation (h)	$\text{Os}(\text{CO})_4[\eta^2\text{-alkene}]^a$		$\text{Os}_2(\text{CO})_8[\mu\text{-alkene}]$		b
		$\text{3c}(\text{mg})$	alkene(g)			isomers Z	isomers E(mg,%)	Z(mg,%)	E(mg,%)	
i	DNM	536.4	8.52	100	6.5	b	IR <sup>c</sup>	5.0 (1)	183.0 (41)	8.3
ii	DMF	409.0	3.60	55	7	b	IR <sup>c</sup>		204.0 (60)	
iii	DNM	511.0	4.95	61	12	c	IR <sup>c</sup>	236.0 (56)	2.0 (<1)	3.1
iv	DNM	515.8	9.45	115	5	b	IR <sup>c</sup>	d	100.0 (24)	6.0
v	DNM	523.0	10.37	125	6.5	a	IR <sup>c</sup>	50.0 (12)	d	e
vi	DNM	503.4	16.13	202	4	a	IR <sup>c</sup>	147.0 (35)	d	10.6
vii	DNM	507.0	16.13	200	4	a	IR <sup>c</sup> +20(18)	96.3 (23)	62.5 (15)	10.9
viii	DEM	523.0	10.64	107	6	b	IR	d	111.0 (25)	e
ix	DEF	317.4	1.21	20	11	b	56.0 (34)		110.0 (40)	
x	cis-stilbene	203.6	4.04	100	7.5	b	d	d	d	2.7

(a) IR identification; (b) isomerized alkene recovered in grams; (c) also observed in sublimates;

(d) not observed; (e) not available.

DNM-dimethyl maleate, DMF-dimethyl fumarate, DEM-diethyl maleate, DEF-diethyl fumarate.

\* E/Z designations refer to the stereochemistry of the "free" olefinic ligand.

to a final solution IR spectrum whose carbonyl region closely resembled those obtained from the monosubstituted alkenes. It is important to note here that the IR spectra were obtained in benzene solution which gave broad absorption bands, resulting in only impressions about the product distribution. A particularly puzzling aspect of the IR spectra taken during the reaction involved the carboxylate carbonyl stretching band. Due almost exclusively to the large excess of free ligand used, the band shifted from 1738 to 1727  $\text{cm}^{-1}$ , a value close to that of free DMF. Confirmation of the isomerization of DMM to DMF occurred when a copious amount of a crystalline white solid separated upon concentrating the reaction solution. IR and  $^1\text{H}$  NMR analyses and melting point determination firmly established that the solid was DMF. After filtration, the solvent was evaporated to leave a solid which still indicated the presence of free DMF which was removed by sublimation.

In the later stages of the sublimation, metal-carbonyl species could be identified in the sublimates. The first compound exhibited an IR pattern (Figure Va) virtually identical to that of  $\text{Ru}(\text{CO})_4[\eta^2\text{-DMM}]$ .<sup>55</sup> The IR spectrum of a second compound (Figure Vb), which also sublimed and appeared in the residue, closely corresponded to the DMF analog in the same report.<sup>55</sup> On this basis, the metal-carbonyl species were identified as the osmium derivatives  $\text{Os}(\text{CO})_4[\eta^2\text{-Z-C}_2\text{H}_2(\text{CO}_2\text{CH}_3)_2](27)$  and  $\text{Os}(\text{CO})_4[\eta^2\text{-E-C}_2\text{H}_2(\text{CO}_2\text{CH}_3)_2](29)$  respectively. An interesting feature of the IR spectra is the appearance of more than one carboxylate carbonyl stretching bands. For compound 27, two equally intense bands around 1700  $\text{cm}^{-1}$  suggest that the expected mirror symmetry of the molecule is disturbed. Rotational isomers which place the two

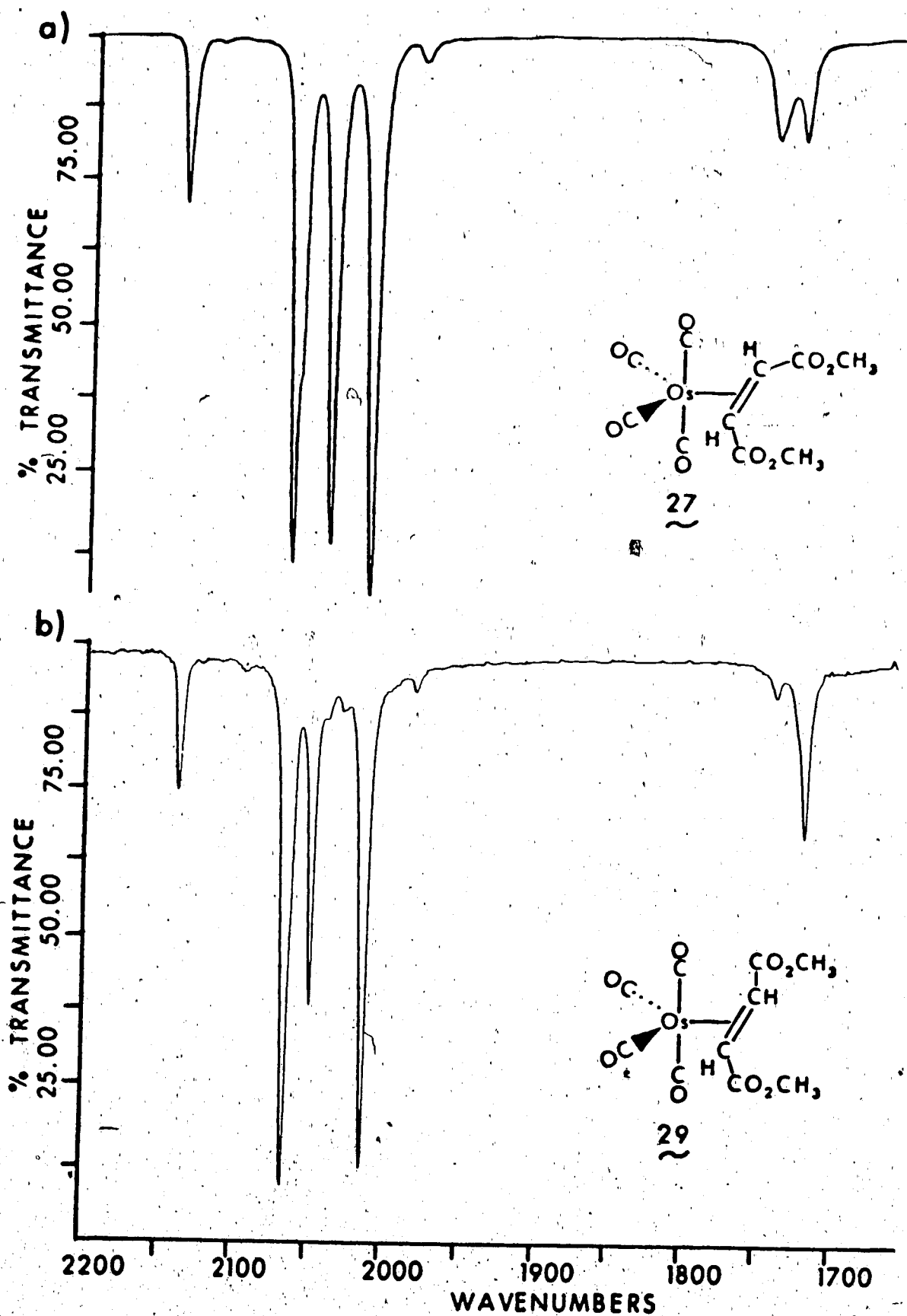


Figure V. IR spectra for [η²-DMM]- and [η²-DMF]Os(CO)₄.



ends of the bound alkene in different environments could also affect the number of terminal carbonyl bands. The shoulder on the band at  $2062\text{ cm}^{-1}$  may be the result of such a phenomenon. Corroboration of this argument is provided by the X-ray analysis of  $\text{Fe}(\text{CO})_3(\text{PPh}_3)[\eta^2\text{-Z-C}_2\text{H}_2(\text{CO}_2\text{CH}_2\text{CH}_3)_2]$ <sup>94</sup> in which one carboethoxy substituent lies in the plane of the olefin while the other group is orthogonally disposed to reduce steric interactions between the two adjacent bulky substituents (Figure VI). In the carboxylate region for 29, a shoulder on one  $\nu_{\text{CO}_2}$  band and a weaker second one implies that if rotational isomers exist here, the greatest proportion of them adopt a single structure where the molecule maintains  $\text{C}_2$  symmetry.

NMR spectroscopy, in particular  $^{13}\text{C}$ , was diagnostic in confirming the above mononuclear molecular formulations. The anticipated 3:1 ratios of methyl to olefinic proton resonances (Table XII) showed only minor differences between the two compounds. Whereas for 29, the two-fold symmetry imposes identical environments for the pairs of axial and equatorial carbonyl ligands giving rise to two equal intensity  $^{13}\text{C}$  signals, the average  $\text{C}_s$  symmetry of 27 results in distinct axial and equivalent equatorial groups, and a 2:1:1 pattern for terminal carbonyl resonances was observed (Table XIII). In a qualitative variable temperature  $^{13}\text{C}$  study of 29 the metal-carbonyl resonances significantly broadened at  $90^\circ\text{C}$  but failed to coalesce. The implication of this is a higher free energy of activation for carbonyl scrambling than in the MA derivative<sup>87</sup> and in the analogous iron and ruthenium derivatives.<sup>55</sup>

Following the sublimation, a yellow residue remained and IR

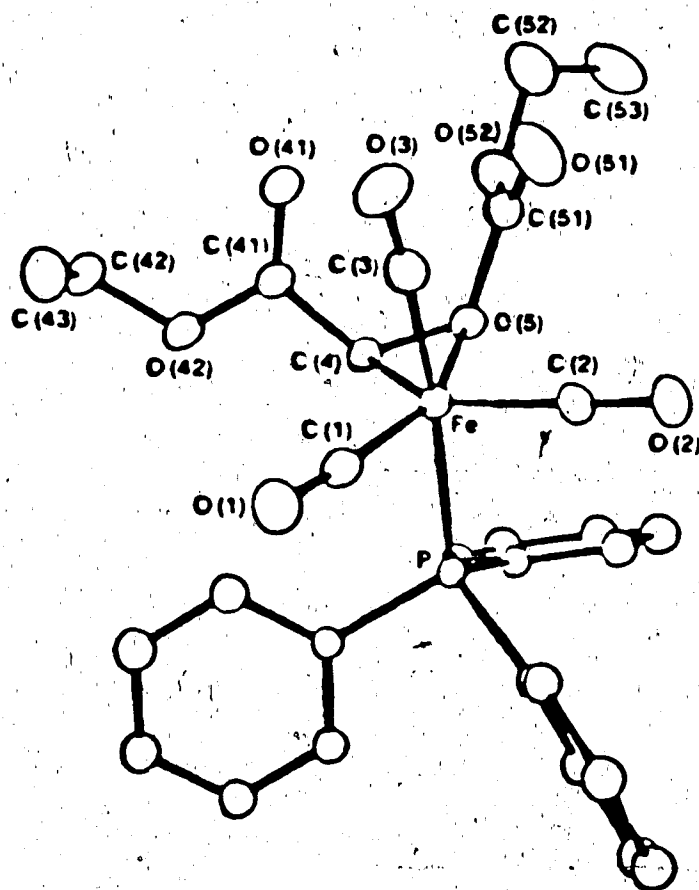
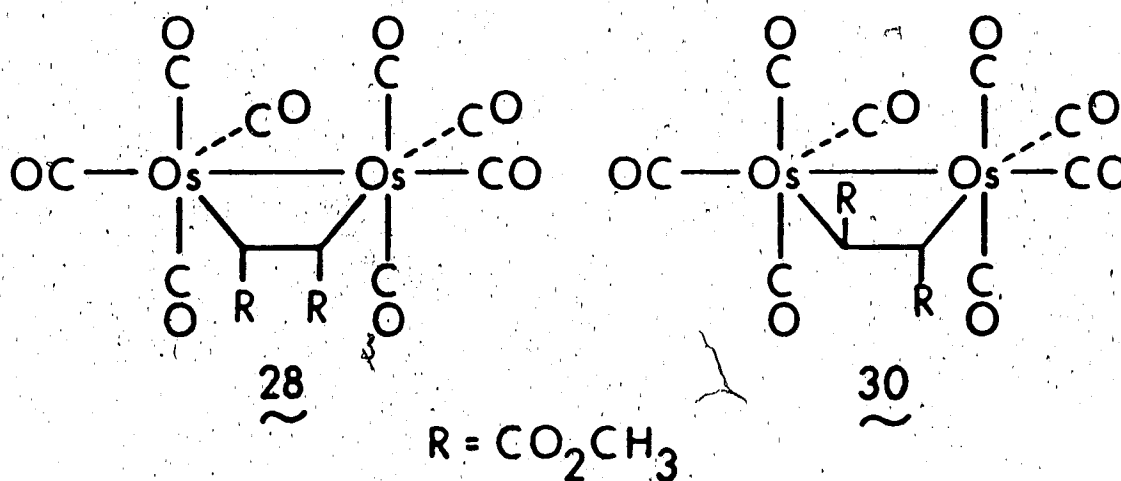


Figure VI. Structure of  $\text{Fe}(\text{CO})_3(\text{PPh}_3)[\eta^2\text{-DEN}]$ .<sup>94</sup>

spectroscopy indicated a mixture of compounds. Successful separation was achieved by chromatography on a Chromatotron (see Chapter Seven for details) which first delivered a small quantity of free DMF and 29. After two hours, two slowly moving bands could be collected individually. The solubility characteristics of these species suggested that two different compounds had formed. While both can be dissolved in  $\text{CH}_2\text{Cl}_2$  to give marginally different IR spectra, characteristic of diosmacyclobutanes, only one of the compounds is soluble in hydrocarbon solvents. With reasonable surety, both the DMF and DMF bridged dinuclear complexes had been obtained, but an ambiguity concerning their identification prevailed. Irrespective of their molecular symmetries ( $C_s$  for DMF, 28 and  $C_2$  for DMF, 30), the two complexes should show the same number of resonances in their  $^1\text{H}$  and  $^{13}\text{C}$  NMR spectra.



Experimentally, the hydrocarbon-soluble species (which proved to be 28) exhibited three metal-carbonyl  $^{13}\text{C}$  signals in a 2:1:1 ratio, while the other compound (30) gave four equal-intensity  $^{13}\text{C}$  resonances as expected. The unforeseen dissimilarities did not assist in resolving

the issue. A small, tentative hint came from examination of the IR spectra, which for 28 showed two closely spaced carboxylate carbonyl bands reminiscent of the mononuclear DMM compound 27. However, it was by no means certain that the analogy could be extended to the dinuclear compound as well.

In an attempt to resolve the ambiguity the photoreaction of 3c with DMF was carried out. Since trans-to-cis geometric isomerization is not expected, this reaction should only yield the mono- and dinuclear DMF derivatives. Solvent removal and sublimation of excess free DMF from the resulting mixture gave a pale yellow solid. Some of 29 was detected in the sublimates as before and the remainder was removed from the residue via pentane extractions. Recrystallization of the remaining white solid from a mixture of  $\text{CH}_2\text{Cl}_2$  and hexanes afforded a fluffy white material whose IR spectrum was identical to that observed for the hydrocarbon-insoluble material from the DMM reaction, compound 30. Even though the nature of the dinuclear complexes 28 and 30 was undoubtedly secure with the supplementary DMF reaction, it was still considered necessary to confirm the deduction beyond all doubt by X-ray diffraction experiments.

B. Solid State Structure of Isomeric  $\text{Os}_2(\text{CO})_8[\mu\text{-DMM}]$  and

$\text{Os}_2(\text{CO})_8[\mu\text{-DMF}]$ .

X-ray quality crystals could be grown, and the two molecules were found to adopt identical space groups with vaguely similar crystal parameters (Table XV). A perspective view of each (Figure VII) clearly shows the diosmacyclic structures whereby the bridging moieties maintain their respective geometric disposition. This is more con-

Table XV. Summary of Crystallographic Data for the Isomeric  
Compounds  $\text{Os}_2(\text{CO})_8[\mu-\eta^1, \eta^1-\text{C}_2\text{H}_2(\text{CO}_2\text{CH}_3)_2]$ .

	28	30
temperature	-65°C	23°C
formula	$\text{C}_{14}\text{H}_8\text{O}_{12}\text{Os}_2$	
formula weight	748.61	
crystal dimensions, mm	0.15 x 0.13 x 0.42	0.20 x 0.40 x 0.28
crystal system, space group	Monoclinic, $P2_1/C$	
a, Å	7.068 (6)	14.885 (2)
b, Å	14.386 (5)	8.466 (2)
c, Å	17.834 (6)	14.979 (4)
$\beta$ , deg	95.30 (5)	93.82 (2)
volume, Å <sup>3</sup>	1805	1883
Z	4	4
d, g cm <sup>-3</sup>	2.770	2.640
$\mu$ , cm <sup>-1</sup>	142.2	135.59
take-off angle, deg	3.0	3.0
detector aperture	2.0 + 0.50 tan $\theta$ mm horizontal 4.0 mm vertical	
crystal-to-detector distance, mm	250	
scan type	$\omega - 2\theta$	
scan rate, deg min <sup>-1</sup>	10.1 - 1.0	
scan width, deg	0.70 + 0.35 tan $\theta$	
2 $\theta$ limit, deg	54.0	52.0
reflections measured	unique 4419	3704
	$I > 3.0\sigma(I)$	

Table XV. (continued).

absorption correction		yes	yes
parameters refined		253	259
agreement factors	R	0.038	0.034
	R <sub>w</sub>	0.051	0.047

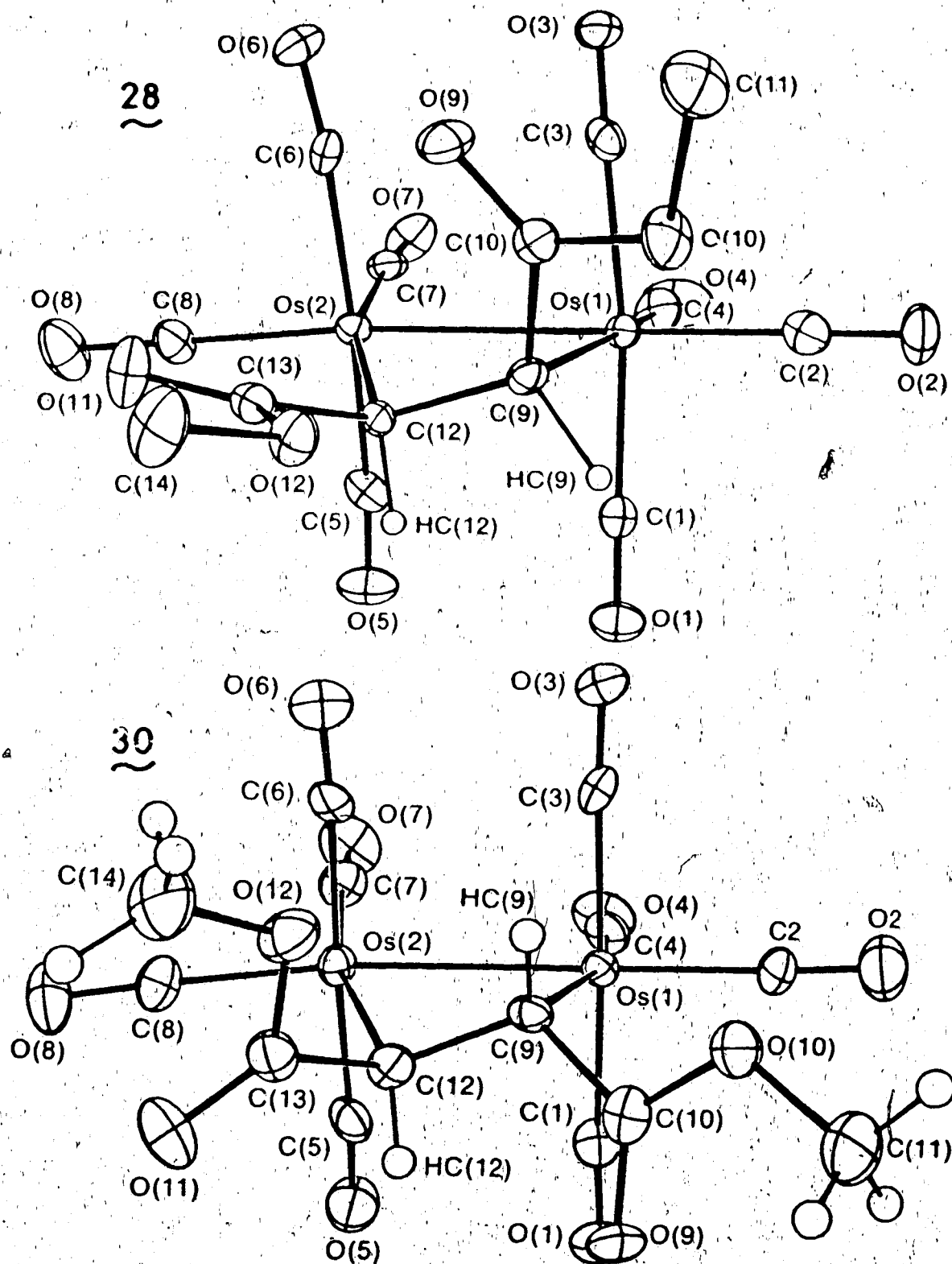


Figure VII. Molecular structures of  $\text{Os}_2(\text{CO})_8[\mu\text{-DMM}]$  (28) and  $\text{Os}_2(\text{CO})_8[\mu\text{-DMF}]$  (30) (Dr. R.G. Ball, SDL/U of A, 1985).

Also noteworthy is the sterically favoured orthogonal displacement of these groups as determined for the previously mentioned iron- $\eta^2$ -diethyl maleate complex (Figure VI).<sup>94</sup> As expected for  $\text{Os}_2(\text{CO})_8[\mu-\eta^1, \eta^1-\text{E}-\text{C}_2\text{H}_2(\text{CO}_2\text{CH}_3)_2](30)$ , the trans conformation persists in the dinuclear molecule as the substituents adopt a more staggered arrangement. As well, the carboxylate groups are bent sufficiently away from the  $\text{Os}_2(\text{CO})_8$  unit to reduce steric interference with the ancillary carbonyl ligands.

Elucidation of the subtle changes brought about by the bridging ligand can be accomplished by a comparison of structural parameters for the two molecules. A listing of the relevant bond lengths (Table XVI) for 28 and 30 shows little variation and in fact parallel those of the MA analog 14 (Table VII), with the notable exception of the bridging distance. Including the C-C bond distances for 14 and the parent compound 16, the to-date observed bridging distances fall in the order  $1.501(9)\text{\AA}$  (30) <  $1.52(1)\text{\AA}$  (14) <  $1.53(3)\text{\AA}$  (16) <  $1.54(1)\text{\AA}$  (28). Correspondingly, an inverse relationship involving the intra-diosma-cycle torsional angles (Table XVII) has those within 30 on the average  $5^\circ$  greater than the comparable angles in 28 while values for 14 are interdisposed (Table IX). The expansion of the ethanediyl bridge in 28 can be attributed to the steric interference caused by the gauche-type arrangement of the two bulky carbomethoxy substituents. Apparently this increase is adequate enough to accommodate a slightly less distorted four-membered ring in this molecule. Even though the differences under consideration are rather small, the structural changes



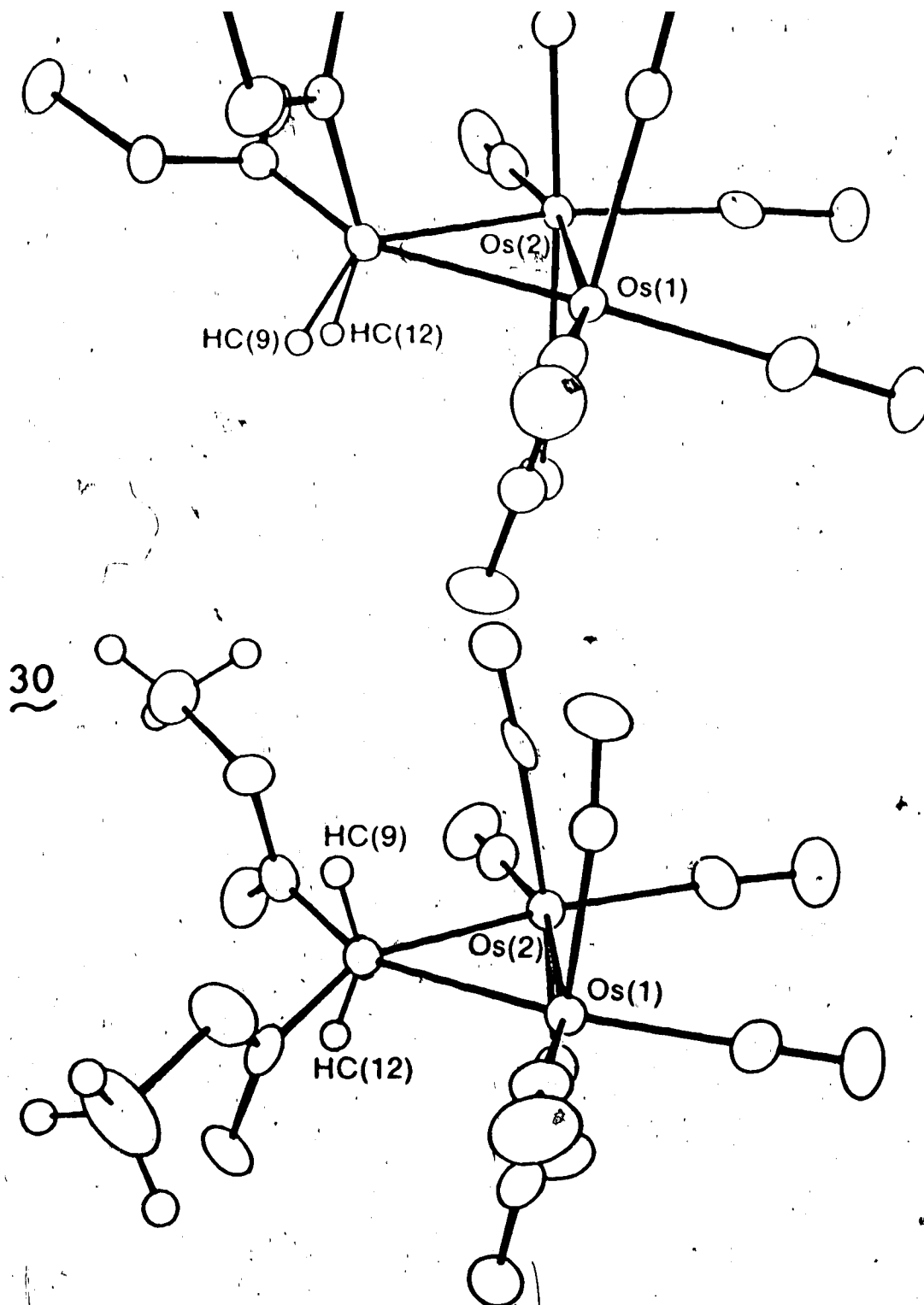


Figure VIII. Views of 28 and 30 looking down the C(9)-C(12) vector.

	Z-isomer 28	E-isomer 30
Metal-Metal		
Os(1)-Os(2)	2.8788(4)	2.8719(4)
Metal-C (bridging)		
Os(1)-C(9)	2.220(7)	2.205(6)
Os(2)-C(12)	2.202(6)	2.221(7)
C-C (bridging)		
C(9)-C(12)	1.54(1)	1.501(9)
Metal-C (carbonyl)		
Os(1)-C(1)	1.954(8)	1.944(7)
Os(1)-C(2)	1.941(9)	1.927(7)
Os(1)-C(3)	2.001(8)	1.949(7)
Os(1)-C(4)	1.942(9)	1.949(8)
Os(2)-C(5)	1.926(9)	1.962(8)
Os(2)-C(6)	1.974(8)	1.967(7)
Os(2)-C(7)	1.941(9)	1.947(8)
Os(2)-C(8)	1.910(9)	1.928(7)
C-O (carbonyl ligands)		
C(1)-O(1)	1.11(1)	1.143(8)
C(2)-O(2)	1.13(1)	1.118(9)
C(3)-O(3)	1.104(9)	1.120(8)
C(4)-O(4)	1.12(1)	1.127(9)
C(5)-O(5)	1.15(1)	1.133(9)
C(6)-O(6)	1.119(9)	1.121(9)
C(7)-O(7)	1.15(1)	1.135(9)
C(8)-O(8)	1.16(1)	1.142(8)

Numbers in parentheses are estimated standard deviations in the least significant digits.

Table XVII. Comparison of Torsional Angles (deg) for Isomeric

Compounds  $\text{Os}_2(\text{CO})_8[\mu\text{-}\eta^1, \eta^1\text{-C}_2\text{H}_2(\text{CO}_2\text{CH}_3)_2]$ .

	Z-isomer 28	E-isomer 30
Carbonyl ligands		
C(1)-Os(1)-Os(2)-C(5)	-16.4	-16.8
C(2)-Os(1)-Os(2)-C(6)	-24.7	-27.2
C(3)-Os(1)-Os(2)-C(7)	-17.2	-16.6
C(4)-Os(1)-Os(2)-C(8)	-16.0	-16.7
Bridging ligand		
C(9)-Os(1)-Os(2)-C(12)	-13.0	-15.9
Os(1)-Os(2)-C(12)-C(9)	18.8	23.2
Os(1)-C(9)-C(12)-Os(2)	-24.0	-29.9
Os(2)-Os(1)-C(9)-C(12)	18.2	23.2

Numbers in parentheses are estimated standard deviations in the least significant digits.

from 30 to 28 (1.949(7) versus 2.001(8)Å) while the other Os-CO(axial) distances remain unchanged within their esd's. The proximity of the carbomethoxy group at C(10) to CO(3) in 28 can account for the stretching of the Os-C distance.

An equally useful comparison to gauge steric effects in these molecules comes from an analysis of the C(axial)-Os-C(bridge) angles (Table XVIII). The major distinction between the two structures is the disposition of the substituent anchored by C(10) at the bridgehead carbon C(9). It moves from above to below the four-membered ring on going from 28 to 30, while the region surrounding C(12) remains relatively unaffected. Consistent with this, the C(5)-Os(2)-C(12) angle shows little change between the two structures (86.9(3) and 87.6(3)° for 28 and 30 respectively). Concomitantly, the movement described above decreases both the angles C(3)-Os(1)-C(9) and C(6)-Os(2)-C(12) by 6.1(3) and 4.9(3)°, respectively, and increases the angle C(1)-Os(1)-C(9) from 83.0(3) to 87.6(3)°. Although electronic factors also may influence the structural features, especially in view of substituent orientations with respect to the ethanediyl C-C bond, consideration of steric effects alone seems to adequately rationalize the changes seen between the diosmacycles 28 and 30.

C. Experimental Attempts to Identify the Origin of the Isomerization Process.

The unambiguous identification of both isomeric forms for the mononuclear and dinuclear osmium derivatives of  $C_2H_2(CO_2CH_3)_2$ , coupled with the isolation of isomerized free alkene, suggested that a more detailed investigation into the photoreactivity of DMM with 3c was

Table A-11. Comparison of relevant Bond Angles (deg) for Isomeric  
Compounds  $\text{Os}_2(\text{CO})_8[\mu\text{-}\eta^1, \eta^1\text{-C}_2\text{H}_2(\text{CO}_2\text{CH}_3)_2]$ .

	Z-isomer 28	E-isomer 30
Angles at Os(1)		
Os(2)-Os(1)-C(1)	88.6(2)	90.3(2)
Os(2)-Os(1)-C(2)	166.1(2)	168.0(2)
Os(2)-Os(1)-C(3)	85.2(2)	88.1(2)
Os(2)-Os(1)-C(4)	96.6(3)	93.3(2)
Os(2)-Os(1)-C(9)	71.9(2)	70.9(2)
C(1)-Os(1)-C(2)	92.5(3)	91.7(3)
C(1)-Os(1)-C(3)	173.3(3)	174.2(3)
C(1)-Os(1)-C(4)	91.7(4)	92.8(3)
C(1)-Os(1)-C(9)	83.0(3)	87.6(3)
C(2)-Os(1)-C(3)	93.0(3)	88.8(3)
C(2)-Os(1)-C(4)	97.3(4)	98.4(3)
C(2)-Os(1)-C(9)	94.4(3)	97.4(3)
C(3)-Os(1)-C(4)	91.4(4)	92.8(3)
C(3)-Os(1)-C(9)	92.7(3)	86.6(3)
C(4)-Os(1)-C(9)	167.4(4)	164.2(3)
Angles at Os(2)		
Os(1)-Os(2)-C(5)	90.4(3)	87.7(2)
Os(1)-Os(2)-C(6)	92.9(2)	89.0(2)
Os(1)-Os(2)-C(7)	91.6(3)	94.4(2)
Os(1)-Os(2)-C(8)	167.8(3)	166.1(2)
Os(1)-Os(2)-C(12)	70.7(2)	69.9(2)
C(5)-Os(2)-C(6)	175.5(3)	173.7(3)
C(5)-Os(2)-C(7)	91.1(3)	92.9(3)
C(5)-Os(2)-C(8)	88.9(4)	92.0(3)
C(5)-Os(2)-C(12)	86.9(3)	87.6(3)
C(6)-Os(2)-C(7)	92.0(3)	92.7(3)
C(6)-Os(2)-C(8)	87.3(4)	90.0(3)
C(6)-Os(2)-C(12)	94.2(3)	86.3(3)
C(7)-Os(2)-C(8)	100.6(4)	99.5(3)
C(7)-Os(2)-C(12)	162.2(3)	164.2(3)
C(8)-Os(2)-C(12)	97.1(3)	96.2(3)

Table XVIII. (continued).

---

	Z-isomer 28	E-isomer 30
Angles at C (carbonyl)		
Os(1)-C(1)-O(1)	177.5(8)	176.9(6)
Os(1)-C(2)-O(2)	177.9(7)	175.8(7)
Os(1)-C(3)-O(3)	178.0(8)	173.4(6)
Os(1)-C(4)-O(4)	180.(1)	175.5(7)
Os(2)-C(5)-O(5)	175.4(8)	176.8(7)
Os(2)-C(6)-O(6)	171.8(7)	174.8(6)
Os(2)-C(7)-O(7)	174.9(7)	176.6(7)
Os(2)-C(8)-O(8)	179.0(8)	178.5(7)
Angles at C (bridging ligand)		
Os(1)-C(9)-C(12)	104.0(4)	104.7(4)
Os(2)-C(12)-C(9)	107.5(4)	105.4(4)

---

Numbers in parentheses are estimated standard deviations in the least significant digits.

studied as a function of alkene concentration. It was hoped that higher concentrations of DMM would yield a product distribution favouring the cis-olefin derivatives. The results of this study are compiled in Table XIV which shows the range of alkene-to-3c varying from 61:1 to 202:1. An initial observation was a decrease, though nonlinear, in irradiation time (i.e., when 3c was judged totally consumed) as the alkene concentration was increased. Yet, in every case, a large portion of the starting DMM was recovered as isomerized DMF. Inspection and comparison of solution IR spectra from each reaction showed a similar rapid shift to lower frequency of the free ligand  $\nu_{\text{CO}_2}$  band to the value for free DMF. More salient to the present goal, the product distribution indicated no change when the original DMM concentration was increased or decreased. In fact, the proportions of the four osmium products could not even be reproduced when the reactions were repeated at the same olefin concentrations. The volatility of the mononuclear species could account for some of their erratic behaviour, but variations in the remarkably stable and nonvolatile  $\text{Os}_2$ -derivatives remained an anomaly. In order to define the possible roles of these osmium species in the bulk alkene isomerization and to determine whether under the present reaction conditions the same species are undergoing secondary photoreactivity, a qualitative photochemical study of the derived products was undertaken.

The long wavelength irradiation ( $\lambda \geq 370 \text{ nm}$ ) of  $\text{Os}(\text{CO})_4[\eta^2\text{-DMM}](27)$  with an excess of DMM left both starting materials unchanged (by IR spectroscopy). This should remove speculation on the involvement of 27 in the isomerization process. In parallel experiments,  $\text{Os}_2(\text{CO})_8$ -

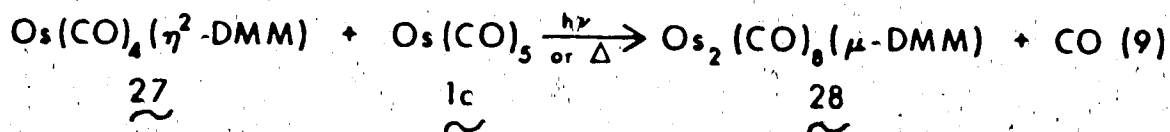
the presence of DMM, ca. 13.5h. IR monitoring showed no change in the position of the unbound olefin  $\nu_{\text{CO}_2}$  band. However, both 28 and 30 did react, to give virtually identical final solution IR spectra. What was surprising was the appearance of 28 in lieu of 30 in the residue from the reaction of the latter. This result implies an exchange of bound for free bulk alkene, perhaps entailing the intermediacy of an unsaturated  $[\text{Os}_2(\text{CO})_8]$  fragment.

In an effort to generate the putative  $[\text{Os}_2(\text{CO})_8]$  intermediate, the photoinduced metathesis of  $\text{Os}_2(\text{CO})_8[\mu\text{-MA}](\text{14})$  also was examined. The ready availability of 14 and what should be a driving force in replacing a "singly-activated" alkene with a "doubly-activated" one were factors in favour of attempting this exchange. With considerable puzzlement and distress it was discovered that, contrary to the reactions of 28 and 30, free DMM had isomerized to DMF and the major species isolated was the dinuclear DMF complex 30. Even with this unexpected behaviour, the intermediacy of an  $[\text{Os}_2(\text{CO})_8]$  fragment must be questioned, specifically in terms of its role in alkene isomerization (which was not indicated for 28 nor 30).

Even though the mononuclear 27 did not bring about isomerization of free DMM, the plausibility of an  $[\text{Os}(\text{CO})_4]$  moiety resulting from the fragmentation of 3c and its participation in the DMM-DMF conversion required investigation. The reaction of  $\text{Os}(\text{CO})_5(\text{1c})$  with the alkene thus was pursued. Thermolysis of 1c with DMM required high temperature ( $88^\circ\text{C}$ ) and a longer reaction time than the photoreaction of 3c, and the lack of isomerized free alkene rules out a thermally-activated conversion through  $[\text{Os}(\text{CO})_4]$ . The photolysis of 1c and DMM gave a



Consequently this became the preferred synthetic route to and allowed the spectroscopic characterization of 27. In the hope of improving on the isolation of 27, a stoichiometric photoreaction was carried out. Free ligand isomerization was not apparent, but a number of species which could be identified included a minor amount of 3c, 27 and a few crystals of 28. The last compound most probably arose from a secondary photoreaction (or thermal reaction) as depicted below (equation (9)):



However, the prominent observation of this study is the minor role played by an  $[\text{Os}(\text{CO})_4]$  fragment in the isomerization process.

### III. Photoreactions of 3c with Other Disubstituted Alkenes.

To test the capacity of the reaction system to isomerize olefins, the photolysis of 3c also was studied with diethyl maleate (DEM,  $\text{Z-C}_2\text{H}_2(\text{CO}_2\text{CH}_2\text{CH}_3)_2$ ) and cis-stilbene ( $\text{Z-C}_2\text{H}_2\text{Ph}_2$ ). The reaction with DEM (Table XIV, entry viii) seemed to follow a course similar to DMM. Diagnostic of alkene isomerization was a lowering of the free ligand  $\nu_{\text{CO}_2}$  frequencies in the IR spectra of the reaction solution. Contrary to the DMM reaction, only two products were observed whose identity was unsure until the analogous diethyl fumarate (DEF,  $\text{E-C}_2\text{H}_2(\text{CO}_2\text{CH}_2\text{CH}_3)_2$ ) reaction gave the same species. Thus, isomerization

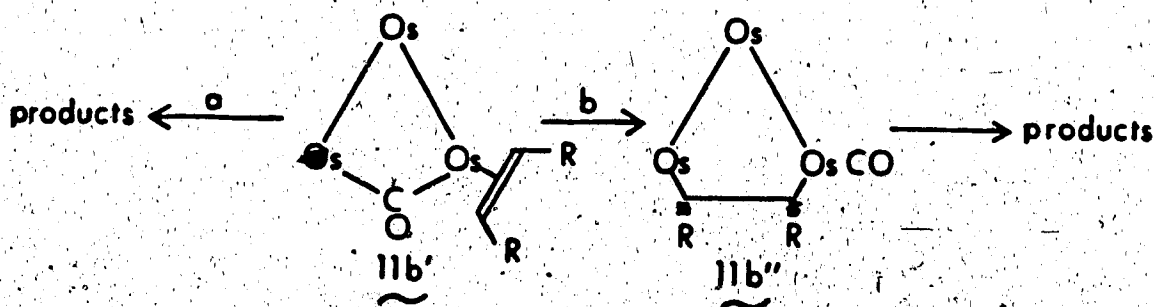
of DEM to DEM appears more facile than DMM to DMM conversion such that no DEM derivatives have been produced. Perhaps more valuable to the entire scheme of things was the reaction with cis-stilbene. IR spectra of the reaction solution gave no indication of the desired products, but as with DMM, a copious quantity of solid material obtained upon solvent removal. Sublimation of the residue gave a pale yellow solid which was identified as trans-stilbene ( $E-C_2H_2Ph_2$ ).

Therefore, even though osmium products did not form, geometric isomerization of the organic ligand nevertheless occurred.

#### IV. Conclusions.

The observation of remarkably facile cis  $\rightarrow$  trans isomerization of the olefinic ligand as the focal point of this chapter also holds relevance to the photofragmentation of  $Os_3(CO)_{12}$ . The results reported in Section II.C., even though the reaction of 14 might suggest otherwise, seem to rule against the involvement of either  $[Os(CO)_4]$  or  $[Os_2(CO)_8]$  as isomerization catalysts. This, in conjunction with the cis-stilbene reaction, implicates a reactive entity prior to cluster fragmentation and suggests that the scheme presented in equation (8)(Chapter Two) is best abandoned.

The intermediacy of  $Os_3(CO)_{12}(\eta^2\text{-alkene})(11b')$  proposed in Chapter Two remains plausible. Fragmentation directly to products (path a)



or rearrangement to an alkane bridged species ( $11b''$ ) prior to frag-

reduction (path b) would require in either case a reduction in the C-C bond order as the alkene would span two metal centers. This reduction, if accompanied by rotation around the newly-forming C-C single bond, can effect isomerization of the bound ligand, most logically, in the dinuclear products. To account for the cis  $\rightarrow$  trans conversion of bulk alkene, a rapid reversal of path b is necessary, since path a leads to products that do not isomerize bulk alkenes readily. The lack of isomerization in the ruthenium system can be seen as a consequence of weaker Ru-Ru bonds<sup>44</sup> and the greater propensity to support a bridging carbonyl group<sup>9c</sup> to form 11a which gives fragmentation to mononuclear products, most likely via path a. However, strong Os-C bonds in 11b", reasonably assumed from the stability of the resulting dinuclear products (except for cis-stilbene), in fact may inhibit a rapid reversal. An alternate pathway which could circumvent this troublesome aspect entails the photoinduced homolysis of an Os-Os bond to produce a diradical species.<sup>21</sup> Such an intermediate, though it could explain both the isomerization of free ligand and the multiple products from the DMN reaction, has been largely discounted based on quantum yield studies with chlorocarbons.<sup>50,66</sup> Their comparably higher quantum yields<sup>66</sup> and moderately facile photofragmentation of 3c may place olefins ahead of chlorocarbons as better radical traps, at least under the present conditions. An assessment of this discrimination was not available prior to this work since these are the first reported photoreactions of 3c with cis-disubstituted olefins. The intention here is not to necessarily revitalize the diradical approach, but to emphasize the need to consider and accommodate the isomerization results in future mechanistic studies.

## CHAPTER FOUR

### PHOTOREACTIONS OF $\text{Os}_3(\text{CO})_{12}$ WITH ALKYNES

#### I. Introduction.

A dominant feature in the reported chemistry of the  $\text{M}_3(\text{CO})_{12}$  complexes involves their thermal reactivity towards alkynes (see Chapter One). In these reactions, the trinuclear framework was either maintained or expansion with the formation of larger clusters was observed. Consequently, mono- and binuclear alkyne derivatives of the iron-triad metals are rare. Of the binuclear derivatives obtained from the trinuclear clusters, two structural types have been identified: (1) "fly-over" compounds (i.e.,  $9^{31}$ ) consisting of a metallacyclopentadiene fragment and a metal-metal donor-acceptor bond, and (2) "perpendicular" alkyne-bridged species with the alkyne behaving as a four-electron donor (i.e.,  $\text{Fe}_2(\text{CO})_4(\text{C}_2^t\text{Bu}_2)_2$   $^{95}$ ). With the precedent established by the saturated diosmacycles, the less common "parallel" bonding mode for alkynes  $^{96}$  was anticipated from the photoreaction of  $\text{Os}_3(\text{CO})_{12}$  with alkynes.

#### II. Reaction with Dimethylacetylenedicarboxylate [DMAD]. Preparation and Characterization of $\text{Os}_2[\mu_{||}\text{-alkyne}]$ and an Unusual Alkyne-Linked Species.

With the modest success afforded by "activated" alkenes; especially the disubstituted DMM and DMF (in terms of product stability), dimethylacetylenedicarboxylate [DMAD,  $\text{C}_2(\text{CO}_2\text{CH}_3)_2$ ] was an obvious initial alkyne of choice. The photoreaction of 3c with DMAD (Table XIX, entry i) led to features in the solution IR spectrum recognizable

Table XIX. Summary of Photoreactions of  $\text{Os}_3(\text{CO})_{12}$  (3c) with Alkynes.

entry	alkyne	3c (mg)	Mass of alkyne (g)	mL solvent <sup>a</sup>	apparatus, reaction time (h)	Products (compound number, mg)
i	DMAD	501.0	1.16	250	(f), 26	33, 40; 34, 30.
ii	HFB	319.7	purge	150	(1), 35	b
iii	HFB	536.6	5.0	230	(1), 35	$\text{Os}_2(\text{CO})_8$ (HFB), 5.
iv	BTMSA	319.3	0.63	150	(1), 120	$\text{Os}(\text{CO})_4$ (BTMSA) <sup>c</sup> .
v	$\text{C}_2\text{H}_2$	520.9	purge	200	(1), 5	35, 20; 36, 8; 37, 17.3.
vi	DPA	507.0	1.50	250	(1), 8.5	38, 814; 39, 15; 40, 2; 9, d.
vii	DPA	527.0	6.02	250	(1), 10	38, 1012; 39, e; 9, e.
viii	DPA	78.0	1.53	30	(3), 1	38, f; 39, f; 9, e.
ix	DPA	112.0	0.33	40 <sup>g</sup>	(2a), 146	38, 220; 40, e.
x	DPA	78.7	0.23	30 <sup>h</sup>	(3), 1	38, 20; 40, e; 9, 35.

(a) benzene unless stated otherwise; (b) no products identified/isolated; (c) mass spec only; (d) mixture with 39; (e) minor quantities; (f) ~ 1:1 mixture of 38 and 9 (qualitative); (g) under one atmosphere  $\text{CO}$ ; (h) pentane solvent.

DMAD-dimethylacetylenedicarboxylate, HFB-hexafluoro-2-butyne, BTMSA-bis(trimethylsilyl)acetylene,

DPA-diphenylacetylene.

for an  $\text{Os}_2$ -species, but gave no indication for the presence of the  $\text{Os}[\eta^2\text{-alkyne}]$  derivative, the other expected product of the reaction. The appearance of other terminal carbonyl bands, though, implied that a mixture of compounds was formed. Isolation of products from the crude reaction mixture was tedious. After several trituration "cycles" (see Chapter Seven, Section VI.2), followed by preparative TLC, two osmium-containing complexes were obtained (Table XIX) in poor yields. One of the compounds was readily identified. The IR spectrum of the pure compound, its mass spectrum which exhibited a parent molecular ion at 748 m/e and an elemental analysis were all consistent with the formulation  $\text{Os}_2(\text{CO})_8[\text{DMAD}](33)$ . Three  $^{13}\text{C}$  carbonyl resonances in a 2:1:1 ratio revealed that the symmetry of the molecule was compatible with the 1,2-diosmacyclobutene type structure (cf.  $\text{Os}_2(\text{CO})_8[\mu\text{-C}_2\text{H}_4](16)$ , Table XI). A fourth signal in this region at  $\delta 170.5$  could be assigned to the carboxylate carbonyl upon comparison with the analogous 1,2-diruthenacyclobutene (at 173K,  $\delta(\text{Ru-CO}) = 195.8\text{--}181.2$ ,  $\delta(\text{CO}_2\text{CH}_3) = 170.6$  ppm)<sup>97</sup>. The lone  $^{13}\text{C}$  signal at  $\delta 114.0$ , out of necessity and due to its vicinity to the olefinic carbon region [ $\delta(\text{CH=}) = 130.0$  ppm for DMF], is assigned to the bridgehead carbons of DMAD. To confirm the diosmacyclobutene nature of 33, an X-ray structural analysis was performed. Figure IX shows a perspective view of the molecule together with the numbering scheme. Features of the crystallographic determination appear in Table XX.

The analysis clearly substantiates the unsaturated diosmacyclic core. The C(5)-C(5)' distance of 1.33(1) Å (Table XXI) is indicative of a double bond.<sup>73</sup> Albeit in the range of typical single bonds,<sup>72</sup>

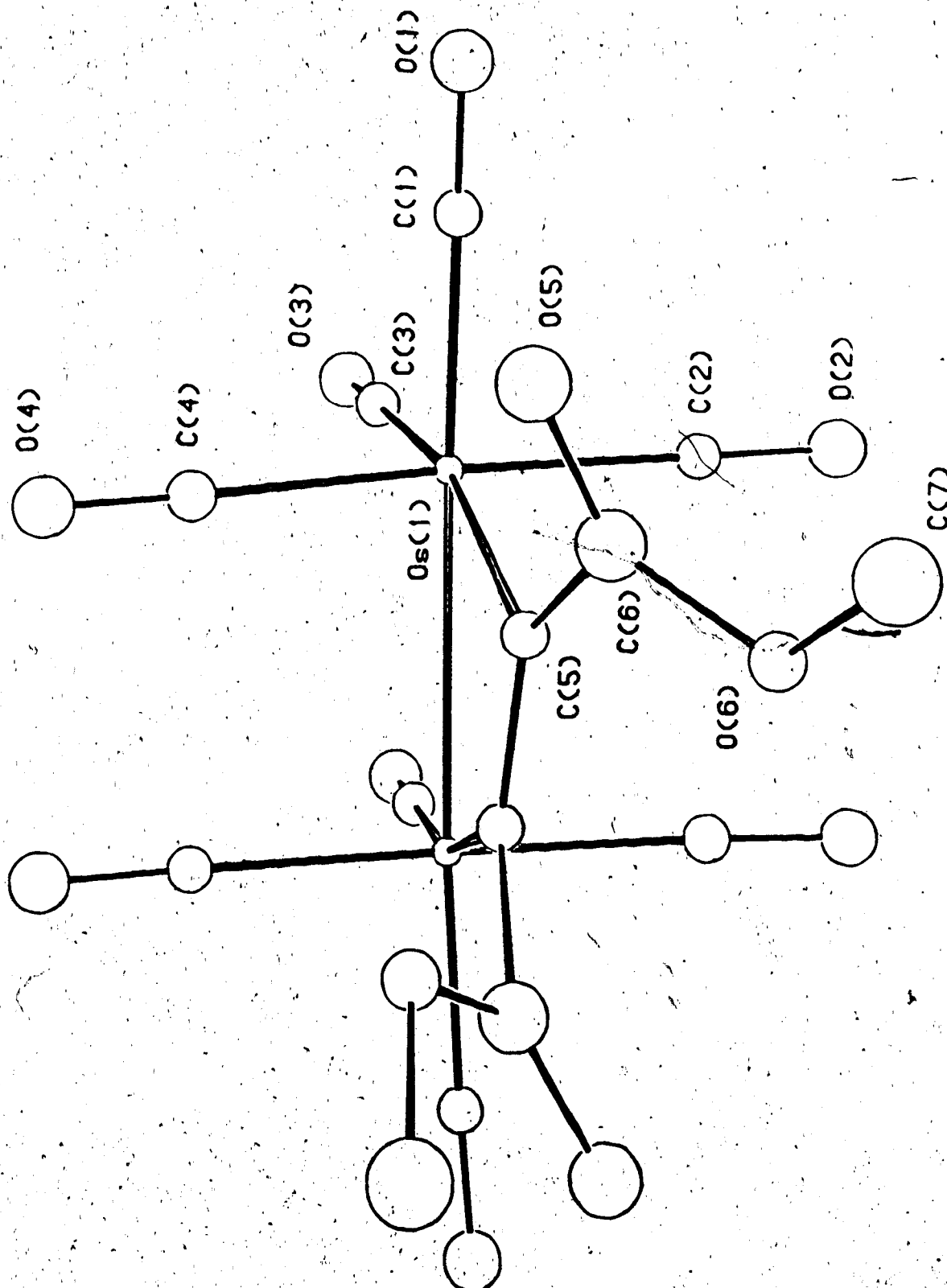


**Figure IX.** Molecular structure of  $\text{Os}_2(\text{CO})_8[\eta\text{-}\eta^1, \eta^1\text{-C}_2(\text{CO}_2\text{CH}_3)_2](33)$   
 (Dr. R.G. Ball, SDL/U of A, 1983).

Table XX. Summary of Crystallographic Data for  $\text{Os}_2(\text{CO})_8[\mu\text{-C}_2(\text{CO}_2\text{CH}_3)_2]_2$  (33) and  $\text{Os}_2(\text{CO})_6(\text{DMAD})_4$  (34).

	33	34
temperature	-50°C	23°C
formulae	$\text{C}_{14}\text{H}_6\text{O}_{12}\text{Os}_2$	$\text{C}_{30}\text{H}_{24}\text{O}_{22}\text{Os}_2$
formula weight	746.60	1116.91
crystal dimensions, mm	0.16x0.20x0.13	0.04x0.13x0.24
crystal system	Monoclinic	Triclinic
space group	$\text{C2/C}$	$\text{P}\bar{1}$
a, Å	13.211 (3)	12.363 (2)
b, Å	11.333 (5)	14.457 (3)
c, Å	11.863 (2)	11.504 (3)
$\alpha$ , deg	90	93.71 (2)
$\beta$ , deg	101.26 (2)	115.99 (2)
$\gamma$ , deg	90	74.04 (2)
volume, Å <sup>3</sup>	1741.87	1773.19
Z	4	2
d, g cm <sup>-3</sup>	2.847	2.092
$\mu$ , cm <sup>-1</sup>	146.60	72.55
take-off angle, deg	3.05	3.05
detector aperture, mm	2.00 + 0.50 tan $\theta$ mm horizontal 4.0 mm vertical	
crystal-to-detector distance, mm	205	205
scan type	$\omega$ -2 $\theta$	$\omega$ -2 $\theta$
scan rate, deg min <sup>-1</sup>	10.1-2.1	10.1-1.7



Table XX. (continued).

scan width, deg		$0.76 + 0.35 \tan \theta$	$0.65 + 0.35 \tan \theta$
2 $\theta$ limit, deg		55.00	60.00
reflections measured	unique	2005	10307
	$I > 3.00(I)$	1707	6514
absorption correction		yes	yes
parameters refined		126	487
agreement factors	R	0.029	0.030
	R <sub>w</sub>	0.042	0.038

Table XXI. Relevant Bond Distances (Å) for  $\text{Os}_2(\text{CO})_8[\mu\text{-C}_2(\text{CO}_2\text{CH}_3)_2](33)$ .

Metal-Metal		C-C (bridging)	
Os-Os'	2.8975(1)	C(5)-C(5)'	1.33(1)
Metal-C (bridging)			
Os-C(5)	2.138(5)		
Metal-C (carbonyl)		C-O (carbonyl)	
Os-C(1)	1.919(6)	C(1)-O(1)	1.116(7)
Os-C(2)	1.940(6)	C(2)-O(2)	1.132(8)
Os-C(3)	1.955(6)	C(3)-O(3)	1.131(8)
Os-C(4)	1.976(6)	C(4)-O(4)	1.096(7)

Numbers in parentheses are estimated standard deviations in the least significant digits.

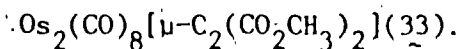
Atoms marked ' are related to the unmarked atoms by the two-fold symmetry axis.

the Os-Os' distance (2.8975(1)Å) is longer than found in the saturated analogs (2.8788(4)Å in 28, 2.872(0)Å in 30). This expansion, and the shortening of the Os-C(5) bond length (2.138(5)Å) from the "normal" Os-C(0) distances observed for 28 (average 2.211(7)Å) and 30 (average 2.213(7)Å) jointly can be suggested to accomodate the change in hybridization of the bridging carbon atoms from  $sp^3$  in the diosmacyclobutanes to  $sp^2$  in 33. It will be seen in Chapter Five that this increased strength of the interaction between DMAD and the dinuclear framework will allow for interesting derivative chemistry not available to the saturated analogs.

As expected from the more rigid parallel alkyne bridge, the four-membered ring in 33 is decidedly less puckered than in the saturated relatives. The torsional angle between the Os-Os' and C(5)-C(5)' vectors is  $8.4^\circ$  in 33 (Table XXII) whereas the corresponding angles in 14, 28 and 30 vary between  $23.0^\circ$ ,  $18.5^\circ$  and  $23.2^\circ$ . Consequently the equatorial carbonyls in 33 are more eclipsed with the average Os-Os' twist angle reduced to  $9^\circ$  from  $19^\circ$  in 28 and 30. It is interesting to note that in two structurally similar compounds, the dimetallacycle either is essentially planar,  $Pt_2(CO)_2(PPh_3)_2(\mu-\eta^1, \eta^1-DMAD)^{98}$ , or only slightly distorted,  $Fe_2(CO)_8(\mu-\eta^1, \eta^1-C_6F_4)$  (C-C and Fe-Fe vectors are skewed by  $1.6^\circ$ )<sup>99</sup>. The sterically less congested environment of the metal in the former and the aromaticity of the bridging o-phenylene unit in the latter can be cited as reasons for the more symmetrical rings.

With regard to the rest of the molecule, the disposition of the ancillary carbonyl ligands shows little difference from the diosma-

Table XXII. Relevant Bond Angles and Torsional Angles (deg) for



## Angles at Os

Os'-Os-C(1)	168.3(2)
Os'-Os-C(2)	90.1(2)
Os'-Os-C(3)	96.1(2)
Os'-Os-C(4)	88.1(2)
Os'-Os-C(5)	68.3(2)
C(1)-Os-C(2)	91.3(3)
C(1)-Os-C(3)	95.5(2)
C(1)-Os-C(4)	89.2
C(1)-Os-C(5)	100.1(2)
C(2)-Os-C(3)	92.5(2)
C(2)-Os-C(4)	172.9(2)
C(2)-Os-C(5)	89.1(2)
C(3)-Os-C(4)	94.6(2)
C(3)-Os-C(5)	164.3(2)
C(4)-Os-C(5)	83.8(2)

## Angles at C (carbonyl)

Os-C(1)-O(1)	179.2(6)
Os-C(2)-O(2)	177.0(5)
Os-C(3)-O(3)	177.4(5)
Os-C(4)-O(4)	175.5(5)

## Angles at C (bridging)

Os-C(5)-C(5)'	111.2(2)
---------------	----------

## Torsional Angles

## Carbonyl ligands

C(1)-Os-Os'-C(1)'	-10.2
C(3)-Os-Os'-C(3)'	8.2

## Bridging ligand

C(5)-Os-Os'-C(5)'	5.2
Os-C(5)-C(5)''-Os'	11.3
Os'-Os-C(5)-C(5)'	-8.4

Numbers in parentheses are estimated standard deviations in the least significant digits.

Atoms marked ' are related to the unmarked atoms by the two-fold symmetry axis.

cyclobutane compounds. The range of Os-C (carbonyl) bond distances (1.919(6) - 1.976(6) Å) parallels those previously reported, but reveals no particular trends corresponding with the location of the carbonyl groups (i.e., axial versus equatorial). Equally, those groups cis to the bridge are bent toward that moiety to the same extent as in 28 and 30 (Table XXII), with the axial carbonyl groups leaning more (11.7°) than the equatorial moieties (3.5° on the average).

The second reaction product presented difficulties in its structural elucidation. Even though mass spectral and analytical data pointed to the molecular formulation  $\text{Os}_2(\text{CO})_6(\text{DMAD})_4$  (34), additional spectroscopic data were not definitive for a specific structural type. The pattern of terminal carbonyl stretching bands in the IR was indicative of a metal tricarbonyl fragment,<sup>83</sup> and the appearance of a band in the low end of the carboxylate carbonyl region hinted at a possible bonding involvement of a  $\text{CO}_2\text{Me}$  group. Four resonances in the  $^1\text{H}$  NMR methoxy region ( $\delta$  ~ 3.7), corresponding to the same number of methoxy carbon  $^{13}\text{C}$  signals around  $\delta$  52.0, and eleven resonances over the  $^{13}\text{C}$  NMR range  $\delta$  198.0 - 59.2 implied a complex connectivity of the organic moieties in 34. In the absence of corroborating evidence, efforts were directed toward a solid state determination. Fortunately, X-ray quality crystals were easily obtained from a slowly evaporating methanol solution. The crystallographic analysis revealed that the unit cell (P1, Table XX) contained two independent dimers, each residing on a center of symmetry. The results are depicted in Figure X, which unveils a unique arrangement of the alkyne groups in

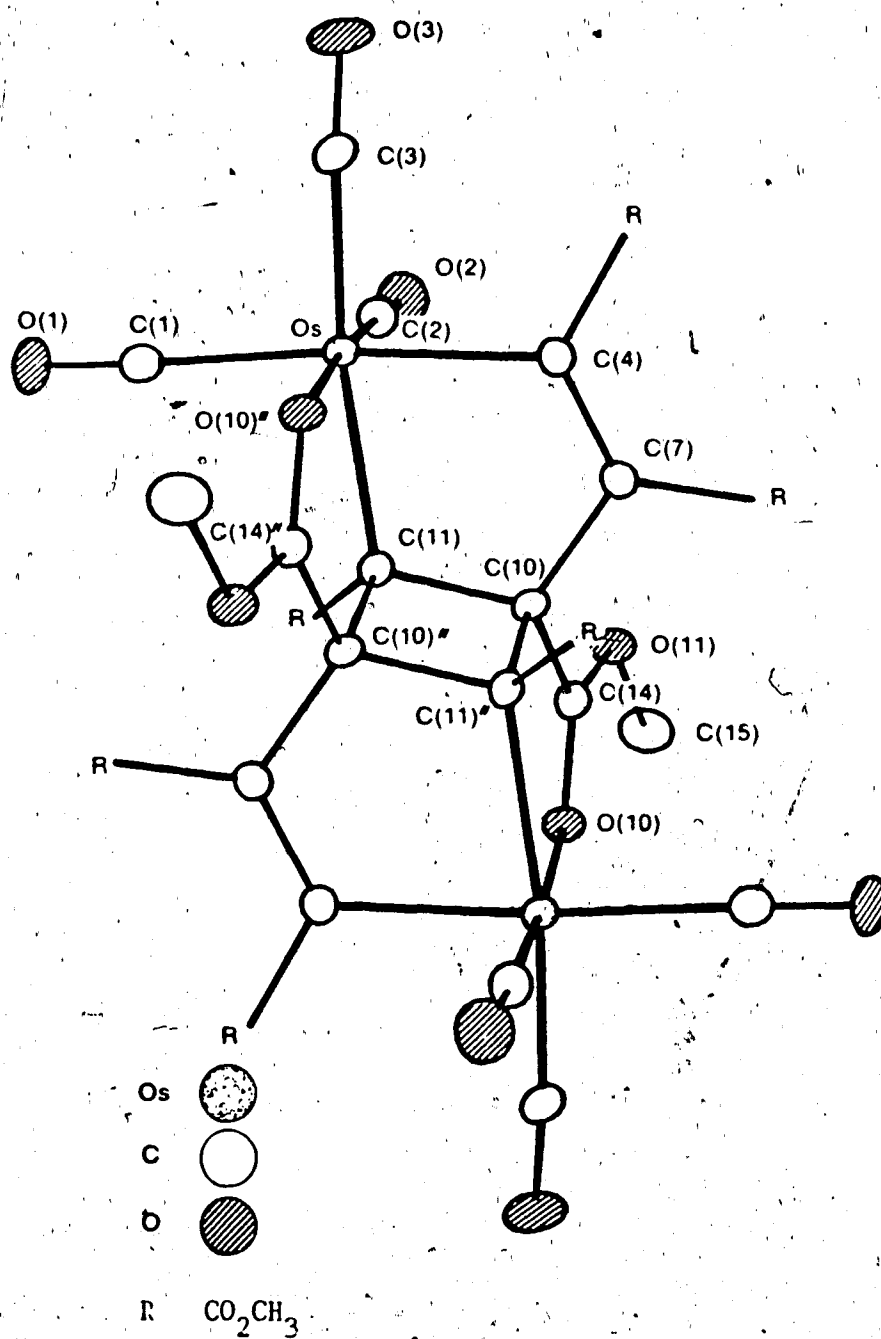


**Figure X.** Molecular structure of  $\text{Os}_2(\text{CO})_6(\text{DMAD})_4$  (34)

(Dr. R.G. Ball, SDL/U of A, 1983).

the centrosymmetric dimeric molecule. A comparison of bond distances (Table XXIII) and angles (Table XXIV) gives two very similar independent molecules.

The dimer is best described as arising from the condensation of two osmacyclopentadiene fragments which then form a central cyclobutane ring (Figure XI). The C-C bond distances within the carbocycle (C(10)-C(11) = 1.578(7) Å and C(10)-C(11)" = 1.592(8) Å are averaged values) are somewhat longer than the "normal" single bond value of 1.54 Å<sup>73</sup> and may be a factor contributing to the strict planarity of the ring. In conjunction with this planarity, the virtually identical bond distances and closely approximate right angles (C(10)-C(11)-C(10)", 90.7(4)° and C(11)-C(10)-C(11)", 89.3(4)°) very nearly define the four-membered ring as a square. Two heterocycles also are featured in these molecules. The difference in the bond lengths Os-C(4) (2.101(5) Å, sp<sup>2</sup> carbon) and Os-C(11) (2.156(5) Å, sp<sup>3</sup> carbon) in the osmacyclopentene moiety mirrors the change in the Os-C(bridging) distance from 33 to 28 or 30. The C(4)-C(7) distance of 1.350(8) Å is that of a double bond<sup>73</sup>, but the value of 1.490(7) Å for C(7)-C(10) lies between a single and a double bond, reflecting the unusual linkage of alkynes.

In order to fulfill the electronic requirements at each osmium, an oxygen atom of a carboxylate carbonyl from the adjacent osmacyclopentene ring coordinates in an end-on fashion and forms the second type of heterocycle. As a result of coordination, the C(14)-O(10) distance lengthens to 1.244(7) Å compared to 1.189(7) Å for the unbound carbonyl moieties. The Os-O(10)" distance is in the range of reported

Table XXIII. Comparison of Relevant Bond Distances (Å) for the  
Independent Molecules of  $\text{Os}_2(\text{CO})_6[\text{C}_2(\text{CO}_2\text{CH}_3)_2]_4(34)$ .

	A	B
Metal-C (carbonyl)		
Os-C(1)	1.981(7)	1.966(6)
Os-C(2)	1.855(6)	1.866(6)
Os-C(3)	1.944(6)	1.932(7)
Metal-C (ring)		
Os-C(4)	2.104(5)	2.098(5)
Os-C(11)	2.154(5)	2.159(5)
Metal-O (carboxylate)		
Os-O(10)"	2.135(4)	2.129(4)
C-O (carbonyl ligands)		
C(1)-O(1)	1.111(8)	1.126(7)
C(2)-O(2)	1.132(7)	1.131(7)
C(3)-O(3)	1.119(8)	1.133(8)
C-O (O bound to Os)		
C(14)-O(10)	1.240(7)	1.248(7)
C-C (ring)		
C(4)-C(7)	1.345(8)	1.356(8)
C(7)-C(10)	1.494(7)	1.486(7)
C(10)-C(11)	1.573(7)	1.584(7)
C(10)-C(11)"	1.596(8)	1.589(7)

Numbers in parentheses are estimated standard deviations in the least significant digits.

The " indicates atoms centrosymmetrically related to unprimed atoms of the same name.



Table XXIV. Comparison of Relevant Bond Angles (deg) for the Independent Molecules of  $\text{Os}_2(\text{CO})_6[\text{C}_2(\text{CO}_2\text{CH}_3)_2]_4$  (34).

	A	B
Angles at Os		
C(1)-Os-C(2)	94.3(3)	95.0(3)
C(1)-Os-C(3)	93.2(3)	91.4(3)
C(1)-Os-C(4)	174.3(2)	174.7(3)
C(1)-Os-C(11)	95.1(2)	95.5(3)
C(2)-Os-C(3)	92.3(3)	91.4(3)
C(2)-Os-C(4)	83.6(2)	83.6(2)
C(2)-Os-C(11)	95.4(2)	95.7(2)
C(3)-Os-C(4)	92.1(2)	93.7(3)
C(3)-Os-C(11)	168.2(2)	169.6(2)
C(4)-Os-C(11)	79.9(2)	79.7(2)
O(10)"-Os-C(1)	87.2(2)	86.8(2)
O(10)"-Os-C(2)	175.3(2)	175.6(2)
O(10)"-Os-C(3)	92.1(2)	92.6(2)
O(10)"-Os-C(4)	94.5(2)	94.3(2)
O(10)"-Os-C(11)	80.1(2)	80.0(2)
Angles at C (carbonyl ligands)		
Os-C(1)-O(1)	177.7(6)	177.1(6)
Os-C(2)-O(2)	177.0(6)	177.3(5)
Os-C(3)-O(3)	175.1(6)	178.3(7)
Angles within ring systems		
Os-C(4)-C(7)	118.5(4)	118.3(4)
C(4)-C(7)-C(10)	117.3(5)	118.0(5)
C(7)-C(10)-C(11)	112.4(4)	111.3(4)
C(7)-C(10)-C(11)"	115.7(5)	115.6(4)
C(10)-C(11)-C(10)"	90.6(4)	90.8(4)
Os-C(11)-C(10)	109.4(3)	111.6(3)
Os-C(11)-C(10)"	111.1(3)	109.2(3)
C(11)-C(10)-C(14)	113.4(5)	113.9(4)
C(11)"-C(10)-C(14)	110.6(4)	111.4(4)
O(10)-C(14)-C(10)	121.4(5)	120.8(5)
Os"-O(10)-C(14)	116.6(4)	117.1(4)

Numbers in parentheses are estimated standard deviations in the least significant digits.

The " indicates atoms centrosymmetrically related to unprimed atoms of the same name.

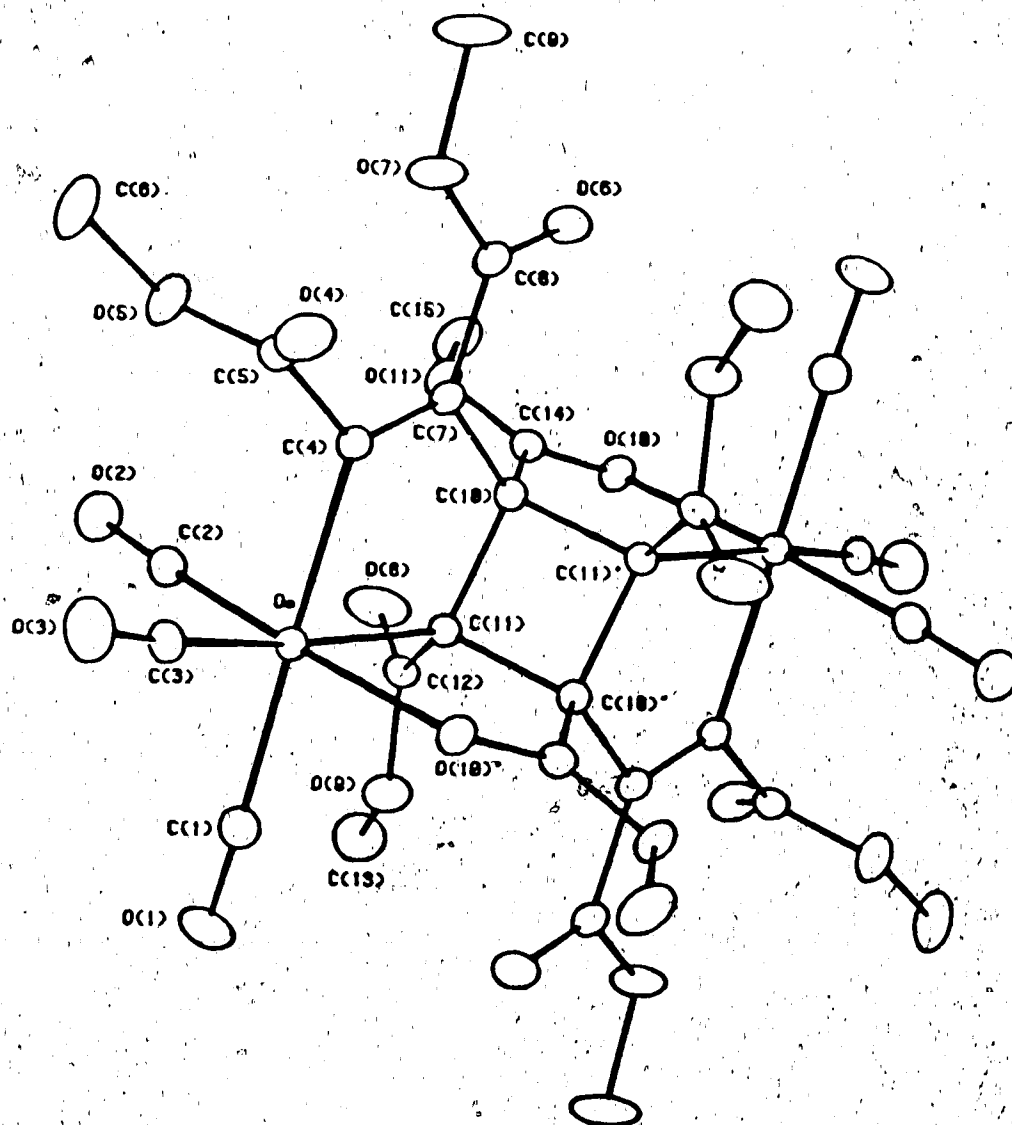


Figure XI. View of cyclobutane ring in 34.

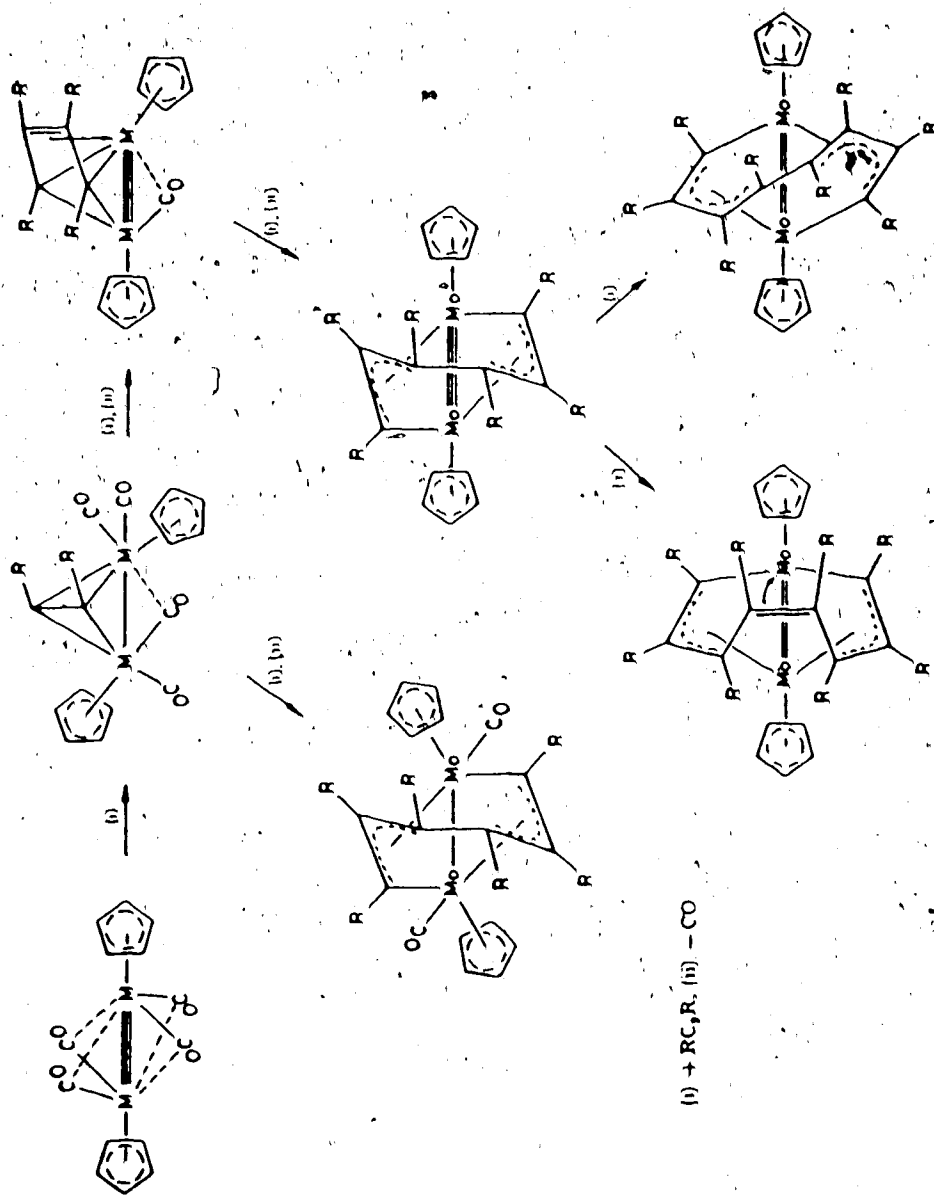
only slightly compressed from the expected  $120^\circ$  for an " $sp^2$ " oxygen atom (with two lone pairs of electrons). Thus, the IR stretching frequency at  $1601\text{ cm}^{-1}$  is confidently assigned to the coordinated acyl group. Similar lowering of stretching frequencies has been observed in a series of  $\text{HOs}_3(\text{CO})_{10}((\text{CHR}-)\text{C}(\text{O}-)\text{OR}')$  complexes<sup>103</sup> which also contain coordinated acyl oxygen donors. As well, the low field  $^{13}\text{C}$  resonance at  $\delta 198.0$  undoubtedly is due to  $\text{C}(14)$ , especially since the remaining carbonyl signals appear ca.  $\delta 175$  as seen for osmium and carboxylate carbonyls (cf. Tables XI and XIII).

A facial arrangement of three carbonyl ligands completes the pseudo-octahedral coordination sphere surrounding each osmium. Distortion of the geometry lies in the direction of the ring structures. The angles  $\text{C}(4)-\text{Os}-\text{C}(11)$  and  $\text{C}(11)-\text{Os}-\text{C}(10)$  are contracted substantially from  $90^\circ$  ( $79.8(2)$  and  $80.0(2)^\circ$  respectively) and, as a result, the tricarbonyl face has opened up with interligand angles averaging  $93^\circ$ . The diversity of atom types trans to the carbonyl ligands has a noticeable influence on the  $\text{Os}-\text{C}$  (carbonyl) bond lengths. The shortest distance,  $\text{Os}-\text{C}(2)$  ( $1.860(6)\text{\AA}$ ), is located opposite the end-on bonded ester carbonyl group. The shortness most probably reflects the increased electron density on the osmium center, now available for back bonding, as a result of  $\sigma$  and  $\pi$  electron donation from the oxygen donor. Bond shortening effects have been seen in an iron complex which contains a similarly coordinated ester group<sup>104</sup> and in  $\text{Mn}(\text{CO})_4^-$

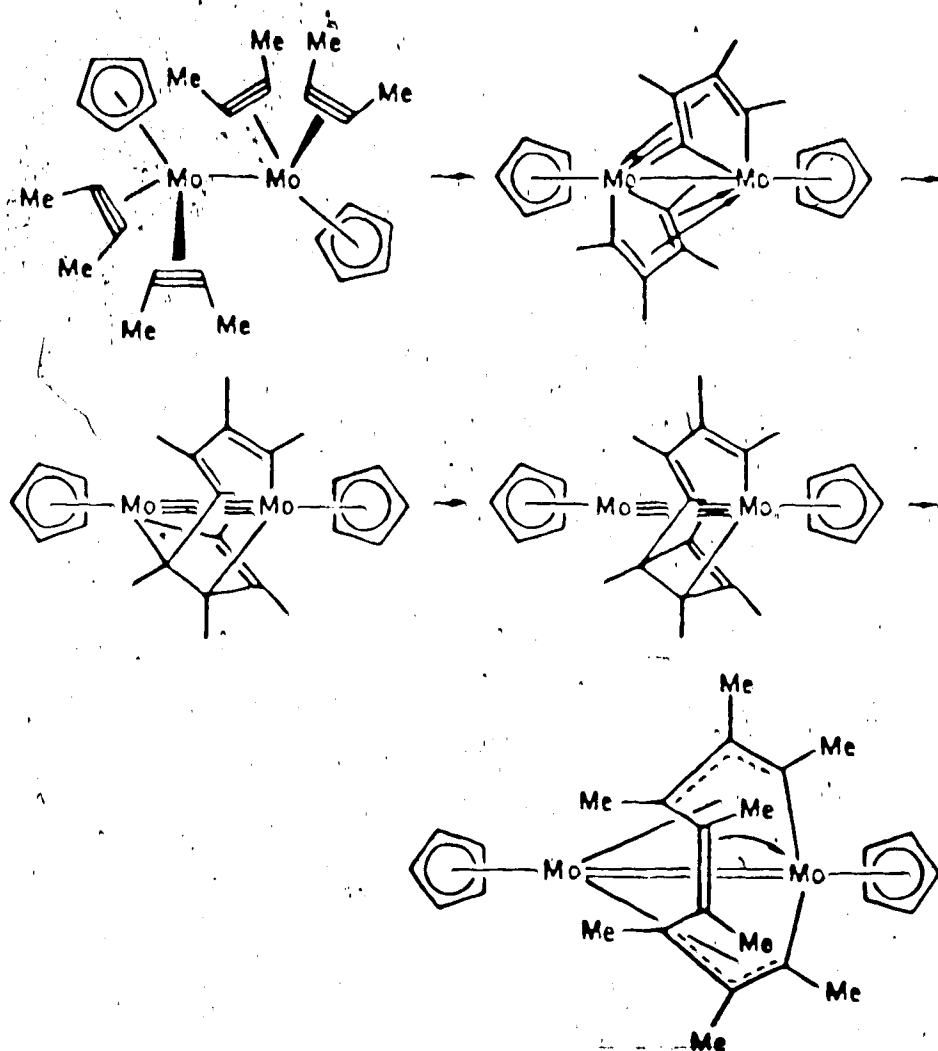
Compound	Os-O distance, Å	reference
H Os <sub>5</sub> C(CO) <sub>14</sub> (C(O-)OEt)	2.118(12)	100
HOs <sub>3</sub> (CO) <sub>10</sub> (C(O-)CH <sub>2</sub> Ph)	2.12(1)	101
HOs <sub>3</sub> (CO) <sub>8</sub> (C(O-)C(CHMe-)CHCHCEt)	2.138(9)	72
Os <sub>3</sub> (CO) <sub>10</sub> (MeO(O-)CN <sub>2</sub> C(O-)OMe)	2.144(6)	102
10s <sub>5</sub> C(CO) <sub>14</sub> (C(O-)OMe)	2.17(3)	100
Os <sub>2</sub> (CO) <sub>6</sub> (DNAD) <sub>4</sub> (34)	2.132(5)	this work

Competition for metal back donation to the  $\pi^*$  orbital on C(4), reinforced by its electron withdrawing carboxylate substituent, may argue for the longer Os-carbonyl bond length.

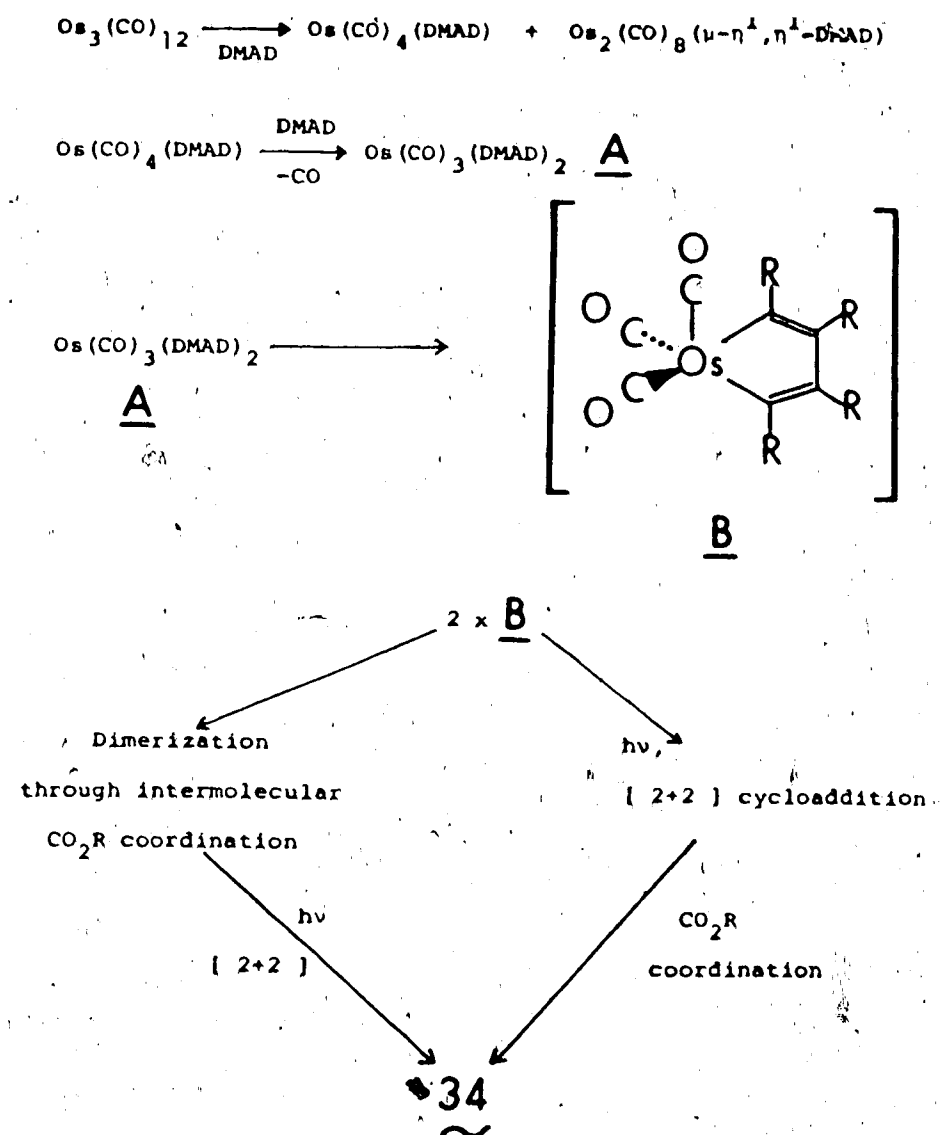
For multiple coupling of alkynes on metal centers, sequential addition to form linear polyenyl subunits with each end attached to intact metal-metal bonded fragments has been observed (Scheme VI<sup>106</sup>). Green also has reported<sup>107</sup> a nine-membered unsaturated metallacycle which interacts with a second metal center in a "fly-over" fashion. It was suggested that the structure could be achieved by "insertion" of a C=C bond from a molybdenacyclopentadiene into an Mo-C bond of an adjacent metallacycle followed by reductive elimination and a ring-opening reaction (Scheme VII<sup>107</sup>). In order to plausibly describe the formation of 34, an osmacyclopentadiene intermediate must be invoked. If the photoreaction proceeds as earlier described for olefins, an extruded  $[\text{Os}(\text{CO})_4]$  should be scavenged by free DNAD (Scheme VIII). The lack of simple mononuclear osmium alkyne carbonyl complexes from the reaction implies either some inherent instability or enhanced reactivity of such a species, which in this case could lead to further substitution to give A. Coupling of the alkynes, a well-known phenomenon in metal-acetylene chemistry<sup>108,109</sup>, would result in the osmacyclopentadiene fragment B. This now coordinatively unsaturated species can condense with a second unit via a two step process. A photochemically-allowed [2+2] cycloaddition will give the central



Scheme VI. Alkyne linkage at a dimetal center (adapted from Knox, et al.<sup>106</sup>).



Scheme VII. Alkyne linkage at a dimetal center  
(adapted from Green, et al.<sup>107</sup>).



Scheme VIII. Proposed formation of 34.



cycloaddition. Isomeric forms of the dimer are then possible. A "head-to-tail" approach of two unsaturated species (Os as the "head") would result in the structure depicted for 34 ("trans" arrangement of the two  $\text{Os}(\text{CO})_3$  fragments). The second isomer ("cis") arising from a "head-to-head" approach was not isolated from the osmium reaction but was obtained along with the "trans" isomer and structurally characterized from the analogous ruthenium reaction.<sup>110</sup> The implications of this are unknown presently, but it should be mentioned that the "cis- $\text{Ru}_2(\text{CO})_6(\text{DNAD})_4$ " was only a minor product in the above reaction. It is nonetheless obvious that the photochemical method does not favour the formation of mononuclear osmium-DNAD derivatives.

### III. Reactions With Other Alkynes.

Even though the marginal success of the DNAD reaction and the propensity of many alkynes to form a variety of osmium carbonyl derivatives were uncomfortable realities, it was important to determine whether the complicated photobehaviour of DNAD was a general phenomenon for alkynes. Thus, a broad range but limited number of electronically different alkynes were enlisted for this investigation.

Since the trifluoromethyl group is known to be strongly electron-withdrawing, hexafluoro-2-butyne [HFB] was anticipated to behave in a fashion similar to DNAD (i.e., toward diosmacycle formation). Irradiation of 3c with HFB (Table XIX, entries ii and iii) produced little change in solution IR spectra over 35 h. Most of the starting

$\text{Os}_2(\text{CO})_8[\mu-\eta^2, \eta^2-\text{C}_2(\text{CF}_3)_2]$  based on the familiar IR pattern. Further characterization of this compound was delayed (Chapter Five) until larger quantities became available from an alternate synthetic procedure.

At the other end of the substituent scale, the reaction with the electron-rich alkyne bis(trimethylsilyl) acetylene [BTMSA,  $\text{C}_2(\text{SiMe}_3)_2$ ] appeared to proceed somewhat better but difficulties in isolating products once again proved frustrating. Following a lengthy photolysis (Table XIX, entry iv) a darkly coloured residue was obtained. A mass spectrum of the residue was complicated. However, a weak isotope pattern at 474 m/e followed by similar ones at intervals of 28 mass units hinted at the probable presence of  $\text{Os}(\text{CO})_4[\eta^2\text{-BTMSA}]$ , the first simple carbonyl-alkyne derivative of osmium. However, no such species could be isolated from the reaction.

It was becoming evident that the anticipation of a simple extension of the photoreactivity to include alkynes may have been premature. Nevertheless, two other alkynes were investigated. Acetylene [ $\text{C}_2\text{H}_2$ ] and diphenylacetylene [DPA] have enjoyed interesting thermal reactivity with  $3c$  in yielding a myriad of products. With the hope of gaining some selectivity, the photoreaction between  $3c$  and these alkynes was carried out.

The rapid consumption of  $3c$  in the presence of  $\text{C}_2\text{H}_2$  ultimately resulted in a mixture of products (Table XIX, entry v). Separation and identification of all the products was not feasible. Two of

IR spectra to the same products afforded previously by the thermal reaction.<sup>41</sup> The identity of the unique component of the mixture presented some early difficulties (see Table XXVI for data). The IR spectrum in the carbonyl region was consistent with an  $\text{Os}(\text{CO})_3(\text{diene})$  formulation<sup>83</sup>, while a mass spectrum of a pure crystalline sample indicated a molecule made up of a tricarbonyl osmium fragment bonded to an organic ligand resulting from two  $\text{C}_2\text{H}_2$  moieties and molecule of solvent benzene. The  $^1\text{H}$  NMR spectrum proved to be the necessary diagnostic tool. A multiplet in the phenyl region and five resonances over the range  $\delta 5.94\text{--}0.63$  integrated as 3:1:1:1:1:1. The multiplicities and chemical shifts of the five equal-intensity multiplets paralleled the  $^1\text{H}$  spectral features reported for  $\text{Os}(\text{CO})_3(\text{anti-1-methyl-cis-1,3-butadiene})$ <sup>47</sup> and confirmed the identity of the present compound as,  $\text{Os}(\text{CO})_3[\eta^4\text{-anti-1-phenyl-cis-1,3-butadiene}]$ (37,<sup>o</sup> Figure XII).

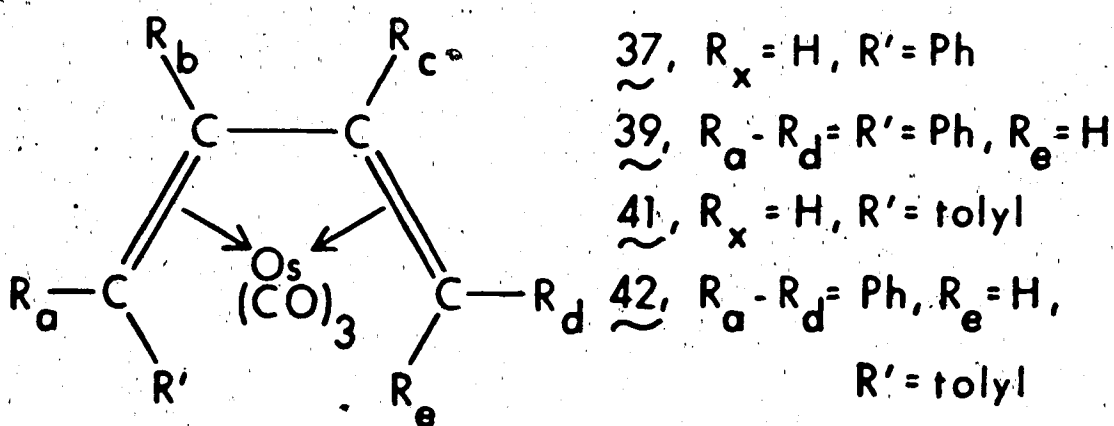


Figure XII. The  $\text{Os}(\text{CO})_3[\eta^4\text{-butadiene}]$  complexes.

	37	39	41	42
IR <sup>a</sup>	2069 1996 1987	2064 1994 1983	2068 1995 1986	2064 1995 1984
<sup>1</sup> H NMR <sup>b</sup>	c	c	N/A	d
Ph	7.10-6.97	7.45-6.15		7.00-6.22
diene	5.94 (ddt, H <sub>b</sub> ) 5.42 (dddd, H <sub>c</sub> ) 2.25 (dd, H <sub>a</sub> ) 1.96 (ddd, H <sub>e</sub> ) 0.63 (ddd, H <sub>d</sub> ) <sup>e</sup>	2.80		(2.85, 2.83, 2.80)
other				(2.29, 2.23, 2.21) <sup>f</sup>
<sup>13</sup> C NMR <sup>g</sup>	c	c	N/A	d
Os-CO	N/O	N/O		181.6 177.5 176.0
Ph	142.7 (1) 128.8 (2) 125.8 (1) 125.7 (2)	147.9-125.2		147.9-125.0
diene				
-inner	83.5 79.1	111.8 104.7		111.4 104.9
-outer	47.5 24.7	67.3 55.0		67.3 55.1
MS <sup>h</sup>	406 (155)	710 (175)	N/A	724 (170)

(a)  $\nu_{\text{CO}}$ , pentane,  $\text{cm}^{-1}$ ; (b) 30°C, 300 MHz, ppm; (c)  $\text{CD}_2\text{Cl}_2$ ; (d)  $\text{CDCl}_3$ ;  
(e)  $J_{\text{a-b}}=7.25$  Hz,  $J_{\text{a-c}}=J_{\text{b-d}}-J_{\text{b-e}}=1.00$  Hz,  $J_{\text{b-c}}=4.50$  Hz,  $J_{\text{c-d}}=7.75$  Hz,  
 $J_{\text{c-e}}=7.13$  Hz,  $J_{\text{d-e}}=3.50$  Hz; (f) methyl protons; (g) 30°C, 75.469 MHz,  
ppm; (h)  $M^+$  (highest abundance isotope), temperature (°C). N/A=not  
available, N/O=not observed.

...presumably via C-H bond activation followed by reductive elimination and  $\Pi$ -coordination of the resultant phenyl-substituted 1,3-diene. Regrettably, there was no sign of the parent diosmacyclobutene  $\text{Os}_2(\text{CO})_8[\mu\text{-C}_2\text{H}_2]$ .

The initial photolysis experiment with DPA (Table XIX, entry vi) also gave the now common-place collection of alkyne derivatives. However, the product distribution was dominated by another type of tricarbonyl compound. IR, mass spectrometric and analytical characterizations conclusively identified this species as  $\text{Os}(\text{CO})_3[\eta^4\text{-2,3,4,5-tetraphenyl-2,4-cyclopentadien-1-one}](38)$ , the missing member of the otherwise well-represented iron triad tricarbonyl cyclopentadienone complexes.<sup>111</sup> The ligand ketonic stretching frequency shows the characteristic dependence on solvent polarity, lowering from  $1677\text{ cm}^{-1}$  in cyclohexane to  $1646\text{ cm}^{-1}$  in  $\text{CH}_2\text{Cl}_2$  solution. Of more current interest and utility has been the recent discovery<sup>112</sup> of the capacity of  $\text{Ru}(\text{CO})_3(\text{C}_5\text{Ph}_4\text{O})$  to function as a catalytic precursor in hydrogen transfer and dehydrogenation reactions. This puts 38 in perspective as a possible candidate for related comparative studies.

Preparative chromatography aided in the separation of three other products from this reaction. Immediately identifiable were  $\text{Os}_2(\text{CO})_6(\text{C}_4\text{Ph}_4)(9)$ , also available from the thermal reaction<sup>31</sup>, and a second example of a mononuclear butadiene complex,  $\text{Os}(\text{CO})_3[\eta^2\text{-1,1,2,3,4-pentaphenyl-cis-1,3-butadiene}](39)$ . Assignment of the lone olefinic hydrogen to an anti position in 39 (Table XXVI, Figure XII) came by

two anti protons resonate at a field similar to 39 (2.87 versus 2.80 ppm respectively), while the low field signal for the syn proton in the latter (5.66 ppm) precludes this configuration in 39. More exciting was the isolation, albeit in very low yield (2 mg), of the third representative of a diosmacyclobutene complex,  $\text{Os}_2(\text{CO})_8[\mu-\eta^1, \eta^1-\text{C}_2\text{Ph}_2]$  (40). Spectral characterization<sup>114</sup> clearly indicated this formulation, and gave hope that perhaps under more favourable conditions this compound can be prepared in larger quantities.

In an effort to establish these conditions in the photochemical preparation, a number of reactions were performed where certain variables were altered. Increasing the concentration of DPA by four times (entry vii, Table XIX) lead to the near exclusive formation of 38. By utilizing higher intensity irradiation (entry viii), a 1:1 mixture of 38 and 39 was accompanied by a minor amount of the "fly-over" compound 9 and no diosmacycle. Since many of the products clearly arose following Os-CO bond cleavage, it was anticipated that carrying out the photolysis under an atmosphere of CO may quench their formation. The reaction appeared to be inhibited, as evidenced by the longer irradiation time (entry ix, Table XIX) but persisted in yielding 38 as the sole product. As a final attempt to affect product distribution, pentane was used as reaction solvent (entry x). Experiments in our laboratories<sup>115</sup> and the recent work of Wrighton<sup>92</sup> show that alkene photoreactions in hydrocarbons lead to chemistry different than has been observed for benzene. The present effects were marked as no

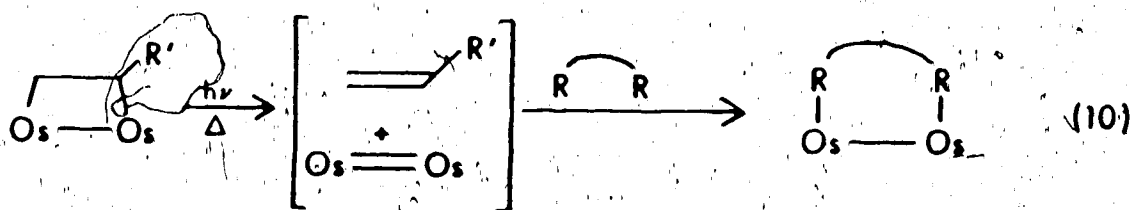
small quantities ended aspirations for a photochemical route to this compound directly from 3c.

#### IV. Conclusions.

An overview of the photoreactivity of alkynes with 3c reveals that the expectation of a facile entry into a series of 1,2-diosma-cyclobutenes remained largely unfulfilled most probably because of an oversimplistic view of the photofragmentation of 3c (eq.(8), Ch. Two). Although three examples of such derivatives were isolated, invariably they accounted for only a very small amount of the available starting material. The history of complicated behaviour for alkynes with 3c may have been a signpost for our attempts with photochemical activation. Other workers have reported similar behaviour. Geoffroy, et al.<sup>116</sup> note that the irradiation of  $H_3Re_3(CO)_{12}$  in the presence of DPA also affords a complex mixture of products. The differences in product distribution stemming from the photochemical and the thermal activation of 3c with alkynes are no better exemplified than with DPA, whereby 38 is almost exclusively produced from the photolytic route. However, the availability of some unsaturated diosma-cycles only in low yields clearly indicates that alternate synthetic pathways must be sought for these derivatives. Attempts to uncover these routes will be presented in Chapter Five.

## I. Introduction.

The difficulties encountered in previous Chapters to extend the photochemical synthesis to a variety of substituted diosmacyclobutanes and diosmacyclobutenes led to a search for an alternate preparative route. Upon reconsideration of the unsuccessful photoreactions, the lack of dinuclear products may be the result of the lability and/or reactivity of the putative diosmacycles. Hence, it was postulated that exchange reactions between easily available 1,2-diosmacyclobutanes and suitable organic substrates may provide an attractive synthesis of these molecules (equation (10)). The possibility that the initial



step represents a heretofore rare example of a dinuclear reductive elimination reaction<sup>117</sup> also added incentive for attempting these reactions. Even though a concerted thermal reductive elimination reaction has been shown to be symmetry forbidden,<sup>118</sup> the energy barrier for the process is lowered substantially when the leaving groups are first bent toward each other. In this respect, the 1,2-diosmacyclobutanes seem well suited. In addition, since prolonged photolysis of some 1,2-diosma-



In this Chapter the thermal exchange reactions of  $\text{Os}_2(\text{CO})_8[\mu\text{-MA}]$  (14) and  $\text{Os}_2(\text{CO})_8[\mu\text{-C}_2\text{H}_4]$  (16) with alkenes and alkynes will be presented. The phosphine substitution chemistry of a series of diosmacycles was investigated also to give an indication of the strength of the bridging ligand-osmium interaction.

## II. Alkyne Exchange Reactions.

### A. Reactions with DMAD, $\text{C}_2\text{H}_2$ and DPA.

To test the validity of the thermal exchange reaction with alkynes, DMAD was the first alkyne tried since the diosmacyclobutene derivative was obtained via photolysis. Since 14 was available in useful quantities and in pure form, it was used as the source of " $\text{Os}_2(\text{CO})_8$ ". The reaction (equation (11)) was conveniently monitored by IR spectroscopy

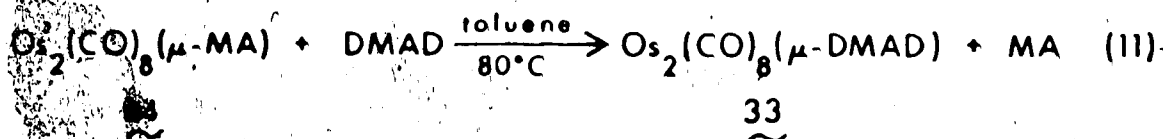


(Figure XIII). The reaction proceeded with the decrease in intensity of  $\nu_{\text{CO}}$  for 14 and the appearance of those for 33. The improved isolated yield of 33 (47%) over that obtained from the photochemical method afforded usable quantities of the compound. The exchange reaction was also carried out with the parent complex 16 which resulted in a drastically reduced yield of 33 (13%). Some difficulties in isolating

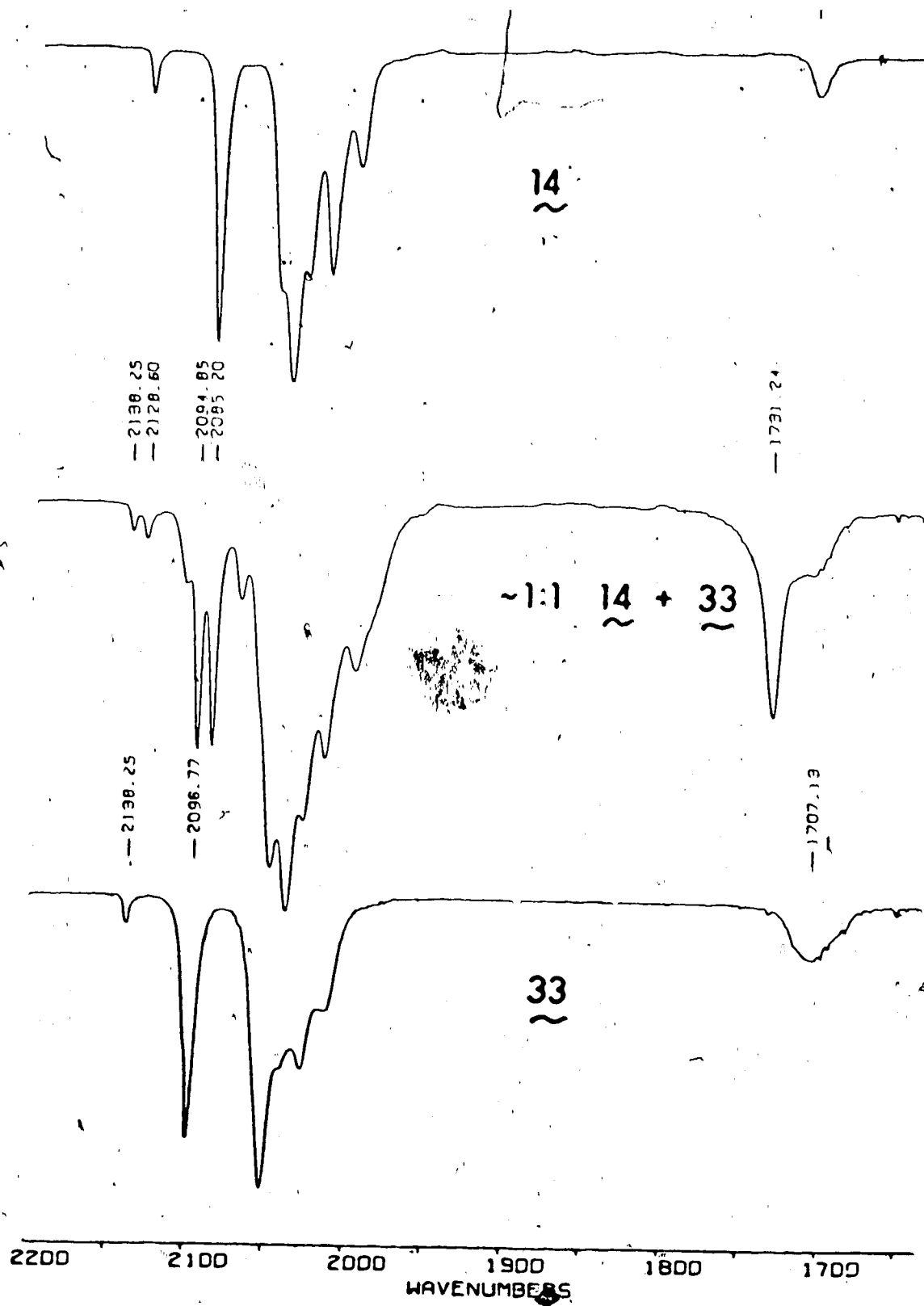
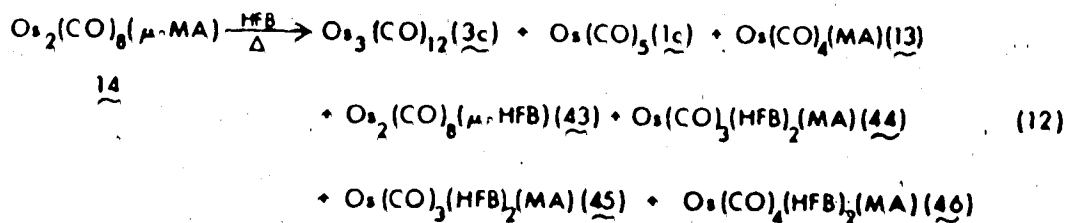


Figure XIII. IR spectra for the thermal exchange reaction of  $\text{Os}_2(\text{CO})_8(\text{u-MA})(14)$  with DMAD.

However, the initial excitement quickly abated. The reaction with acetylene in toluene gave a yellow oily residue, from which the isolation of individual components was very difficult and no pure product was obtained. However, IR spectroscopy did allow the identification of  $\text{Os}_2(\text{CO})_6(\text{C}_4\text{H}_4)(35)^{41}$  and what could be the third example of a butadiene complex,  $\text{Os}(\text{CO})_3[\eta^4\text{-anti-1-tolyl-cis-1,3-butadiene}](41)$ , Figure XII, Table XXVI). Regrettably, no parent diosma-cyclobutene ( $\text{Os}_2(\text{CO})_8[\mu\text{-C}_2\text{H}_2]$ ) was observed. Similarly, the exchange reaction with DPA produced a mixture. In this case,  $\text{Os}_2(\text{CO})_8[\mu\text{-DPA}](40)$  was obtained only in marginally better yields than from the photochemical reaction. Accompanying 40 were the increasingly apparent thermodynamic sink of osmium carbonyl - DPA chemistry,  $\text{Os}_2(\text{CO})_6(\text{C}_4\text{Ph}_4)(9)^{31}$ , and another butadiene derivative,  $\text{Os}(\text{CO})_3[\eta^4\text{-anti-1-tolyl-1,2,3-4-syn-tetraphenyl-cis-1,3-butadiene}](42)$ . Although all three aromatically-substituted isomers (ortho, meta and para) of 42 were seen in the  $^1\text{H}$  NMR spectrum (Table XXVI), there appeared to be a non-random distribution amongst them. The small chemical shift differences in the methyl and olefinic proton resonances forbade assignment and an accurate determination of the ratio of products. Interestingly, no cyclopentadienone complex 38 was observed, which might indicate that it derives more directly from the starting cluster rather than subsequent reaction products.

very low yield, via the photolysis of 3c, the thermal exchange reaction between 14 and 16 and HFB was necessarily attempted in spite of the limited successes of the previous  $C_2H_2$  and DPA reactions. In this case as well, multiple products were obtained. The reaction of 14 did allow easier isolation and as such is detailed below.

The complexity of the attempted exchange reaction is depicted in equation (12). Compounds 3c, 1c and 13 were undesirable side products



and were only identified. The anticipated dinuclear HFB-bridged species 43 could be separated, but its isolated yield was irreproducible over several reaction attempts, ranging from nearly zero to a maximum of 20%. Nevertheless, the compound could be characterized by spectroscopic and analytical techniques (Chapter Seven, Section VII. 2(e)). The familiar IR terminal carbonyl band pattern, parent isotope pattern at 768 m/e in the mass spectrum, and elemental analysis confirmed the dinuclear framework for 43. Whereas a 2:1:1 ratio of carbonyl  $^{13}\text{C}$  NMR resonances mirrors that observed for the DMAD analog 33, the bridgehead and tri-fluoromethyl carbon signals could not be observed in an overnight run

the trifluoromethyl  $^{19}\text{F}$  resonance at  $\delta$ -59.3 ppm is in good agreement with those values for the trans and cis isomers of the above rhodium compound ( $\delta$ -55.09 and -55.12 ppm, respectively).

The nature of the remaining three compounds was somewhat more difficult to deduce. The initial problems began with identical mass spectra obtained for two of the compounds (44 and 45) which pointed to the general formulation  $\text{Os}(\text{CO})_3(\text{HFB})_2(\text{MA})$ . While the IR spectrum of isomer 45 showed a  $\nu_{\text{CO}}$  band pattern typical for a simple tricarbonyl fragment<sup>83</sup> (2117 (s), 2062 (s), 2048 (s);  $\nu_{\text{CO}_2}$  1753 (m)  $\text{cm}^{-1}$ ), compound 44 exhibited an IR spectrum closely resembling that observed for the alkyne-linked complex 34, including a weak band in the  $\nu_{\text{CO}_2}$  region at 1624  $\text{cm}^{-1}$  (cf. 1601  $\text{cm}^{-1}$  for 34). Clearly, the IR features of the isomeric species indicated different structural types. However, the unavailability to date of quality X-ray crystals meant that discrimination of the isomers must come from the battery of spectroscopic analyses.

$^1\text{H}$  and  $^{19}\text{F}$  NMR spectroscopy were helpful in diagnosing the nature of the MA and HFB moieties in 44. The multiplicity of three broad olefinic proton resonances in the  $^1\text{H}$  spectrum for 44 (Table XXVII), although somewhat reminiscent of the dinuclear MA derivative 14, implied additional coupling, especially since lowering the temperature did nothing to improve their resolution. This was borne out in the  $^{19}\text{F}$  spectrum for 44 (Figure XIV) which showed couplings much smaller than the homonuclear  $^{19}\text{F}$  interactions. Reciprocal selective  $^1\text{H}\{^{19}\text{F}\}$  and  $^{19}\text{F}\{^1\text{H}\}$  NMR experiments performed on 44 allowed for the identi-

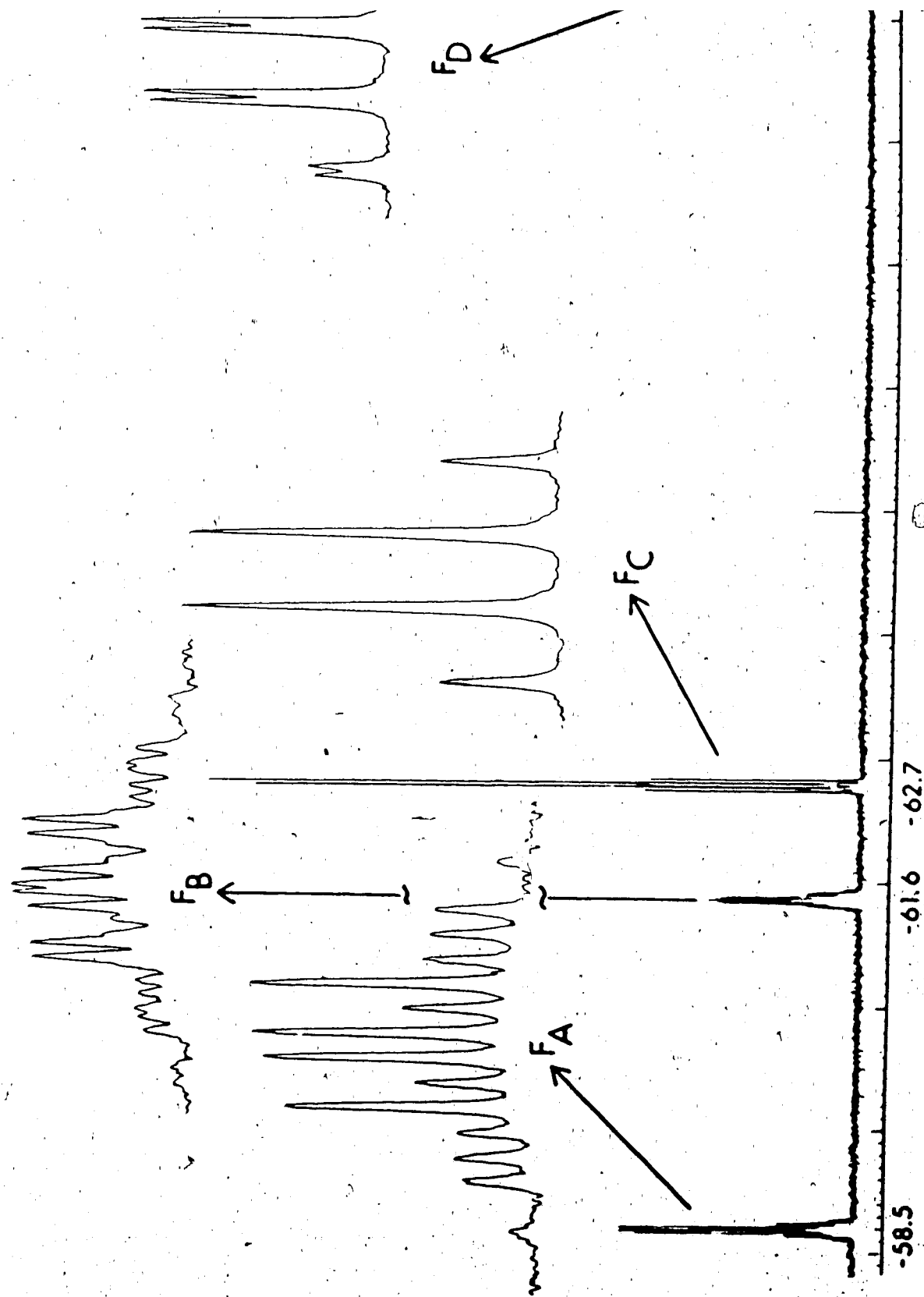


Figure XIV. 376 MHz  $^{19}\text{F}$  NMR spectrum of 44.

Table XXVII. Characterization of the Isomeric Compounds  $\text{Os}(\text{CO})_3[(\text{HFB})_2(\text{MA})]$ .

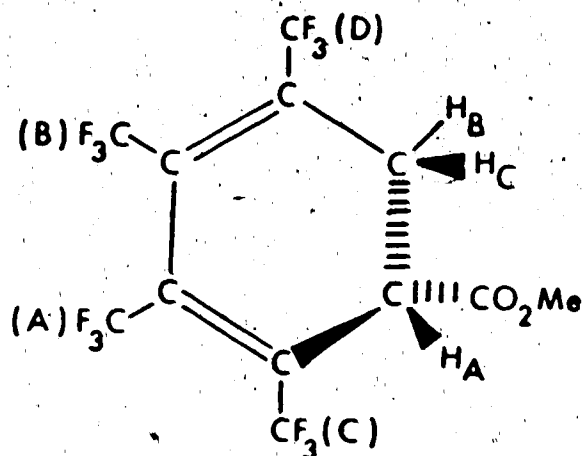
	44	45
IR <sup>a</sup>	2099(s), 2023(s), 2010(s), 1626(w)	2117(s), 2062(s), 2048(s), 1753(
<sup>1</sup> H NMR <sup>b</sup>	3.88(s, $\text{OCH}_3$ ), 3.85(dd, $\text{H}_A$ ) 2.98(ddqq, $\text{H}_B$ ), 2.68(dd, $\text{H}_C$ ) <sup>c</sup> 195.0( $\text{C}=\text{O}$ Os), 179.7, 179.1, 171.0 128.8, 127.9, 121.9, 121.5 <sup>f</sup>	3.72(s, $\text{OCH}_3$ ), 3.08(dd, $\text{H}_A$ ) 2.48(dd, $\text{H}_B$ ), 2.17(dd, $\text{H}_C$ ) <sup>d</sup> 173.3, 171.1, 169.0, 168.4 126.9(2), 121.85(1), 121.5(1) <sup>g</sup>
<sup>13</sup> C NMR <sup>e</sup> $\delta(\text{CO})$	Not observed	inner- 91.9, 91.0 outer- 58.4, 57.9 <sup>h</sup>
$\delta(\text{CF}_3)$		
$\delta(\text{CCF}_3)$		
$\delta(\text{MA})$	57.8( $\text{OCH}_3$ ), 48.5, 30.6( $\text{CH}$ , $\text{CH}_2$ ) -58.5(qq, $\text{F}_A$ ), -61.6(qqd, $\text{F}_B$ ), -62.7(q, $\text{F}_C$ ), -70.4(qd, $\text{F}_D$ ) <sup>j</sup>	52.7( $\text{OCH}_3$ ), 43.8, 32.3( $\text{CH}$ , $\text{CH}_2$ ) -50.0(septet, $\text{F}_A$ ), -56.0(q, $\text{F}_B$ ), -56.7(septet, $\text{F}_C$ ), -57.0(q, $\text{F}_D$ ) <sup>k</sup>
<sup>19</sup> F NMR <sup>i</sup>	$M^+$ 686 m/e, $M^+-n\text{CO}$ ( $n=1-3$ ) <sup>l</sup>	$M^+$ 686 m/e, $M^+-n\text{CO}$ ( $n=1-3$ ) <sup>m</sup>
MS		
melting point	140 - 142°C	65 - 67°C
elemental analysis	%C                      %H	%C                      %H
$\text{C}_{15}\text{F}_{12}\text{H}_6\text{O}_5\text{Os}$	calc                      26.32                      0.88	26.32                      0.88
	found                      not available	26.00                      0.88

Table XXVII. (continued).

- a) pentane solution,  $\text{cm}^{-1}$ ; b) 400 MHz,  $\text{CD}_2\text{Cl}_2$ , ambient; c)  $J_{\text{H}_\text{A}-\text{H}_\text{C}} = 4 \text{ Hz}$ ,  $J_{\text{H}_\text{H}} = 17.5 \text{ Hz}$ ,  $J_{\text{H}_\text{A}-\text{H}_\text{B}} = 3 \text{ Hz}$ ,  $J_{\text{H}_\text{B}-\text{F}_\text{D}} = 2 \text{ Hz}$ ,  $J_{\text{H}_\text{B}-\text{F}_\text{B}} = 3 \text{ Hz}$ ; d)  $J_{\text{H}_\text{A}-\text{H}_\text{B}} = 3.5 \text{ Hz}$ ,  $J_{\text{H}_\text{A}-\text{H}_\text{C}} = 8 \text{ Hz}$ ,  $J_{\text{H}_\text{B}-\text{H}_\text{C}} = 14 \text{ Hz}$ ; e) 75.469 MHz,  $\text{CD}_2\text{Cl}_2$ , ambient
- f) all quartets, average  $J_{\text{C}-\text{F}} = 275 \text{ Hz}$ ; g) quartets in approximate 2:1:1 ratio, average  $J_{\text{C}-\text{F}} = 278 \text{ MHz}$ ; h) all quartets,  $J_{\text{C}-\text{F}} = 42 \text{ Hz}$  for inner, 33 Hz for outer; i) 376. MHz,  $\text{CD}_2\text{Cl}_2$ ; j)  $J_{\text{F}_\text{A}-\text{F}_\text{C}} = 15 \text{ Hz}$ ,  $J_{\text{F}_\text{B}-\text{F}_\text{D}} = 14.5 \text{ Hz}$ ; k) 55°C,  $J_{\text{F}_\text{A}-\text{F}_\text{B}} \approx J_{\text{F}_\text{A}-\text{F}_\text{C}} \approx J_{\text{F}_\text{B}-\text{F}_\text{D}} \approx J_{\text{F}_\text{C}-\text{F}_\text{D}} \approx 16 \text{ Hz}$ ; l) 70eV, 120°C; m) 70eV, 70°C.



connectivity between the alkene and alkyl fragments as depicted below.



Still, there was no clear indication of the bonding mode of this moiety to a tricarbonyl osmium fragment.

An overnight  $^{13}\text{C}$  spectrum of 44 provided the final telling evidence (Table XXVII). The low field resonance at  $\delta 195.0$  is very close to the value obtained for the end-on bound carboxylate carbonyl carbon atom of 34 ( $\delta 198.0$ ) and corroborates with the low frequency  $\nu_{\text{CO}_2}$  band to suggest a similar bonding mode in 44. Although the four quartets ca. 125 ppm and three higher field single peaks correspond nicely to  $\text{CF}_3$  and MA groups respectively, none of the remaining very weak signals could be assigned with confidence to the cyclohexadiene olefinic carbon atoms. However, if the relative upfield shift of  $F_B$  and  $F_D$  with respect to  $F_A$  and  $F_C$  is an effect of the expected upfield coordination shift of the attached olefinic carbons, then the double bond between the  $F_B$ - and  $F_D$ -substituted carbon atoms is responsible for completing the electronic requirements of osmium. What should be the more obvious  $\eta^4$ -diene bonding mode for the cyclohexadiene ligand is negated by the

Assigned coupling of olefinic hydrogens

nucleus(multiplicity)	coupled to
H <sub>A</sub> (t)	H <sub>B</sub> , H <sub>C</sub>
H <sub>B</sub> (ddqq)	H <sub>A</sub> , H <sub>C</sub> , F <sub>B</sub> , F <sub>D</sub>
H <sub>C</sub> (dd)	H <sub>A</sub> , H <sub>B</sub>

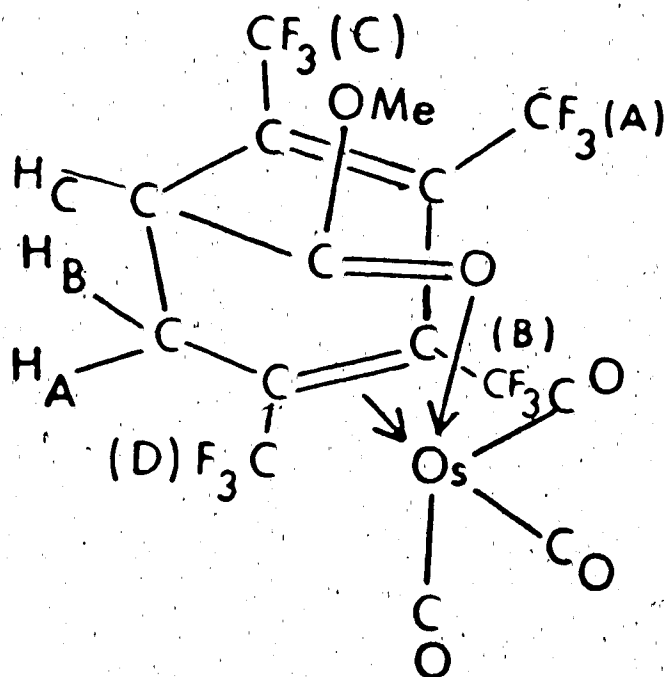
Assigned coupling of trifluoromethyl fluorines

nucleus (multiplicity)	coupled to
F <sub>A</sub> (qq)	F <sub>B</sub> , F <sub>C</sub>
F <sub>B</sub> (qqd)	F <sub>A</sub> , F <sub>D</sub> , H <sub>B</sub>
F <sub>C</sub> (q)	F <sub>A</sub>
F <sub>D</sub> (qd)	F <sub>B</sub> , H <sub>B</sub>

Scheme IX. Homo- and heteronuclear <sup>1</sup>H and <sup>19</sup>F couplings for 44.

carboxylate carbonyl oxygen atom in an axial site to conform to Hoffmann's site preference arguments.<sup>86</sup> The reasons for this are uncertain, but the strongly electron-withdrawing  $\text{CF}_3$  groups may alter the electron density of the diene fragment to the point where bonding through this entity is less favourable than the  $\pi$ -olefin,  $\sigma$ -oxygen mode.

In contrast to 44, the  $^1\text{H}$  NMR spectrum of 45 (Table XXVII) was consistent with a simple  $\pi$ -bound MA, as was found for  $\text{Os}(\text{CO})_4[\eta^2\text{-MA}]$  (13). However, the corresponding room temperature  $^{19}\text{F}$  spectrum was deceptive with the appearance of a septet well-removed to low field of a quartet, each integrating as one against a very broad and seemingly complicated higher field multiplet of intensity two. A variable temperature  $^{19}\text{F}$  study was indicated to resolve the unusual NMR features (Figure XVI). At  $55^\circ\text{C}$ , the resonances were distinguishable as a low field septet ( $\text{F}_\text{A}$ ) and a group of three multiplets consisting of a quartet ( $\text{F}_\text{B}$ ), a septet ( $\text{F}_\text{C}$ ) and a quartet ( $\text{F}_\text{D}$ ) at 7 ppm to higher field. As the probe temperature dropped,  $\text{F}_\text{D}$  began a migration across  $\text{F}_\text{C}$  to regenerate the ambient temperature spectrum then continued toward the other quartet  $\text{F}_\text{B}$  with the concomitant broadening of both signals. The original quartets appeared to coalesce at  $-40^\circ\text{C}$  to one very broad resonance while the septets remained sharp and experienced some minor fluctuations in their chemical shifts. The coalesced resonance continued to broaden until it disappeared into the baseline at  $-90^\circ\text{C}$ , which also resulted in broadening of the septets. Further cooling to the limits of the spectrometer saw the emergence of three pairs of resonances which at  $-125^\circ\text{C}$  resolved as two sets of three triplets each,



44  
~

Figure XV. Proposed structure for 44.

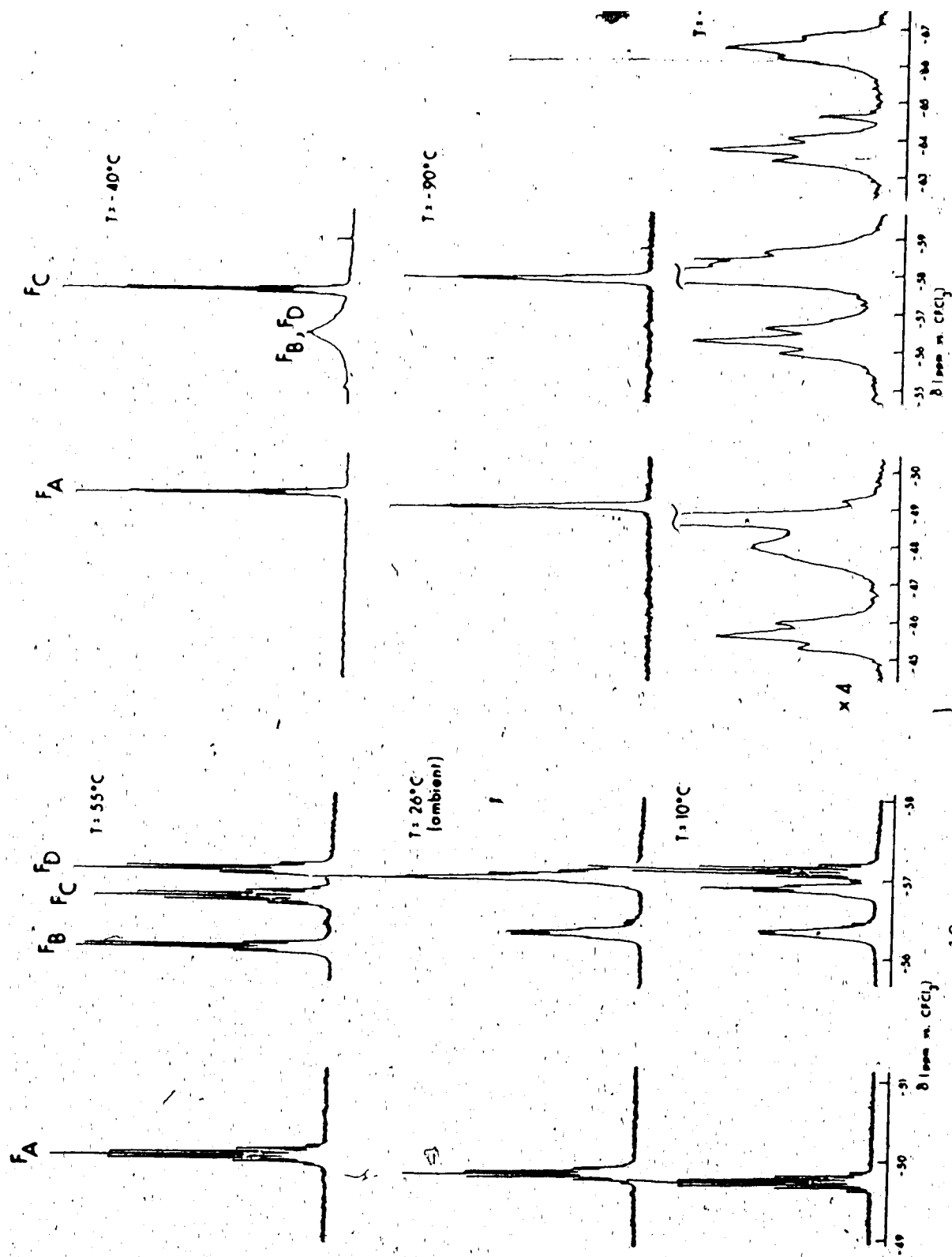


Figure XVI. 376 MHz  $^{19}\text{F}$  variable temperature NMR spectra for 45.

age 127 Hz for resolved signals) closely corresponds to values associated with  $^2J_{F-F}$  interactions<sup>120</sup> and to the only other reported homonuclear geminal couplings for  $CF_3$  groups in  $(CH_3)_2(CF_3)_2PSCH_3$  (or  $OCH_3$ ).<sup>121</sup> In the present case, restricted rotation of the  $CF_3(B)$  and  $CF_3(D)$  groups should give rise to this rarely observed phenomenon, but at this point affords no stereochemical information.

In order to fully assign a structure to 45, the  $^{13}C$  NMR spectrum had to be obtained. The carbonyl resonances show no unusual chemical shift behaviour (Table XXVII), however the three highest field signals are noticeably broader ( $\delta 171.1$ ,  $\Delta\nu_{\frac{1}{2}}=5.5$  Hz;  $\delta 169.0$ ,  $168.4$ ,  $\Delta\nu_{\frac{1}{2}}=10$  Hz) than the fourth resonance ( $\delta 173.3$ ,  $\Delta\nu_{\frac{1}{2}}=3$  Hz) leading to its assignment as the carboxylate carbonyl carbon signal. Three quartets at ca. 125 ppm in a roughly 2:1:1 ratio (cf. ambient temperature  $^{19}F$ , Figure XVI, Table XXVII) along with weak multiplets at 91 ppm and somewhat higher intensity multiplets at 58 ppm clearly indicated that selective  $^{13}C(^{19}F)$  NMR experiments should be performed. However, the close proximity of the  $F_B$ ,  $F_C$ , and  $F_D$  resonances (Figure XVI) did not allow for a completely satisfactory decoupling. The results of this study and what appears to be the most consistent assignment of the cis-diene linkage of two HFB units are given in Scheme X. The broad signal at 126.9 ppm in the decoupling of  $F_C$  is probably due to partial decoupling of the close  $F_D$  resonance, whereas in the  $F_D$  decoupling, the line at 91.9 ppm is weaker than at 57.9 ppm and probably arises from the closeness of  $F_C$  and its partial decoupling. To accommodate these features, along with an intact  $\eta^2$ -MA ligand and a tricarbonyl osmium fragment, two plausible structures

$^{13}\text{C}$  ( $^{19}\text{F}$ ) experimental results

decoupled nucleus	resonances giving single lines (ppm)
$\text{F}_\text{A}$	121.85, 91.0
$\text{F}_\text{B}$	126.9, 58.4
$\text{F}_\text{C}$	126.9(br), 121.5, 91.9, 58.4, 57.9
$\text{F}_\text{D}$	126.9, 121.5, 91.9, 57.9

$^{13}\text{C}$  assignment

fluorine atoms	$\text{CF}_3$	diene carbon
$\text{F}_\text{A}$	121.85	91.0
$\text{F}_\text{B}$	126.9	58.4
$\text{F}_\text{C}$	121.5	91.9
$\text{F}_\text{D}$	126.9	57.9

Scheme X. Assignment of trifluoromethyl and diene carbon resonances from  $^{13}\text{C}$ ( $^{19}\text{F}$ ) experiments for 45 at 45°C.

an axial position (45b) and local  $C_{3v}$  symmetry of the osmium-carbonyl unit. Structure 45b could also account for the low field shift of  $F_A$  as a result of deshielding by the carboxylate moiety pointed in that direction. As well, the restricted rotation of both outer trifluoromethyl substituents could more easily be ascribed to a stereochemical interaction with the axial MA ligand, which in 45a might only affect the proximal rotating group ( $F_B$ ). As a defense of 45b, the anticipated drain of electron density from the metal in the equatorial plane by the  $C_4(CF_3)_4$  unit would not allow for sufficient  $\pi$ -back-donation to an alkene in order to stabilize the bonding interaction. Evidence that this phenomenon occurs comes from the substantially higher carbonyl stretching frequencies in 45 over 44. With great confidence, then, 45b can be postulated as the more plausible isomer.

In retrospect, the seemingly unusual nature of compounds 44 and 45 may not be that unusual after all. Both in the photochemical and thermal reactions of 3c,  $C_2H_2$  and DPA consistently have shown the capacity to couple at the metal center and in some cases to subsequently react further with solvent to form the  $Os(CO)_3$ (butadiene) complexes. Under the present reaction conditions, an MA moiety is maintained in the coordination sphere as HFB substitution ensues. Coupling of two HFB moieties gives rise to 45 which, following insertion of the olefinic double bond into an osmium-carbon bond of the osmacyclopentadiene and reductive elimination, could give the substituted cyclohexadiene ligand as found in 44. A postulated third derivative of this type was isolated



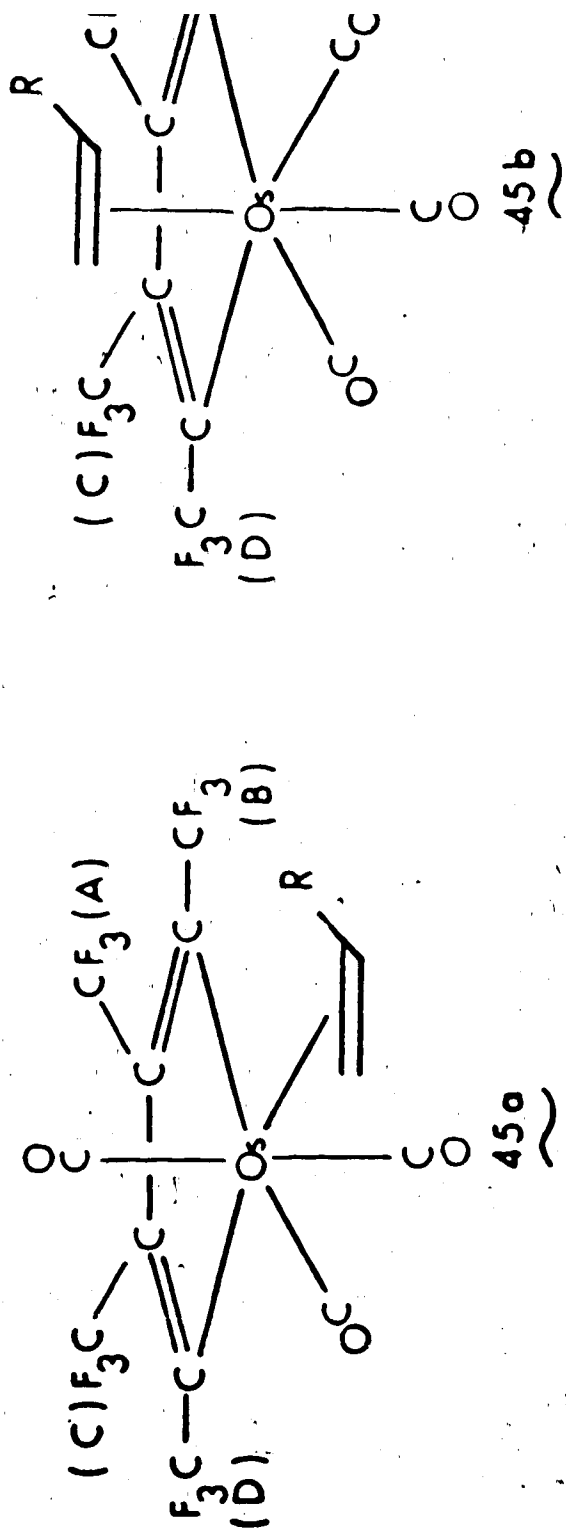


Figure XVII. Proposed possible structures for 45.

of  $\text{Os}(\text{CO})_4(\text{HfD})_2(\text{MA})$  (40). However, as all three compounds were obtained in low yields, investigation of their formation or, perhaps more appropriately, their interconversion was negated.

### III. Alkene Exchange Reactions.

Having established that thermally induced fragmentation of 14 and 16 was feasible it was of interest to examine its utility toward the formation of saturated diosmacycles as well.

The reaction of 14 with dimethyl maleate [DMN] also required moderate temperature ( $64^\circ\text{C}$ ) and resulted in a satisfactorily clean conversion to  $\text{Os}_2(\text{CO})_8[\mu\text{-DMN}]$  (28) with a 65% isolated yield. A byproduct of the reaction was the mononuclear MA compound 13. Interestingly, no isomerization of bulk free alkene was observed. This supports the previous arguments presented in Chapter Three that the dinuclear complexes and the generated  $[\text{Os}_2(\text{CO})_8]$  species have a marginal influence on the alkene isomerization. It is pertinent to mention here that Professor Norton has communicated to us that the parent 16 loses olefins in a stereospecific and reversible fashion under thermal activation thereby confirming in the present context the concerted nature of the dinuclear reductive elimination from 1,2-diosmacycles.

To further test the generality of the thermal exchange reaction, maleic anhydride [MAH] was chosen, mainly due to its nonreactivity in the photochemical experiments with 3c (Chapter Two). Indeed, in accord

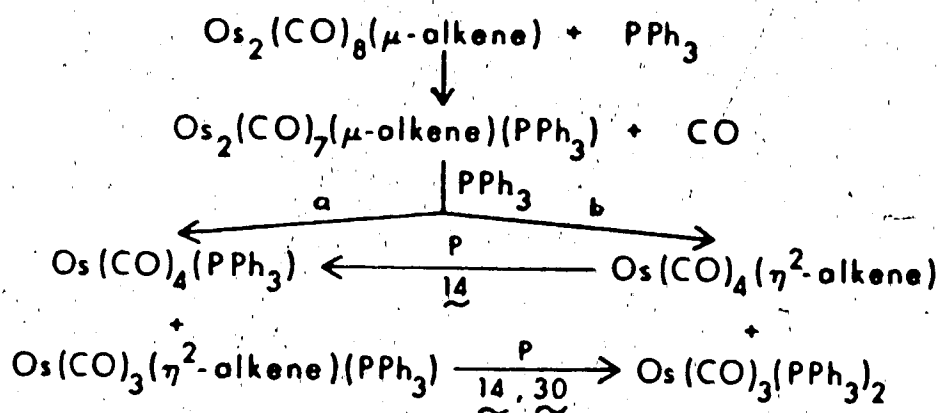
observed for hard donor molecules (i.e., THF). Consequently, this also led us to investigate the possible formation of the mononuclear derivative. Benzene solutions of  $\text{Os}(\text{CO})_4[\eta^2\text{-C}_2\text{H}_4](15)$  were readily available (see Chapter Seven, Section IV. 2(b)) and easily adapted for this type of reactivity study. Successful preparation of the complex  $\text{Os}(\text{CO})_4[\eta^2\text{-MAH}](48)$  was indicated by spectroscopic characterizations (see Tables IV, V, XII and XIII) consistent with a tetracarbonyl formulation and comparison to the reported ruthenium analog.<sup>55</sup> Reminiscent of the photoreaction of  $\text{Os}(\text{CO})_5$  with DMM (equation (9)), a small amount of dinuclear 47 contaminated the isolated sample.

#### IV. Phosphine Substitution Reactions.

In an effort to gauge the relative stability of the dinuclear complexes toward fragmentation versus CO substitution, reactions between the dinuclear derivatives of MA (14), DMF (30) and DMAD (33) and triphenylphosphine were examined.

Disappointingly, 14 fragments to the mononuclear phosphine complexes  $\text{Os}(\text{CO})_3(\text{PPh}_3)_2(49)$  and  $\text{Os}(\text{CO})_4(\text{PPh}_3)(50)$ <sup>122</sup> and free MA was observed by IR spectroscopy ( $\nu_{\text{CO}_2}$  1732  $\text{cm}^{-1}$ ). In a similar manner, but at a much higher temperature (103 versus 62°C for 14), dinuclear 30 collapsed with the additional formation of  $\text{Os}(\text{CO})_4[\eta^2\text{-DMF}](29)$ . These results are consistent with the thermally induced reductive elimination of alkenes in favour of Os-CO bond cleavage. In line with the known thermal instability of  $\text{Os}_2(\text{CO})_9$ <sup>6</sup>, the postulated  $\text{Os}_2(\text{CO})_8(\text{PPh}_3)$

A plausible scenario is shown in Scheme XI.

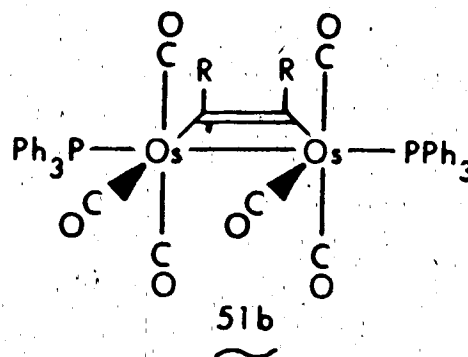
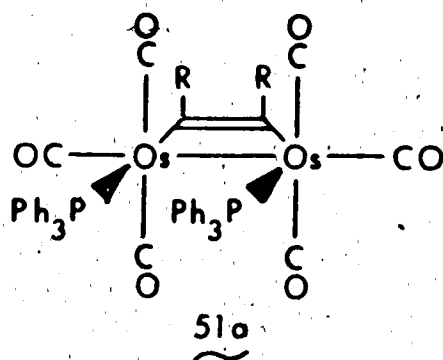


Scheme XI. Proposed fragmentation of  $\text{Os}_2[\mu\text{-alkene}]$  induced by  $\text{PPh}_3$ .

In the reaction of 14, path a would be the favoured route, whereas the appearance of 29 suggests that both pathways are operable for 30.

The stability of 33 under the metathesis conditions gave some hope that here derivative chemistry could be obtained. The reaction between 33 and  $\text{PPh}_3$  gave one main product (51) in good yield. The IR spectrum of 51 was relatively simple ( $\nu_{\text{CO}}$  2083 (w), 2036 (w), 1995 (vs), 1961 (sh);  $\nu_{\text{CO}_2}$  1692 (w)  $\text{cm}^{-1}$ ) but its mass spectrum showed isotope patterns characteristic of a dinuclear complex. Close examination of the mass spectrum resulted in the identification of a weak parent isotope envelope at 1216  $m/e$  followed by losses of six carbonyl units. Although complete purification of the compound proved impossible as

multiplets in the  $^{13}\text{C}$  NMR spectrum at  $\delta 188.3$  and  $172.7$  ppm ultimately led to the proposed isomeric forms for 51 depicted below:



Choosing between structures 51a and 51b is difficult. The multiplet feature of the  $^{13}\text{C}$  resonance for the bridgehead carbon at  $\delta 120.0$  ppm ( $\delta 114.0$  for 33) may be better accommodated by the trans  $^{31}\text{P}$ -bridgehead carbon interaction. However, the large steric interference inherent with two adjacent  $\text{PPh}_3$  moieties in this structure may favour 51b. A similar compound came from the preparation of the  $\text{PPh}_2\text{Me}$  analog 52 which exhibited a virtually identical  $^{13}\text{C}$  NMR spectrum in the carbonyl and bridging carbon regions. As a result of the stronger  $\text{Os}-\text{C}(\text{sp}^2 \text{ bridgehead carbon})$  interaction, 33 has been allowed a derivative chemistry not available to the saturated diosmacycles.

38 with excess  $\text{PPh}_3$  at  $103^\circ\text{C}$  gave no apparent reaction after several days. Phosphine substitution could be induced photochemically (Pyrex filtered light), though, and afforded the isolation of the major product  $\text{Os}(\text{CO})_2(\text{PPh}_3)[\eta^4\text{-2,3,4,5-tetraphenyl-2,4-cyclopentadien-1-one}](53)$ .

#### V. Conclusions.

The thermal reactivity of the saturated diosmacycle 14 with alkynes had some encouraging results in allowing a limited extension of the available diosmacyclobutenes. Clearly, though, alkynes can further react as evidenced by the large number of coupled products. Therefore, there is a real need for a more reactive " $\text{Os}_2$ " transfer reagent. The propylene derivative 18 was considered in this respect, but a high degree of instability precluded its potential utility. More recent results in our laboratory<sup>115</sup> have shown that the parent diosmacycle 16 is proving to be a more suitable candidate, although reactions with DPA and HFB are still problematic.

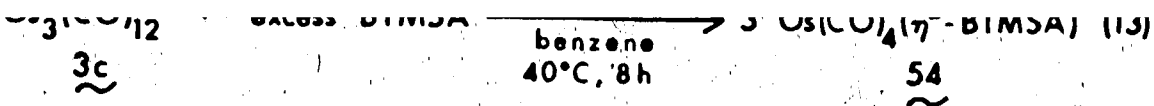
## I. Introduction.

Although the photochemical synthetic route has led to a number of saturated diosmacycles, three examples of alkyne-bridged species could be obtained only in low yields (Chapter Four). Equally, the mononuclear alkyne-tetracarbonyl derivatives of osmium had escaped preparation under similar reaction conditions. This last result is perhaps not surprising in view of the paucity of simple  $\eta^2$ -alkyne complexes of the iron triad transition metal carbonyls.<sup>123</sup> However, an indication of the first example of an  $\text{Os}(\text{CO})_4[\eta^2\text{-alkyne}]$  complex from the photoreaction of 3c with bis(trimethylsilyl)acetylene [BTMSA] was presented in Chapter Four and suggested that, under suitable conditions, such mononuclear alkyne complexes may be accessible. In this Chapter, the preparation of the osmium and analogous ruthenium derivative will be presented. With the previously known iron compound,<sup>123a</sup> a detailed comparison of the iron triad compounds was carried out also.

## II. The $\text{M}[\eta^2\text{-BTMSA}]$ Complexes.

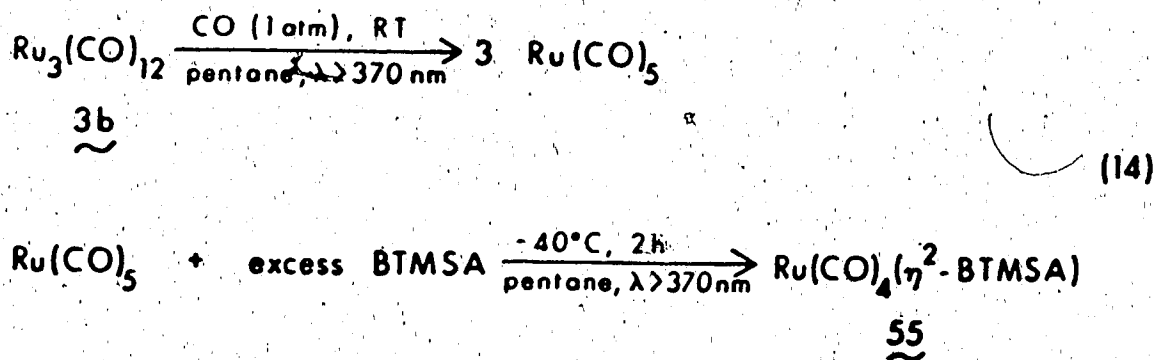
### A. Synthesis and Characterization of $\text{M}(\text{CO})_4[\eta^2\text{-Me}_3\text{SiC}_2\text{SiMe}_3]$ .

An initial photoreaction between 3c and BTMSA under the normal Immersion Well conditions resulted in little overall reaction even after long irradiation periods (Chapter Four). With a higher intensity light source (see Chapter Seven, Section VIII.2), the reaction of 3c with BTMSA went to completion after 8h to afford a



Elemental analysis and spectroscopic characterization (vide infra) confirmed the formulation as 54, the first simple mononuclear carbonyl-alkyne complex of osmium.

Attempts to prepare the analogous ruthenium compound under similar conditions met with failure. Photolysis of  $\text{Ru}_3(\text{CO})_{12}$  (3b) and excess BTMSA in benzene resulted only in precipitation of the orange-red insoluble, polymeric form of ruthenium carbonyl.<sup>65,124</sup> However, application of the metal pentacarbonyl route previously used to prepare the related iron complex<sup>123a</sup> proved to be highly satisfactory. Photolysis of in situ prepared  $\text{Ru}(\text{CO})_5$ <sup>51</sup> and excess BTMSA at  $-40^\circ\text{C}$  gave, after 2h, quantitative conversion (by IR monitoring) to 55 (equation (14)). Removal of the volatiles at  $-25^\circ\text{C}$  left behind pure 55 as a



yellow solid, which is stable only below  $-20^\circ\text{C}$ . A mass spectrum of 55



scopic data on 54 and 55 (Table XXVIII). Although solution IR of 54 can be obtained without any undue precaution, 55 like many other  $\text{Ru}(\text{CO})_4[\eta^2\text{-olefin}]$  complexes,<sup>55</sup> is labile in solution. Solution samples for IR analysis of 55 were stabilized by the addition of a small amount of free BTMSA, otherwise back reaction to 3b occurred rapidly. Nevertheless, the position and intensity distribution of the four terminal carbonyl stretching bands ( $\nu_{\text{CO}}$ ) are fully consistent with the alkyne ligand occupying an equatorial position of a trigonal bipyramidal structure. Also, weak absorptions in the 1800-1900  $\text{cm}^{-1}$  region can be attributed to the carbon-carbon stretching modes ( $\nu_{\text{CC}}$ ) of the complexed alkyne. The low temperature  $^{13}\text{C}$  NMR spectra show two equally intense signals, one each for the equivalent axial and equatorial carbonyl ligands of  $\text{eq-M}(\text{CO})_4[\eta^2\text{-BTMSA}]$  of  $\text{C}_{2v}$  symmetry.

#### B. Molecular Structure of 54.

In order to substantiate the molecular geometry of the  $\eta^2$ -alkyne compounds as suggested by the spectroscopic data, an X-ray structure analysis of 54 was carried out. Figure XVIII shows a perspective view of the molecule with the atom numbering scheme. A summary of crystallographic parameters appears in Table XXIX, while relevant bond distances and angles are collected in Tables XXX and XXXI, respectively.

The view clearly shows the trigonal-bipyramidal arrangement of the ligands around osmium, with the alkyne carbon atoms lying in the equatorial plane (torsional angles  $\text{C}(1)\text{-Os-C}(5)\text{-C}(6)$ ,  $-178.9^\circ$  and

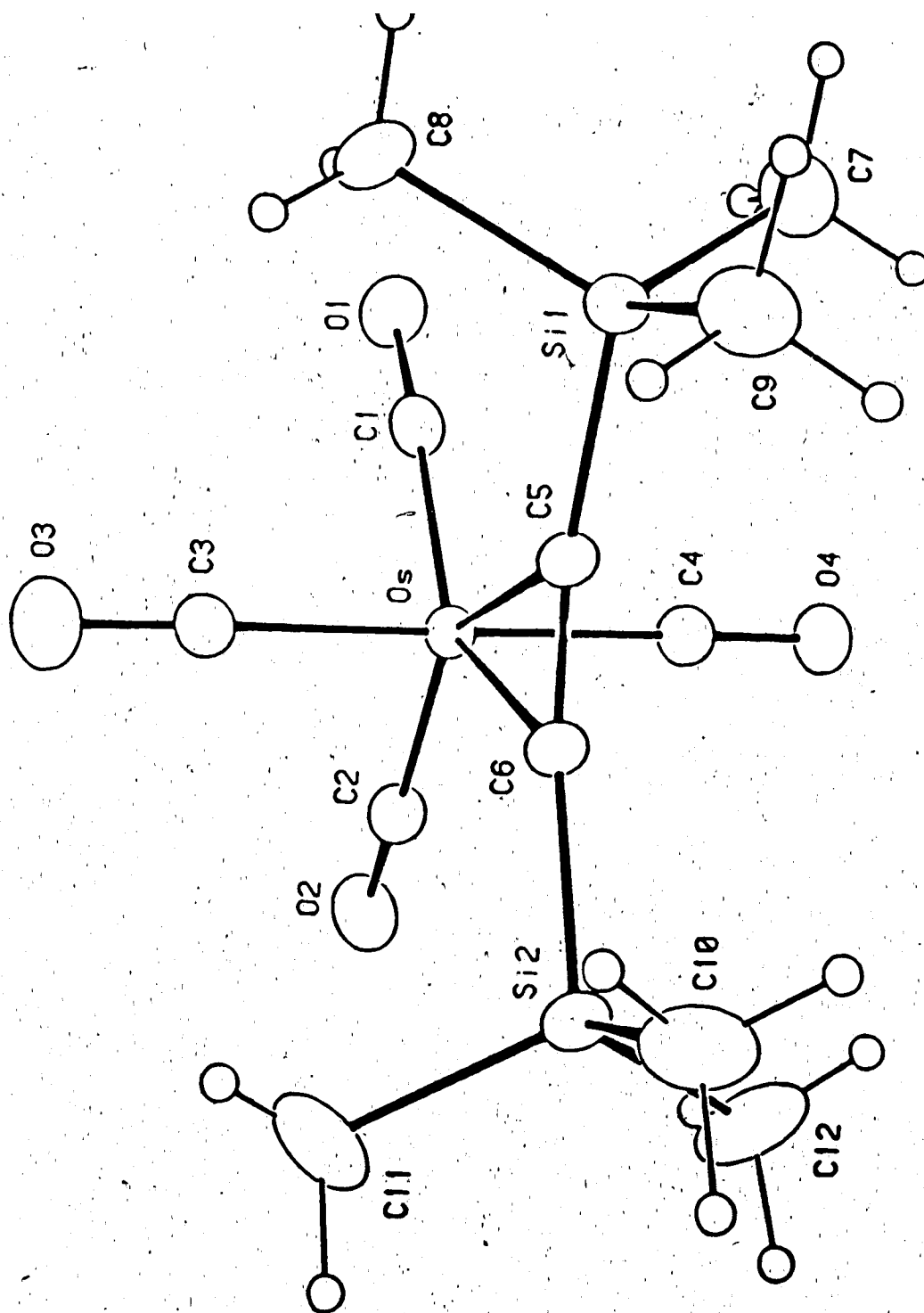


Figure XVIII. Perspective view of  $\text{Os(CO)}_4[\eta^2\text{-C}_2(\text{SiMe}_3)_2](54)$  (Dr. R.G. Ball, SDL/U of

Table XVIII. Spectral Data for Complexes  $M(CO)_4[\eta^2-C_2(SiMe_3)_2]$ .

M	Ir, $cm^{-1}$ <sup>a</sup>		<sup>13</sup> C NMR <sup>b</sup>				
	$\nu_{CO}$	$\nu_{CC}$	T(°C)	$\delta_{CO}$	T(°C)	$\delta_{CO}^c$	$\delta_{CSiMe_3}$
Fe, 56	2078(w) 1998(m)	2003(vs) 1969(s)	1875(w)	-64 <sub>int</sub> 214.1	-92	216.2 211.9	87.8
Ru, 55	2097(w) 2006(m)	2019(vs) 1981(s)	1860(w)	-50 201.5	-80	205.9 198.8	89.5
Os, 54	20999(w) 2003(m)	2016(vs) 1976(s)	1809(w)	+10 183.2	-40	186.4 179.8	92.7

<sup>a</sup>In pentane solution. Abbreviations:

<sup>b</sup>In  $CD_2Cl_2$  solution at 100.6 MHz. Chemical shifts in ppm from  $Me_4Si$ .

<sup>c</sup>The two signals at low temperatures are in the ratio 1:1.

formula	$C_{12}H_{18}O_4Si_2O_s$
formula weight	472.64
crystal dimensions, mm	• 0.25 x 0.37 x 0.32
crystal system, space group	Orthorhombic, $P2_12_12_1$
a, Å	13.391 (3)
b, Å	13.871 (3)
c, Å	9.879 (3)
volume, Å <sup>3</sup>	1835
Z	4
d, g cm <sup>-3</sup>	1.711
$\mu$ , cm <sup>-1</sup>	70.92
take-off angle, deg	3.0
detector aperture, mm	2.40 horizontal, 4.0 vertical
crystal-to-detector distance, mm	205
scan type	$\omega$ -2 $\theta$
scan rate, deg min <sup>-1</sup>	10.1 ~ 2.0
scan width, deg	$0.70 + 0.35 \tan \theta$
2 $\theta$ limit, deg	55.0
reflections measured	2408 unique, 2073 with $I > 3.0\sigma(I)$
absorption correction	yes
parameters refined	172
agreement factors	R, 0.038; $R_w$ , 0.052

---

Metal-C (carbonyl)

Os-C(1)	1.88(1)	Os-C(3)	1.94(1)
Os-C(2)	1.91(1)	Os-C(4)	1.92(1)

Metal-C (alkyne)

Os-C(5)	2.278(9)	Os-C(6)	2.240(9)
---------	----------	---------	----------

C-C (alkyne)

C(5)-C(6)	1.28(1)
-----------	---------

C-O (carbonyl)

C(1)-O(1)	1.17(1)	C(3)-O(3)	1.17(1)
C(2)-O(2)	1.12(1)	C(4)-O(4)	1.16(1)

Si-C

Si(1)-C(5)	1.820(9)	Si(2)-C(6)	1.851(9)
Si(1)-C(7)	1.85(1)	Si(2)-C(10)	1.86(1)
Si(1)-C(8)	1.87(1)	Si(2)-C(11)	1.85(1)
Si(1)-C(9)	1.87(1)	Si(2)-C(12)	1.85(1)

---

Numbers in parentheses are estimated standard deviations in the least significant digits.

---

Angles at Os

C(1)-Os-C(2)	108.6(4)	C(1)-Os-C(5)	108.0(6)
C(1)-Os-C(3)	92.1(5)	C(1)-Os-C(6)	140.9(4)
C(1)-Os-C(4)	90.9(5)	C(2)-Os-C(5)	143.3(4)
C(2)-Os-C(3)	93.0(5)	C(2)-Os-C(6)	110.5(4)
C(2)-Os-C(4)	92.1(4)	C(3)-Os-C(5)	87.9(4)
C(3)-Os-C(4)	172.9(4)	C(3)-Os-C(6)	88.0(5)
C(5)-Os-C(6)	32.9(3)	C(4)-Os-C(5)	85.1(3)
		C(4)-Os-C(6)	85.6(4)

Angles at C (carbonyl)

Os-C(1)-O(1)	177.(1)	Os-C(3)-O(3)	178.(1)
Os-C(2)-O(2)	178.(1)	Os-C(4)-O(4)	178.(1)

Angles at C (alkyne)

Os-C(5)-C(6)	71.9(6)	Os-C(6)-C(5)	75.2(6)
Os-C(5)-Si(1)	128.1(5)	Os-C(6)-Si(2)	131.5(5)

---

Numbers in parentheses are estimated standard deviations in the least significant digits.

characterized  $M(CO)_4[\eta^2\text{-alkyne}]$  fragment encountered in  $Fe_2(CO)_8(Ph_2P\equiv C^tBu)$ .<sup>127</sup> The average Os-CO(axial) (1.93(1)Å) and Os-CO(equatorial) (1.90(1)Å) bond distances are marginally different. The shorter Os-CO (equatorial) bonds indicate that the BTMSA ligand is a poorer  $\pi$ -acid than the CO group and allows for greater back bonding to the carbonyl moieties from osmium in the equatorial plane than toward the axial carbonyls. Similar differences between axial and equatorial carbonyl groups have been observed in the previously mentioned iron complex (1.832(3) and 1.807(9)Å) and in  $eq\text{-Os}(CO)_4(SbPh_3)$  (1.946(6) and 1.918(7)Å).<sup>128</sup>

The strength of the metal-alkyne interaction can be assessed with the aid of structural parameters, i.e., C-C bond distance, the back-bending angle of the alkyne substituents, and the metal-C(alkyne) bond length.<sup>129</sup> In 54, the C(5)-C(6) bond length is 1.28(1)Å which lies midway between the accepted values for C-C double and triple bonds.<sup>73</sup> This distance and the back-bending angles of the  $SiMe_3$  moieties are compared to values obtained for  $Fe_2(CO)_8(Ph_2P\equiv C^tBu)$ <sup>127</sup> and a number of zero valent trigonal nickel triad alkyne complexes<sup>130</sup> in Table XXXII. The somewhat smaller angles in 54, taken together with the length of the C-C bond, indicate slight changes in the relative importance of the retrodonative Os-alkyne interaction in 54 compared to the nickel-group transition metal complexes.

		angle, deg	
$(^t\text{BuN}\equiv\text{C})_2\text{Ni}(\text{PhC}\equiv\text{CPh})$	1.28(2)	$\overline{31}(1)$	b
$(\text{Ph}_3\text{P})_2\text{Pt}(\text{F}_3\text{CC}\equiv\text{CCF}_3)$	1.255(9)	39.9(5)	c
$(\text{Ph}_3\text{P})_2\text{Pt}(\text{C}-\text{C}_7\text{H}_{10})$	1.294(17)	39, 43	d
$(\text{Ph}_3\text{P})_2\text{Pt}(\text{RhC}\equiv\text{CPh})$	1.32(9)	40	d
$\text{Fe}_2(\text{CO})_8(\text{Ph}_2\text{PC}\equiv\text{C}^t\text{Bu})$	1.275(7)	27, 30	e
$(\text{OC})_4\text{Os}(\text{Me}_3\text{SiC}\equiv\text{CSiMe}_3)$	1.28(1)	20.0(8) 27.0(8)	this work

a) Taken in part from reference 130. b) Dickson, R.S.; Ibers, J.A. J. Organomet. Chem. 1972, 36, 191. c) reference 130. d) Glanville, J.O.; Stewart, J.M.; Grim, S.O. J. Organomet. Chem. 1967, 7, P9. e) reference 127.



of the  $\text{SiMe}_3$  groups. As it is, the Os-CO(equatorial) bond axis lies along the favorable Me-Si-Me angle bisector.

A direct comparison of the Os-C(alkyne) distances in 54 with other simple  $\text{Os}[\eta^2\text{-alkyne}]$  fragments is not possible. However, as expected, these bond lengths (Os-C(5), 2.278(9) Å and Os-C(6), 2.240(9) Å) are longer than those observed in alkyne-bridged polynuclear derivatives. For instance, in  $\text{Os}_2(\text{CO})_8[\mu\text{-}\eta^1, \eta^1\text{-DMAD}](33)$ , the two Os-C(alkyne)  $\sigma$ -bonds are 2.138(5) Å. Whereas, in  $\text{Os}_3(\text{CO})_{10}(\text{C}_2\text{Ph}_2)^{131}$  the bridging alkyne unit displays two Os-C  $\sigma$ -bonds of 2.182(8) and 2.070(9) Å and two Os-C  $\pi$ -interactions of 2.188(8) and 2.293(9) Å. Consistent with the stronger osmium-alkyne interaction in these bridged species, the C-C bond lengths, 1.33(1) and 1.439(10) Å respectively, are longer than in 54.

A final point of interest of the present structure is the distinct, if not severe, bending of the axial carbonyl groups towards the equatorial alkyne moiety. A clear view of this is provided in Figure XIX. The C(3)-Os-C(4) angle is 172.9(4)°. Interestingly, a similar type of distortion, with a virtually identical canting angle of 173.5(2) has been observed also in the  $\text{Fe}[\eta^2\text{-alkyne}]$  complex,  $\text{Fe}_2(\text{CO})_8(\text{Ph}_2\text{PC}^t\text{Bu})$ .<sup>127</sup> Since the latter compound presents a different type of alkyne ligand and crystal environment to the iron center, packing forces can be dismissed and it is believed that electronic factors are at the

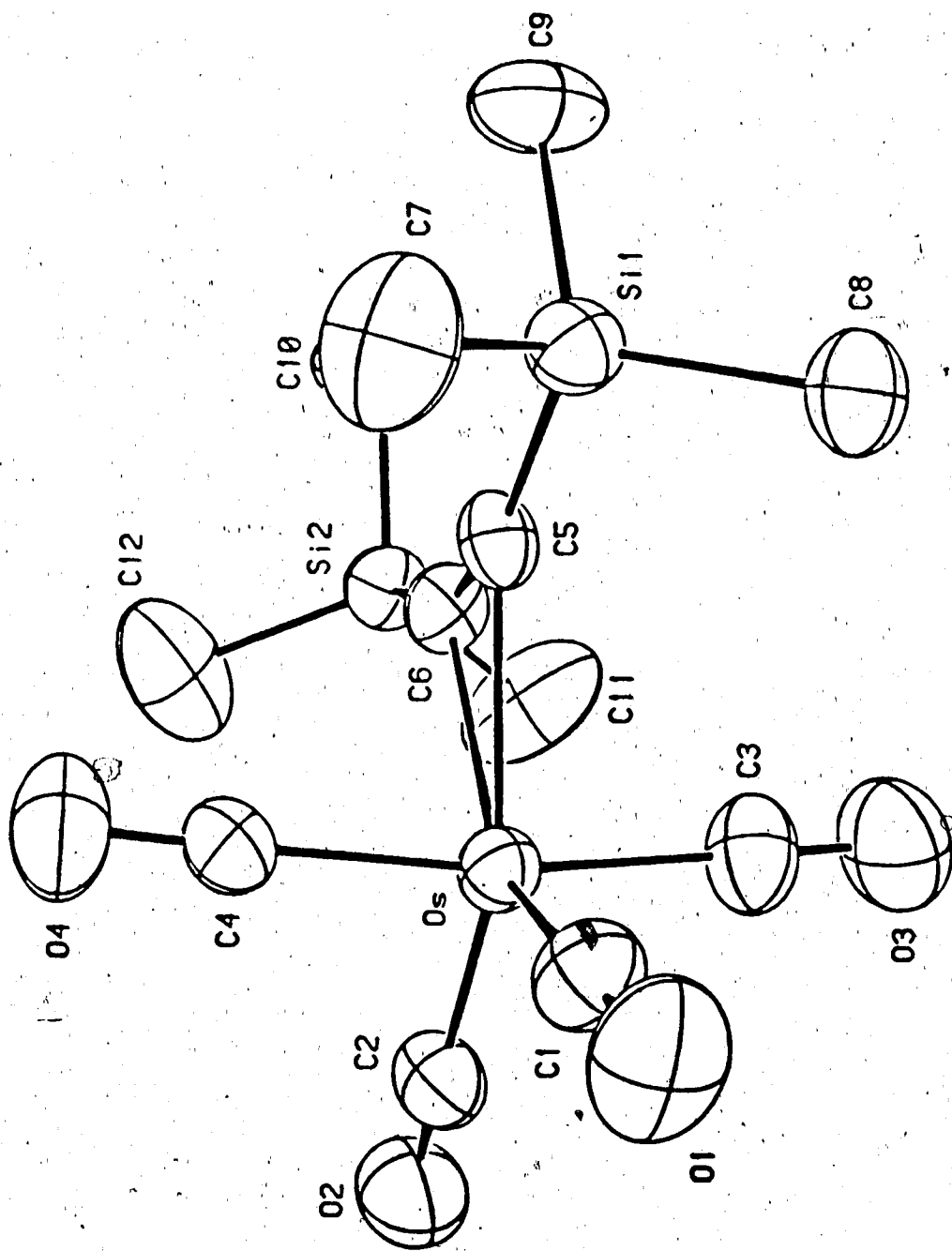
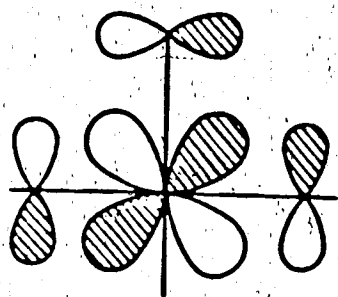


Figure XIX. View of 54 emphasizing the axial carbonyls bending toward the equatorial alkyne.

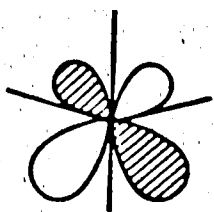
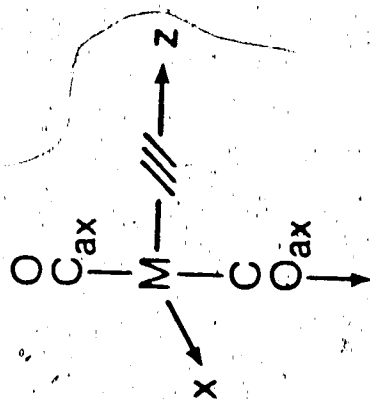
$M(CO)_4[\eta^2\text{-alkene}]$  complexes, the  $CO_{ax}-M-CO_{ax}$  angle is very close to  $180^\circ$  and often the axial CO groups bend slightly away from the equatorial olefin.<sup>132</sup>

Focussing on the  $Os(CO_{ax})_2[\eta^2\text{-alkyne}]$  fragment, Scheme XII, shows the orbitals of interest. The choice of axis system and orbital designations follow the development by Hoffmann.<sup>86</sup> Only the combination which results in positive overlap between metal  $d_{yz}$  ( $b_1$ ),  $CO_{ax}(\pi_{yz}^*)$  and acetylene  $\pi_1$  orbitals is shown in A. Since the equatorial CO groups also compete, via back-bonding, for the electron density in the metal  $d_{yz}$  orbital, the axial carbonyl ligands move slightly toward the alkyne  $\pi_1$  orbital to compensate for this competition. It is recognized that in the present context with both metal  $d_{yz}$  and alkyne  $\pi_1$  orbitals being full, the antibonding combination between these two orbitals will also contain an electron pair. However, movement of axial CO groups toward the equatorial alkyne may result in a "rehybridization" of  $d_{yz}$  as shown in B, which should reduce the two electron repulsion between  $d_{yz}$  and  $\pi_1$ . Although symmetry considerations allow for possible overlap between metal d and alkyne  $\pi_1^*$  orbitals, this is thought to be of minor importance and not readily adapted to account for the kind of axial carbonyl groups movement seen in these molecules.

Of course, the importance of the second full MO of alkynes ( $\pi_1$ ) in electron deficient mononuclear complexes is well recognized and the



A



B

Scheme XII. Proposed orbital interaction to account for axial carbonyl bending.

...three metal centers via a  $\pi$  binding mode, as in  $\text{Os}_3(\text{CO})_{10}(\text{C}_2\text{Ph}_2)^{131}$  and related compounds.<sup>134</sup> It appears from the present observation and analysis, that under appropriate circumstances even electron precise compounds may involve the  $\pi$  MO of the coordinated alkyne. It would be of interest to establish both experimentally and theoretically how the nature of the alkyne and of the transition metal effects the magnitude of this involvement.

### C. Variable Temperature $^{13}\text{C}$ NMR Behaviour.

The variable temperature  $^{13}\text{C}$  NMR spectra of the  $\eta^2$ -alkyne compounds are shown in Figure XX. As expected from the well known behaviour of the related  $\text{M}(\text{CO})_4[\eta^2\text{-olefin}]$  complexes,<sup>135</sup> the tetracarbonyl-alkyne complexes are fluxional as well. At the low temperature limit consistent with the solid state structure of 54, each spectrum exhibits two signals of equal intensity in the carbonyl region. The simplicity of the spectra and the observation that in  $\text{M}(\text{CO})_4[\eta^2\text{-olefin}]$  complexes axial carbonyl groups may resonate both at higher<sup>55,79,135a</sup> and at lower<sup>85,135c</sup> fields than the equatorial carbonyl moieties, precludes unambiguous assignment of the resonances of compounds 54-56. As the temperature is raised the resonances broaden, coalesce and emerge as single sharp signals at the expected averaged positions. The high temperature limiting, sharp singlet could not be observed for the ruthenium derivative due to its instability in solution much above  $-50^\circ\text{C}$ . The observed line shape changes are temperature reversible and indepen-

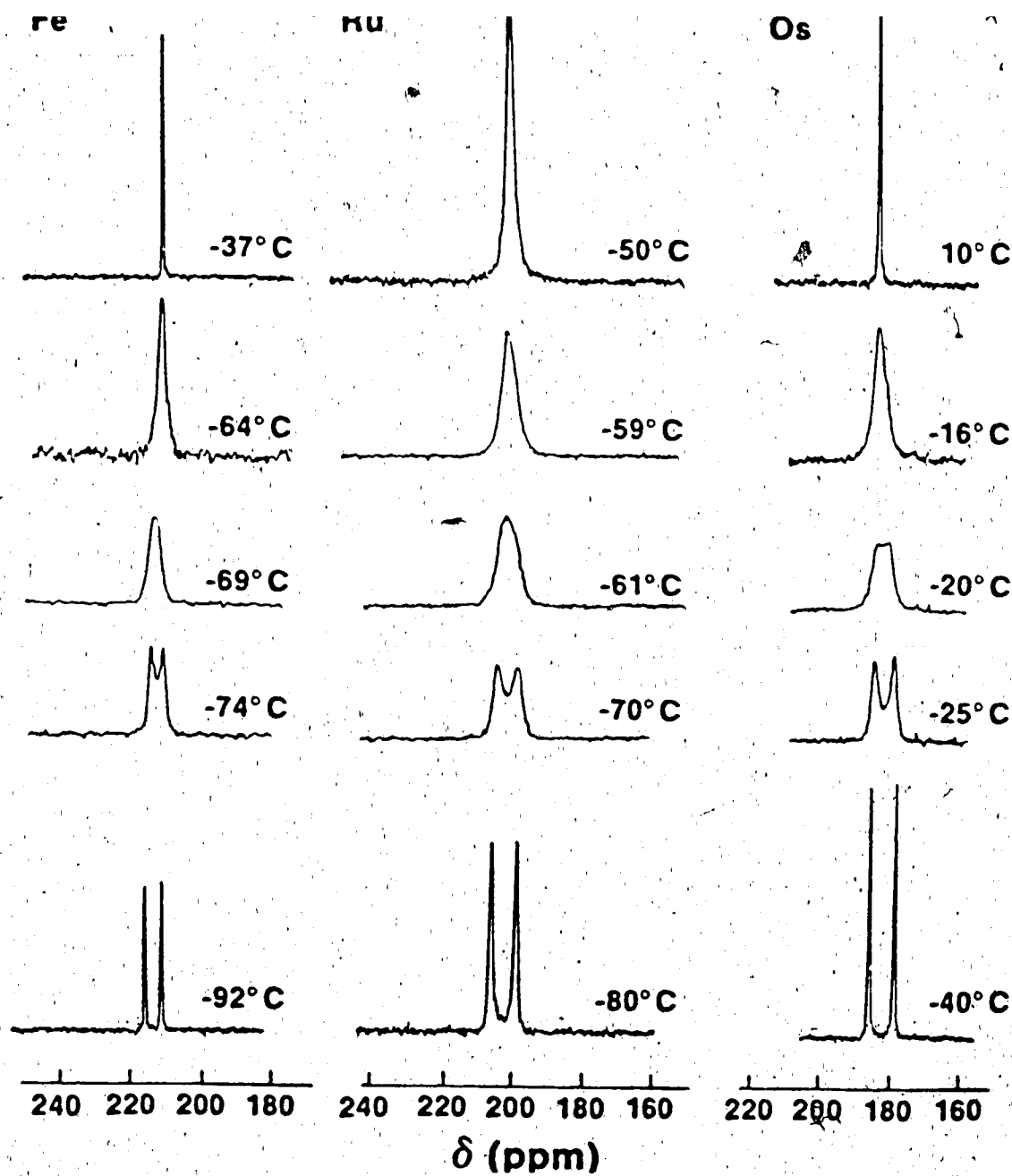


Figure XX. 100.6 MHz  $^{13}\text{C}$  variable temperature NMR spectra for  
Complexes  $\text{M}(\text{CO})_4[\eta^2\text{-C}_2(\text{SiMe}_3)_2]$ .

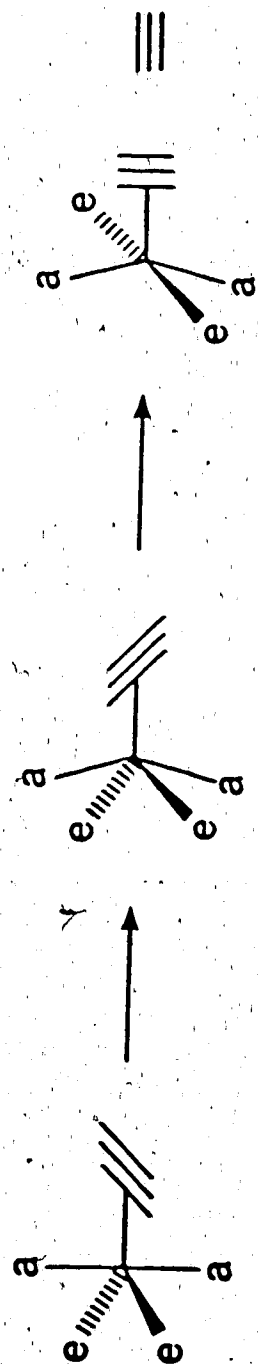
negated by the simplicity of the coalescence pattern, an attractive possibility is the coupled alkyne rotation - Berry pseudorotation (Scheme XIII) which is operationally identical to the well established, although not exclusive,<sup>85,135c</sup> coupled olefin rotation-carbonyl exchange process in the related  $M(CO)_4[\eta^2\text{-olefin}]$  complexes.<sup>55,79,135a,b</sup> Free energies of activation have been calculated (Table XXXIII). Discussion of the observed trend is deferred to the next section.

### III. Triad Comparison of $M(CO)_4[\eta^2\text{-Me}_3\text{SiC}_2\text{SiMe}_3]$ Compounds and Nature of the $M\text{-}[\eta^2\text{-alkyne}]$ Interaction.

The bonding, structure and reactivity of transition metal complexes are under the influence of numerous and often subtly interdependent factors. To gauge the hierarchy of importance of these factors is very difficult. However, triad comparison of homologous series of compounds is well recognized to be extremely valuable in this regard. The observation of metal dependent trends in properties often clarifies bonding ideas and may serve as a guide for structure and reactivity predictions.

In this section we wish to compare the available data on compounds 54-56, especially as they pertain to the major point of interest, the  $M\text{-}[\eta^2\text{-alkyne}]$  interaction. The relevant spectroscopic and energetic data are compared in Table XXXIII.

As usual,<sup>139</sup> metal-alkyne  $\pi$  interaction lowers the  $C\equiv C$  stretching



Scheme XIII. The coupled alkyne rotation - Berry pseudorotation.



Table XXXIII. Comparison of Spectroscopic and Energetic Data on Complexes  
 $M(CO)_4[\eta^2-C_2(SiMe_3)_2]$ .

M	$\Delta(\nu_{CC})^a$	$\Delta(\delta_{C_{alk}})^b$	$\Delta G_{T_c}^\ddagger$ (kcal/mol) <sup>c</sup>	$T_c$ (°)
Fe	233	25.2	9.0	-61
Ru	248	23.5	9.5	-54
Os	299	20.3	11.0	-20

<sup>a</sup> $\Delta(\nu_{CC}) = \nu_{CC}(\text{free BTMSA}) - \nu_{CC}(\text{complexed BTMSA})$ ,  $\nu_{CC}(\text{free BTMSA}) = 2108$ .<sup>136</sup>

<sup>b</sup> $\Delta(\delta_{C_{alk}}) = \delta(\underline{CSiMe_3}, \text{free}) - \delta(\underline{CSiMe_3}, \text{complexed})$ ,  $\delta(\underline{CSiMe_3}, \text{free}) = 113.0$ .<sup>137</sup>

<sup>c</sup>Free energies of activation at the coalescence temperature,  $T_c$ , were calculated using the approximate expression applicable to the coalescence of two equal singlets.<sup>138</sup>

represented by the metallacyclopropene formulation. This conclusion is further reinforced by the Os-C(alkyne) distances which, vide supra, are significantly longer than in the corresponding diosmacyclobutene compound 33. The coordination shift increases in the order Fe<Ru<<Os and reflects<sup>139,140</sup> a concomitant reduction in C≡C bond order.

Another measure of this bond order reduction is the chemical shift of the coordinated alkyne carbon atoms. Deshielding of the alkyne carbons upon coordination to a metal has been attributed to an increase in the olefinic character of the alkyne as its  $\pi$ -bond order is reduced.<sup>141</sup> Indeed, Templeton<sup>142</sup> has established an empirical relationship between the number of electrons donated by the alkyne and its  $^{13}\text{C}$  chemical shifts. Although the progressively lower field shifts of the alkyne carbons ( $\delta\text{C}_{\text{alk}}$ ) from Fe to Os (Table XXVIII) parallels the variation in  $\Delta(\nu_{\text{CC}})$  (and indicates reduced C≡C bond order down the triad), the sign and magnitude of the coordination shift requires some further comments. Reference to Table XXXIII reveals that contrary to previous cases with normal, carbon substituted alkynes, the coordination shift in the  $\eta^2$ -alkyne complexes is positive (i.e., complexed BTMSA resonates at higher field than the free ligand). This anomaly can be traced not to a suddenly different metal-alkyne bonding in these compounds but to the influence of the  $\text{SiMe}_3$  moiety on the carbon chemical shift in free BTMSA. The chemical shift of the alkyne carbon in free BTMSA is at  $\delta 113.0$  ppm,<sup>137</sup> some 35 ppm to lower field than in related carbon sub-

bond and the  $\text{SiMe}_3$  moiety,<sup>137,144</sup> giving rise to reduced  $\pi$ -bond order in free BTMSA. The situation, of course, is very different in complexes 54-56 where the bending back of the  $\text{SiMe}_3$  moieties from the  $\text{C}\equiv\text{C}$  bond (Figures XVIII and XIX) greatly reduces this type of interaction. As a result the chemical shift of the alkyne carbons of "free" BTMSA but in a geometry as seen in 54 should arguably resonate at a field significantly higher than 113 ppm. Regretably, the magnitude of this predicted chemical shift is not easily available and therefore discussion concerning the absolute magnitude of the observed  $^{13}\text{C}$  coordination shifts in compounds 54-56 would be futile. Nevertheless, we believe that neglect of this "correction term" is indeed the reason for the sign reversal of  $\Delta\delta$  and consequently for the trend of decreasing coordination shift down the triad in the alkyne compounds (i.e., smaller positive  $\Delta\delta$ , after "correction" would translate into a larger negative  $\Delta\delta$ ).

Finally, we wish to consider the trend in the free energies of activation,  $\Delta G_{\text{T}}^{\ddagger}$ , for carbonyl group scrambling in these molecules. Although the energetics of the related process in  $\text{M}(\text{CO})_4[\eta^2\text{-olefin}]$  ( $\text{M} = \text{Fe}, \text{Ru}, \text{Os}$ ) compounds are not simply dependent on a single variable,<sup>86,145</sup> the available experimental data supports the view that the trends in activation energies are mainly controlled by the  $\pi$ -component of the metal-olefin bond.<sup>135</sup> The same rationale is expected to hold for the present compounds. The trend of increasing  $\Delta G^{\ddagger}$  in order  $\text{Fe} < \text{Ru} < \text{Os}$  mirrors the changes observed in the analogous  $\eta^2$ -olefin com-

metals is descended. It is noteworthy that the increase in back bonding from Fe to Ru is apparently more than offset by a concomitant decrease in  $\pi(\text{alkyne})$  to metal d orbital donor interaction since the ruthenium compound is much less stable than its iron analog. The stability sequence is  $\text{Os}(54) > \text{Fe}(56) \gg \text{Ru}(55)$ . It is worth emphasizing that the importance of the  $\sigma$  component of the metal-alkyne bonding interaction became clear only when the stability of the complexes and the variation in barriers for the coupled alkyne rotation-carbonyl scrambling process were scrutinized together. The successful identification of the individual components of the metal-alkyne bond resides in the fact that the trend in  $\Delta G^\ddagger$  is uniquely modulated by the  $\pi$ -component of this bond. The coordination shifts,  $\Delta(\nu_{\text{CC}})$  and  $\Delta(\delta\text{C}_{\text{alk}})$ , indicate variations in  $\text{C}\equiv\text{C}$  bond order and therefore reflect composite changes in forward donation and back acceptance from the alkyne moiety. To further probe the relative importance of these two factors on the coordination shifts, the variations in  $\Delta(\delta\text{C}_{\text{alk}})$  vs.  $\Delta G^\ddagger$  and  $\Delta(\nu_{\text{CC}})$  vs.  $\Delta G^\ddagger$  were investigated. Figure XXI nicely shows the inverse relation between  $\Delta G^\ddagger$  and  $\Delta\delta$  and  $\Delta\nu_{\text{CC}}$  which is due to the apparent anomaly in  $\Delta\delta$ , vide supra. It also establishes that, despite the non-uniform changes between Fe/Ru and Ru/Os, there is a good linear relationship between these properties as the metal is changed. Clearly this implies that, as long as the assumption about the dependence of  $\Delta G^\ddagger$  on metal-alkyne  $\pi$  component is valid, at least in this class of compounds  $\pi$ -back bonding also dominates changes affecting  $\nu_{\text{CC}}$  and  $\delta\text{C}_{\text{alk}}$ .

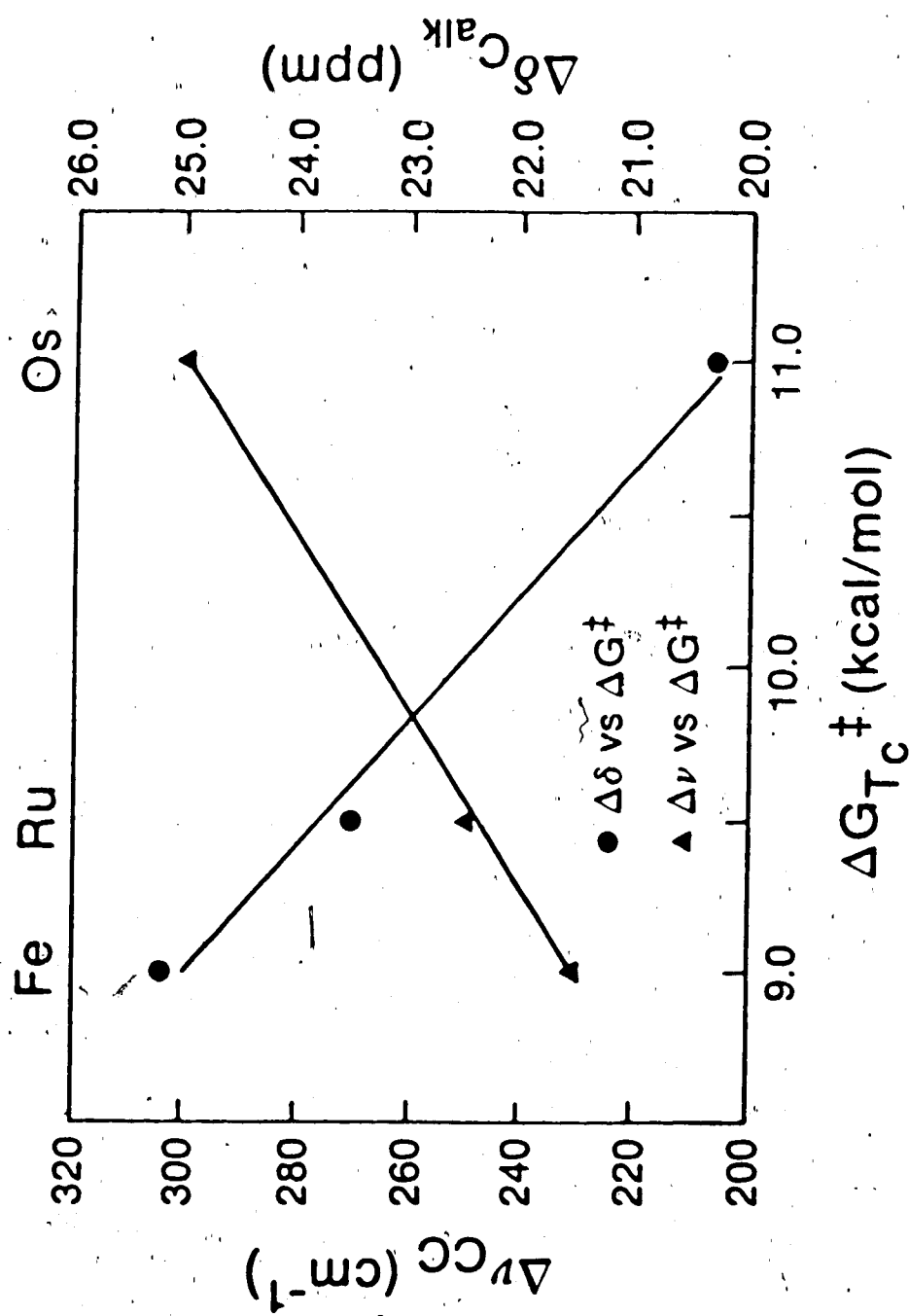


Figure XXI. Graphical comparison of the variation in coordination shifts (IR and NMR) versus  $\Delta G^\ddagger$  for carbonyl scrambling in Complexes  $M(CO)_4[\eta^2-C_2(SiMe_3)_2]$ .

the lesser stability of 55 compared to 56. Similarly,  $\text{Ru}(\text{CO})_4[\eta^2\text{-olefin}]$  compounds are less stable than their iron analogs.<sup>55</sup> Discontinuity in stability at the second row transition metal is not confined to the Fe triad but appears to be a general phenomenon for metal  $\pi$ -complexes. For instance, Maitlis et al.<sup>137</sup> found that in the series of complexes,  $(\text{Ph}_3\text{P})_2\text{M}(\eta^2\text{-CF}_3\text{C}_2\text{CF}_3)$ , the stability decreased in the order  $\text{Pt} > \text{Ni} > \text{Pd}$ . Moreover, for this class of alkyne-transition metal derivatives the variation in  $\Delta(\nu_{\text{CC}})$ ,  $\text{Pt} > \text{Ni} > \text{Pd}$ , reflects exactly the stability sequence and implies that with these highly basic  $\text{d}^{10} \text{M}(\text{PPh}_3)_2$  fragments metal d to  $\pi^*(\text{alkyne})$  back-bonding dominates the metal-alkyne interactions. This is clearly not the case with  $\text{M}(\text{CO})_4[\eta^2\text{-BTMSA}]$  compounds. Here, due to the presence of the electron acceptor  $\text{M}(\text{CO})_4$  metal carbonyl fragment and the electron rich bis(trimethylsilyl) acetylene, both  $\sigma$  and  $\pi$  component of the metal-alkyne interaction appear to play an important role in determining the overall thermodynamic stability of the bond.

#### IV. Conclusions.

The availability now of the first simple  $\text{Os}(\text{CO})_4[\eta^2\text{-alkyne}]$  derivative should provide enough incentive to seek out other examples. This would be most important in view of the structural features which suggest the participation of the second set of  $\pi$  orbitals on the alkyne in the overall bonding picture. By altering the electronic character of the alkyne, it would be of interest to meter the extent of this participation. Initial efforts to this end are presently underway in

over the BTMSA derivatives. As well, a reasonable yield of the corresponding ruthenacyclobutene complex has been obtained in a fashion similar to equation (9), and may imply a rich derivative chemistry heretofore unknown for ruthenium.

## I. General Techniques.

Solvents were dried by refluxing and distilling from the appropriate drying agents (Table XXXIV). When necessary they were further freed of oxygen by repeated freeze-pump-thaw cycles or purged with purified nitrogen or argon. Pentane and hexanes were preconditioned before drying by firstly washing with  $\text{H}_2\text{SO}_4$  until no colour appeared in the acid layer, then washing with water to remove residual acid, and finally drying over  $\text{Na}_2\text{SO}_4$ . Deuterated solvents were dried over molecular sieves.

Glassware was treated with KOH-Ethanol solution and dried at  $120^\circ\text{C}$ . All reactions were performed using standard Schlenk techniques under purified inert atmospheres. Nitrogen and argon were passed through a heated column ( $100^\circ\text{C}$ ) containing BASF Cu-based catalyst (R3-11) to remove oxygen and a column of Mallinkrodt Aquasorb ( $\text{P}_2\text{O}_5$  on inert base) to remove water.

Chromatographic separations were carried out either on preparative TLC plates (EM Reagents; Silica Gel 60 F-254,  $20 \times 20 \times 0.2$  cm) or on a Chromatotron (Harrison Research; preparative, centrifugally accelerated, radial thin-layer chromatography, Silica Gel PF-254 with  $\text{CaSO}_4 \cdot \frac{1}{2}\text{H}_2\text{O}$ , OD 21.8 cm, ID 6.8 cm, 2 mm thickness, argon atmosphere).

## II. Photochemical Techniques.

Photochemical experiments were performed with the following apparatus:

- (1) Pyrex Immersion Well apparatus [Figure XXII] using cold

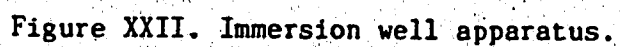


Table XXXIV. Drying Agents for Solvents.

---

Pentane	$\text{CaH}_2$
Hexanes	Potassium metal
Heptane	$\text{CaH}_2$
Benzene	Potassium metal
Toluene	Sodium metal
THF	Potassium metal/benzophenone
$\text{CH}_2\text{Cl}_2$	$\text{P}_2\text{O}_5$

---



(Glasswerk Wertheim) glass; (2) Immersion Well only [Figure XXII, right], with the sample solution held in a Schlenk tube positioned adjacent to the Well. This could be used (a) with or (b) without the GWV filter sleeve for external photolysis; (3) Oriel 500W Variable Power Focused Beam High Pressure Mercury Lamp used for external photolysis. Samples were held in Schlenk tubes, which were surrounded by a GWV filter sleeve, at a distance of approximately 10 cm from the focusing lens.

### III. Physical Measurements.

Reactions were monitored by IR with the aid of a Nicolet MX-1 Fourier Transform Interferometer over the range  $2200-1600\text{ cm}^{-1}$ . Solution samples were held between either KBr (0.1 mm or 0.5 mm path length) or  $\text{CaF}_2$  (0.1 mm path length) plates.  $^1\text{H}$ ,  $^{13}\text{C}$ ,  $^{19}\text{F}$ , and  $^{31}\text{P}$  NMR spectra were obtained on either a Bruker WP-200 or a WP-400 Fourier Transform Spectrometer. Routine  $^1\text{H}$  and overnight  $^{13}\text{C}$  spectra were collected on a Bruker AM-300 FT Spectrometer. Variable temperature NMR experiments were carried out on the Bruker WP-400 either in vacuum-sealed medium-walled sample tubes or thin-walled sample tubes with the plastic caps wrapped in Parafilm. Solvent resonances (vs. TMS) were used as internal standards for  $^1\text{H}$  and  $^{13}\text{C}$  NMR spectra.  $\text{H}_3\text{PO}_4$  and  $\text{CFCI}_3$  were used as calculated external standards for  $^{31}\text{P}$  and  $^{19}\text{F}$  NMR spectra, respectively.

Mass spectra were recorded on an AEI MS-12 Mass Spectrometer operating at 70 eV. Solid samples were injected directly into the source at temperatures just sufficient to obtain data. Parent molecular ions were identified by the highest abundance isotopes of Ru(102),

analyses were performed in the Microanalytical Laboratory of this Department and at the Analytische Laboratorien, Gummersbach, West Germany.

Complete X-ray solid state structure determinations for compounds 14, 28, 33, 34 and 54 were carried out by Dr. R.G. Ball of the Structure Determination Laboratory of this Department. For compound 30, Dr. Ball collected the diffraction data, and structure solution was performed by this author under the guidance of Professor Martin Cowie of this Department. All data was collected on an Enraf Nonius CAD4 Diffractometer using MoK $\alpha$  radiation ( $\lambda = 0.71073 \text{ \AA}$ ) and an incident beam graphite crystal monochromator. Other pertinent crystallographic information will appear together with the appropriate structures.

#### IV. Reagents and Reactions, Chapter Two.

##### 1. Reagents.

$\text{Os}_3(\text{CO})_{12}$  (3c) was prepared by the literature method.<sup>7</sup> The following alkenes were used as received: ethylene [ $\text{C}_2\text{H}_4$ ](Linde-Union Carbide Canada); propylene [ $\text{C}_3\text{H}_6$ ](Matheson of Canada); methyl acrylate [MA], ethyl acrylate [EA](Eastman Kodak); acrylic acid [AA], methyl vinyl ketone [MVK](Aldrich Chemical Company); maleic anhydride [MAH](BDH Chemicals Ltd.); cis-cyclooctene [COE](Matheson, Coleman, Bell); tetrafluoroethylene [TFE](PCR); perfluoro-2-butene [OFB](Pierce Chemical Company). 3-penten-2-one [3P2O](Aldrich) was distilled prior to use.

##### 2. Photoreactions of $\text{Os}_3(\text{CO})_{12}$ (3c) with alkenes.

###### (a) General Method.

Photoapparatus (1) was charged with approximately 500 mg (0.60 mmol)

til a clear solution was obtained and IR bands for  $3c$  ( $\nu_{CO}$  2070 (vs), 2034 (s), 2015 (m), 2000 (m)  $\text{cm}^{-1}$ ) had disappeared. The solution was filtered through a medium-porosity glass frit if necessary, and the solvent and excess alkene were removed on a Rotavapor R110 (trapped at  $-78^\circ\text{C}$ ) or in vacuo ( $35^\circ\text{--}40^\circ\text{C}/0.1$  mm Hg). Treatment of the crude reaction mixture varied with the alkene. In a typical experiment with methyl acrylate [MA], the crude product was extracted with 10 mL portions of hot pentane until no further solids dissolved. The combined extracts (50–60 mL) were filtered through a glass frit and concentrated in volume until crystals formed (ca. 15 mL). The pentane solution was cooled to  $-15^\circ\text{C}$  which precipitated pale yellow crystals of  $\text{Os}_2(\text{CO})_8[\mu-\eta^1, \eta^1\text{-CH}_2\text{CH}(\text{CO}_2\text{CH}_3)]$  ( $14$ ). A further crop of crystals could be obtained by reducing the supernatant volume and recooling to  $-15^\circ\text{C}$  (average total yields:  $180 + 20$  mg, 48%). The other Os-containing product,  $\text{Os}(\text{CO})_4[\eta^2\text{-CH}_2\text{CH}(\text{CO}_2\text{CH}_3)]$  ( $13$ ) could be isolated from the mother liquor after all of  $14$  had precipitated (average yield: 150 mg, 65%).

The same reaction could be carried out in a 200 mL Schlenk tube (5.0 x 15.0 cm) in 120 mL of benzene using photoapparatus (3). Compound  $14$  was obtained in a maximum yield of 69% following identical isolation procedures.

Results from photoreactions between  $3c$  and other alkenes are reported in Table III.  $\nu_{CO}$  of the carbonyl ligands and alkenes for the obtained products appear in Table IV. Analytical and mass spectral data (where available) appear in Table V.  $^1\text{H}$  NMR data for compounds

... data for the mononuclear and dinuclear compounds are given in Tables XI and XIII respectively.

Variations in the isolation procedure are reported below:

(b)  $C_2H_4$ :

The formed  $Os(CO)_4[\eta^2-C_2H_4]$  (15) is volatile and was removed along with the benzene. The resulting solution was used in subsequent reactions [see Section VII. 2(i)]. Pentane extracts of the orange residue were combined and filtered through a short pad (1.0 x 2.0 cm) of silica gel before concentrating and cooling.

(c)  $C_3H_6$ :

$Os(CO)_4[\eta^2-CH_2CH(CH_3)]$  (17) also is volatile and was obtained as a benzene solution. Small quantities of impure  $Os_2(CO)_8[\mu-\eta^1, \eta^1-CH_2-CH(CH_3)]$  (18) could be obtained but appeared to decompose to 3c, even under a propylene atmosphere.

(d) COE.

$Os(CO)_4[\eta^2-cis-cyclooctene]$  (19) was characterized by IR in the pentane extracts as the only identifiable reaction product. Extended recrystallization attempts resulted in the apparent decomposition of 19.

(e) EA.

Following the isolation procedure in (a), crystalline  $Os_2(CO)_8[\mu-\eta^1, \eta^1-CH_2CH(CO_2CH_2CH_3)]$  (21) was obtained. However,  $Os(CO)_4[\eta^2-CH_2CH(CO_2CH_2CH_3)]$  (20) could not be isolated due to apparent decomposition to an unidentifiable solid material.

two 7 mL pentane extractions left behind 168.5 mg of a highly insoluble white solid, which displayed very broad  $\nu_{\text{CO}}$  and was not identified. The cooled yellow pentane solution afforded a mixture of solids. Fractional crystallization and preparative TLC ( $\text{CH}_2\text{Cl}_2$  eluent) were not successful in separating the mixture, but the two compounds could be identified spectroscopically.

(g) MVK.

A brown involatile liquid remained after solvent removal. Cooling the liquid to  $-15^\circ\text{C}$  gave 11.0 mg (0.0163 mmol, 3%) of yellow crystalline  $\text{Os}_2(\text{CO})_8[\mu-\eta^1, \eta^1-\text{CH}_2\text{CH}(\text{C}(\text{O})\text{CH}_3)]$  (25). Further attempts to isolate pure compounds (distillation of the liquid, extraction/fractional crystallization, preparative TLC) failed.

(h) 3P20.

Several 10 mL hexanes extractions of the orange oil following solvent removal gave only  $\text{Os}(\text{CO})_4[\eta^2-\text{CH}(\text{CH}_3)-\text{CH}(\text{C}(\text{O})\text{CH}_3)]$  (26) in small quantities. Attempted purification (fractional crystallization, chromatography) resulted in decomposition of 26 to 3g.

(i) TFE.

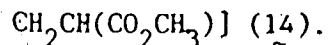
No net reaction occurred over a 12h irradiation period.

(j) OFB.

Compound 3c was recovered after 20h of photolysis using photoapparatus (2a).

(k) MAH.

No products were formed and 3c was recovered.



X-ray quality crystals of 14 were obtained from a cooled (-15°C) pentane solution. Table VI gives a summary of crystal data and features of the data collection and structure refinement.

The two Os atom positions were located using the direct methods program MULTAN.<sup>147</sup> The remaining non-hydrogen atoms were located by the usual combination of least-squares refinement and difference Fourier synthesis. Refinement of atomic parameters was carried out using full-matrix least-squares techniques on  $\underline{F}_o$  minimizing the function

$$\sum \omega (|\underline{F}_o| - |\underline{F}_c|)^2$$

where  $|\underline{F}_o|$  and  $|\underline{F}_c|$  are the observed and calculated structure factor amplitudes respectively, and the weighting factor  $\omega$  is given by

$$\omega = 4 \underline{F}_o^2 [\sigma^2(\underline{F}_o)]^{-1}$$

Atomic scattering factors were calculated from the analytical expression for the scattering factor curves.<sup>148</sup> The  $\underline{f}'$  and  $\underline{f}''$  components of anomalous dispersion<sup>149</sup> were included in the calculations for all non-hydrogen atoms.

Five of the six H atoms were revealed in the final difference Fourier cycles. These were included at their observed positions while the sixth (a methyl H) was subsequently fixed. Isotropic thermal parameters for the H atoms were fixed at 1.5 Å<sup>2</sup>.

The anisotropic thermal parameters of O(10) refined to impossible values during the final refinement and so was assigned an isotropic thermal parameter.

A list of positional and thermal parameters with their esd's is



Table XXXV. Positional and Thermal Parameters for  $\text{Os}_2(\text{CO})_8[\eta-\eta^1, \eta^1-\text{CH}_2\text{CH}(\text{CO}_2\text{CH}_3)](14\gamma)$ .

Atom	x	y	z	$U_{11}$	$U_{22}$	$U_{33}$	$U_{12}$	$U_{13}$	$U_{23}$
Os(1)	220.94(2)	341.91(3)	384.16(6)	9.0(2)	14.0(2)	8.3(2)	1.0(2)	0	0
Os(2)	55.12(2)	326.04(3)	232.79(6)	7.8(2)	14.4(2)	13.0(2)	-0.4(2)	2	2
O(1)	396.1(5)	397.3(7)	486(1)	29(4)	24(5)	44(5)	4(4)	0	0
O(2)	170.2(5)	514.2(6)	636(1)	27(4)	15(4)	13(3)	1(3)	3	3
O(3)	206.3(5)	189.0(6)	703(1)	34(5)	19(4)	23(4)	-4(4)	-7	-7
O(4)	271.6(5)	175.5(6)	120(1)	21(4)	28(4)	15(4)	11(4)	2	2
O(5)	-107.8(5)	335.4(8)	-5(1)	15(4)	19(4)	45(5)	-3(3)	-10	-10
O(6)	37.1(5)	544.8(6)	6(1)	18(4)	22(4)	26(4)	2(4)	6	6
O(7)	2.9(6)	238.9(7)	609(1)	41(5)	47(6)	16(4)	-1(5)	14	14
O(8)	94.0(5)	129.3(7)	42(1)	17(4)	26(4)	30(4)	0(4)	4	4
O(9)	289.8(5)	380.3(6)	-101(1)	17(4)	26(4)	16(4)	-2(4)	4	4
C(1)	331.6(7)	374.9(9)	450(2)	15(5)	25(6)	19(5)	4(5)	-4	-4
C(2)	187.6(7)	450.7(8)	545(2)	17(5)	23(6)	11(5)	-4(5)	-1	-1
C(3)	213.6(6)	246.5(8)	587(1)	1(4)	22(6)	16(5)	0(4)	2	2
C(4)	250.4(7)	237.4(8)	210(1)	19(5)	16(5)	5(5)	-1(5)	3	3
C(5)	-46.6(7)	330.0(8)	87(2)	17(5)	15(5)	21(5)	-2(5)	12	12
C(6)	44.5(6)	464.2(8)	302(1)	9(5)	19(5)	14(5)	3(4)	10	10
C(7)	20.3(7)	271.2(9)	468(2)	19(6)	16(6)	30(6)	3(5)	-7	-7
C(8)	81.3(6)	199.3(8)	126(2)	11(5)	9(5)	22(5)	0(4)	-2	-2
C(9)	126.7(6)	392.7(9)	17(2)	3(4)	22(6)	19(5)	1(4)	-1	-1
C(10)	200.7(6)	437.5(8)	127(1)	14(5)	17(5)	10(5)	6(5)	-7	-7

Table XXV. (continued).

Atom	x	y	z	U <sub>11</sub>	U <sub>22</sub>	U <sub>33</sub>	U <sub>12</sub>	U <sub>13</sub>
C(11)	273.4(6)	437.8(8)	22(1)	14(5)	20(5)	8(5)	0(5)	1(5)
C(12)	401.8(7)	509(1)	10(2)	15(5)	30(7)	51(7)	-12(5)	21(5)
-----								
Atom	x	y	z	U <sub>11</sub>	Atom	x	y	z
O(10)	325.1(5)	508.8(6)	86(1)	19(2)	H1C(12)	434	562	62
H1C(9)	137(7)	336(8)	-39(17)	19	H2C(12)	425(7)	447(9)	22(5)
H2C(9)	91(7)	438(8)	-69(16)	19	H3C(12)	399(7)	520(9)	-128(5)
H3C(10)	195(7)	504(9)	161(16)	19				

The atomic positional parameters have been multiplied by 10<sup>3</sup>. The anisotropic thermal parameters multiplied by 10<sup>3</sup>.

The isotropic thermal parameters have been multiplied by 10<sup>3</sup>.

The form of the anisotropic thermal parameter is:

$$\exp[-2\pi^2(h^2a^2U_{11} + 12hkaU_{12} + 12k^2a^2U_{22} + 2hla^2cU_{13} + 2hla^2cU_{23} + 2k^2l^2c^2U_{33})]$$

Estimated standard deviations in the least significant digits are shown in parentheses. Those per without an error were not refined.

Dimethyl fumarate [DMF], a gift from the MPI für Strahlenchemie, West Germany, was sublimed before use. Diethyl fumarate [DEF] (Baker Chemical Co.), dimethyl maleate [DMM] (Eastman Kodak), diethyl maleate [DEM] and cis-stilbene (Aldrich Chemical Company) were used without further purification.  $\text{Os}(\text{CO})_5(1c)$  was prepared by the method of Pomeroy.<sup>88</sup>  $\text{Os}_2(\text{CO})_8[\mu-\eta^1, \eta^1-\text{CH}_2\text{CH}(\text{CO}_2\text{CH}_3)]$  (14) was synthesized as described in Section IV. 2(a).

## 2. Photochemical Reactions of 3c with DMM.

These reactions were carried out as described in Section IV. 2(a) in an attempt to prepare the analogous complexes  $\text{Os}(\text{CO})_4[\eta^2-\text{Z}-\text{C}_2\text{H}_2(\text{CO}_2\text{CH}_3)_2]$  (27) and  $\text{Os}_2(\text{CO})_8[\mu-\eta^1, \eta^1-\text{Z}-\text{C}_2\text{H}_2(\text{CO}_2\text{CH}_3)_2]$  (28). However, during the reactions, a shift to higher frequency of the carboxylate  $\nu_{\text{CO}}$  of the free alkene was seen. This proved to be indicative of the isomerization of DMM to DMF.

Following each reaction (see Table XIV for reaction conditions), the excess DMF was isolated by one of the following procedures: (a) Solvent was removed on a Rotavapor R110 (trapped at  $-78^\circ\text{C}$ ) until some DMF separated from solution. The solution was decanted and the solid residue washed with 10 mL of benzene, which was added to the previously removed supernatant. The solution was returned to the Rotavapor and the cycle was repeated several times to a final volume of 10 mL. After the final decanting, the benzene solvent was removed, the residue was dried in vacuo and loaded into a sublimator and the

due was treated as in (b).

In the later stages of sublimation, compound 27 and in greater quantities  $\text{Os}(\text{CO})_4[\eta^2\text{-E-C}_2\text{H}_2(\text{CO}_2\text{CH}_3)_2]$  (29) were identified in the sublimes by IR. These species could not be separated from the bulk of the sublimed DMF and in most cases their yields were not determined. The residues remaining after sublimation contained varying quantities of the isomeric dinuclear compounds  $\text{Os}_2(\text{CO})_8[\mu\text{-}\eta^1, \eta^1\text{-Z-C}_2\text{H}_2(\text{CO}_2\text{CH}_3)_2]$  (28) and  $\text{Os}_2(\text{CO})_8[\mu\text{-}\eta^1, \eta^1\text{-E-C}_2\text{H}_2(\text{CO}_2\text{CH}_3)_2]$  (30). The most effective separation of these compounds was accomplished with the Chromatotron ( $\text{CH}_2\text{Cl}_2$  eluent, ca. 2h). As well, 28 could be removed by extraction with pentane, since 30 showed limited solubility in hydrocarbon solvents.

### 3. Photoreaction of 3c with DMF.

In the usual manner (Section IV. 2(a) and Table XIV), the photolysis of 3c with excess DMF was carried out. Following isolation procedure (b), a yellow powder remained after sublimation of the alkene. Pentane extraction of the powder removed the remainder of compound 29 which did not sublime and left almost pure dinuclear 30. Compound 30 could be recrystallized from 1:1  $\text{CH}_2\text{Cl}_2$ :hexanes at  $-40^\circ\text{C}$  to give a fluffy white solid.

### 4. Photoreaction of 3c with DEM.

Twelve mL of a yellow liquid remained after removal of benzene

4 4

( $\text{CO}_2\text{CH}_2\text{CH}_3$ )<sub>2</sub>] (31) and some unreacted 3c. Distillation of the excess alkene left an oily orange solid from which 31 could not be isolated.

5. Photoreaction of 3c with DEF.

To confirm the identity of products from reaction 4, the photolysis of 3c with DEF was performed (Table XIV). The wet yellow solid which resulted after solvent removal was treated with 6 - 7 mL portions of pentane to remove 31 and leave almost pure 32. The pentane extracts were combined and reduced in volume to 10 mL and cooled to  $-15^\circ\text{C}$ . The initial precipitate was identified as free DEF (literature mp  $1 - 2^\circ\text{C}$ ). Concentrating the mother liquor to one-half and storing at  $-78^\circ\text{C}$  afforded a pure white solid of  $\text{Os}(\text{CO})_4[\eta^2\text{-E-C}_2\text{H}_2(\text{CO}_2\text{CH}_2\text{CH}_3)_2]$  (31), which appears as a colourless liquid at room temperature.

6. Photoreaction of 3c with cis-stilbene.

Upon removing all volatiles, a golden-brown residue remained. The solid was loaded into a sublimator and sublimation at  $50^\circ\text{C}/0.1\text{ mm Hg}$  afforded 2.75 g of a yellow crystalline solid identified as trans-stilbene (mp:  $121^\circ\text{C}$ ; literature mp:  $122-4^\circ\text{C}$ ; bp cis-stilbene:  $82-4^\circ\text{C}/0.4\text{ mm Hg}$ ). The remaining brown residue contained unreacted 3c and unidentifiable materials.

These reactions were carried out in 70 mL Schlenk tubes (3.6 x 14.0 cm) using filtered u.v. light (GWV filter sleeve,  $\lambda \geq 370$  nm) and photoapparatus (2a)[see Figure XXII]. (a) A pentane solution of 27 (from a previous reaction) was irradiated for 5.5 h with an excess of DMM (estimated 100-fold excess). No reaction had occurred over this time period (as monitored by IR) and free DMM remained unchanged; (b) In parallel experiments, 43 mg each of 28 and 30 (0.057 mmol) were irradiated for 13.5 h in the presence of excess DMM (0.72 mL each, 0.83 g, 5.8 mmol) in 20 mL of benzene. From the reaction of 28, an orange-brown oil remained after solvent removal in vacuo. A 5 mL pentane extraction of the oil contained a number of compounds, of which 27, 28 and 29 were identified by IR. The excess alkene appeared to remain unchanged. The oily orange-brown solid that was obtained from the reaction of 30 also was extracted with 5 mL of pentane and gave a virtually identical IR spectrum (i.e., dinuclear 28 and not 30 was identified along with 27 and 29). The excess alkene also remained unchanged in this reaction.

#### 8. Thermal and Photochemical Reactions of $\text{Os}(\text{CO})_5(1c)$ with DMM.

(a) An excess of DMM (1.15 mL, 1.32 g, 9.16 mmol) was added to a 10 mL heptane solution of 1c (approximately 43 mg, 0.13 mmol) in a 30 mL Schlenk tube (2.7 x 11.5 cm) closed with a serum stopper. The mixture was heated at 88°C for 132 h which produced a quantitative yield (by IR) of  $\text{Os}(\text{CO})_4[\eta^2\text{-ZrC}_2\text{H}_2(\text{CO}_2\text{CH}_3)_2]$  (27). Compound 27 could not be freed of excess DMM on this scale of reaction. No free DMF was

... 2.10 mmol) of DMM. The vessel was closed with a serum stopper, and irradiation for 1.5 h gave an apparent quantitative yield (by IR) of 27. The solution separated into two layers - heptane above DMM - and the upper heptane layer was syringed off and evaporated to dryness. Recrystallization of the resulting solid residue from pentane (-78°C) gave 24.8 mg (0.055 mmol, 21%) of white solid 27; (c) In a stoichiometric reaction, a 20 mL pentane solution of 1c (approximately 118 mg, 0.357 mmol) and 45  $\mu$ L (52 mg, 0.36 mmol) of DMM were photolysed as in (b) until most of 1c was consumed (by IR, ca. 2h). Solvent was removed and the solid residue was extracted with 10 mL of pentane. After cooling the pentane solution to -15°C, some solid formed which was shown by IR to be a mixture of 3c, 27, 28 and free DMM (which melted upon warming). Further purification was not possible due to the small quantities obtained. A solid remained undissolved after the original pentane extraction. Upon standing as a damp solid following decantation, two large crystals grew from the solid matrix. These were identified as  $\text{Os}_2(\text{CO})_8[\mu\text{-}\eta^1, \eta^1\text{-Z-C}_2\text{H}_2(\text{CO}_2\text{CH}_3)_2]$  (28, approximately 15 mg).

9. Photochemical Reaction of  $\text{Os}_2(\text{CO})_8[\mu\text{-}\eta^1, \eta^1\text{-CH}_2\text{CH}(\text{CO}_2\text{CH}_3)]$  (14) with DMM.

Using photoapparatus (3) and a 70 mL Schlenk tube (3.6 x 14.0 cm), 124.4 mg (0.166 mmol) of 14 was irradiated with a five-fold excess of DMM (0.11 mL, 0.13 g, 0.88 mmol) for 1 h in 20 mL of benzene.

... contaminated with  $\text{Os}(\text{CO})_4[\mu-\eta^1, \eta^1-\text{C}_2\text{H}_2(\text{CO}_2\text{CH}_3)_2]$  (29) was obtained. The yellow residue was dissolved in a minimum of  $\text{CH}_2\text{Cl}_2$  and carefully layered with 10 mL of pentane. The mixture was cooled to  $-78^\circ\text{C}$  and a white solid, which was identified as dinuclear 30 (23.0 mg, 17%) precipitated. The supernatant was evaporated to dryness. Another IR spectrum (pentane) still showed a number of products (24) in the remaining residue. Further separation could not be effected, but compounds 28 and 29 could be identified in the IR spectrum of the mixture.

10. X-Ray Solid State Structure Determinations of the Isomeric Compounds of  $\text{Os}_2(\text{CO})_8[\mu-\eta^1, \eta^1-\text{C}_2\text{H}_2(\text{CO}_2\text{CH}_3)_2]$  (28 and 30)

A summary of crystallographic data for the two structures appears in Table XV. The Os atomic positions were located using a three-dimensional Patterson synthesis in both cases. The remaining non-hydrogen atoms were located as previously described (Section IV. 3). For compound 28, two peaks of reasonable position appeared near C(9) and C(12) in a difference Fourier map, and subsequently were included with fixed isotropic thermal parameters. The methyl H atoms were not located and were not included in the calculations. In the structure solution for 30, all H atom positions were calculated assuming idealized  $\text{sp}^3$  hybridization for the methyl and alkene C atoms. The obtained H atoms were constrained to "ride" on the parent C atoms and were included in the refinement with fixed isotropic thermal parameters.



## VI. Reagents and Reactions, Chapter Four.

### 1. Reagents.

Acetylene [ $C_2H_2$ ] (Linde-Union Carbide Canada) was purified by passing through a saturated aqueous solution of sodium bisulphite to remove the acetone stabilizer.<sup>150</sup> The gaseous alkyne was dried by passing through a column (3.3 x 10.0 cm) of molecular sieves (Davison Type 4A, Fischer Scientific Company). Dimethylacetylenedicarboxylate [DMAD], diphenyl acetylene [DPA], bis(trimethylsilyl)acetylene [BTMSA] (Aldrich Chemical Company) and hexafluoro-2-butyne [HFB] (PCR Research Chemicals, Inc.) were used without further purification.

### 2. Photoreactions of 3c with alkynes.

These reactions were carried out as described in Section IV. 2(a). Results are tabulated in Table XIX, and isolation procedures are described below.

#### (a) DMAD.

A viscous red oil was obtained after the volatiles were removed in vacuo. A white solid could be separated from the oil by the following procedure: trituration of the oil with 5 mL of THF gave a small quantity of the solid; decanting the supernatant and removing the THF in vacuo gave back a red oil which could be treated again with THF to give a second crop of solid; repeating this procedure until no further solids were obtained resulted in 80 mg in total. The white solid proved to be a mixture of two compounds which could be separated by

Table XXXVI. Positional and Thermal Parameters for  $\text{Os}_2(\text{CO})_8[\mu-\eta^1, \eta^1-\text{Z-C}_2\text{H}_2(\text{CO}_2\text{CH}_3)_2](28)$ .

Atom	x	y	z	U <sub>11</sub>	U <sub>22</sub>	U <sub>33</sub>	U <sub>12</sub>	U <sub>13</sub>	U <sub>23</sub>
Os(1)	321.72(2)	-6.97(4)	-181.20(2)	28.4(2)	28.9(2)	36.8(2)	4.6(1)	3.2(1)	3.2(1)
Os(2)	302.03(2)	273.71(4)	-75.77(2)	33.8(2)	33.0(2)	26.5(2)	-1.6(2)	1.6(1)	1.6(1)
O(1)	486.4(5)	143(1)	-260.2(7)	51(4)	81(6)	102(6)	-23(4)	31(4)	31(4)
O(2)	311.6(6)	-268.2(9)	-323.9(5)	84(8)	46(4)	64(5)	9(4)	10(4)	10(4)
O(3)	146.2(5)	-121.7(9)	-100.8(5)	52(4)	41(4)	91(5)	-2(3)	34(3)	34(3)
O(4)	438.7(6)	-190(1)	-40.7(6)	57(5)	131(7)	104(6)	23(5)	-17(4)	-17(4)
O(5)	494.2(5)	381(1)	-109.6(5)	42(4)	95(6)	70(5)	-16(4)	1(4)	1(4)
O(6)	104.1(4)	210.8(9)	-37.3(5)	41(3)	70(5)	46(4)	5(4)	15(3)	15(3)
O(7)	371.2(5)	93(1)	94.5(5)	81(5)	96(6)	36(4)	30(5)	4(4)	4(4)
O(8)	269.9(7)	604(1)	-1.0(5)	140(8)	49(5)	51(5)	-12(6)	2(5)	2(5)
O(9)	94.9(4)	169(1)	-229.8(5)	29(3)	66(5)	55(4)	-4(3)	6(3)	6(3)
O(10)	132.5(5)	38.8(9)	-350.9(5)	50(4)	58(4)	48(4)	-2(4)	-13(3)	-13(3)
O(11)	176.8(5)	558(1)	-190.0(5)	76(4)	53(4)	48(4)	29(4)	-9(4)	-9(4)
O(12)	166.7(4)	448.9(9)	-324.4(4)	52(4)	42(4)	37(3)	14(3)	1(3)	1(3)
C(1)	427.6(6)	89(1)	-229.6(7)	46(5)	39(5)	50(5)	2(5)	8(4)	8(4)
C(2)	314.3(6)	-170(1)	-272.4(7)	34(5)	40(5)	57(6)	6(4)	-1(4)	-1(4)
C(3)	209.0(6)	-79(1)	-128.0(7)	45(5)	28(5)	53(6)	3(4)	-1(4)	-1(4)
C(4)	395.9(7)	-123(2)	-92.0(8)	51(6)	63(7)	70(7)	17(6)	1(5)	1(5)
C(5)	429.7(7)	335(1)	-95.7(7)	47(5)	40(5)	49(5)	-3(5)	-14(5)	-14(5)
C(6)	174.5(6)	228(1)	-57.3(6)	46(5)	35(5)	38(4)	11(4)	7(4)	7(4)
C(7)	342.4(6)	164(1)	33.3(6)	43(5)	51(6)	42(5)	-8(5)	13(4)	13(4)
C(8)	281.9(8)	480(1)	-29.9(7)	70(7)	43(6)	33(5)	-9(5)	5(5)	5(5)

Table XXXVI. (continued).

Atom	$\bar{x}$	$\bar{y}$	$\bar{z}$	$\bar{U}_{11}$	$\bar{U}_{22}$	$\bar{U}_{33}$	$\bar{U}_{12}$	$\bar{U}_{13}$
C(9)	248.7(6)	172(1)	-266.7(5)	34(4)	32(4)	26(4)	4(4)	5(3)
C(10)	150.4(6)	129(1)	-278.9(6)	37(4)	33(5)	36(5)	6(4)	2(4)
C(11)	38.9(8)	-11(2)	-365.9(9)	55(6)	72(8)	67(7)	-10(6)	-12(6)
C(12)	268.8(6)	329(1)	-217.8(5)	39(4)	20(4)	27(4)	6(4)	3(3)
C(13)	199.3(6)	457(1)	-239.2(6)	37(4)	34(5)	40(5)	-4(4)	3(4)
C(14)	100.0(7)	565(1)	-354.1(8)	64(6)	67(7)	57(6)	40(5)	-8(5)

All atomic parameters have been multiplied by 103.

The form of the anisotropic thermal parameter is:

$$\exp[-2\pi^2(h^2a^2U_{11} + k^2b^2U_{22} + l^2c^2U_{33} + 2hka^2b^2U_{12} + 2hla^2c^2U_{13} + 2klb^2c^2U_{23})]$$

Estimated standard deviations in the least significant digits are shown in parentheses.

Table XXXVII. Positional and Thermal Parameters for  $\text{Os}_2(\text{CO})_8[\text{u-n}^1\text{-E-C.H}_2(\text{CO}_2\text{CH}_3)_2](30)$ .

Atom	x	y	z	U <sub>11</sub>	U <sub>22</sub>	U <sub>33</sub>	U <sub>12</sub>	U <sub>13</sub>
Os (1)	129.17(3)	186.31(2)	-115.89(2)	15.0(2)	18.1(2)	16.3(1)	-8(1)	1.1(1)
Os (2)	-2.65(5)	71.31(2)	-241.64(2)	19.7(2)	16.1(2)	18.6(1)	1.2(1)	2.4(1)
O (1)	-132(1)	85.1(5)	-12.9(4)	30(4)	37(4)	37(4)	-1(4)	-11(3)
O (2)	221(1)	335.8(6)	2.7(4)	67(6)	32(4)	32(4)	-10(4)	4(4)
O (3)	343(1)	306.4(5)	-222.1(4)	34(4)	34(4)	26(3)	-6(3)	13(3)
O (4)	463(1)	54.5(6)	-71.7(5)	23(4)	43(4)	58(5)	8(4)	-2(4)
O (5)	-158(1)	-66.8(5)	-131(4)	58(5)	32(4)	35(4)	-11(4)	7(4)
O (6)	109(1)	223.6(5)	-351.1(4)	30(4)	32(4)	34(3)	1(3)	9(3)
O (7)	376(1)	-35.5(6)	-239.9(5)	36(4)	34(4)	65(5)	11(4)	4(4)
O (8)	-233(1)	-25.2(5)	-373.8(4)	55(5)	37(4)	33(4)	-6(4)	-14(4)
O (9)	-363.3(9)	261.4(5)	-85.5(4)	18(3)	38(4)	30(3)	-1(3)	12(3)
O (10)	-182(1)	384.2(5)	-107.7(4)	38(4)	24(3)	38(4)	-7(3)	14(3)
O (11)	-492(1)	142.7(5)	-309.7(4)	25(4)	34(4)	45(4)	-3(3)	-10(3)
O (12)	-301(1)	264.6(5)	-322.0(4)	27(3)	38(4)	21(3)	1(3)	3(3)
C (1)	-36(1)	120.6(7)	-52.5(5)	30(5)	18(4)	25(4)	2(4)	-0(4)
C (2)	180(1)	281.9(7)	-41.1(5)	31(5)	28(5)	16(4)	-4(5)	1(4)
C (3)	272(1)	258.2(7)	-184.2(5)	25(5)	23(4)	14(4)	6(4)	2(4)
C (4)	345(1)	105.7(7)	-86.2(6)	21(5)	36(5)	25(4)	-6(4)	-5(4)

Table XXXVII. (continued).

Atom	x	y	z	U <sub>11</sub>	U <sub>22</sub>	U <sub>33</sub>	U <sub>12</sub>	U <sub>13</sub>
C (5)	-99(1)	-14.2(7)	-170.0(5)	19(5)	31(5)	28(5)	-4(4)	-4(4)
C (6)	77(1)	168.4(7)	-309.7(5)	9(4)	24(4)	31(4)	-0(4)	8(3)
C (7)	236(1)	4.1(7)	-242.9(6)	29(5)	26(5)	35(5)	5(4)	10(4)
C (8)	-147(1)	11.6(7)	-325.3(5)	34(5)	20(4)	24(4)	7(4)	2(3)
C (9)	-129(1)	248.9(6)	-174.2(5)	12(4)	20(4)	17(4)	-1(4)	0(3)
C (10)	-240(1)	298.0(7)	-119.1(5)	21(4)	23(4)	19(4)	7(4)	-6(4)
C (11)	-279(2)	435.0(8)	-53.5(7)	47(7)	45(6)	63(7)	-7(6)	22(6)
C (12)	-230(1)	169.4(7)	-215.0(5)	12(4)	28(4)	21(4)	5(4)	-0(3)
C (13)	-358(1)	188.4(6)	-285.5(5)	19(4)	24(5)	27(4)	1(4)	3(4)
C (14)	-412(2)	288.1(9)	-390.7(6)	30(6)	52(6)	29(5)	4(6)	-8(5)

All atomic parameters have been multiplied by  $10^3$ .

The form of the anisotropic thermal parameter is:

$$\exp[-2\pi^2(h^2a^{*2}U_{11} + k^2b^{*2}U_{22} + l^2c^{*2}U_{33} + 2hka^*b^*U_{12} + 2hla^*c^*U_{13} + 2klb^*c^*U_{23})]$$

Estimated standard deviations in the least significant digits are shown in parentheses.

2011 (m);  $\nu_{\text{CO}_2}$  1704 (w), 1693 (w),  $\text{cm}^{-1}$ .  $^1\text{H}$  NMR (25°C,  $\text{CD}_2\text{Cl}_2$ , 200 MHz)  $\delta$  3.66 ( $\text{OCH}_3$ ).  $^{13}\text{C}$  NMR (30°C,  $\text{CDCl}_3$ , 75.469 MHz)  $\delta$  176.0 (axial Os-CO), 172.3, 165.0 (equatorial Os-CO), 170.5 ( $\text{CO}_2\text{Me}$ ), 114.0 ("bridging" C), 51.9 ( $\text{OCH}_3$ ). Mass spectrum (125°C)  $\text{M}^+$  748 m/e. Anal. calcd. for  $\text{C}_{14}\text{H}_{12}\text{O}_{12}\text{Os}_2$ : C, 22.52; H, 0.81. Found: C, 22.55; H, 0.81.

(ii)  $\text{Os}_2(\text{CO})_6[\text{C}_2(\text{CO}_2\text{CH}_3)_2]_4$  (34, ~30 mg, 10%).

IR ( $\text{CH}_2\text{Cl}_2$ )  $\nu_{\text{CO}}$  2101 (s), 2033 (m), 2014 (m);  $\nu_{\text{CO}_2}$  1711 (w), 1601 (w),  $\text{cm}^{-1}$ .  $^1\text{H}$  NMR (25°C,  $\text{CD}_2\text{Cl}_2$ , 200 MHz)  $\delta$  3.96, 3.82, 3.64, 3.48 (s,  $\text{OCH}_3$ ).  $^{13}\text{C}$  NMR (28°C,  $\text{CD}_2\text{Cl}_2$ , 100.62 MHz)  $\delta$  198.0 (Os + OC), 177.9, 177.0, 176.8, 175.4, 172.6, 163.8 (Os-CO +  $\text{CO}_2\text{Me}$ ), 169.0, 147.7, 72.1, 59.2 (carbons of ring systems), 56.1, 52.0, 51.4, 51.1 ( $\text{OCH}_3$ ). Mass spectrum (190°C)  $\text{M}^+$  1118 m/e. Anal. calcd. for  $\text{C}_{30}\text{H}_{24}\text{O}_{22}\text{Os}_2$ : C, 33.26; H, 2.23. Found: C, 32.16; H, 2.17.

No other Os-containing compounds could be isolated nor identified. Hexamethylmellitate [ $\text{C}_6(\text{CO}_2\text{CH}_3)_6$ ] was formed in this reaction [IR  $\nu_{\text{CO}_2}$  1746  $\text{cm}^{-1}$ ], but no attempts were made to isolate this material.

(b) HFB.

300 mg of 3c was recovered as the only organometallic species.

(c) HFB.

A second reaction was carried out in a closed system, whereby a ~~one~~ flask containing approximately 5.0 g (30.9 mmol) of HFB was connected to photoapparatus (1) via a varistaltic pump. The yellow solid obtained after solvent removal (0.35 g) was extracted with 2 x 7 mL portions of pentane, which removed a component that dis-

played  $\nu_{\text{CO}}$  different from  $3c$ . Reducing the volume and cooling to  $-15^\circ\text{C}$  precipitated a pale yellow solid. IR ( $\text{CH}_2\text{Cl}_2$ )  $\nu_{\text{CO}}$  2144 (w), 2103 (s), 2055 (vs), 2040 (sh), 2034 (m), 2017 (m),  $\text{cm}^{-1}$ . The familiar  $\nu_{\text{CO}}$  pattern suggested the compound  $\text{Os}_2(\text{CO})_8[\mu-\eta^1-\eta^1-\text{C}_2(\text{CF}_3)_2]$  which could be prepared by another route (see Section VII. 2(e)). The bulk of the originally obtained yellow solid proved to be unreacted  $3c$ . No other compounds were observed.

(d) BTMSA.

A mass spectrum of the reaction residue gave an isotope pattern at 474 m/e, which corresponds to  $\text{Os}(\text{CO})_4[\eta^2-\text{C}_2(\text{SiMe}_3)_2]$ . A pure sample could not be isolated from this preparation but was obtained from a latter reaction (see Section VIII. 2).

(e)  $\text{C}_2\text{H}_2$ .

After solvent removal, the resulting red-orange residue was dissolved in a minimum of  $\text{CH}_2\text{Cl}_2$  and loaded onto a rotor of the Chromatotron. Elution with pentane gave a yellow and a red band. A second yellow band was obtained by eluting with  $\text{CH}_2\text{Cl}_2$  and finally an orange band was removed with Methanol flushing.

The first yellow band contained two compounds. The head of the band was a mixture while the remainder was mostly one compound. Separately collecting the last half of the band, concentrating it to one-half its original volume and cooling to  $-78^\circ\text{C}$  afforded white crystals of  $\text{Os}(\text{CO})_3[\eta^4\text{-1-phenyl-1,3-butadiene}](37)$ . Table XXVI gives the spectral characteristics of this and similar compounds obtained later in this study.

The head of the first yellow band was shown to be a mixture of 37 and  $\text{Os}_2(\text{CO})_6(\text{C}_4\text{H}_6)(35)$ . Compound 35, although not isolated in

pure form, was identified on the basis of a comparison of IR, mass and  $^1\text{H}$  NMR spectroscopic data to those previously published.<sup>41</sup>

The red band was evaporated to dryness to yield a red solid,  $\text{Os}_3(\text{CO})_9(\text{C}_6\text{H}_5)_3$  (36), which was identified by its  $\nu_{\text{CO}}$  bands.<sup>41</sup>

The second yellow band (eluted with  $\text{CH}_2\text{Cl}_2$ ) appeared to be a mixture of compounds which could not be separated by further chromatography. IR (pentane)  $\nu_{\text{CO}}$  2119 (m), 2075, 2068 (sh), 2046 (vs), 2040 (s), 2036 (sh), 2029 (m), 2011 (m), 2004 (s), 1988 (m), 1982 (w), 1975 (w),  $\text{cm}^{-1}$ . A mass spectrum ( $85^\circ\text{C}$ ) gave parent isotope patterns for 3c and 35. Further spectroscopic investigations did not assist in the identification of the components of this mixture of compounds.

The final orange band gave an IR spectrum (pentane) with  $\nu_{\text{CO}}$  2101 (m), 2070 (m), 2065 (m), 2046 (s br), 2030 (m), 2018, 2011 (w), 2001 (s), 1986 (w),  $\text{cm}^{-1}$ . Attempts to isolate pure compounds from this apparent mixture resulted in decomposition of the material to 3c.

(f) DPA.

After all volatiles were removed in vacuo, excess DPA was sublimed at  $40^\circ\text{C}/0.1$  mm Hg to leave a mixture of beige and brown solids. These solids were washed with 10 mL aliquots of cyclohexane until the residue was shown to be one compound by IR. The beige residue was the major product (see Table XIX) and was formulated as  $\text{Os}(\text{CO})_3[\eta^4\text{-}2,3,4,5\text{-tetraphenyl-}2,4\text{-cyclopentadien-1-one}]$  (38) based on the following:

IR ( $\text{CH}_2\text{Cl}_2$ )  $\nu_{\text{CO}}$  2083 (s), 2018 (s), 2005 (s), 1646 (m);  
 $(\text{O}_6\text{H}_{12}) \nu_{\text{CO}}$  2079 (s), 2015 (s), 2013 (sh), 1997 (s), 1677 (m),  $\text{cm}^{-1}$ .  
 $^1\text{H}$  NMR ( $25^\circ\text{C}$ ,  $\text{CDCl}_3$ , 200 MHz)  $\delta$  7.24 (m, phenyl).  $^{13}\text{C}$  NMR ( $-60^\circ\text{C}$ ,  $\text{CDCl}_3$ , 50.323 MHz)  $\delta$  173.9 (keto  $\text{CO}$ ), 173.6 ( $\text{Os-CO}$ ), 129.5 (m, phenyl), 102.9 (inner diene), 78.4 (outer diene). Mass spectrum ( $165^\circ\text{C}$ )  $\text{M}^+$



660 m/e,  $M^+ - nCO$  ( $n=1-3$ ). Anal. Calcd. for  $C_{32}H_{20}O_4Os$ : C, 58.35; H, 3.06. Found: C, 57.91; H, 3.08.

The cyclohexane washings were evaporated and the resulting solid was separated via the Chromatotron using hexanes,  $CH_2Cl_2$  and methanol successively as eluents. Several bands were collected:

(i) colourless (hexanes) - mixture of 3c and 3PA;  
 (ii) colourless (hexanes) - as in Section VI. 2(b), this band was shown to be a mixture of  $Os_2(CO)_6(C_4Ph_4)(9)^{31}$  and  $Os(CO)_3[\eta^4-1,1,2,3,4\text{-pentaphenyl-1,3-butadiene}](39)$  (see Table XXVI). 39 could be isolated by cooling the hexanes solution to  $-78^\circ C$ .

(iii) yellow-orange (hexanes) - slow evaporation of the solvent afforded several colourless crystals. IR (pentane)  $\nu_{CO}$  2125 (w), 2083 (s), 2046 (m), 2040 (vs), 2026 (m), 2018 (s), 2000 (m),  $cm^{-1}$ .  $^{13}C$  NMR ( $30^\circ C$ ,  $CD_2Cl_2$ , 75.469 MHz)  $\delta$  178.9 (axial  $Os-CO$ ), 173.0, 167.6 (equatorial  $Os-CO$ ), 153.7, 128.0, 127.4, 124.8 (1:2:2:1, phenyl carbons), 113.4 ("alkyne" carbon). Mass spectrum ( $120^\circ C$ )  $M^+$  784 m/e,  $M^+ - nCO$  ( $n=1-8$ ). The familiar  $\nu_{CO}$  pattern and other spectroscopic data lead to the formulation  $Os_2(CO)_8[\mu-\eta^1, \eta^1-C_2(C_6H_5)_2](40)$ ;

(iv) colourless ( $CH_2Cl_2$ ) - 10.0 mg of  $C_6(C_6H_5)_6$  ( $M^+$  534 m/e) with a small impurity of 39.

(v) orange-yellow (methanol) - extraction of the resulting solid with cyclohexane gave unidentified impurities and left 20.0 mg of 38.

Reactions (g)-(j) are reported in Table XIX. The isolation procedures were identical to those reported in (f).

### 3. X-Ray Solid State Structure Determinations of Compounds

#### 33 and 34.

Pertinent crystallographic data for each structure is summarized in Table XX. Data collection (see Section IV. 3) and structure refinement (see Section V. 10) methods have been described elsewhere.

For compound 33, the molecule occupies a two-fold symmetry site where the symmetry axis bisects the Os-Os and C(5)-C(5) bonds. Three methyl H atoms were located and their positions were used to calculate idealized coordinates for the remaining H atoms. The derived H atoms were constricted to "ride" the parent C atoms in subsequent refinement cycles. In the solution of structure 34, two independent molecules were observed per asymmetric unit, each sitting on a center of symmetry. No attempt was made to locate H atoms nor were they included in the refinement due to time constraints on the PDP 11/34 computer.

Positional and thermal parameters for the two structures are given in Tables XXXVIII (33) and XXXIX (34). Relevant bond distances for 33 are collected in Table XXI, while relevant bond and torsional angles for 34 are given in Table XXII. A comparison of relevant bond distances and bond angles for the independent molecules of 34 are included in Tables XXIII and XXIV, respectively.

### VII. Reagents and Reactions, Chapter Five.

#### 1. Reagents.

Compounds 14, 16, 30, 33 and 38 were prepared as previously described. Compound 15 was obtained as a benzene solution from the photoreaction of 3c with  $C_2H_4$  (see Section IV. 2(b)).  $PPh_3$  was obtained from Aldrich and used as received.  $PPh_2Me$  was a gift from Dr. J. Hoyano of this Department.

Table XXXVIII. Positional and Thermal Parameters for  $\text{Os}_2(\text{CO})_8[\eta^1-\eta^1-\text{C}_2(\text{CO}_2\text{CH}_3)_2](33)$ .

Atom	x	y	z	$U_{11}$	$U_{22}$	$U_{33}$	$U_{12}$	$U_{13}$	$U_{23}$
Os	8920	1182.3(2)	6949	6.7(1)	6.7(1)	7.0(1)	0.15(9)	1.08(9)	-0.21(9)
O(1)	6691(5)	1720(5)	5871(5)	21(3)	22(3)	34(3)	4(2)	-1(2)	-9(2)
O(2)	9307(5)	1150(4)	4569(5)	27(3)	22(3)	12(2)	7(2)	6(2)	2(2)
O(3)	8671(4)	-1523(5)	7010(4)	27(3)	11(2)	23(2)	-3(2)	12(2)	-4(2)
O(4)	8366(4)	1651(5)	9304(5)	20(2)	32(3)	20(2)	-7(2)	10(2)	-11(2)
O(6)	9555(4)	4754(4)	6265(4)	14(2)	10(2)	19(2)	-1(2)	8(2)	2(2)
O(5)	8067(4)	4214(5)	6742(5)	18(2)	18(2)	41(3)	7(2)	15(2)	5(2)
C(1)	7513(5)	1525(6)	6261(6)	10(3)	13(3)	16(3)	2(3)	1(2)	-3(3)
C(2)	9306(6)	1135(5)	5454(6)	15(3)	8(3)	8(3)	3(2)	-1(3)	1(2)
C(3)	8738(5)	-529(6)	6976(6)	10(3)	12(3)	11(3)	-1(2)	2(2)	-3(2)
C(4)	8579(5)	1439(6)	8480(6)	8(3)	13(3)	13(3)	1(3)	4(2)	1(3)
C(5)	9528(6)	2933(6)	7181(6)	16(3)	12(3)	11(3)	1(3)	8(2)	0(2)
C(6)	8949(5)	4022(7)	6734(6)	15(3)	14(3)	19(3)	3(3)	7(2)	3(3)
C(7)	9075(6)	5821(7)	5813(8)	23(4)	19(3)	36(4)	2(3)	8(3)	9(3)

The atomic positional parameters have been multiplied by  $10^4$ . The anisotropic thermal parameters have been multiplied by  $10^3$ .

The form of the anisotropic thermal parameter is:

$$\exp[-2\pi^2(h^2a^2U_{11} + k^2b^2U_{22} + l^2c^2U_{33} + 2hkaU_{12} + 2hlcU_{13} + 2klcU_{23})]$$

Estimated standard deviations in the least significant digits are shown in parentheses. Those parameters without an error were not refined.

Table XXXIX. Positional and Thermal Parameters for  $\text{Os}_2(\text{CO})_6[\text{C}_2(\text{CO}_2\text{CH}_3)_2]_4(34)$ .

Atom	x	y	z	U <sub>11</sub>	U <sub>22</sub>	U <sub>33</sub>	U <sub>12</sub>	U <sub>13</sub>	U <sub>23</sub>
Os	-72.5(2)	-137.1(2)	-2532.6(2)	27.17(8)	25.73(9)	22.96(8)	-7.28(7)	11.93(6)	-3.11(7)
Os'	-473.8(2)	-4135.0(2)	2578.3(2)	22.74(7)	24.05(9)	24.67(8)	-6.00(6)	9.12(6)	0.81(7)
O(1)	2643(4)	-668(5)	-2222(5)	37(2)	112(5)	70(3)	-10(2)	34(2)	-7(3)
O(2)	-763(4)	1858(4)	-3671(5)	64(2)	40(2)	70(3)	-18(2)	29(2)	8(2)
O(3)	-1115(5)	-914(4)	-5228(5)	86(3)	79(4)	34(2)	-25(3)	27(2)	-24(2)
O(4)	-3370(4)	-364(4)	-4246(5)	40(2)	44(2)	59(3)	-18(2)	10(2)	-14(2)
O(5)	-3326(4)	1113(4)	-4642(5)	40(2)	73(3)	36(2)	-25(2)	-3(2)	18(2)
O(6)	-3311(4)	1534(4)	-988(4)	39(2)	53(3)	41(2)	-3(2)	19(1)	-12(2)
O(7)	-4217(4)	1125(4)	-2633(5)	25(2)	75(3)	46(2)	0(2)	9(2)	-21(2)
O(8)	876(4)	1788(4)	-92(6)	54(2)	36(2)	131(4)	-22(2)	50(2)	-29(3)
O(9)	2368(4)	497(3)	40(5)	28(2)	46(2)	68(3)	-20(1)	15(2)	-5(2)
O(10)	-385(4)	1503(3)	1573(4)	40(2)	23(2)	27(2)	-5(1)	13(1)	-5(1)
O(11)	-1448(4)	2350(3)	-313(4)	46(2)	21(2)	30(2)	1(2)	13(1)	-2(2)
O(11')	1969(4)	-3799(4)	2794(5)	44(2)	91(3)	69(3)	-30(2)	32(1)	6(2)
O(2')	-1809(4)	-2043(3)	2430(5)	49(2)	31(2)	58(2)	-4(2)	24(2)	-2(2)
O(3')	-1482(5)	-4161(5)	-374(5)	88(3)	95(4)	34(2)	-26(3)	21(2)	-6(3)
O(4')	-3369(4)	-5006(4)	717(5)	40(2)	42(3)	59(3)	-9(2)	0(2)	-20(2)
O(5')	-3840(4)	-3408(3)	834(4)	38(2)	39(2)	33(2)	-8(2)	-4(2)	1(2)
O(6')	-3263(4)	-4452(4)	4927(4)	36(2)	61(3)	49(2)	-13(2)	22(1)	3(2)
O(7')	-4272(4)	-4330(5)	2766(5)	21(2)	154(5)	48(3)	-25(2)	4(2)	10(3)
O(8')	390(4)	-3065(4)	6038(5)	59(2)	57(3)	80(3)	-33(2)	42(2)	-42(2)

Table XXXIX. (continued).

Atom	Z	X	Y	Z	U <sub>11</sub>	U <sub>22</sub>	U <sub>33</sub>	U <sub>12</sub>	U <sub>13</sub>	U <sub>23</sub>
O(9)	8	-3723(3)	5414(4)	33(2)	39(2)	49(2)	-23(1)	14(1)	-3(2)	
O(10)	8	-4363(3)	7163(4)	36(2)	27(2)	33(2)	-3(1)	19(1)	0(2)	
O(11)	8	-3159(3)	5740(4)	33(2)	29(2)	43(2)	-1(2)	18(1)	1(2)	
C(1)	6	-485(5)	-2308(6)	40(3)	51(4)	31(3)	-11(3)	15(2)	-6(3)	
C(2)	6	1096(4)	-3246(6)	37(2)	35(3)	38(3)	-16(2)	18(2)	-3(2)	
C(3)	6	-657(5)	-4230(5)	44(2)	38(3)	32(2)	-6(2)	22(2)	-1(2)	
C(4)	6	330(4)	-2628(5)	27(2)	20(2)	30(2)	-7(2)	12(2)	0(2)	
C(5)	6	310(4)	-3901(5)	26(2)	36(3)	30(2)	-8(2)	12(2)	-3(2)	
C(6)	6	1162(7)	-5916(8)	61(4)	124(6)	39(4)	-45(4)	-9(3)	34(4)	
C(7)	6	716(4)	-1585(5)	28(2)	19(2)	29(2)	-7(2)	10(2)	-2(2)	
C(8)	6	1169(4)	-1522(6)	31(2)	32(3)	30(2)	-3(2)	10(2)	0(2)	
C(9)	6	1575(7)	-2690(9)	25(3)	88(6)	92(5)	1(4)	20(3)	-34(5)	
C(10)	6	647(4)	-362(5)	31(2)	23(2)	24(2)	-6(2)	14(1)	-6(2)	
C(11)	6	287(4)	-583(5)	28(2)	25(2)	28(2)	-6(2)	14(1)	-2(2)	
C(12)	6	947(4)	-176(5)	29(2)	30(3)	35(2)	-11(2)	17(2)	-7(2)	
C(13)	6	1063(6)	575(8)	36(2)	80(4)	73(5)	-42(2)	11(3)	-6(4)	
C(14)	6	1544(4)	372(5)	29(2)	29(3)	31(2)	-7(2)	15(2)	-9(2)	
C(15)	6	3227(5)	379(7)	68(4)	17(3)	49(3)	-3(3)	16(3)	-12(3)	
C(1)	6	-3929(5)	2750(6)	30(2)	42(3)	34(2)	-11(2)	15(2)	0(2)	
C(2)	6	-2826(4)	2475(5)	37(2)	33(3)	26(2)	-17(2)	11(2)	-1(2)	
C(3)	6	-4137(5)	716(6)	45(3)	46(4)	30(3)	-12(3)	11(2)	2(3)	

Table XXXIX. (continued).

Atom	$x$	$y$	$z$	$U_{11}$	$U_{22}$	$U_{33}$	$U_{12}$	$U_{13}$	$U_{23}$
C(4)'	-2102(5)	-4318(4)	2372(5)	23(2)	22(2)	26(2)	-7(2)	5(2)	-3(2)
C(5)'	-3183(5)	-4307(5)	1304(6)	27(2)	36(3)	29(2)	-5(2)	7(2)	-4(2)
C(6)'	-4894(7)	-3326(7)	-453(8)	43(4)	79(6)	35(4)	-1(4)	-17(3)	7(4)
C(7)'	-2130(4)	-4396(4)	3726(5)	15(2)	23(2)	30(2)	-2(2)	5(2)	1(2)
C(8)'	-3265(5)	-4404(5)	3891(6)	23(2)	46(4)	47(3)	-2(2)	12(2)	7(3)
C(9)'	-5419(7)	-4298(10)	2876(10)	30(3)	200(11)	97(6)	-40(4)	24(3)	-3(7)
C(10)'	-934(4)	-4543(4)	4923(5)	23(2)	27(2)	27(2)	-8(2)	11(1)	0(2)
C(11)'	135(4)	-4368(4)	4631(5)	19(2)	20(2)	31(2)	-3(2)	11(1)	-1(2)
C(12)'	780(5)	-3649(4)	5441(5)	29(2)	31(3)	28(2)	-11(2)	8(2)	2(2)
C(13)'	2631(6)	-3136(5)	6281(8)	53(3)	75(4)	51(4)	-51(2)	-1(3)	-9(3)
C(14)'	-1078(4)	-4005(4)	6026(5)	21(2)	22(2)	33(2)	-5(2)	10(2)	0(2)
C(15)'	-2019(7)	-2630(6)	6804(7)	61(4)	46(4)	56(3)	5(3)	31(3)	-16(3)

The atomic positional parameters have been multiplied by  $10^4$ . The anisotropic thermal parameters have been multiplied by  $10^3$ .

The form of the anisotropic thermal parameter is:

$$\exp[-2\pi^2(h^2a^2U_{11} + k^2b^2U_{22} + l^2c^2U_{33} + 2hkaU_{12} + 2hlcU_{13} + 2klbU_{23})]$$

Estimated standard deviations in the least significant digits are shown in parentheses. In this and other tables the ' indicates the atoms in the second independent molecule.

## 2. Attempted Thermal Exchange Reactions.

a) Reaction of  $\text{Os}_2(\text{CO})_8[\mu-\eta^1, \eta^1-\text{CH}_2\text{CH}(\text{CO}_2\text{CH}_3)](14)$  with DMAD. 51.5 mg (0.0745 mmol) of 14 and 15  $\mu\text{L}$  (17 mg, 0.12 mmol) of DMAD were heated gradually to  $80^\circ\text{C}$  over 24h in 20 mL of toluene. Cooling the solution to  $-5^\circ\text{C}$  gave a yellow solid which upon preparative chromatography (TLC, silica gel,  $\text{CH}_2\text{Cl}_2$ ) yielded 26.0 mg (0.0348 mmol, 47%) of  $\text{Os}_2(\text{CO})_8[\mu-\eta^1, \eta^1-\text{C}_2(\text{CO}_2\text{CH}_3)_2](33)$ . A scaled-up reaction [0.512 g (0.741 mmol) 14, 0.50 mL (0.57 g, 4.1 mmol) DMAD] afforded a 30% yield (164.8 mg) of 33.

b) Reaction of  $\text{Os}_2(\text{CO})_8[\mu-\eta^1, \eta^1-\text{C}_2\text{H}_4](16)$  with DMAD. In a manner similar to (a), 101.6 mg (0.161 mmol) of 16 and 30  $\mu\text{L}$  (34.7 mg, 0.244 mmol) of DMAD in 15 mL of toluene at  $80^\circ\text{C}$  for 19h gave 16.0 mg (0.0214 mmol, 13%) of 33.

c) Reaction of 14 with  $\text{C}_2\text{H}_2$ . A 100 mL cylindrical Pyrex vessel (2.8x17.5 cm) with a side-arm containing a glass frit for dispersing gas, was charged with 164.8 mg (0.239 mmol) of 14 and 30 mL of toluene. Purified  $\text{C}_2\text{H}_2$  (see Section VI. 1) was purged through the solution, which was maintained at  $80^\circ\text{C}$ , for 16h (a water-cooled condensor fixed to an outlet reduced solvent loss). Upon solvent removal, a yellow oil remained. Attempts to separate the mixture failed (fractional crystallization, chromatography) the following compounds could be identified by IR spectroscopy:

(i)  $\text{Os}_2(\text{CO})_6(\text{C}_4\text{H}_4)(35)^{41}$  (see also Section VI. 2(e));

(ii)  $\text{Os}(\text{CO})_3[\eta^4\text{-1-tolyl-1,3-butadiene}](41)$ , see Table XXVI).

d) Reaction of 14 with DPA. Compound 14 (104.0 mg, 0.151 mmol) and an excess of DPA (139.0 mg, 0.780 mmol) were heated in 17 mL of toluene at  $82^\circ\text{C}$  for 1h, then at  $62^\circ\text{C}$  for 23h. Cooling the resulting

yellow solution ( $-15^{\circ}\text{C}$ ) precipitated 5.0 mg of 3c. Toluene was removed in vacuo and the unused portion of DPA was sublimed ( $50^{\circ}\text{C}/0.1\text{ mm Hg}$ ) to leave a brown solid. Addition of pentane (7 mL) dissolved all but 10.0 mg of a tan solid, identified as  $\text{C}_6(\text{C}_6\text{H}_5)_6$  ( $M^+$  534 m/e,  $180^{\circ}\text{C}$ ).

The pentane solution was cooled to  $-15^{\circ}\text{C}$  to precipitate pale yellow crystals of the mono-tolyl derivative of 39,  $\text{Os}(\text{CO})_3[\eta^4-1,2,3,4\text{-tetraphenyl-1-tolyl-1,3-butadiene}](42, 15.0\text{ mg. See Table XX})$ .

The mother liquor contained a number of components which could be separated on the Chromatotron ( $\text{CH}_2\text{Cl}_2$  eluent). Three major bands appeared, and the compounds isolated were:

- (i)  $\text{Os}_2(\text{CO})_8[\mu-\eta^1, \eta^1-\text{C}_2(\text{C}_6\text{H}_5)_2](40, \sim 3\text{ mg, } 3\%)$ ;
- (ii) a mixture of compounds 9 and 39; and
- (iii) unreacted 14 ( $\sim 5\text{ mg}$ ).

When the same reaction was carried out in hexanes solution, compounds 9, 39, and 40 could be separated as described above (N.B. No 1-hexyl derivative of 42 was observed).

e) Reaction of 14 with HFB. In a typical reaction, 158.0 mg (0.229 mmol) of 14 and 20 mL of toluene were added to a 60 mL Carius tube (4.0x11.0 cm) and the solution was subjected to several freeze-pump-thaw-degas cycles. HFB was condensed into the vessel (0.930 g, 3.89 mmol) and the mixture was heated at  $68-75^{\circ}\text{C}$  for 28h. The solution was cooled to  $-78^{\circ}\text{C}$ , giving the separation of a yellow precipitate. Preparative TLC (1%  $\text{CH}_2\text{Cl}_2$  in hexanes) of the solid gave 43.0 mg (0.0474 mmol) of 3c and 34.3 mg (0.0447 mmol, 20%) of colourless crystalline  $\text{Os}_2(\text{CO})_8[\mu-\eta^1, \eta^1-\text{C}_2(\text{CF}_3)_2](43)$  (see Section VI. 2(c)).  $^{13}\text{C}$  NMR ( $34^{\circ}\text{C}$ ,  $\text{CD}_2\text{Cl}_2$ , 75.469 MHz)  $\delta$  175.8(axial Os-CO), 171.9, 164.4 (equatorial Os-CO). No alkyne or trifluoromethyl carbon signals were



observed.  $^{19}\text{F}$  NMR ( $28^\circ\text{C}$ ,  $\text{CD}_2\text{Cl}_2$ , 75.26 MHz)  $\delta$  -59.3 [CFC $\text{Cl}_3$  external reference]. Mass spectrum ( $105^\circ\text{C}$ )  $M^+$  768 m/e,  $M^+ - n\text{CO}$  ( $n=1-8$ ). Anal. calcd. for  $\text{C}_{12}\text{F}_6\text{O}_8\text{Os}_2$ : C, 18.80; F, 14.87. Found: C, 18.67; F, 14.99. In several subsequent reactions the isolated yields of 43 varied from nearly zero to 20%.

Removal of the volatiles from the original toluene mother liquor resulted in the trapping of  $\text{Os}(\text{CO})_5$  ( $\nu_{\text{CO}}$  2038 (m), 1987 (s)) and free MA ( $1732\text{ cm}^{-1}$ ) and left an oily yellow solid. The bulk of this solid was extracted into 5 mL of pentane, and upon cooling the solution to  $-15^\circ\text{C}$ , a small number of white crystals formed. When the reaction was performed on a larger scale (0.5 g 14) the same white solid remained mostly out of solution. The compound could be recrystallized from  $\text{CH}_2\text{Cl}_2$ /pentane (44, average yield 15.0 mg) Mass spectrum ( $120^\circ\text{C}$ )  $M^+$  686 m/e,  $M^+ - n\text{CO}$  ( $n=1-3$ ). A second product was initially isolated by slow evaporation of the toluene solvent at  $-15^\circ\text{C}$  to give white solid hemispheres as pure compound 45 (18.0 mg). This compound could also be obtained from the pentane extracts by cooling to  $-78^\circ\text{C}$  after 44 had been separated. Mass spectrum 45 ( $70^\circ\text{C}$ )  $M^+$  686 m/e,  $M^+ - n\text{CO}$  ( $n=1-3$ ). On the basis of mass spectral data, both compound 44 and 45 were formulated as isomers of the general formula  $\text{Os}(\text{CO})_3[(\text{HFB})_2(\text{MA})]$ . Table XXVI shows a comparison of spectral parameters for compounds 44 and 45.

Upon the precipitation of both 44 and 45,  $\text{Os}(\text{CO})_4[\text{n}^2\text{-CH}_2\text{CH}(\text{CO}_2\text{-CH}_3)]$  (13) remained in solution and was not isolated (estimated yield <5%).

A seventh product was obtained by preparative TLC ( $\text{CH}_2\text{Cl}_2$  eluent) performed on the oily yellow solid. Compounds 13, 44 and 45 followed

closely behind the solvent front and a colourless band eluted with  $R_f=0.4$ . The isolated colourless fibrous solid (3.0 mg) was tentatively formulated as  $\text{Os}(\text{CO})_4[(\text{HFB})_2(\text{ASM})](46)$  on the basis of the following data: Mass spectrum ( $100^\circ\text{C}$ )  $M^+$  714 m/e,  $M^+-n\text{CO}$  ( $n=1-3$ ). IR (pentane)  $\nu_{\text{CO}}$  2160 (w), 2090 (m), 2079 (s), 2060 (m);  $\nu_{\text{CO}_2}$  1728 (vw)  $\text{cm}^{-1}$ .

f) Reaction of 16 with HFB. This reaction was carried out under conditions analogous to (b). Freshly prepared 16 (200 mg, 0.316 mmol) and 1.44 g (10.0 mmol) of HFB in 20 mL of toluene were heated at  $74^\circ\text{C}$  for 36h. The resulting solution was reduced by one-half and cooled to  $-78^\circ\text{C}$ . The precipitate consisted of 3c and very little (~5 mg) of 43. The supernatant solution was shown by IR to be a mixture of several compounds which could not be separated nor identified.

g) Reaction of 14 with DMM. 31.0 mg (0.0449 mmol) of 14 and 30  $\mu\text{L}$  (34 mg, 0.24 mmol) of DMM were heated in 10 mL of hexanes at  $64^\circ\text{C}$  for 39h. Removing the solvent and excess ligand in vacuo, and treating the resulting solid with cold ( $0^\circ\text{C}$ ) pentane, gave 22.0 mg (0.0294 mmol, 65%) of  $\text{Os}_2(\text{CO})_8[\mu-\eta^1, \eta^1\text{-Z-C}_2\text{H}_2(\text{CO}_2\text{CH}_3)_2](28)$ . No isomerization of DMM to DMF was observed.

h) Reaction of 14 with MAH. 81.3 mg (0.118 mmol) of 14 and 56.3 mg (0.574 mmol) of MAH were heated at  $80^\circ\text{C}$  for 13h in 20 mL of toluene. Volatiles were removed to leave a yellow solid, which was washed successively with one-10 mL and 3x6 mL aliquots of pentane and 2x5 mL portions of cold ( $0^\circ\text{C}$ ) THF. The remaining white solid was spectroscopically characterized as  $\text{Os}_2(\text{CO})_8[\mu-\eta^1, \eta^1\text{-CHCHC(O)OC(O)}](47)$ , 45.0 mg, 54%. See Tables IV, V, X and XI for spectral data).

i) Reaction of  $\text{Os}(\text{CO})_4[\eta^2\text{-C}_2\text{H}_4](15)$  with MAH. To an in-situ-prepared benzene solution of 15 (see Section IV. 2(b)) 113 mg (1.15 mmol) of MAH was added and the solution was heated at  $80^\circ\text{C}$  until all of 15 had been consumed (by IR ca. 54.5h). The solution was evaporated to dryness and the resulting solid was loaded into a sublimation apparatus. Sublimation at  $50^\circ\text{C}/0.1$  mm Hg removed 57 mg of MAH to leave 57 mg of a tan-coloured residue, which proved to be a mixture of a small quantity of 47 and  $\text{Os}(\text{CO})_4[\eta^2\text{-CHCHC(O)OC(O)}](48)$ . Separation could not be effected, but 48 was spectroscopically characterized (see Tables IV, V, XII and XIII for details).

### 3. Phosphine Substitution Reactions.

a) Reaction of 14 with  $\text{PPh}_3$ . In 20 mL of toluene, an excess of  $\text{PPh}_3$  (203.0 mg, 0.774 mmol) was heated at  $62^\circ\text{C}$  with 53.7 mg (0.0778 mmol) of 14 for 30h. A yellow solid remained after the volatiles were removed. Extraction of the solid with 5x10 mL of pentane left 29.0 mg of a beige solid, identified as  $\text{Os}(\text{CO})_3(\text{PPh}_3)_2^{122}$  (49, 0.0376 mmol). The extracts were combined and reduced in volume to 5 mL and stored at  $-78^\circ\text{C}$  until a pale yellow precipitate formed. This solid was identified as  $\text{Os}(\text{CO})_4(\text{PPh}_3)^{122}$  (50, 66.5 mg, 0.118 mmol).

b) Reaction of  $\text{Os}_2(\text{CO})_8[\mu\text{-}\eta^1, \eta^1\text{-E-C}_2\text{H}_2(\text{CO}_2\text{CH}_3)_2](30)$  with  $\text{PPh}_3$ . 46.7 mg (0.0624 mmol) of 30 and an excess of  $\text{PPh}_3$  (100.5 mg, 0.383 mmol) were heated at  $103^\circ\text{C}$  for 48h in 20 mL of toluene. After solvent removal the remaining yellow residue was extracted with 5- and 7- mL of pentane. An IR spectrum of the combined extracts showed them to be an approximate 1:1 ratio of compounds  $\text{Os}(\text{CO})_4[\eta^2\text{-E-C}_2\text{H}_2\text{-}(\text{CO}_2\text{CH}_3)_2](29)$  and 50 along with free DMF. The undissolved beige solid was isolated and identified as 49 (10.0 mg, 0.013 mmol).

$\text{PPh}_3$  in 50 mL of toluene were heated at  $103^\circ\text{C}$  for 3.5h. The resulting oily yellow residue was washed with 20- and 15-mL aliquots of cyclohexane, which left 100.5 mg of a tan solid. Removing the cyclohexane and redissolving the residue in 3 mL of cyclohexane yielded another crop of the same solid (13.0 mg). IR ( $\text{CH}_2\text{Cl}_2$ )  $\nu_{\text{CO}}$  2083 (w), 2036 (w), 1995 (vs), 1961 (sh);  $\nu_{\text{CO}}$  1692 (w);  $\text{cm}^{-1}$ .  $^1\text{H}$  NMR ( $30^\circ\text{C}$ ,  $\text{CD}_2\text{Cl}_2$ , 300 MHz)  $\delta$  7.50 (m, phenyl), 2.75 (s,  $\text{OCH}_3$ ).  $^{13}\text{C}$  NMR ( $30^\circ\text{C}$ ,  $\text{CD}_2\text{Cl}_2$ , 75.469 MHz)  $\delta$  188.3 (m,  $2(\text{Os}-\text{CO})$ ), 182.6 (s,  $\text{CO}_2\text{CH}_3$ ), 172.7 (d,  $1(\text{Os}-\text{CO})$ ,  $^2J_{\text{P}-\text{C}} = 3$  Hz), 135.1-128.8 (m, phenyl), 120.0 (m, "alkyne" carbon), 50.8 (s,  $\text{OCH}_3$ ).  $^{31}\text{P}$  NMR ( $30^\circ\text{C}$ ,  $\text{CD}_2\text{Cl}_2$ , 161.977 MHz)  $\delta$  -2.16. Mass spectrum ( $185^\circ\text{C}$ )  $\text{M}^+$  1216 m/e. Reproducible elemental analyses were not obtained. This compound was formulated as  $\text{Os}_2(\text{CO})_6(\text{PPh}_3)_2[\text{C}_2(\text{CO}_2\text{CH}_3)_2]$  (51.113.5 mg total, 0.0934 mmol).

d) Reaction of 33 with  $\text{PPh}_2\text{Me}$ . In an analogous fashion to (c), 43.7 mg (0.0585 mmol) of 33 and 50  $\mu\text{L}$  (53 mg, 0.26 mmol) of  $\text{PPh}_2\text{Me}$  in 20 mL of toluene were heated to  $100^\circ\text{C}$  for 13h. The analogous phosphine-substituted product,  $\text{Os}_2(\text{CO})_6(\text{PPh}_2\text{Me})_2[\text{C}_2(\text{CO}_2\text{CH}_3)_2]$  (52.24.8 mg, 0.0227 mmol) was obtained as a tan solid following several 5 mL pentane washings. IR ( $\text{CH}_2\text{Cl}_2$ )  $\nu_{\text{CO}}$  2080 (w), 2028 (w), 1992 (vs), 1971 (sh;  $\nu_{\text{CO}_2}$  1685 (w).  $\text{cm}^{-1}$ .  $^1\text{H}$  NMR ( $30^\circ\text{C}$ ,  $\text{CD}_2\text{Cl}_2$ , 300 MHz)  $\delta$  7.80-7.05 (m, phenyl), 3.00 (s,  $\text{OCH}_3$ ), 2.57 (d,  $\text{PCH}_3$ ,  $^2J_{\text{P}-\text{H}} = 9.0$  Hz).  $^{13}\text{C}$  NMR ( $30^\circ\text{C}$ ,  $\text{CD}_2\text{Cl}_2$ , 75.469 MHz)  $\delta$  188.7 (m,  $2(\text{Os}-\text{CO})$ ), 181.3 (s,  $\text{CO}_2\text{CH}_3$ ), 173.1 (d,  $1(\text{Os}-\text{CO})$ ,  $^2J_{\text{PC}} \approx 1$  Hz), 137.0-128.8 (m, phenyl), 119.4 (m, "alkyne" carbon), 50.8 (s,  $\text{OCH}_3$ ), 19.6 (d,  $\text{P}-\text{CH}_3$ ,  $^1J_{\text{P}-\text{C}} = 37$  Hz).  $^{31}\text{P}$  NMR ( $30^\circ\text{C}$ ,  $\text{CD}_2\text{Cl}_2$ , 161.977 MHz)  $\delta$  -25.9. Mass spectrum ( $220^\circ\text{C}$ )  $\text{M}^+$  1092 m/e. Reproducible elemental analyses were not obtained.

1-one](38) with  $\text{PPh}_3$ . Heating 100.0 mg (0.159 mmol) of 38 and 225.0 mg (0.858 mmol) of  $\text{PPh}_3$  in 15 mL of toluene at  $103^\circ\text{C}$  over several days resulted in no reaction. Transferring the solution to a 30 mL Schlenk tube (3.0x12.0 cm) and irradiating with photoapparatus (2b) (Figure XXII, right, without GWV) for 68h resulted in the total consumption of 38. The volatiles were removed and the resulting residue was dissolved in a minimum of  $\text{CH}_2\text{Cl}_2$  and loaded onto a rotor of the Chromatron. Elution with pentane only removed unused  $\text{PPh}_3$ . Further elution with  $\text{CH}_2\text{Cl}_2$  separated a previously ill-resolved band into two bands. The first band (orange) contained a small amount of an unidentifiable product. The second colourless band gave 33.0 mg of a tan solid. IR ( $\text{CH}_2\text{Cl}_2$ )  $\nu_{\text{CO}}$  2008 (s), 1948 (s), 1612 (m br),  $\text{cm}^{-1}$ .  $^1\text{H}$  NMR ( $30^\circ\text{C}$ ,  $\text{CD}_2\text{Cl}_2$ , 300 MHz)  $\delta$  7.25-6.85 (m, phenyl).  $^{13}\text{C}$  NMR ( $30^\circ\text{C}$ ,  $\text{CD}_2\text{Cl}_2$ , 75.469 MHz)  $\delta$  183.2 (d, Os-CO,  $^2J_{\text{P-C}}=7$  Hz), 170.6 (d, keto CO,  $^3J_{\text{P-C}}=4$  Hz), 134.0-126.0 (m, phenyl), 101.7 (d, inner diene,  $^2J_{\text{P-C}}=4.5$  Hz), 77.9 (s, outer diene).  $^{31}\text{P}$  NMR ( $28^\circ\text{C}$ ,  $\text{CD}_2\text{Cl}_2$ , 161.977 MHz)  $\delta$  3.12. Mass spectrum ( $170^\circ\text{C}$ )  $\text{M}^+$  894 m/e. This compound was identified as  $\text{Os}(\text{CO})_2(\text{PPh}_3)[\eta^4\text{-}2,3,4,5\text{-tetraphenyl-}2,4\text{-cyclopentadien-1-one}]$  (53, 0.0370 mmol, 23%).

### VIII. Reagents and Reactions, Chapter Six.

#### 1. Reagents.

Hydrated  $\text{RuCl}_3$  was obtained from Engelhard Industries.  $^{13}\text{CO}$  (99%  $^{13}\text{C}$  enriched) was purchased from Isotec, Inc.  $\text{Ru}_3(\text{CO})_{12}$  (3b)<sup>7</sup>,  $\text{Fe}(^{13}\text{CO})_5^{151}$  and  $\text{Os}_3(^{13}\text{CO})_{12}^{152}$  were prepared by published procedures.

2. Synthesis of  $\text{Os}(\text{CO})_4[\eta^2\text{-C}_2(\text{SiMe}_3)_2](54)$ .

A 200 mL Schlenk tube (5.0x15.0 cm) was charged with 203.5 mg (0.224 mmol) of 3c, 5.00 mL (3.76 g, 22.1 mmol) of BTMSA and 100 mL of benzene under a nitrogen atmosphere. The vessel was closed with a serum stopper and irradiated (photoapparatus (3) with GWV filter sleeve,  $\lambda \approx 370$  nm) until 3c was completely consumed (ca. 8h). Solvent and excess alkyne were removed in vacuo from the yellow brown solution. Several X-ray quality crystals were obtained as yellow blocks as the solvent evaporated. Sublimation (40°C/0.1 mm Hg) of the remainder of the brown residue onto a dry ice-cooled finger yielded 143.8 mg (0.304 mmol, 45%) of the yellow powder of 56 (mp 49°C). Mass spectrum (90°C)  $M^+$  474 m/e,  $M^+ - n\text{CO}$  ( $n=1-4$ ). Anal. calcd. for  $\text{C}_{12}\text{H}_{18}\text{O}_4\text{Si}_2\text{Os}$ : C, 30.49; H, 3.84. Found: C, 29.99; H, 3.88. IR and  $^{13}\text{C}$  NMR spectral data for this and compounds 55 and 56 appear in Table XXVII.

3. Synthesis of  $\text{Ru}(\text{CO})_4[\eta^2\text{-C}_2(\text{SiMe}_3)_2](55)$ .

This preparation was carried out in a two-step fashion: (a) 54.0 mg (0.0845 mmol) of  $\text{Ru}_3(\text{CO})_{12}$  (3b) and 70 mL of pentane were loaded into a 130 mL Schlenk tube (3.3x21.0 cm) and closed with a serum stopper. After several freeze-pump-thaw-degas cycles, an atmosphere of CO was introduced into the vessel. Photolysis (photoapparatus (2a),  $\lambda \approx 370$  nm) over 30 min resulted in a clear, colourless solution of  $\text{Ru}(\text{CO})_5$  (1b); (b) The Schlenk tube containing the pentane solution of 1b was quickly transferred to a Dewar kept at -40°C with a dry ice-acetone bath. Photoapparatus (2b) (without GWV filter sleeve) was placed into the

while the Schlenk tube and photoparatus (2b) were maintained at  $-40^{\circ}\text{C}$ , 1.00 mL (0.75 g, 4.42 mmol) of BTMSA was injected through the stopper to the stirred solution. Irradiation for 2h afforded a quantitative conversion (by IR) of 1b to 55. Removing the volatiles in vacuo at  $-25^{\circ}\text{C}$  left a fine yellow powder which was unstable above  $-20^{\circ}\text{C}$ . Mass spectrum ( $30^{\circ}\text{C}$ )  $M^{+}$  384,  $M^{+}-n\text{CO}$  ( $n=1-4$ ).

#### 4. Synthesis of $\text{Fe}(\text{CO})_4[\eta^2-\text{C}_2(\text{SiMe}_3)_2]$ (56).

This compound was obtained via two published synthetic routes<sup>123a</sup>:

- (a)  $\text{Fe}_2(\text{CO})_9 + \text{BTMSA}$ , room temperature in hexanes for 12h -yield 42%;
- (b) photolysis of  $\text{Fe}(\text{CO})_5 + \text{BTMSA}$  (photoapparatus (3)) in hexanes for 5h -yield 39%.

#### 5. Preparation of $^{13}\text{CO}$ -enriched $\text{M}(\text{CO})_4[\eta^2-\text{C}_2(\text{SiMe}_3)_2]$ .

- (a)  $\text{Fe}(^{13}\text{CO})_4[\eta^2-\text{C}_2(\text{SiMe}_3)_2]$  was obtained from  $\text{Fe}(^{13}\text{CO})_5$  and BTMSA as per Section VIII. 4(b); (b)  $\text{Ru}(^{13}\text{CO})_5$  was generated from  $\text{Ru}_3(^{13}\text{CO})_{12}$  and  $^{13}\text{CO}$  as per Section VIII. 3(a), and  $\text{Ru}(^{13}\text{CO})_4[\eta^2-\text{C}_2(\text{SiMe}_3)_2]$  was subsequently prepared as per Section VIII. 3(b); (c)  $\text{Os}(^{13}\text{CO})_4[\eta^2-\text{C}_2(\text{SiMe}_3)_2]$  was obtained from  $\text{Os}_3(^{13}\text{CO})_{12}$  as per Section VIII. 2.

#### 6. X-Ray Solid State Structure Determination of $\text{Os}(\text{CO})_4[\eta^2-\text{C}_2(\text{SiMe}_3)_2]$ (54).

A summary of pertinent crystallographic data appears in Table XXVIII. Data collection and structure refinement procedures are similar to those described in Section IV. 3. All H atomic positions were calculated using idealized methyl group geometry, and were con-

thermal parameters is found in Table XL. Relevant bond distances appear in Table XXIX and bond angles are given in Table XXX.



Table XL. Positional and Thermal Parameters for  $\text{Os}(\text{CO})_4[\eta^2\text{-C}_2(\text{SiMe}_3)_2](54)$ .

Atom	x	y	z	$U_{11}$	$U_{22}$	$U_{33}$	$U_{12}$	$U_{13}$	$U_{23}$
Os	358.14(3)	115.37(3)	201.58(4)	3.59(2)	3.63(2)	3.67(2)	0.07(2)	-0.24(2)	0.0
S11	617.3(2)	125.9(3)	75.0(3)	4.3(2)	4.8(2)	3.8(1)	0.2(1)	0.4(1)	0.2
S12	507.1(3)	125.4(3)	520.8(3)	4.9(2)	5.2(2)	3.3(1)	0.0(2)	-0.5(1)	0.2
O1	295.4(9)	112.8(7)	-93(1)	10.3(7)	7.1(6)	5.5(5)	0.2(7)	-2.6(6)	-0.3
O2	169.9(7)	104.9(8)	372(1)	5.4(5)	7.2(7)	10.0(7)	0.1(5)	2.1(5)	-0.2
O3	361.0(8)	339.6(8)	208(1)	9.5(7)	5.5(5)	9.9(8)	-0.6(6)	-0.6(8)	-0.6
O4	387.2(9)	-104.6(6)	206(1)	9.7(7)	4.3(5)	8.0(7)	0.7(5)	1.5(6)	0.7
C1	321.8(9)	112.7(9)	17(1)	4.9(6)	4.7(6)	5.4(6)	0.3(6)	-0.7(6)	-0.6
C2	240(1)	107.4(9)	309(1)	5.2(6)	4.7(6)	5.4(7)	-0.6(6)	0.0(6)	0.2
C3	359(1)	255(1)	203(1)	6.6(7)	5.1(6)	5.4(6)	1.3(7)	1.0(9)	0.2
C4	375.0(8)	-21.9(9)	203(1)	4.0(6)	4.5(6)	5.1(6)	-0.8(5)	-0.3(6)	-0.2
C5	528.0(9)	120.6(7)	214(1)	5.1(5)	3.5(5)	3.5(5)	-0.5(5)	0.5(5)	0.3
C6	493.6(9)	118.9(9)	335(1)	4.6(6)	4.8(6)	3.2(4)	0.3(6)	-0.2(5)	0.3
C7	610(1)	14(1)	-27(2)	13(1)	6.7(9)	6.3(9)	1(1)	-1(1)	-2.0(8)
C8	589(1)	234(1)	-31(1)	6.7(9)	7.3(9)	4.9(7)	0.2(8)	0.0(7)	2.4(6)
C9	746(1)	128(1)	150(2)	4.1(6)	10(1)	6.8(8)	-0.4(9)	-0.2(7)	-0.3(9)
C10	643(1)	131(1)	560(1)	4.6(7)	15(2)	5.5(7)	0(1)	-1.2(7)	-1(1)
C11	435(2)	231(1)	583(2)	14(2)	13(1)	9(1)	7(1)	-4(1)	-0.5(9)
C12	458(2)	10(1)	587(2)	15(2)	11(1)	6.0(9)	-5(1)	-3(1)	3(1)

The atomic positional parameters have been multiplied by 10<sup>3</sup>. The anisotropic thermal parameters have been multiplied by 10<sup>3</sup>.

The form of the anisotropic thermal parameter is:  
 $\exp[-2\pi^2(h^2a^{*2}U_{11} + k^2b^{*2}U_{22} + l^2c^{*2}U_{33} + 2hka^*b^*U_{12} + 2hla^*c^*U_{13} + 2klb^*c^*U_{23})]$   
 Estimated standard deviations in the least significant digits are shown in parentheses.

- Abel, E.W. (Eds) "Comprehensive Organometallic Chemistry", Pergamon Press, Oxford, 1982; Volume 4, Chapter 31.1, p. 245. b) Ibid., Chapters 31.1-31.4, p. 243-613. c) Ibid., Chapter 31.1, references 155-159. d) Wei, C.H.; Dahl, L.H. J. Am. Chem. Soc. 1969, 91, 1351.
2. Braye, D.H.; Hübel, W. Inorg. Synth. 1966, 8, 178.
  3. Hieber, W.; Stallman, W. Z. Electrochem. 1943, 49, 258.
  4. Speyer, E.; Wolf, H. Ber. 1927, 60, 1424.
  5. Corey, E.R.; Dahl, L.F. Inorg. Chem. 1962, 1, 521.
  6. Moss, J.R.; Graham, W.A.G. J. Chem. Soc., Dalton Trans. 1977, 95.
  7. Johnson, B.F.G.; Lewis, J. Inorg. Synth. 1972, 13, 92.
  8. Huggins, D.K.; Flitcroft, N.; Kaesz, H.D. Inorg. Chem. 1965, 4, 166.
  9. a) Forster, A.; Johnson, B.F.G.; Lewis, J.; Matheson, T.W.; Robinson, B.A.; Jackson, W.G. J. Chem. Soc., Chem. Commun. 1974, 1042.  
 b) Cotton, F.A.; Hunter, D.L. Inorg. Chim. Acta 1974, 11, L9.  
 c) Aime, S.; Gambino, O.; Milone, L.; Sappa, E.; Rosenberg, E. Inorg. Chim. Acta 1975, 15, 53.
  10. Johnson, B.F.G.; Lewis, J.; Williams, I.G.; Wilson, J. J. Chem. Soc., Chem. Commun. 1966, 391.
  11. Lewis, J.; Manning, A.R.; Miller, J.R.; Wilson, J.M. J. Chem. Soc. A 1966, 1663.
  12. Bradford, C.W.; Nyholm, R.S. J. Chem. Soc., Chem. Commun. 1967, 384.
  13. For a review, see Adams, R.D.; Selegue, J.D. in Wilkinson, G. (Ed.) "Comprehensive Organometallic Chemistry" Pergamon Press, Oxford, 1982; Volume 4, Chapter 33, Section 3.
  14. Deeming, A.J.; Underhill, M.J. J. Chem. Soc., Dalton Trans. 1974, 1415.
  15. Jackson, W.G.; Johnson, B.F.G.; Lewis, J. J. Organomet. Chem. 1977, 139, 125.
  16. Canty, A.J.; Johnson, B.F.G.; Lewis, J. J. Organomet. Chem. 1972, 43, C35.

18. Manuel, I.A. J. Org. Chem. 1962, 27, 3941.
19. Casey, C.P.; Cyr, C.R. J. Am. Chem. Soc. 1973, 95, 2248.
20. Bingham, D.; Hudson, B.; Webster, D.E.; Wells, P.B. J. Chem. Soc., Dalton Trans. 1974, 1521 and references therein.
21. Austan, R.G.; Paonessa, R.S.; Giordano, P.J.; Wrighton, M.S. Adv. Chem. Ser. 1978, 168, 189.
22. Murdoch, H.D.; Weiss, E. Helv. Chim. Acta 1963, 46, 1588.
23. Deeming, A.J.; Hasso, S.; Underhill, M.; Canty, A.J.; Johnson, B.F.G.; Jackson, W.G.; Lewis, J.; Matheson, T.W. J. Chem. Soc. Chem. Commun. 1974, 807.
24. Johnson, B.F.G.; Lewis, J.; Sankey, S.W.; Wong, K.; McPartlin, M.; Nelson, W.J.H. J. Organomet. Chem. 1980, 191, C3.
25. Jackson, P.F.; Johnson, B.F.G.; Lewis, J.; Raithby, P.R.; Will, G.J.; McPartlin, M. J. Chem. Soc., Chem. Commun. 1980, 1190.
26. Evans, J.; McNulty, G.S. J. Chem. Soc., Dalton Trans. 1981, 2017.
27. Castiglioni, M.; Milone, L.; Osella, D.; Vaglio, G.A.; Valle, M. Inorg. Chem. 1976, 15, 394.
28. Johnson, B.F.G.; Lewis, J.; Aime, S.; Milone, L.; Osella, D. J. Organomet. Chem. 1982, 233, 247.
29. Raithby, P.R.; Rosales, M.J. Adv. Inorg. Chem. Radiochem. 1985, 29, 169.
30. King, R.B. Prog. Inorg. Chem. 1972, 15, 287.
31. Gambino, O.; Vaglio, G.A.; Ferrari, R.P.; Cetini, G.J. Organomet. Chem. 1971, 30, 381.
32. Ferrari, R.P.; Vaglio, G.A.; Gambino, O.; Valle, M.; Cetini, G. J. Chem. Soc., Dalton Trans. 1972, 1998.
33. Vaglio, G.A.; Gambino, O.; Ferrari, R.P.; Cetini, G. Inorg. Chim. Acta 1973, 7, 193.
34. X-ray structure: Ferraris, G.; Gervasio, G. J. Chem. Soc., Dalton Trans. 1972, 1057. <sup>1</sup>H NMR: Ferrari, R.P.; Vaglio, G.A. Transition Met. Chem. 1983, 8, 155.

37. Hübel, W.; Braye, E.J.; Clauss, A.; Weiss, E.; Krüerke, U.; Brown, D.A.; King, G.S.D.; Hoogzand, C. *J. Inorg. Nucl. Chem.* 1959, 9, 204.
38. Cetini, G.; Gambino, O.; Sappà, E.; Valle, M. *J. Organomet. Chem.* 1969, 17, 437.
39. Bruce, M.I.; Cooke, M.; Green, M.; Westlake, D.J. *J. Chem. Soc. A.*, 1969, 987.
40. Aime, S.; Milone, L.; Deeming, A.J. *J. Chem. Soc., Chem. Commun.* 1980, 1168.
41. Ferrari, R.P.; Vaglio, G.A. *Gazz. Chim. Ital.* 1975, 105, 939.
42. Gervasio, G. *J. Chem. Soc., Chem. Commun.* 1976, 25.
43. Sappà, E.; Tirripicchio, A.; Manotti Lanfredi, A.M. *J. Organomet. Chem.* 1983, 249, 391.
44. Quicksall, C.O.; Spiro, T.G. *Inorg. Chem.* 1968, 7, 2365.
45. Cotton, F.A.; Deeming, A.J.; Josty, P.L.; Ullah, S.S.; Domingos, A.J.P.; Johnson, B.F.G.; Lewis, J. *J. Am. Chem. Soc.* 1971, 93, 4624.
46. Bryan, E.G.; Burrows, A.L.; Johnson, B.F.G.; Lewis, J.; Schiavon, G.M. *J. Organomet. Chem.* 1977, 129, C19.
47. Zobl-Ruh, S.; Von Philipsborn, W. *Helv. Chim. Acta* 1980, 63, 773.
48. Dickens, B.; Lipscomb, W.N. *J. Chem. Phys.* 1962, 37, 2084.
49. Cotton, F.A.; Eiss, R. *J. Am. Chem. Soc.* 1969, 91, 6593.
50. Tyler, D.R.; Altobelli, M.; Gray, H.B. *J. Am. Chem. Soc.* 1980, 102, 3022.
51. Johnson, B.F.G.; Lewis, J.; Twigg, M.V. *J. Organomet. Chem.* 1974, 67, C75.
52. Johnson, B.F.G.; Lewis, J.; Twigg, M.V. *J. Chem. Soc., Dalton Trans.* 1975, 1876.
53. Desrosiers, M.F.; Ford, P.C. *Organometallics* 1982, 1, 1715.
54. Malito, J.; Markiewicz, S.; Poe, A.J. *Inorg. Chem.* 1982, 21, 4335.

- Soc. 1984, 106, 2027.
57. Tyler, D.R.; Levenson, R.A.; Gray, H.B. J. Am. Chem. Soc. 1978, 100, 7888.
  58. a) Green, J.C.; Seddon, E.A.; Mingos, D.M.P. J. Chem. Soc., Chem. Commun. 1979, 94. b) Green, J.C.; Mingos, D.M.P.; Seddon, E.A. J. Organomet. Chem. 1980, 185, C20. c) Green, J.C.; Mingos, D.M.P.; Seddon, E.A. Inorg. Chem. 1981, 20, 2595.
  59. Ajó, D.; Granozzi, G.; Tondello, E.; Fragalá, I. Inorg. Chim. Acta 1979, 37, 191.
  60. Sherwood, D.E., Jr.; Hall, M.B. Inorg. Chem. 1982, 21, 3458.
  61. Sherwood, D.E., Jr.; Hall, M.B. Organometallics 1982, 1, 1519.
  62. Delley, B.; Manning, M.C.; Ellis, D.E.; Berkowitz, J.; Trogler, W.C. Inorg. Chem. 1982, 21, 2247.
  63. Geoffroy, G.L.; Wrighton, M.S. "Organometallic Photochemistry" Academic Press, New York, 1979.
  64. Desrosiers, M.F.; Wink, D.A.; Ford, P.C. Inorg. Chem. 1985, 24, 1.
  65. Desrosiers, M.F.; Wink, D.A.; Trautman, R.; Friedman, A.E.; Ford, P.C. J. Am. Chem. Soc. 1986, 108, 1917.
  66. Poë, A.J.; Sekhar, C.V. J. Am. Chem. Soc. 1986, 108, 3673.
  67. Vioget, P.; Bonivento, M.; Roulet, R.; Vogel, P. Helv. Chim. Acta. 1984, 67, 1630.
  68. Weiss, E.; Stark, K.; Lancaster, J.E.; Murdoch, H.D. Helv. Chim. Acta 1963, 46, 288.
  69. Kao, S.C.; Lu, P.P.Y.; Pettit, R. Organometallics 1982, 1, 911 and references therein.
  70. Churchill, M.R.; De Boer, B.G. Inorg. Chem. 1977, 16, 878.
  71. Motyl, K.M.; Norton, J.R.; Schauer, C.K.; Anderson, O.P. J. Am. Chem. Soc. 1982, 104, 7325.
  72. Churchill, M.R.; Lashewycz, R.A. Inorg. Chem. 1978, 17, 1291.
  73. "International Tables for X-ray Crystallography" Kynoch Press, Birmingham, England, 1974, Vol. III, Table 4.2.2.

75. Carter, W.J.; Kelland, J.W.; Okrasinski, S.J.; Warner, K.E.; Norton, J.R. *Inorg. Chem.* 1982, 21, 3955.
76. Kiel, G.-Y.; Kiel, W.A., personal communication.
77. Ball, R.G.; Kiel, G.-Y.; Takats, J.; Grevels, F.-W., manuscript in preparation.
78. Kiel, G.-Y.; Seils, F., personal communication.
79. Kruczynski, L.; Martin, J.L.; Takats, J. *J. Organomet. Chem.* 1974, 80, C9.
80.  $C_2H_4$ . Davis, M.I.; Speed, C.S. *J. Organomet. Chem.* 1970, 21, 401.  
 $C_2F_4$ . Beagley, B.; Schmidling, D.G.; Cruickshank, D.W.J. *Acta Crystallogr., Sect. B* 1973, 29, 1499.
81. Fields, R.; Germain, M.M.; Haszeldine, R.N.; Wiggins, D.W. *J. Chem. Soc. A* 1970, 1969.
82. Bamford, C.H.; Mullik, S.U. *Polymer* 1976, 17, 225.
83. Braterman, P.S. "Metal Carbonyl Spectra"; Academic Press, London, England, 1975.
84. Ugi, I.; Marquarding, D.; Klusacek, H.; Gillespie, P.; Ramirez, F. *Acc. Chem. Res.* 1971, 4, 288.
85. Cosandey, M.; von Buren, M.; Hansen, J.-J. *Helv. Chim. Acta* 1983, 66, 1.
86. Allbright, T.A.; Hoffmann, R.; Thibeault, J.C.; Thorn, D.L. *J. Am. Chem. Soc.* 1979, 101, 3801.
87. Hager, D.; Matisons, J.G.; Takats, J. manuscript in preparation.
88. Rushman, P.; van Buuren, G.N.; Shiralian, M.; Pomeroy, R.K. *Organometallics* 1983, 2, 693.
89. Green, M.; Laguna, A.; Spencer, J.L.; Stone, F.G.A. *J. Chem. Soc., Dalton Trans.* 1977, 1010.
90. Theopold, K.H.; Bergman, R.G. *Organometallics* 1982, 1, 1571.
91. Norton, J.R. private communication.
92. Bentson, J.C.; Wrighton, M.S. *J. Am. Chem. Soc.* submitted for publication.

95. Nicholas, K.; Bray, L.S.; Davis, R.E.; Pettit, R. J. Chem. Soc., Chem. Commun. 1971, 608.
96. Hoffman, D.M.; Hoffmann, R.; Fisel, C.R. J. Am. Chem. Soc. 1982, 104, 3858.
97. Gagné, M., private communication.
98. Kore, Y.; Shimada, S.; Saito, Y.; Fitzgerald, B.J.; Peirpont, C.G. Inorg. Chem. 1980, 19, 770.
99. Bennett, M.J.; Graham, W.A.G.; Stewart, R.P., Jr.; Tuggle, R.M. Inorg. Chem. 1973, 12, 2944.
100. Braga, D.; Johnson, B.F.G.; Lewis, J.; McPartlin, M.; Nelson, W.J.H.; Nicholls, J.N.; Vargas, M.D. J. Chem. Soc., Chem. Commun. 1982, 966.
101. Johnson, B.F.G.; Lewis, J.; Odiaka, T.I.; Raithby, P.R. J. Organomet. Chem. 1981, 216, C56.
102. Einstein, F.W.B.; Nussbaum, S.; Sutton, D.; Willis, A.C. Organometallics 1983, 2, 1259.
103. Keister, J.B.; Shapley, J.R. J. Am. Chem. Soc. 1976, 98, 1056.
104. Krüger, C.; Tray, Y.-H. Cryst. Struct. Commun. 1976, 5, 219.
105. Knobler, C.B.; Crawford, S.S.; Kaesz, H. Inorg. Chem. 1975, 14, 2062.
106. Knox, S.A.R.; Stansfield, R.F.D.; Stone, F.G.A.; Winter, M.J.; Woodward, P. J. Chem. Soc., Chem. Commun. 1978, 221; J. Chem. Soc., Dalton Trans. 1982, 173.
107. Green, M.; Norman, N.C.; Orpen, A.G. J. Am. Chem. Soc. 1981, 103, 1269.
108. Yamazaki, H.; Wakatsuki, Y. J. Organomet. Chem. 1977, 139, 157 and references therein.
109. Maitlis, P.M. J. Organomet. Chem. 1980, 200, 161 and references therein.
110. Ball, R.G.; Gagné, M. private communication.
111. Fe: see reference 37. Ru: Bruce, M.I.; Knight, J.R. J. Organomet. Chem. 1968, 12, 411. Os: see reference 39.

J. Am. Chem. Soc. 1986, 108, 7400.

113. Brammer, L.; Crocker, M.; Dunne, B.J.; Green, M.; Morton, C.E.; Nagle, K.R.; Orpen, A.G. J. Chem. Soc., Chem. Commun. 1986, 1226.
114. Acknowledgement to Dr. F. Seils for  $^{13}\text{C}$  data.
115. Seils, F. private communication.
116. Pourreau, D.B.; Whittle, R.R.; Geoffroy, G.L. J. Organomet. Chem. 1984, 273, 333.
117. Hersch, W.H.; Bergman, R.G. J. Am. Chem. Soc. 1983, 105, 5846.
118. Trinquier, G.; Hoffmann, R. Organometallics 1984, 3, 370.
119. Dickson, R.S.; Mok, C.; Pain, G. J. Organomet. Chem. 1979, 166, 385.
120. Emsley, J.W.; Feeney, J.; Sutcliffe, L.H. "High Resolution Nuclear Magnetic Resonance Spectroscopy", vol. 2, Pergamon Press, New York, 1966.
121. a) The, K.I.; Cavell, R.G. Inorg. Chem. 1977, 16, 1463. b) Cavell, R.G.; The, K.I. Inorg. Chem. 1978, 17, 355.
122. L'Eplattenier, F.; Calderazzo, F. Inorg. Chem. 1968, 7, 1290.
123. For M=Fe see (a) Pannell, K.H.; Crawford, G.M. J. Coord. Chem. 1973, 2, 251; for M=Ru see (b) Cavit, B.E.; Grundy, K.R.; Roper, W.R. J. Chem. Soc., Chem. Commun. 1972, 60; (c) Lehmann, H.; Schlenk, K.J.; Chapuis, G.; Ludi, A. J. Am. Chem. Soc. 1979, 101, 6197; for M=Os see (d) Burt, R.; Cooke, M.; Green, M. J. Chem. Soc. (A) 1970, 2981; (e) Segal, S.A.; Johnson, B.F.G. J. Chem. Soc., Dalton Trans. 1975, 677.
124. Hastings, W.R.; Baird, M.C. Inorg. Chem. 1986, 25, 2913.
125. Cotton, F.A.; Lahuerta, P. Inorg. Chem. 1975, 14, 116.
126. Ball, R.; Gagné, M.; Takats, J. manuscript in preparation.
127. Carty, A.J.; Smith, W.F.; Taylor, N.J. J. Organomet. Chem. 1978, 146, C1.
128. Martin, L.R.; Einstein, F.W.B.; Pomeroy, R.K. Inorg. Chem. 1985, 24, 2777.
129. Ittel, S.D.; Ibers, J.A. Adv. Organomet. Chem. 1976, 14, 33.
130. Davies, B.W.; Payne, N.C. Inorg. Chem. 1974, 13, 1848.
131. Pierpont, C.G. Inorg. Chem. 1977, 16, 636.



133. (a) Iatsumi, K.; Hoffmann, R.; Templeton, J. - Inorg. Chem. 1982, 21, 466. (b) Morrow, J.R.; Tonker, T.L.; Templeton, J.L. J. Am. Chem. Soc. 1985, 107, 6956.
134. Sappa, E.; Tiripicchio, A.; Braunstein, P. Chem. Rev. 1983, 83, 203.
135. For M=Fe see (a) Kruczinski, L.; LiShingMan, L.K.K.; Takats, J. J. Am. Chem. Soc. 1974, 96, 4006. (b) Wilson, S.T.; Coville, N.J.; Shapley, J.R.; Osborn, J. J. Am. Chem. Soc. 1974, 96, 4038. (c) von Buren, M.; Cosandey, M.; Hansen, H.-J. Helv. Chim. Acta 1980, 63, 738. (d) See reference 85. M=Ru, see references 55 and 79. M=Os, see reference 88 and Chapter Two.
136. Kriegsman, H.; Beyer, H. Z. Anorg. Allgem. Chem. 1961, 311, 180.
137. Wrackmeyer, B. J. Organomet. Chem. 1979, 166, 353.
138. Kost, D.; Carlson, E.H.; Raban, M. J. Chem. Soc., Chem. Commun. 1971, 656.
139. Maslowsky, J.E. "Vibrational Spectra of Organometallic Compounds" Wiley-Interscience, 1977, pp. 248-263.
140. Greaves, E.O.; Lock, C.J.L.; Maitlis, P.M. Can. J. Chem. 1968, 46, 3879.
141. Chisholm, M.H.; Clark, H.C.; Manzer, L.E.; Stothers, J.B. J. Am. Chem. Soc. 1972, 94, 5087.
142. Templeton, J.L.; Ward, B.C. J. Am. Chem. Soc. 1980, 102, 3288.
143. Stothers, J.B. "Carbon-13 NMR Spectroscopy" Academic Press, 1972, pp. 85-90.
144. Adridge, C.J. Organomet. Chem. Rev. 1970, 5A, 323.
145. (a) Demuyne, J.; Strich, A.; Veillard, A. Nouv. J. Chim. 1977, 1, 217. (b) Axe, F.U.; Maynick, D.S. J. Am. Chem. Soc. 1984, 106, 6230.
146. Gagné, M. private communication.
147. Main, P.; Lessinger, L.; Woolfson, M.M.; Germain, G.; Declercq, J.P. "MULTAN 80. A System of Computer Programs for the Automatic Solution of Crystal Structures from X-Ray Diffraction Data".
148. "International Tables for X-Ray Crystallography", Kynoch Press, Birmingham, England, 1974, Vol. IV, Table 2.2B.
149. Ibid., Table 2.3.1.
150. Landon, S.J.; Stalman, P.R.; Geoffroy, G.L. J. Am. Chem. Soc. 1985, 107, 6739.

Chem. 1981, 20, 1528.